The role of platelets in the innate inflammatory response to TB

Dr. Daniela Elisa Kirwan

Institute for Infection and Immunity

St. George's, University of London

Thesis submitted for the degree of Doctor of Philosophy (PhD)

February 2022

Declaration of Authenticity

I confirm that I am the sole author of this thesis and the work to which it refers. All referenced studies have been appropriately cited and included in the bibliography. This thesis has not been previously submitted, in part or in whole, to any university or institution.

Daniela E. Kirwan

Copyright Declaration

"Revolution will free society of its afflictions, while science will free the individual of his."

- Mario Vargas Llosa

Abstract

Introduction: Platelets are increasingly recognized for their roles in infection. Tuberculosis (TB) is characterized by excessive inflammation leading to disease and long-term sequelae. Platelets may be key drivers of immunopathology in TB, but the mechanisms involved are poorly understood. My hypothesis is that platelets regulate innate immune responses to TB.

Methods: An *in vitro* model of M.tb-infected monocytes co-cultured with autologous platelets was interrogated using specific inhibitors and recombinant proteins. Gene expression of matrix metalloproteinases (MMPs) was assessed using quantitative PCR, and secretion using ELISA.

Pulmonary TB patients, healthy controls, and patients undergoing diagnostic bronchoscopy were prospectively recruited. Agonist-induced platelet aggregation was quantified using light transmission aggregometry, and platelet activation and platelet-leukocyte binding measured using flow cytometry. Concentrations of cytokines, MMPs, and platelet-associated factors were assessed in bronchoalveolar lavage fluid (BALF) and plasma using Luminex multiplex analysis. Inflammatory responses were compared with those identified in a separate cohort of SARS-CoV-2-infected patients using multiplex analysis.

Results: Platelets respond to M.tb-secreted antigens. Co-culture with platelets increases MMP gene expression and secretion by M.tb-stimulated monocytes. Platelets enhance M.tb-induced upregulation of monocyte phosphorylated phosphatidylinositol 3-kinase (PI3K) and mitogen activated protein kinase (MAPK) pathways through a combination of direct receptor-mediated and indirect secretory stimulation.

Platelets from TB patients display a pro-inflammatory phenotype with decreased agonist-induced aggregation. Platelet-monocyte aggregation is increased in patients with TB and non-TB lung disease compared to healthy controls, but platelet-granulocyte aggregation was increased in TB patients only. Increased levels of inflammatory mediators including IP-10, platelet markers including von Willebrand factor (vWF), and MMPs were seen in both TB and SARS-CoV-2 infection; others including IL-8 showed divergent responses.

Conclusions: This study presents cellular and clinical evidence that platelets adopt a TB-specific pro-inflammatory phenotype in pulmonary TB. This will inform the development of therapeutic agents aiming to limit harmful platelet-driven inflammation in TB.

Contents

Tables and Figures

Acknowledgements

First and foremost I would like to wholeheartedly thank my two supervisors, Prof. Jon Friedland at St. George's University of London and Prof. Bob Gilman at Johns Hopkins University. I shall be eternally grateful for their unwavering support, encouragement, mentorship, and belief in my abilities, as well as their friendship. I look forward to continuing to work together.

In Peru Dr. Oscar Gayoso and Dr. Cesar Ugarte-Gil facilitated implementation of the clinical study at the Hospital Cayetano Heredia. I am grateful to all the staff at CENEX and the TB clinics for their good will in identification and recruitment of patients, my study nurses Lic. Liset Nazario and Lic. Karen Rojas, and most importantly to each of the patients who participated in my study. At UPCH, Jorge Coronel, Omar Melo, Carolina Maynari, Dina Patilla, and Valeria Chancafe were extremely helpful in the laboratory, and Lic. Lilia Cabrera, Karina Roman, and Henry Torres Mori in coordinating project administration and fieldwork. Dr Ivan Lozada provided valuable support with flow cytometry design as well as access to his cytometer. Working alongside fellow UK PhD candidate Cristina Loader made it all much easier and more enjoyable.

The Friedland research group are like a family. My thanks to Sara Brilha, Kate Fox, Radha Asher, Ash Whittington, Cristina Loader, Deborah Chong, Keira Skolimowska, Sally Hayward, Sajeel Shah, Julia Kutschenreuter, and others for their patience, encouragement, and company.

The COVID-19 pandemic may have interrupted my clinical TB project, but it also presented a unique opportunity to work on the frontline of research. I thank Prof. Sanjeev Krishna, Drs. Tim Planche, Henry Staines, David Clark, Yolanda Augustin, Nick Eckersley, and Ben Davies at SGUL, and the wider collaboration for this valuable experience, and Will Elson for support with analysis.

I am grateful to Prof. Michael Emerson, Dr. Kirk Taylor, and their team at Imperial College for welcoming me into their research group in the early stages of my PhD, and for training in platelet techniques including light transmission aggregometry which I was able to transfer to Peru.

I am grateful to the Medical Research Council, for having sufficient faith in myself and my project to fund my Fellowship, and for their flexibility and support during the pandemic.

Above all, I would like to thank my parents, Michael and Silvia, and my brother Joseph, the three most important people in my life without whose love and support I would not be where, or who, I am today.

Chapter 1 Introduction

1.1 Immunopathology and Tissue Destruction in Tuberculosis

1.1.1 Tuberculosis remains a significant public health concern

Tuberculosis (TB) is one of the most important infectious diseases of our time. In 2019 10.0 million people developed symptomatic disease and 1.2 million died(1) with little change in these figures over the preceding decade. Although many patients are never diagnosed or treated, a significant proportion of deaths occur in individuals who have received appropriate anti-TB treatment(2). This is largely due to the inflammatory immune response to *Mycobacterium tuberculosis* (M.tb), the causative agent of TB. This response is highly complex encompassing both the innate and adaptive immune systems, resulting in severe disease manifestations and facilitating onwards transmission(3). In addition, the co-evolution of M.tb and humans has led to bi-directional adaptations that enable the bacteria to persist in a semi-dormant state, and consequently current treatment regimens require a minimum of six months of therapy to ensure eradication of all viable bacilli within the patient(4). Treatment is further complicated by the rise of single-, multi- and extensively drug-resistant disease which require longer and yet more complex regimens, associated with higher cost and worse side effect profiles.

1.1.2 Tuberculosis leads to impaired lung function and reduced quality of life in survivors

In TB, excess inflammation causes tissue destruction that resolves with fibrosis, so even when successfully treated patients often suffer long-term sequelae including impaired lung function and quality of life(5-11). TB survivors have a shortened life expectancy with one model predicting an average loss of 3.6 years of life(12). This has been well documented in the literature for over a century(13-18).

Residual damage following TB includes fibrosis, emphysema, and bronchiectasis(19). TB is a risk factor for developing chronic obstructive pulmonary disease (COPD)(20) independent of smoking status(21, 22) and in a large South African study was the strongest predictor of chronic bronchitis

(men: odds ratio (OR) 4.9 [95% confidence interval (CI) 2.6-9.2]; women: OR 6.6 [95% CI 3.7-11.9])(23).

Lung function can be objectively assessed using spirometry, which is commonly used to evaluate patients with chronic lung diseases and is useful for quantifying the degree of functional lung damage post TB. Following TB treatment lung function can range from normal to severely impaired, and patients can have restrictive, obstructive, or mixed abnormalities(24, 25). Studies conducted across a variety of geographical locations have identified rates of impairment following TB of up to 68% (8, 24, 26-28). The Burden of Obstructive Lung Disease (BOLD) study, a large, population-based study, investigated the association between history of TB and airflow obstruction in 18,664 adults aged 40 years or older from 27 sites. Participants underwent a questionnaire and pulmonary function testing, and a history of TB was associated with a restrictive spirometric pattern (adjusted odds ratio 2.13, 95% CI 1.42-3.19) and with airflow obstruction (adjusted OR 2.51, 95% CI 1.83-3.42)(8). Similarly, the PLATINO study evaluated 5,571 adults aged 40 years or older from five Latin American metropolitan areas, and found a prevalence of airflow obstruction (defined as a forced expiratory volume in 1 second (FEV1)/ forced vital capacity (FVC) ratio post bronchodilator of <0.7) of 30.7% in individuals with a history of TB and 13.9% in those without; the difference was greater for males than for females(26). A retrospective cohort study of South African gold miners also found that previous TB was associated with symptomatic breathlessness and a loss of lung function which was greater in those with more severe disease at presentation(27).

The degree of radiological severity at diagnosis has been shown to be the most important determinant of residual pulmonary function post treatment(27-29). Patients with chronic pulmonary disease following TB are affected at a younger age than patients with other aetiologies(7) and this may lead to cumulative lung damage when subsequently exposed to other insults. Loss of lung function also accumulates with repeated episodes of TB. Hnzido *et al* elegantly demonstrated this in a series of 27,660 South African gold miners at ongoing risk of re-exposure. Loss of lung function was greatest within six months of diagnosis and stabilised by 12 months, and the average deficit in FEV1 was 153ml, 326ml, and 410ml, and deficits in FVC were 96ml, 286ml and 345ml after one, two, or three or more episodes of TB, respectively. In these groups the percentage who had a FEV1 <80% of predicted was 18.4%, 27.1%, and 35.2% respectively(19).

This substantial burden of disease has significant public health and economic implications. Given that TB primarily affects young adults within the economically active age group and residing in low- and middle-income countries, these countries are disproportionately affected. It is important to identify patients with post-TB sequelae so that they can be appropriately managed: loss of pulmonary function can be mitigated with interventions including pulmonary rehabilitation(30), and therapies that can reverse or prevent progression of sequelae including lung fibrosis are in development and may be shortly available for use in this patient group.

1.1.3 Pulmonary TB is associated with a matrix degrading phenotype

Pulmonary TB is characterised by pathophysiology that is disproportionate to the mycobacterial load, and even in paucibacillary disease severe inflammation of the lung may occur. It is commonly understood that following inhalation M.tb are phagocytosed by macrophages, the main innate immune effector cells and hosts for bacterial replication. Macrophages become activated and recruit other innate immune cells including neutrophils(31) which are important early responders to TB infection, involved in both pathogen elimination and in inflammation(32). A secondary cell-mediated immune reaction involving cross-presentation and priming of CD8+ T cells occurs days after initial antigen exposure(33), known as delayed-type hypersensitivity. These processes may lead to the formation of a granuloma whereby lymphocytes and neutrophils surround infected macrophages to isolate and contain the bacteria, often for decades; if this containment is unsuccessful, bacterial replication, disease, and dissemination occur.

A classic feature of pulmonary TB that is often present at diagnosis is cavitation of the lung. Here, lung parenchymal destruction leads to the formation of large, air-filled spaces that provide relatively immunoprivileged sites where M.tb can proliferate exponentially. Cavitating disease is associated with treatment failure(34) and drug resistance(35), and patients are highly contagious and represent the main drivers of transmission(36). Despite a high burden of viable bacteria within the cavities patients can remain relatively well for years or decades, existing in a state of symbiosis with the bacterium. For example, George Orwell who is thought to have caught TB in 1937 during the Spanish civil war(37) suffered several severe exacerbations, and finally died of the disease in 1950; some of his most distinguished works were written during this time.

Cavity formation results from the activity of enzymes called matrix metalloproteinases (MMPs) that are the final effectors of the host innate inflammatory response(38, 39). MMPs are a family of zinc-dependent proteases that collectively degrade all components of the extracellular matrix (ECM), and also have immunological functions including modulating cytokine and chemokine activity, activating defensins, and cleavage of proteinase-activated receptors(40, 41). They are tightly regulated through gene expression, secretion as proenzymes, compartmentalisation, enzymatic inactivation, and by specific tissue inhibitors of metalloproteinases (TIMPs). MMPs are responsible for the turnover of healthy tissues, but if produced in excess they cause tissue damage. They are produced by many different cell types including epithelial cells, macrophages, and other cells, and their production is induced in response to specific stimuli(42). MMPs are secreted by leukocytes and stromal cells during *M.tb* infection(43, 44) and in pulmonary TB MMP-1, interstitial collagenase, is the rate limiting step in the degradation of type I collagen(45) and is the main effector of lung degradation and cavity formation(39, 46). High levels of MMP-1 are also found in other lung diseases involving loss of pulmonary architecture including emphysema(47-49). Different MMPs have distinct roles and are active at different stages in TB pathology: for example, MMP-1 drives early macrophage-dependent collagen degradation, MMP-8 (neutrophil elastase) may predominate in advanced cavitary disease where there is marked neutrophil infiltration(50), and MMP-9 is involved in macrophage recruitment and granuloma formation(51) and predominates in TB meningitis(52).

MMP concentrations have consistently been shown to be elevated in patients with acute TB, and correlate with clinical and radiological disease severity(46, 53-55). In one study, concentrations of MMP-1 and -3 were significantly higher in induced sputum and bronchoalveolar lavage fluid from patients with TB compared to respiratory symptomatics (increased by 15.6-fold and 3.6-fold respectively), whilst concentrations of TIMP-1 and TIMP-2 were reduced by 4.7-fold and 138-fold respectively(54). Separately, sputum samples from patients with TB had high levels of MMP-1, -2, -3, -8, and -9(46, 55) and sputum MMP-1 concentrations correlated with radiological evidence of tissue destruction(55). These levels reduce markedly within the first 2 weeks of anti-TB treatment(46). Raised pleural fluid concentrations of MMP-1, -8 and -9 have also been found in patients with TB pleuritis compared to those with other causes of pleural effusions(56). Using immunohistochemistry, MMP-1 and -7 have been demonstrated within epithelioid macrophages and Langhans giant cells within lung granulomas(57) and MMP-9 has been identified in multinucleate giant cells in lymph node tissue(58). Gene expression profiling of macrophages has

shown that among patients with pulmonary TB the most highly upregulated gene was *mmp-1* compared to people with latent TB(59) and genetic predispositions have also been shown as risk factors for developing fibrosis following TB(60).

1.2 Platelets as Immune Cells

Platelets, small, anucleate cells, are the second most abundant cell type in the circulation. Traditionally known as effectors of haemostasis and thrombosis, they also have important functions in immunity and inflammation for which they are increasingly gaining recognition. Although platelets do not contain any genomic DNA, they have functional non-coding and coding RNAs and translational machinery which they acquire from the parent megakaryocytes in a highly regulated manner. This enables platelets to synthesise proteins, and also enables post-transcriptional gene regulation(61). This is thought to occur primarily through miRNAs binding to the 3'-UTR of the target transcript and thus regulating RNA degradation and protein translation, as well as through RNA-binding proteins (RBPs) which mediate transport of RNA from megakaryocytes to platelets and within the platelet itself can modify RNA translation, splicing, transport, decaying, and editing(62, 63).

Platelets circulate in a resting state maintained by nitric oxide (NO) and prostacyclin (Prostaglandin I_2) released from the vascular endothelium, and upon contact with a stimulant they rapidly activate and exert a range of effects. Despite their small size they contain a number of structures including three types of granules: alpha, dense, and lysosomal. Alpha granules are the most abundant, storing over 300 different proteins which are rapidly released during platelet activation through degranulation. Proteomics studies have found many of these to be involved in the regulation of inflammation and tissue repair(64) including, among others, RANTES, IL-1β, monocyte chemoattractant factor (MCP-1), platelet factor 4 (PF4), and platelet activating factor (PAF). Some of these proteins are acquired from the megakaryocyte, and others including fibrinogen and albumin are obtained from the plasma through endocytosis(65). Following stimulation platelets also express functional immune receptors which facilitate intracellular interactions. Some receptors are externalised from the alpha granule membrane, such as P-selectin which is involved in leukocyte tethering and migration; others including integrins are already present on the platelet surface and undergo conformational change to an active state(66).

Following insults such as endothelial injury, platelets are well placed to respond and to initiate inflammation. They recruit, activate and influence the differentiation of cells of the innate system, including monocytes, macrophages, natural killer (NK) cells, and dendritic cells(67), and they form a bridge between the innate and adaptive immune systems for example through the secretion of soluble CD40 ligand (sCD40L) which influences antibody class switching, cell maturation, and cell adhesion(68), and by acting as antigen presenting cells to recruit T-cells(69).

1.3 Platelets in Infection

Platelet directly target and eliminate viral and bacterial pathogens. At sites of microbial entry into the body such as a wound or cut, platelets are the first to arrive and initiate a response. As well as limiting blood loss and closure of the defect, the process of thrombosis allows platelets to entrap pathogens, and to kill them directly by secreting anti-microbial peptides(70) or indirectly through complement factors such as C5a(71). Platelets sense pathogens directly via expressed Toll-like receptors (TLRs) such as TLR2 and TLR4(72, 73) leading to activation and release of reactive oxygen species(74) and pro-inflammatory cytokines(75). Most notably, platelet TLR4 binds to lipopolysaccharides (LPS) from Gram-negative bacteria, which induces secretion of pro-inflammatory cytokines including tumour necrosis factor alpha (TNF-α), soluble CD40 ligand (sCD40L), and interleukin 1 beta (IL-1β)(75). This is a sophisticated system, able to distinguish different LPS moieties to induce distinct secretory profiles(76). TLR2 stimulation, more frequently by Gram-positive organisms, can lead to bacterial phagocytosis by the platelets(74, 77).

While platelet-mediated killing of the pathogens is ongoing, platelets also recruit other immune cells to sites of infection. They do this through chemokine secretion and by interacting with other immune cells via a number of surface receptors forming platelet-leukocyte aggregates, which can enhance the anti-pathogen function of these other cells for example by enhancing neutrophil extracellular trap (NET) formation or enhancing the phagocytic abilities of monocytes and macrophages(78, 79).

Whilst these responses are effective in the eradication of microbes and repair damaged tissues, uncontrolled inflammation can result in over-activity of platelets and coagulation factors as well as downregulation of anticoagulant mechanisms. This can in turn lead to disseminated

intravascular coagulation (DIC) characterised by microthrombi formation, consumption of coagulation factors and platelets, and bleeding(80). Immunocoagulation, a relatively recent addition to the immunology lexicon, describes the combination of these processes and is considered a pathologic response in sepsis(81). Hence, platelets are implicated both in coagulopathy itself as well as in modulating coagulation and inflammation in sepsis(82) and indeed, platelets may form a powerful link between thrombosis and inflammation(83).

1.4 Platelets in Tuberculosis

1.4.1 Clinical and pre-clinical evidence for the involvement of platelets in TB immunopathology

Thrombocytosis (elevated platelet count) has repeatedly been reported in patients with tuberculosis (84-89). This has been shown to correlate with severity of tuberculosis and with levels of acute phase reactants such as C-reactive Protein (CRP)(89-92) and this response may be absent in patients with community acquired pneumonia(93). Other studies have identified thrombocytopaenia (low platelet count) instead, and it has been postulated that this may occur where there is disseminated tuberculosis involving marrow infiltration(94).

Platelet-associated gene transcripts have been found to be upregulated in TB patients(95). As platelet RNA is formed in the megakaryocyte prior to platelet formation, the megakaryocyte itself may be influenced by the disease state and platelets may be pre-programmed to respond specifically to TB. This has been identified in other diseases such as cancer, where the platelet transcriptome can be used to accurately diagnose different types of cancer and in some situations to inform on prognosis(96).

Changes in platelet structure and function have been described in TB patients. In acute TB there are increased numbers of alpha granules(97) which contain pro-inflammatory mediators such as TNFα and IL-1β, which are elevated in the serum of TB patients(98). In contrast, patients with chronic TB have elongated platelets and in addition to alpha granules also have large numbers of dense granules which contain a range of mediators including adenosine diphosphate (ADP), adenosine triphosphate (ATP), serotonin, and ionized calcium, involved in the coagulation cascade(97). These differences may reflect distinct functional roles at different disease stages,

with a predominantly pro-inflammatory phenotype in acute TB and a mixed inflammatory-thrombotic state in chronic disease.

Functionally, this may translate to a hypercoagulable state in TB. Kutiyal *et al* found that APTT was deranged in 18% of patients with TB, Factor VII levels in 35%, fibrinogen levels in 57%, and D-dimers were positive in 57.8%, alterations that are all in keeping with hypercoagulability(94). Schoeman *et al* also identified a hypercoagulable state occurring in children with advanced TB disease, with a higher risk of developing thrombosis and stroke(99). This is also described in patients with HIV-associated TB in whom it was associated with increased risk of death(100). Thrombosis frequently occurs in cerebral TB(101), although the pathophysiology of cerebral tuberculosis is different from that of pulmonary disease.

Increased platelet activity can be detected by quantifying markers released from platelet granules. Elevated plasma concentrations of Platelet Factor 4 (PF4; CXCL4), a component of alpha granules specific to platelets, have been identified in patients with pulmonary TB and correlate with radiological disease severity(102). To see whether we could find any evidence of platelet activity in patients with TB, our group recruited 50 adult patients with newly diagnosed, drug-sensitive smear positive pulmonary TB, and 50 age- and sex-matched controls in Lima, Peru. At diagnosis, levels of platelet factor 4 (PF4), platelet-derived growth factor (PDGF)-BB, C-C motif chemokine ligand 5 (CCL5; RANTES), MMP-9, soluble CD40 ligand (sCD40-L), and Pentraxin-3 (PTX-3; TNF-stimulated gene (TSG)-14) were elevated compared to age- and sex-matched controls, but levels of soluble P-selectin were not. Among the TB patients there was a strong correlation between several of these factors, in particular PDGF-BB, PF4 and RANTES, which is in keeping with co-secretion of these factors. 50% of these patients were followed up during their anti-TB treatment, and the plasma concentrations of all markers increased at Day 14 and then decreased, returning to normal by Day 60(103). Levels of platelet-derived mediators such as PF4 have been shown to correlate with disease progression and severity in other chronic inflammatory conditions including inflammatory bowel disease(104), atherosclerosis(105), and rheumatoid arthritis(106). Platelet-derived mediators may also drive inflammatory processes in TB, and could be important in the resolution of inflammation and/or development of fibrosis.

Finally, there is evidence that platelets are present at the site of disease, either as a result of extravasation and localisation to the lesion, or secondary to platelet biogenesis within the lung itself; megakaryocytes have been identified within the lungs and may have the capacity to scale

up platelet generation in response to specific stimuli(107). Concentrations of PDGF-BB, P-selectin and RANTES were elevated in samples of human broncho-alveolar lavage fluid (BALF) collected from patients with TB compared to controls with non-TB respiratory disease(103). Platelet aggregations and platelet-neutrophil adhesions have been observed within pulmonary lesions and M.tb have been visualised within the platelets, located mainly along the edges of the mitochondria(97). We stained sections of M.tb-infected and uninfected mouse lung for CD41, a ubiquitous platelet marker, and observed staining in infected but not uninfected lung tissue. This was seen predominantly within the alveoli and, although most of the staining occurred in association with anucleate cells consistent with the morphology of platelets, we also noted some staining of nucleated cells which indicates platelet phagocytosis and/or adherence to leukocytes(103). Similarly, Feng *et al* observed platelet-specific marker CD42b within epithelioid cells and multinuclear giant cells in granulomas within lung biopsies from human TB patients(108), and microthrombi occur around tuberculosis cavities and have been proposed to prevent dissemination(109).

1.4.2 Platelet-leukocyte signalling and cellular interactions in TB

Although little is known about platelet-leukocyte signalling in TB, much can be inferred from mechanisms known to be important in response to other micro-organisms. During infection, activated platelets interact directly with leukocytes to facilitate cellular recruitment towards the site of infection(110). These adhesive interactions can form platelet-monocyte aggregates (PMA) and platelet-neutrophil aggregates (PNA) which lead to cell activation and enhance immune function such as cytokine or MMP production. Platelets can stimulate neutrophils to release neutrophil extracellular traps (NETs)(111), which are increased in the plasma of TB patients(112) and have been associated with severe TB-associated lung damage and subsequent sequelae(113). These adhesive interactions are mediated by the two main families of cell adhesion molecules, selectins and integrins.

Selectins are single transmembrane glycoproteins that initiate leukocyte tethering and rolling along inflamed endothelium prior to transmigration(114). Platelets express P-selectin (CD62P), which is translocated from alpha granules to the surface membrane in response to stimulation. P-selectin ligation can activate platelets leading to aggregation, enhanced adhesion, and

activation of other platelet expressed integrins such as GPIIb/IIIa(115). It is also sheared into the circulation; levels of soluble P-selectin are higher in TB patients compared to healthy controls(103, 116). Moreover, P-selectin on platelets can interact with P-selectin glycoprotein ligand-1 (PSGL-1) expressed on leukocytes to form PMA(117), an important process in the pathology of chronic inflammatory diseases including atherosclerosis(118) and heart disease(119). Increased circulating PMA are found in TB patients compared to healthy controls(120), and treatment of M.tb-infected whole blood with anti-P-selectin antibody decreases PMA(120).

Following rolling and tethering, integrins facilitate platelet binding to inflamed endothelium or leukocytes. Platelets express three families of integrins, β1 (CD29), β2 (CD18), and β3 (CD61). αIIbβ3 is the most dominant integrin expressed on platelets(121) and can recognise arginine-glycine-aspartic acid (RGD)-containing ligands such as fibrinogen and fibrin(122). Ligation of integrins on platelets initiates "inside-out" or "outside-in" signalling pathways to result in functional outcomes such as cell activation, adhesion, or degranulation(123). Other important adhesive interactions demonstrated between platelets and leukocytes include the binding of surface expressed glycoprotein-Ibα (GPIbα, CD42a), part of a receptor complex that binds von Willebrand factor (vWF), to αMβ2 (CD11b/CD18, Mac-1) on monocytes(124). In atherosclerosis platelet-derived CD40L (CD154) can interact with CD40 (TNF receptor) expressed on leukocytes to form platelet-leukocyte aggregates(125). Whilst these cellular interactions have been observed *in vitro* or in animal models, the specific interactions important in TB patients remain unclear.

In TB, cellular networks involving resident and influxing leukocytes, stromal cells, and other cells enable amplification of initial responses, leading to secretion of MMPs and other pro-inflammatory mediators(126). Cross-talk between platelets and leukocytes, particularly monocytes, may be key to driving TB immunopathology: platelets have been shown to significantly upregulate MMP secretion from M.tb-infected monocytes(103) and are important in the development of granulomas and macrophage differentiation in TB(108). Although the effect of platelets on inflammatory responses in TB depends upon the stage, site, and severity of TB infection, they appear to predominantly steer monocyte differentiation towards an anti-inflammatory phenotype.

What remain unexplored are the mechanisms by which platelets induce leukocyte activation during M.tb infection to cause reported cellular responses. Data from *in vitro* studies utilising uninfected cells show that following engagement of platelet expressed P-selectin and PSGL-1 on

leukocytes, signal transduction pathways are initiated to enhance tyrosine phosphorylation and activation of mitogen-activated protein kinase (MAPK)(127). MAPK are phosphorylation-dependent signal-transducing enzymes involved in immune responses and cellular regulation(128). The p38 and extracellular signal-related kinase (ERK)/MAPK pathways are key in regulating MMP and cytokine secretion during M.tb infection(129-133). Therefore, we hypothesize that P-selectin-PSGL-1 binding between platelets and leukocytes in M.tb infection could lead to MMP and pro-inflammatory cytokine gene and protein production via MAPK signalling. In contrast, phosphatidyl inositol 3-kinase (PI3K) signalling negatively regulates MMP-1 secretion from M.tb-infected macrophages(134). PSGL-1 activation can induce signalling via PI3K(135) and activation of mTOR and Rho-associated kinases (ROCKs) in macrophages to facilitate cell motility and phagocytosis(136). Whether platelets interacting with macrophages during M.tb infection also utilise PSGL-1-PI3K/mTOR signalling is unknown.

Taken together, these studies indicate that platelets have a key role in directing cellular outcomes in response to M.tb through interactions with cell adhesion molecules and by manoeuvring intracellular signalling pathways. These interactions are summarised in Figure 1.1. A better understanding of these cellular interactions may reveal which signalling mechanisms could be targeted to decrease TB immunopathology.

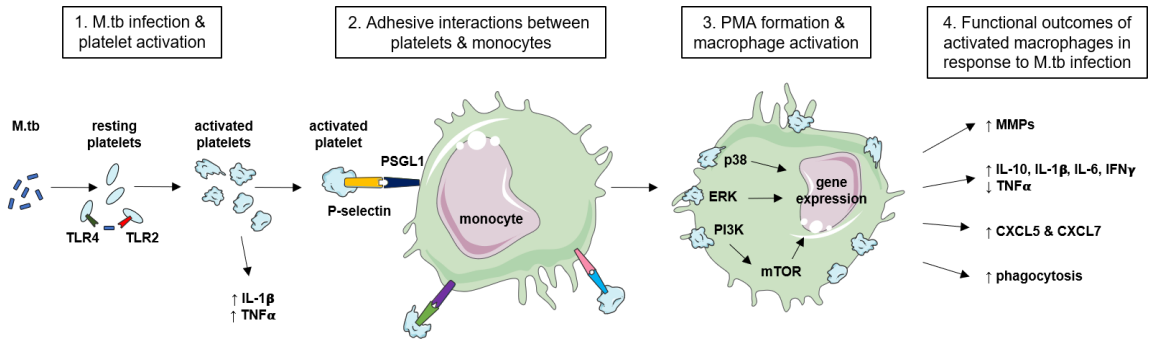

Figure 1.1 Hypothesized platelet-monocyte signalling in M.tb infection.

Figure courtesy of Dr. Deborah Chong. (137)

1.4.3 Anti-platelet agents for the treatment of TB

Imbalances in eicosanoids have been associated with the development of TB(138, 139). Eicosanoids are lipid mediators derived from the activity of the enzymes cyclooxygenase (COX)-1 and -2 on arachidonic acid, which enter either the cyclooxygenase or the lipoxygenase pathway. The cyclooxygenase pathway leads to prostaglandins D, E and F, prostacyclin, and thromboxane A2 (TXA A2) production. Prostaglandins are powerful vasodilators, inhibit platelet aggregation, and act as signalling molecules linking the innate immune system to acute inflammatory pathways(140), whereas thromboxanes are vasoconstrictors that trigger platelet aggregation(141). The lipoxygenase pathway causes the production of lipoxins, which reduce pro-inflammatory cytokine production and neutrophil recruitment(142). Non-steroidal anti-inflammatory drugs (NSAIDs) inhibit COX-1 and -2, and include aspirin (Acetylsalicylic acid, ASA), the most commonly prescribed anti-platelet agent. Aspirin irreversibly inhibits both COX enzymes and displays powerful anti-thrombotic effects at low doses as well as anti-inflammatory activity at higher doses.

Repurposing anti-platelet and anti-inflammatory NSAIDs for use in TB is attractive because they are already approved for use and have well-established safety profiles. Data indicate they may be effective at enhancing TB control(143); animal and human studies are presented in the Appendix (Table 13). Although NSAIDs have some direct anti-mycobacterial activity(142, 144-149), their main effect in TB is likely to be due to their action on the host immune system, particularly by modulating inflammatory pathways that are active in TB disease(142, 144, 150-152). Administration of ibuprofen to TB-infected C3HeB/FeJ mice led to fewer and smaller lung lesions, decreased neutrophil infiltration, reduced bacillary load, and enhanced survival(153). Whether the effects of NSAID treatment are protective, by enabling effective clearance of pathogens, or harmful by causing tissue destruction, will depend upon multiple factors including timing, route of administration, and dose, all of which must be considered when proposing NSAIDs as a potential adjunctive treatment.

Data from TB patients suggest that anti-platelet agents can be beneficial. One of the first drugs in use for TB, P-amino-salicylic acid (PAS), is an aspirin homologue that was deemed effective despite an unknown mechanism of action when it was first given to a patient in 1944. It has been shown that PAS modulates anti-inflammatory immune activity, and suppresses MMP-1 secretion through a PGE2-dependent mechanism without affecting M.tb replication(130). PAS therefore may

represent the first example of a host-directed therapy used to treat TB. More recently, a Taiwanese population-based study of patients with drug-sensitive TB found that use of antiplatelet drugs was associated with significantly improved overall survival and a lower 12-month mortality rate, as well as lower rates of smear positivity and fewer cavities. Benefits were greater with aspirin compared to non-aspirin antiplatelet agents such as clopidogrel(154). In a randomised controlled trial, giving 100mg aspirin to diabetic patients with pulmonary TB resulted in decreased secretion of inflammatory mediators including ESR and CRP, a higher sputum-negative conversion rate (87% versus 54%), and fewer and smaller cavities following treatment, compared to placebo-treated control patients(155). In TB meningitis, both inflammation and thrombosis are associated with higher mortality and complications including stroke in survivors; randomised controlled trials of aspirin have shown benefits in morbidity and mortality(156, 157). Further studies are currently underway to evaluate NSAIDS including meloxicam and ibuprofen as adjuncts to standard TB treatment regimens(158-160).

Drugs blocking other platelet signalling pathways are potentially important in the management of TB. ADP is the endogenous ligand for $P2Y_{12}$ and $P2Y_{13}$ receptors, which are implicated in platelet aggregation. ADP induces MCP-1 expression to enhance macrophage migration, and $P2Y_{13}$ expression is increased in TB patients(161). Ticagrelor and clopidogrel, both $P2Y_{12}$ inhibitors, given to healthy volunteers significantly reduced inflammatory and prothrombotic mechanisms including PMA formation and pro-inflammatory cytokine release following endotoxin challenge(162). In a double-blind placebo-controlled study a single dose of oral ticagrelor reduced PMA formation in healthy volunteers, and this was associated with an increase in pro-inflammatory cytokines in blood exposed to the TLR2 ligand Pam3CSK4 and a decrease in blood exposed to TLR4 ligand LPS, suggesting that platelets may differentially modulate cytokine responses depending upon the receptors involved(163).

1.5 Conclusions and aims of this study

The data above provide evidence that platelets are a key component of the innate immune system, and likely to be important in the response to tuberculosis. Both observational and experimental data show that the administration of anti-platelet agents in patients with TB may be effective at limiting disease manifestations and improving long-term outcomes in patients who

are successfully treated. However, much remains to be understood about the exact mechanisms of platelet engagement with mycobacteria and with other cells in the orchestration of the complex immune response to M.tb.

Hypothesis: Platelets regulate the innate immune response to TB.

Objective 1: To investigate the mechanisms by which platelets upregulate M.tb-driven monocyte activation in a cellular model. This was investigated using an *in vitro* cell culture model. Signalling pathways known to be important in TB were interrogated using specific inhibitors. The contribution of platelets and their secreted products to the activation of M.tb-infected monocytes was investigated.

Objective 2: **To investigate whether platelet activation and activity are increased in patients with pulmonary TB.** A prospective clinical study was conducted. Platelet activity was evaluated in patients with pulmonary TB compared to healthy controls and to respiratory symptomatic controls. This was done using light transmission aggregometry, flow cytometry, and measurement of plasma concentrations of soluble mediators using Luminex.

Objective 3: To determine whether platelets manifest a unique phenotype in M.tb compared to other pulmonary infections. This was evaluated first by the incorporation of respiratory symptomatic controls into the clinical study design, and also by comparing findings in TB patients with inflammatory responses seen in patients with COVID-19.

1.5.1 Experimental approach

The first aspect of this study was to evaluate whether any direct effect of M.tb on platelet activity could be demonstrated, using bacterial lipopolysaccharide (LPS) as a control. Next, the effect of the presence of platelets on M.tb-driven monocyte activation was investigated. A platelet-monocyte co-culture model was developed, and after confirmation that platelets enhance M.tb-driven monocyte activation, the model was manipulated using specific inhibitors to evaluate which signalling pathways were important in this process. Platelets were found to enhance well

established mechanisms of M.tb-associated monocyte activation including via the PI3 Kinase and MAP-Kinase pathways. Therefore, the effect of contact-dependent and -independent interactions between monocytes and platelets were investigated in this model. Finally, a clinical study was set up to investigate whether evidence of differential platelet activity could be identified in patients with pulmonary tuberculosis.

The information presented in this thesis and in planned future work will facilitate the identification of specific targets for therapeutic intervention, bringing us closer to the eventual goal of interruption of harmful tissue destructive processes whilst preserving, or even enhancing, the immune system's anti-infective properties.

Chapter 2 Materials and Methods

2.1 M.tb culture

All work involving M.tb was carried out in a Category 3 laboratory following standard operating procedures. A stock of *Mycobacterium tuberculosis* H37Rv Pasteur (M.tb) was maintained stored at -80 degrees in 30-50% glycerol. A working stock was prepared by defrosting an aliquot and immediate centrifugation and resuspension of the bacterial pellet in fresh media. The bacteria were grown in Middlebrook 7H9 medium supplemented with 0.2% glycerol, 0.02% Tween 80, and 10% OADC enrichment medium (BD Diagnostics, Oxford, UK). Volumes of approximately 2ml were incubated at 37°C with agitation at 120 rotations per minute (RPM). Sub-culture was performed weekly, when the optical density (O.D.), which was measured with a Biowave cell density meter (WPA, Cambridge, UK), reached approximately 1.0. For monocyte culture infections, M.tb was used at an O.D. of 0.6, representing mid-log growth phase, at pre-determined volumes to achieve a final multiplicity of infection (MOI) of 1.

2.2 Preparation of soluble M.tb-secreted antigens

To obtain soluble M.tb-secreted antigens, M.tb at an O.D. of 0.6 were transferred to an Eppendorf and centrifuged at 12,000 x *g* for 2 minutes. The supernatant was removed, leaving the pelleted M.tb undisturbed, and added to a 0.22µm Durapore PVDF centrifugal filter unit (Merck Millipore, UK) and centrifuged at 12,000 x *g* for 2 minutes. This process removed any remaining M.tb from the media which contained soluble factors secreted by the bacteria. This enabled the now sterile preparation to be removed from the Category 3 suite. M.tb-secreted antigens were prepared in large batches, aliquoted, and stored at -20°C until further use in order to ensure consistency across experiments.

2.3 Platelet isolation

Whole blood was collected in 10% sodium citrate (BD Vacutainer® Sodium Citrate tubes) using a vacutainer system. The first tube was partially filled and discarded to avoid activation of platelets by venepuncture and to ensure maximal heterogeneity between the tubes; although this is no longer recommended practice(164), it is still considered advisable for certain investigations involving platelets(165). Blood was poured into 15ml Falcons and spun for 15 minutes at 200 x *g* at room temperature with slow acceleration and deceleration. Platelet rich plasma (PRP) was gently removed with a Pasteur pipette avoiding the Buffy coat layer. 1mM Prostaglandin E1 (PGE1) was added at a dilution of 1 in 500 (i.e. final concentration of 2µM), and the PRP was centrifuged for 15 minutes at 1200 x *g* at room temperature. The platelet-poor plasma (PPP) was discarded and the pellet resuspended in 10mls of platelet wash buffer and rested in an incubator at 37°C. Platelet wash buffer comprised HEPES (10mM), glucose (5mM), KCl (5mM), MgSO4 (1mM), KH2PO4 (1mM), and NaCl (145mM) adjusted to a pH of 7.4 and then filter sterilised with a 0.2µm filter.

To perform a cell count, an aliquot of platelets was diluted 1 in 100 and 20µl added to a Neubauer haemocytometer chamber incubated for 3 minutes after which the cells were counted. After the platelets had been rested for approximately 30 minutes, 1mM PGE1 was added at a dilution of 1 in 500 and the platelets were centrifuged for 10 minutes at 1200 x *g* at room temperature. The resulting pellet was resuspended to the desired concentration in the appropriate media and used immediately. Staining with Trypan blue confirmed that >95% of platelets isolated using this method are viable by visual estimation.

2.4 Preparation of platelet releasate

Platelets were isolated as described above. They were suspended at a concentration of $2.5x10^8$ cells/ml and incubated at room temperature with platelet agonists at the desired concentration for 15 minutes. The platelet suspensions were then centrifuged at 12,000 x *g* for 1 minute to pellet the cells, then the supernatant transferred to a 0.22µm Durapore PVDF centrifugal filter unit (Merck Millipore, UK) and centrifuged at 12,000 x *g* for 1 minute to remove any residual platelets. Supernatants were then frozen at -20°C if not being used immediately.

2.5 Monocyte isolation

Monocytes were isolated through density centrifugation and adherence purification. Whole blood was collected in lithium heparin (BD Vacutainer® lithium heparin tubes) using a vacutainer system. This was diluted 2:1 with HBSS then gently layered onto Histopaque in 50ml Falcon tubes and spun at 500 x *g* at room temperature for 30 minutes with the brake off. The cell layer was removed into a separate Falcon tube, topped up to 50ml with HBSS, and washed three times at 300 x *g* for 5 minutes with the brake on. After the third wash a cell count was performed, and the pellet was resuspended in a final volume of DMEM at a concentration of 5×10^5 cells/ml. Cells were plated in a 24- or 12-well plate at 2.5×10^5 cells/cm^2. The plate was incubated at 37°C, 5% CO_2 for 1 hour, after which the wells were washed 3 times with HBSS to remove non-adherent cells, then DMEM supplemented with 10% fetal calf serum (FCS) and 10µg/ml ampicillin was added.

2.6 Platelet-monocyte co-culture

Autologous monocytes and platelets were isolated as described above from whole blood taken from the same donor. Platelets were resuspended in DMEM supplemented with 10% FCS and 10µg/ml ampicillin to the appropriate concentration and added to the monocytes. Unless otherwise specified, platelets were added at a ratio of 25:1. The final volume in the well was 400µl for a 24 well plate or 760µl for a 12 well plate. After 24 hours, cell supernatants and/or cell lysates were collected and stored at -20°C or -80°C respectively.

2.7 M.tb infection of platelet-monocyte co-culture model

Monocytes were infected with *Mycobacterium tuberculosis* at an O.D. of 0.60, representing the mid-log growth phase, or an equal volume of control 7H9 media. Infection was performed at a multiplicity of infection (MOI) of 1, which corresponds to $1 \times 10^8 – 2 \times 10^8$ colony forming units (CFU)/ml.

2.8 Sterilisation of cell culture supernatants

M.tb-infected cell culture supernatants were transferred to 0.22µm Durapore PVDF centrifugal filter units (Merck Millipore, UK) and centrifuged at 12,000 x *g* for 1-3 minutes, then removed from the Category 3 suite and stored at -20°C until further use. This technique has been validated as a reliable method of removal of M.tb without binding MMPs(166).

2.9 Chemical inhibition and recombinant proteins

A list of inhibitors is supplied in Table 1.

Table 1 Chemical inhibitors and recombinant proteins used in co-culture experiments

Reagent	Target action	Company supplier	Catalogue number	Working concentration
LY294002	Pi3-kinase p110 subunit inhibition	Sigma Aldrich, UK	440202	1-10 µM
SB203580	Selective p38 MAPK inhibition	Enzo Life Sciences, Exeter, UK	BML-EI286	10 µM
PD98059	Inhibits MEK/ERK pathway by preventing activation of MEK1 and MEK2 by upstream kinases.	Calbiochem, Merck Millipore, Watford, UK	513000	10 µM
Rapamycin	mTORC1 and mTORC2 inhibition	Calbiochem, Merck Millipore, Watford, UK	553210	0.5-5 µM
Recombinant P-selectin	Binds to PSGL-1 receptor	Bio-Techne	ADP3	1-2 µg/ml
Anti-P-selectin antibody (BBA30)	Binds to Human P-Selectin/CD62P. Monoclonal Mouse IgG1 Clone #9E1	R&D Systems, UK	BBA30	10 µg/ml
Anti-P-selectin antibody (Psel.KO2.12)	Binds to Human P-Selectin/CD62P. Monoclonal mouse IgG1, clone #Psel.KO2.12	eBioscience™	16-0622-81	10 µg/ml
Anti-PSGL-1 antibody	Ligates P-Selectin Glycoprotein Ligand-1 (PSGL-1) receptor	Sigma-Aldrich	MAB4092	10 µg/ml

For reagents targeting monocyte signalling pathways, monocytes were incubated with the corresponding reagent for 1 hour prior to addition of platelets and/or infection with *M.tb.* For reagents targeting platelet pathways, the platelets were incubated with the corresponding reagent for 15 minutes (unless otherwise specified) prior to incorporation with monocytes followed by infection with *M.tb*. Timings of monocyte and platelet extraction were adjusted accordingly to ensure both cell types were ready for use simultaneously.

2.10 Enzyme-linked immunosorbent assay (ELISA)

Concentrations of the required marker were measured in cell supernatants using the Duoset ELISA Development System (R&D Systems, Abingdon, UK) according to the manufacturer's protocol. Briefly, transparent flat-bottomed 96-well plates (Costar, Sigma-Aldrich, UK) were coated with 100µl of capture antibody in PBS overnight at room temperature, then washed 3 times with wash buffer (PBS/0.05% v/v Tween). The plates were then blocked with reagent diluent (PBS/1% w/v BSA) for 1 hour at room temperature, then washed 3 times. Standards in serial 1 in 2 dilutions were loaded in duplicate, and samples loaded at dilutions appropriate for the assay. The plates were incubated for 2 hours at room temperature, then washed 3 times. 100µl of detection antibody was added per well, the plate was incubated for 2 hours at room temperature. After washing, 100µl streptavidin-HRP was added to each well and the plate was incubated in the dark at room temperature for 20 minutes. The plate was washed one final time, then 100µl tetramethylbenzidine (TMB, Sigma-Aldrich, Poole, UK) substrate solution was added to each well and the plate incubated in the dark for up to 20 minutes. Once a satisfactory colour change had taken place, the reaction was terminated with 50µl of 2M sulphuric acid. The plate was read on a Tecan Infinite® 200 PRO Life Sciences microplate reader at an absorbance of 450nm with a reference wavelength of 560nm. The results were downloaded on Excel and analysed using GraphPad PRISM v9.1.2 software.

2.11 Luminex bead array

Samples were processed using custom designed human premixed muti-analyte kit Luminex Discovery assays from BioTechne. These highly sensitive assays use magnetic microbeads coated with target analyte antibodies labelled with fluorophores, and enable measurement of multiple analytes from a single small volume of sample. Samples were processed following the manufacturer's instructions with minor modifications that reduce the proportion of microbeads in the assay and have been found by our group to obtain comparable results(167).

Thawed samples were centrifuged at 16,000 x *g* for 4 minutes to remove any residue, then diluted in calibrator diluent RD6-52 at the recommended dilution factors. Serial 1 in 3 dilutions of standards were prepared in calibrator diluent RD6-52. 50µl of standards and samples were loaded in duplicate to a 96 well plate, and 50µl of resuspended microparticle cocktail was added to each well. The plates were covered with a foil plate sealer and incubated for 2 hours at room temperature on a horizontal orbital microplate shaker set at 800 rpm. The plates were then washed three times with wash buffer using a magnetic device to keep the microbeads in the wells, then 50µl diluted Biotin-antibody cocktail added to each well. The plates were covered with a foil sealer and incubated for 1h at room temperature on the shaker. The plates were washed three times, then 50µl diluted Streptavidin-PE was added to each well and the plates were incubated for 30 mins at room temperature on the shaker before being washed again. The microparticles were resuspended by adding 100µl wash buffer to each well, incubated with shaking for 2 minutes, and read using a Bio-Plex 200 analyser (Bio-Rad™ Laboratories, Inc.).

Results were downloaded in Excel format. Concentrations were interpolated from standards fitted with a five parameter logistic regression (5PL) curve. Samples with a coefficient of variation (%CV) across duplicates of over 30% were excluded from analysis. Results that fell below the limit of detection were replaced with a value equal to half of the lower limit of detection for that analyte, and samples with results that were above the limit of detection were re-run at a higher dilution factor until the value was within range.

2.12 RNA extraction, cDNA synthesis, and RT-PCR

Immediately following collection of supernatants, cells were washed with sterile PBS and lysed using Tri-Reagent® RNA isolation reagent (Sigma-Aldrich, Poole, UK). Cell lysates were stored at -80°C until further use.

RNA extraction was performed using the Direct-zol™ RNA Miniprep Kit (ZymoResearch, Irvine, California, USA) according to the manufacturer's instructions. Cell lysates were defrosted on ice, then mixed with equal volumes of 100% ethanol and vortexed. The mixture was inserted into ZymoSpin™ columns and centrifuged for 1 minute at 12,000 x *g.* The liquid from the collection tube was discarded, 400µl Direct-zol RNA PreWash added to the column which was centrifuged for 1 minute at 12,000 x *g.* This step was repeated, then 700µl RNA Wash Buffer added to the column and centrifuged twice to ensure dryness of the membrane. The spin columns were then inserted into pre-labelled clean eppendorfs, 30µl DNase/RNase free water added, and centrifuged for 1 minute at 12,000 x *g*. The amount and purity of RNA was quantified by spectrophotometry (Nanodrop ND 1000, ThermoFisher Scientific, UK). The samples were stored at -80°C if not proceeding to cDNA synthesis immediately.

cDNA was synthesized from RNA using the Quantitect® Reverse Transcription Kit (Qiagen, Manchester, UK). Samples were defrosted on ice. RNA was diluted up to 12µl with DNase/RNase-free water and 2µl of wipeout buffer was added, the samples mixed then placed in a heat block at 42°C for 2 minutes. They were then returned to the ice bucket and 6µl reverse transcription mastermix (comprising 1µl Quantiscript® reverse transcriptase, 1µl RT primer mix, and 4 µl Quantiscript® RT buffer 5x per sample) was added. Samples were heated at 42°C for 15 minutes to facilitate primer annealing and strand extension then at 95°C for 3 minutes to stop the reaction, after which they were immediately returned to ice and stored at -20°C if not proceeding to RT-PCR straight away.

To perform real-time polymerase chain reaction (RT-PCR), synthesized cDNA was diluted 1:25 to a total volume of 200 µl in nuclease-free water. PCR master mix was made up comprising Brilliant II (Agilent Technologies, USA) and the primer and probes for the gene of interest and housekeeping gene (18S rRNA). 15 µl mastermix and 10µl samples or standards prepared in serial 1:10 dilutions were added to a 96 well plate (ThermoFisher Scientific, UK) which was carefully covered with plate sealant and loaded onto a CFX Connect Real-Time System Instrument (Bio-Rad

Laboratories, UK). The RT-PCR thermal profile was 95°C for 10 minutes followed by 40 cycles of 95°C for 30 seconds then 60°C for 1 minute.

2.13 Platelet light transmission aggregometry

Platelet aggregometry has conventionally been performed using cuvette-based systems, regarded as the gold standard for the assessment of platelet function(168). However, this approach is cumbersome and limited by the rapid deterioration of platelet functions *ex vivo*. Thus, newer methods have been developed using multiple recording wells to enable the measurement of a range of responses simultaneously(169). The protocol below uses a 96 well plate to assess platelet responses to three different agonists over time.

Whole blood was collected in blue-top citrate vacutainer tubes. 1ml collected into the first tube was discarded to avoid inclusion of platelets activated by venepuncture. The blood was decanted into two 15ml Falcon tubes and centrifuged for 15 mins at 150 x *g* at room temperature, with slow acceleration and deceleration (centrifuge settings 3 and 1 respectively). Platelet rich plasma (PRP) was then transferred using a Pasteur pipette to a new 15ml Falcon tube, taking care to avoid disrupting the cell layer, and this was inverted gently four times. PRP was incubated in a ratio of 2:1 with M.tb-secreted antigen preparation (see methods section 2.2), bacterial lipopolysaccharide (LPS, 0111:B4, from Sigma Aldrich #L2630) diluted in 7H9 to give a final concentration of 100 µg/ml, or 7H9 control for 30 minutes at room temperature. 90µl of the sample was then added to a 96 well plate that had been pre-loaded with serial dilutions of platelet agonists ADP, TRAP-6, and collagen using a multichannel pipette and a reverse pipetting technique to corresponding wells as quickly as possible whilst avoiding the formation of bubbles. Control wells containing PRP and PPP (platelet poor plasma, prepared by centrifugation of 1ml PRP at max speed and separation of the plasma) were included. The plate was immediately inserted into a TECAN Sunrise™ plate reader and absorbance read at 595nm every 20 seconds at 37°C and with shaking for a total of 40 cycles. Data were downloaded in Excel format.

2.14 Flow cytometry

Whole blood was collected in 10% sodium citrate (BD Vacutainer® Sodium Citrate tubes) using a vacutainer system. The first tube was partially filled and discarded to avoid activation of platelets by venepuncture, and the sample was processed immediately to minimize post-venepuncture phenotypic changes(170).

25µl whole blood was incubated with binding buffer (1% w/v BSA), antibody mastermix, and any stimulants, to a final volume of 100µl. The antibodies used are listed in Table 2, and the concentrations of each were selected following a process of antibody titration (see Results section 3.1.3). The samples were incubated for 20 minutes in the dark and at room temperature. 500µl 1x eBioScience™ 1-step fix/lysis solution (ThermoFisher Scientific, UK) was then added and the samples mixed by pipetting. The samples were incubated for a further 15 minutes in the dark, and then 1ml PBS was added to terminate any reactions. Samples were stored at 4°C until analysis, which was performed ideally the same day, or within a maximum of 72 hours. Analysis was performed on a BD FACSCalibur™ flow cytometer (BD Biosciences) in Peru or a CytoFLEX S analyser (Beckman Coulter Life Sciences, UK) in the UK. Data were analysed using FlowJo™ v10 software.

Table 2 Antibodies used for flow cytometric analysis

Antibody	Clone	Isotype	Catalogue number	Manufacturer
CD14-PerCP	MφP9	Mouse BALB/c IgG2b, κ	340585	BD Pharmingen™
CD42b-PE	HIP1	Mouse IgG1, κ	555473	BD Pharmingen™
CD62P-APC	AK-4	Mouse BALB/c IgG1, κ	550888	BD Pharmingen™
PAC-1-FITC	PAC-1	Mouse BALB/c IgM, κ	340507	BD Pharmingen™

2.15 Clinical studies

To assess platelet activity in patients with TB, a prospective clinical study was performed in Peru. Details of the study design and methods are described in Chapter 4.

A separate prospective study of patients with COVID-19 was performed, the methods of which can be found in Chapter 5.

2.16 Statistics

Data were mainly attained in Excel format and analysed using GraphPad PRISM v9.1.2 or *R* statistical software package version 4.0.5. Numerical values were tested for a normal distribution using the Pearson-D'Agostino test. PCR data were analysed in Excel using the Delta-Delta CT method to generate fold change. Continuous variables were compared using a *t*-test (parametric distribution) or a Mann-Whitney U test (non-parametric distribution), and multiple observations were compared using a one- or two- way ANOVA with Šídák's correction for multiple comparisons, or with a Kruskall-Wallis test with Dunn's *post hoc* correction for multiple comparisons. Correlations were assessed using the Spearman's test.

Specific approaches towards statistical analysis are described in more detail in the relevant chapters.

Chapter 3 Platelets regulate monocyte responses to M.tb in a cellular model of infection

3.1 Investigating the effect of M.tb on platelet activation and functional responses

As discussed in the introduction, platelets exert direct anti-infective functions that are largely underappreciated. This begins with the detection of pathogens, leading to platelet activation, the recruitment and mobilisation of immune effector cells, and ultimately control of the pathogen. Platelets detect pathogens via a range of receptors, including Toll-like receptors (TLR) and C-type lectin receptors (CLR), which recognize pathogen-associated molecular patterns (PAMPs) including bacterial cell wall components (171, 172). For example, the Gram-positive bacterium *Streptococcus pneumoniae* causes platelet aggregation following interactions between bacterial peptidoglycan and TLR-2 and αIIbβ3 receptors(173). Lipopolysaccharide (LPS), a major component of the cell wall of many gram-negative bacteria, binds to platelet TLR-4.

The effect of LPS on platelets has been widely studied and is well characterised in the literature(174-176). Following binding to TLR-4, LPS induces rapid secretion of soluble mediators, potentiates platelet aggregation initiated by platelet agonists, even at sub-threshold agonist concentrations(177), and enhances platelet-leukocyte aggregation enabling bacterial trapping through the production of neutrophil extracellular traps (NETs)(79, 178). LPS has also been shown to lead to increased expression of platelet P-selectin(179), and P-selectin and TLR-4 co-localise on the surface of thrombin-activated platelets(180). The secretory profile is known to include IL-1-β, TNF-α, and sCD40L(181), and moreover different LPS moieties are known to lead to differential patterns of cytokine secretion(73, 75, 76, 174, 182-184).

M.tb signalling in innate immune cells is known to occur through toll-like receptors(185), therefore it is plausible that M.tb may also activate platelets through this mechanism. However, a literature search did not yield any data in this area. Therefore, LPS was utilised to first establish reliable methods of demonstrating platelet activation *in vitro*, and subsequently to use as a positive control in experiments involving M.tb.

3.1.1 The effect of LPS on platelet activation and functional responses

To verify that platelet responses to LPS could be demonstrated, platelets were isolated (see methods section 2.3) then incubated with or without 100µg/ml LPS in the presence of increasing concentrations of thrombin for 30 minutes. Supernatants were then collected and stored at -20°C. Concentrations of platelet factor 4 (PF4), one of the predominant platelet secretory components, were later measured by ELISA.

As shown in Figure 3.1, platelet PF4 secretion increased in the presence of LPS, and this was augmented by the addition of thrombin. A very high concentration of 100µg/ml was selected for this experiment in order to determine whether a response to LPS could be seen. A dose-response to LPS was also subsequently demonstrated (data not shown).

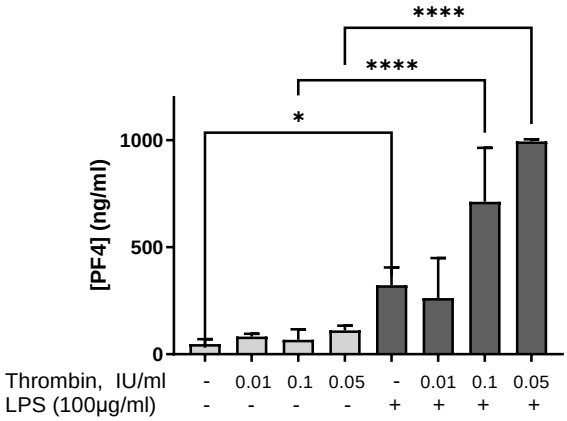

Figure 3.1 Secretion of platelet factor 4 (PF4) by platelets incubated in the presence or absence of thrombin and lipopolysaccharide (LPS).

LPS increased PF4 secretion from thrombin-stimulated platelets in a dose dependent manner. Figure representative of three separate experiments, each carried out in triplicate. Data compared with one-way ANOVA with Šídák's correction for multiple comparisons; **p<0.01, ****p<0.0001.

To evaluate functional platelet aggregation in response to LPS, platelet rich plasma (PRP) was isolated from whole blood. This was incubated with 1µg/ml LPS, 10µg/ml LPS, 100µg/ml LPS, or phosphate buffered saline (PBS) control for 30 minutes before being added to a 96 well plate that

had been pre-prepared with serial dilutions of adenosine diphosphate (ADP), collagen, and thrombin receptor activator peptide 6 (TRAP-6). The plate was immediately inserted into a plate reader for kinetic analysis (see methods section 2.13).

Inclusion of three agonists enables the assessment of different mechanisms of platelet aggregation. ADP is considered a gentle platelet agonist. It acts on the G-protein coupled purinergic receptor $P2Y_{12}$ which inhibits adenylyl cyclase and cyclic AMP (cAMP) production and thereby mediates platelet aggregation. $P2Y_{12}$ is the target of antiplatelet drugs used in clinical practice to prevent clotting, including clopidogrel and ticagrelor. ADP is also released from platelet dense granules, leading to a gradual potentiation of its effect(186). Collagen is important to platelet adhesion and aggregation. It acts through GP1a/IIa ($\alpha_2\beta_1$ integrin) receptors, which are involved in adhesion, and GPVI receptors resulting in formation of thromboxane A_2 (TxA_2)(187). Thrombin is generally considered the most potent of the platelet activators, acting via platelet protease-activating receptor (PAR) -1 and PAR-4. However, its experimental use is complicated by the fact that in addition to activating platelets it is also involved in fibrinogen cleavage in the plasma leading to fibrin clot formation. Thrombin receptor activator peptide 6 (TRAP-6) is a six amino acid synthetic peptide that is analogous to the new amino acid terminus following cleavage of PAR-1 which acts as a tethered ligand. TRAP-6 mimics the effect of thrombin through the activation of PAR-1 but does not cleave fibrinogen, leading to a more specific receptor effect. Like thrombin, platelet stimulation with TRAP-6 requires a critical dose threshold to be met, upon which it elicits a very strong activation response(188).

Figure 3.2 shows an example of a real-time plot of platelet aggregation in response to increasing concentrations of ADP, in the presence of LPS; Figure 3.3 and Figure 3.4 show platelet aggregation in response to increasing concentrations of collagen or TRAP-6 respectively, also in the presence of LPS.

These graph series clearly demonstrate the different effects that each agonist has on the platelets: ADP-induced platelet aggregation commences immediately and steadily increases, with a plateauing occurring after around 100-300 seconds. Collagen gives a delayed initiation with a more erratic output. On microscopic observation of the wells following completion of the assay, clumps of platelets were visible that were not observed in wells stimulated with ADP or TRAP-6;

these clumps are responsible for the irregularity of light passing through the wells, giving rise to the jagged curves seen below. Platelet stimulation with TRAP-6 showed a rapid and intense response in wells that crossed a critical threshold for activation.

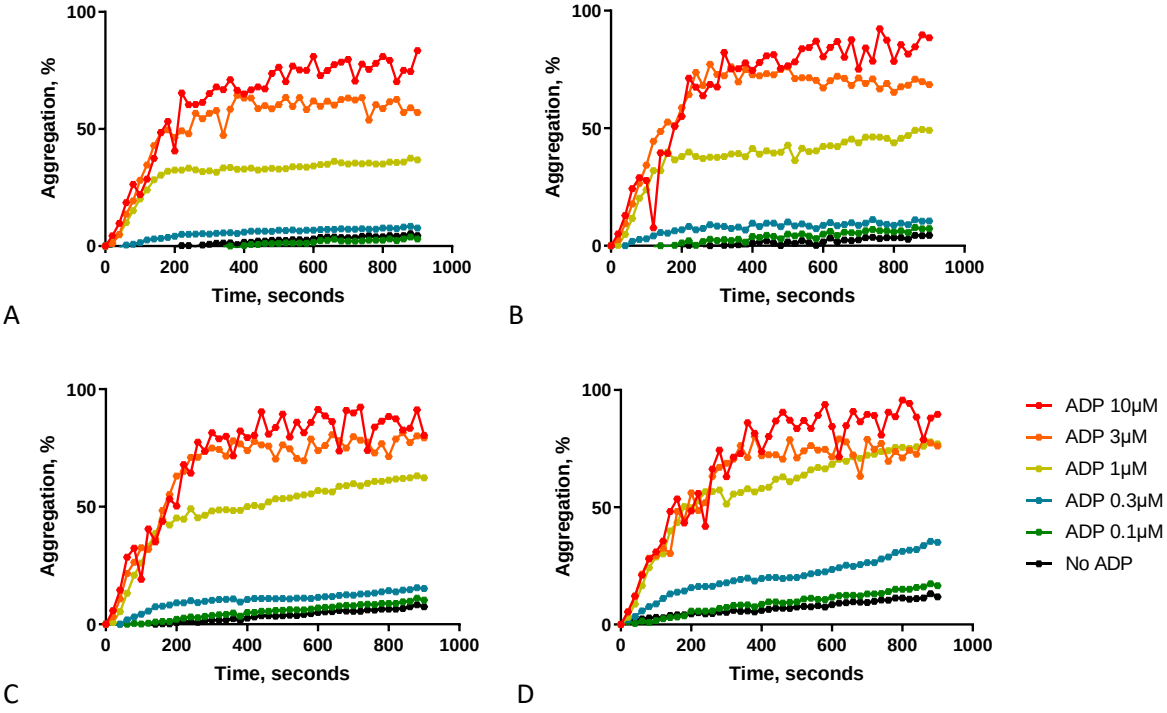

Figure 3.2 Platelet aggregation over time in response to increasing concentrations of adenosine diphosphate (ADP).

Experiment performed in the presence of (A) no LPS, (B) 1µg/ml LPS, (C) 10µg/ml LPS, (D) 100µg/ml LPS. Graphs show a characteristic smooth and gradual response to ADP, which is dose-responsive. This response is enhanced by increasing concentrations of LPS.

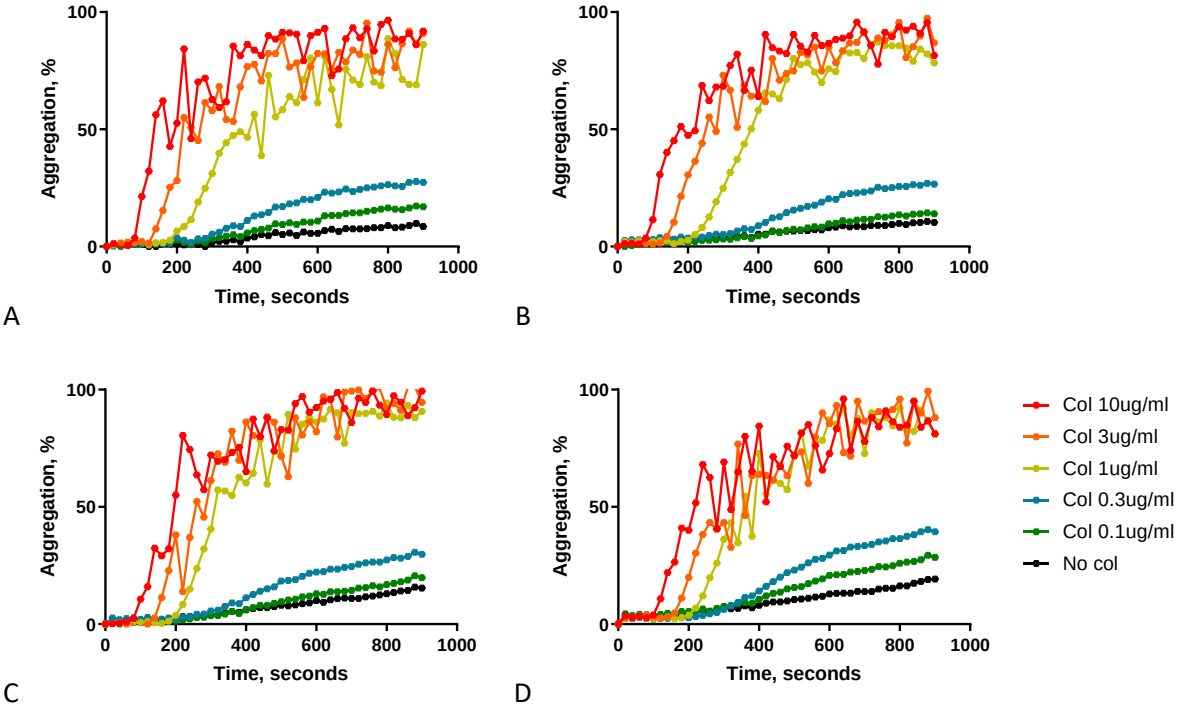

Figure 3.3 Platelet aggregation over time in response to increasing concentrations of collagen.

Experiment performed in the presence of (A) no LPS, (B) 1µg/ml LPS, (C) 10µg/ml LPS, (D) 100µg/ml LPS. Graphs show a characteristic erratic response, which is enhanced by increasing concentrations of LPS. Col = collagen.

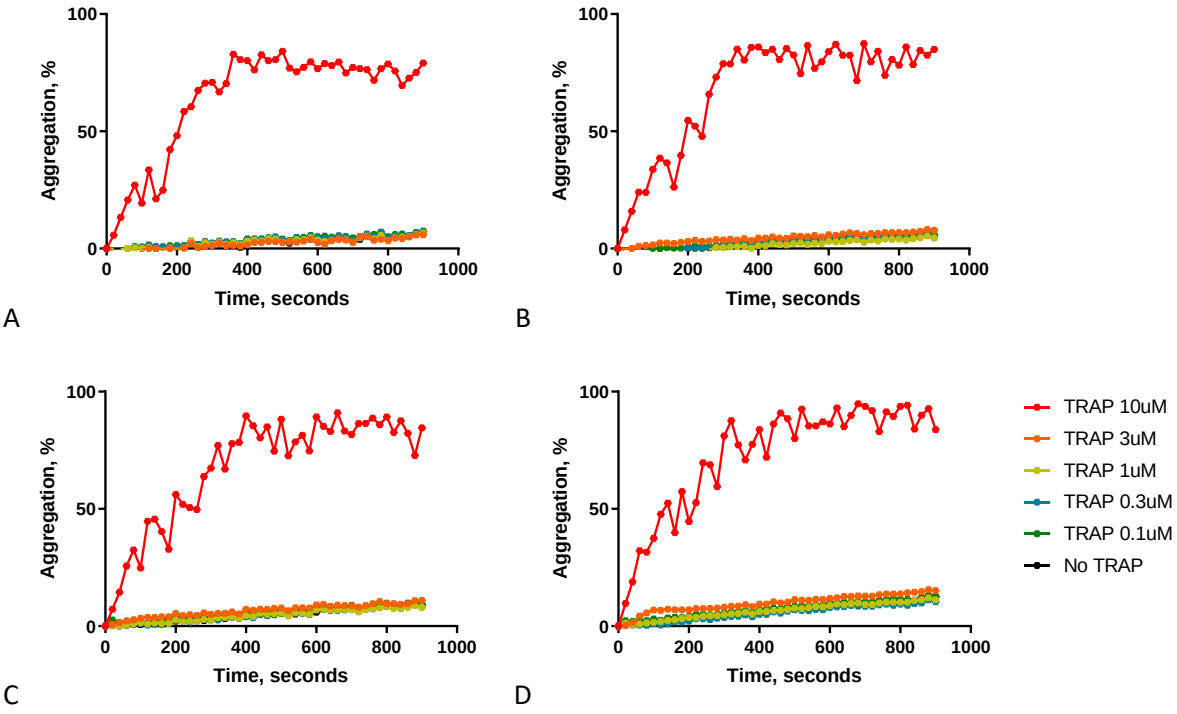

Figure 3.4 Platelet aggregation over time in response to increasing concentrations of thrombin receptor activator peptide 6 (TRAP-6).

Experiment performed in the presence of (A) no LPS, (B) 1µg/ml LPS, (C) 10µg/ml LPS, (D) 100µg/ml LPS. Graphs indicate an all-or-nothing response that is characteristic of platelet responses to TRAP-6.

The above graphs can more usefully be converted into a measure of maximal platelet aggregation, as presented in Figure 3.5. The addition of LPS augmented agonist-induced maximum aggregation in a dose-dependent manner (Figure 3.5 A); again, the difference in mechanisms of activation can be clearly visualised, with the smoothest and most gradual dose response seen in response to ADP, a similar but less clear picture seen in response to collagen, and a threshold response seen in response to TRAP-6. This effect was further enhanced by the pre-incubation of PRP with LPS prior to addition to agonists (Figure 3.5 B) and occurred even in the absence of stimulation of the platelet with any agonist (Figure 3.5 C-D).

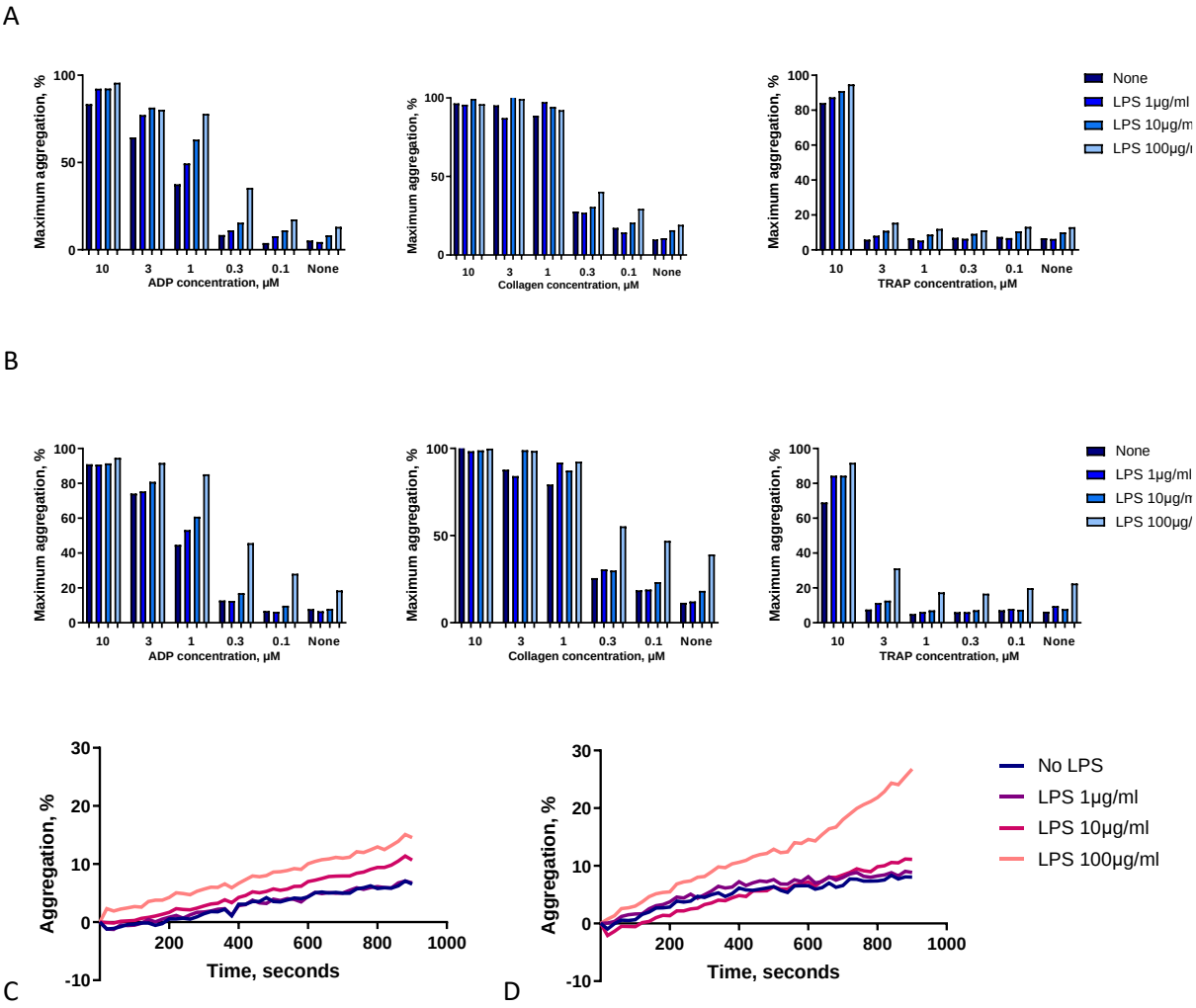

Figure 3.5 Maximal platelet aggregation in response to stimulation with ADP, Collagen, or TRAP-6.

Agonist-induced platelet aggregation is enhanced by LPS in a dose-dependent manner in response to all agonists (A). This is further potentiated by the incubation of platelets with LPS for 30 minutes prior to addition to the plate (B). Platelet aggregation in the presence of LPS occurs in a dose dependent manner even in the absence of any agonists (C) after immediate addition of PRP +/- LPS to plate pre-loaded with agonists or (D) after incubation of platelets with LPS for 30 minutes prior to addition to the plate. Graphs representative of three independent experiments.

3.1.2 The effect of M.tb on platelet activation and functional responses

Having established this methodology using LPS, these techniques were next applied to M.tb in order to investigate whether M.tb activates platelets, about which there are no published data in the international literature to date. High concentration LPS was included as a positive control against which responses observed to M.tb could be compared.

Platelets were isolated as described and suspended in platelet buffer at 1 x 10^8 cells/ml. They were then taken into the Category 3 laboratory. M.tb at an O.D. of approximately 0.6 was centrifuged at 11,000 rpm for 5 minutes. The supernatant was collected and sterile-filtered, and the pellets were resuspended in fresh 7H9 media. Platelets were incubated with washed M.tb, the filtered supernatant containing M.tb-secreted mediators, or 7H9 control, in the presence or absence of 0.1IU/ml thrombin. 1IU/ml thrombin was included as a positive control. After incubation for 30 minutes, the platelets were centrifuged at 4,000rpm for 1 minute to pellet the platelets then sterile-filtered. The supernatants were evaluated by ELISA.

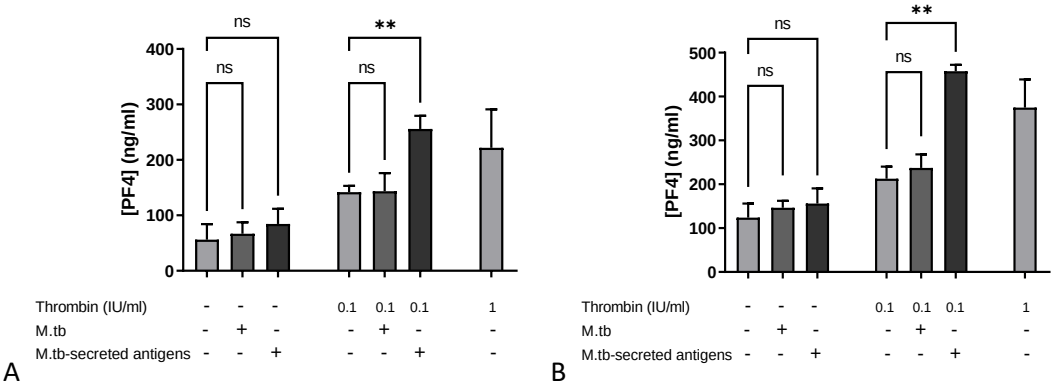

Figure 3.6 Secretion of platelet factor 4 (PF4) by platelets incubated with or without thrombin, washed M.tb, or M.tb-secreted antigens.

M.tb-secreted antigens, but not washed M.tb, significantly upregulated platelet PF4 secretion in the presence of thrombin after incubation for (A) 30 minutes or (B) 45 minutes. Data compared with one-way ANOVA with Šídák's correction for multiple comparisons. Representative of three separate experiments.

In the presence of thrombin, incubation of platelets for 30 minutes with washed M.tb did not affect PF4 secretion, however incubation with M.tb-secreted antigens significantly upregulated PF4 secretion compared to platelets incubated with 7H9 control (255.8 +/- 23.8 vs 141/8 +/- 11.4 ng/ml, p=0.0053). (Figure 3.6 A). A similar effect was observed after incubation for 45 minutes (Figure 3.6 B).

To further investigate platelet reactivity to M.tb-derived antigens, dilution of M.tb-secreted antigens in fresh 7H9 media were prepared at a ratio of 1 in 3, 2 in 3, and neat. Platelets were incubated with M.tb-secreted antigens at increasing concentrations for 30 minutes in the presence of 0.1IU/ml thrombin, before supernatants were sterile-filtered and PF4 and soluble CD40-ligand (sCD40-L) concentrations measured by ELISA.

Enhanced platelet secretion of both PF4 and sCD40L in response to M.tb-secreted antigens was found to occur in a dose-dependent manner (Figure 3.7).

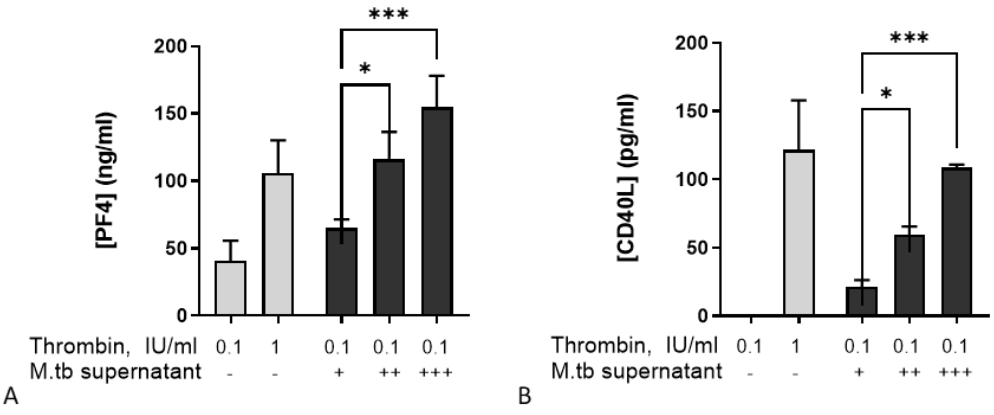

Figure 3.7 Platelet factor 4 (PF4) and soluble CD40 ligand (sCD40L) secretion by platelets after incubation with M.tb-secreted antigens and thrombin for 30 minutes.

Secretion of both PF4 (A) and sCD40L (B) increased in a dose-responsive manner in response to M.tb-secreted antigens. 1 IU/ml thrombin was included as a positive control. M.tb-secreted antigens used at preparations of a 1 in 3 dilution (+), 2 in 3 dilution (++), or neat (+++). Data compared with one-way ANOVA with Šídák's correction for multiple comparisons; *p<0.5, ***p<0.001. Graphs representative of two separate experiments.

Finally, the effect of M.tb-secreted antigens on functional aggregation responses in platelets was investigated. Our group does not have access to a plate reader capable of kinetic measurements within a Category 3 laboratory and thus platelet aggregometry performed with live, virulent M.tb is not possible in our laboratory. The establishment that M.tb-secreted antigens, rather than the M.tb themselves, lead to platelet activation enabled the subsequent investigation of M.tb on functional responses in platelets.

4mls platelet rich plasma (PRP) was incubated for 30 minutes with 2mls M.tb-secreted antigen preparation (see Section 2.2), 1ml M.tb-secreted antigen preparation and 1ml 7H9 control media, or LPS in 7H9 media at a final concentration of 100µg/ml as a positive control. The PRP was added to a 96 well plate pre-loaded with serial dilutions of platelet agonists adenosine diphosphate (ADP), collagen, or thrombin receptor activator protein 6 (TRAP-6), and read immediately.

M.tb-secreted antigen enhanced agonist-induced maximal platelet aggregation in a dose-dependent manner. This was comparable to aggregation enhancement by LPS. M.tb-secreted antigen enhanced platelet aggregation is seen most clearly in the presence of ADP (Figure 3.8 A) where high concentrations of M.tb secreted antigens increased platelet aggregation to a greater extent than 100µg/ml LPS, the positive control. A less marked effect was seen with collagen (Figure 3.8 B). In the presence of TRAP-6, M.tb-secreted antigens again enhanced maximal platelet aggregation; this was most evident at intermediate concentrations of TRAP-6, and this did not reach the level induced by LPS (Figure 3.8 C).

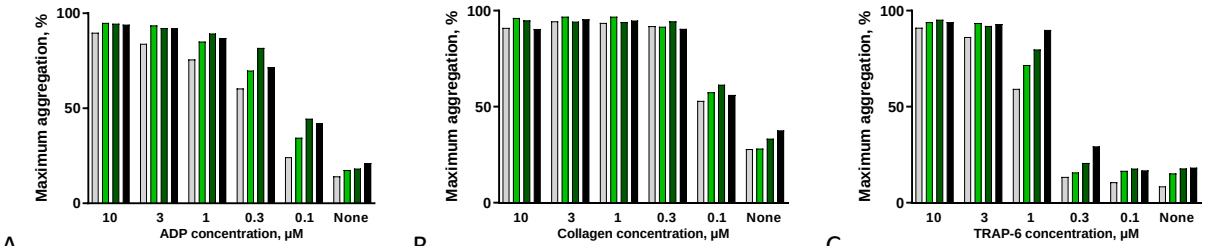

Figure 3.8 Maximal agonist-induced platelet aggregation following stimulation with LPS.

Maximal platelet aggregation in response to reducing concentrations of (A) ADP, (B) collagen, or (C) TRAP-6 following pre-incubation for 30 minutes with 7H9 control (grey bars), low (light green bars) or high (dark green bars) concentrations of M.tb-secreted antigens, or 100µg/ml LPS (black

bars). M.tb-secreted antigens enhanced agonist-induced platelet aggregation in a dose-dependent manner. This was comparable to enhancement induced by LPS. Graphs representative of four separate experiments.

Pooled data from maximal ADP-induced platelet aggregation in the presence of LPS M.tb secreted antigens are presented in Figure 3.9 A and B respectively. Aggregation induced by LPS was significantly greater only at an ADP concentration of 0.3µM (maximal aggregation of 56.6% vs 26.2% respectively, p=0.0084). M.tb-secreted antigens induced significantly higher maximal aggregation at 0.3µM ADP (maximal aggregation induced by low concentration M.tb-secreted antigens of 47.3% vs 26.2% by 7H9 control, p=0.0052; and by high concentration M.tb-secreted antigens 60.1% vs 26.2% by 7H9 control, p<0.0001) and also at 1µM ADP (maximal aggregation induced by high M.tb-secreted antigens 86.4% vs 67.7% by 7H9 control, p=0.024).

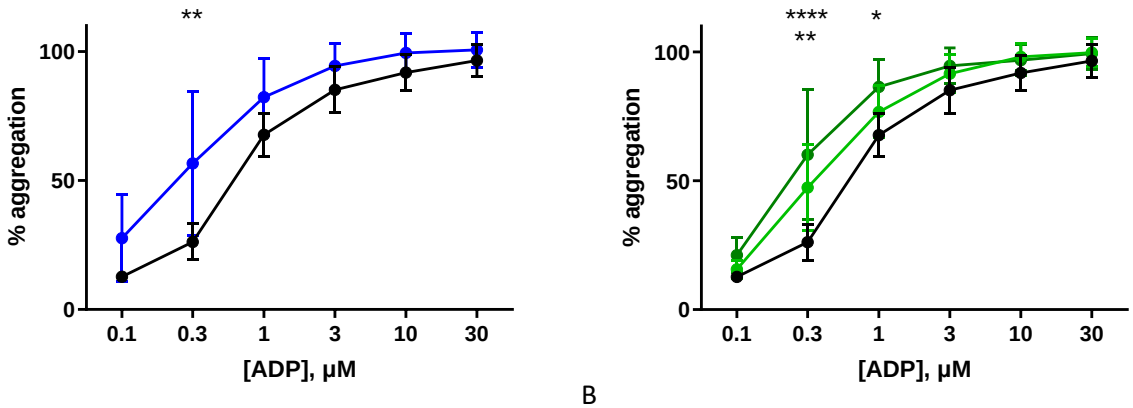

A B

Figure 3.9 Maximum platelet aggregation in response to ADP following stimulation with LPS and M.tb-secreted antigens.

(A) Maximal platelet aggregation was significantly greater in the presence of LPS (blue line) than 7H9 control (black line) at an ADP concentration of 0.3µl. (B) Maximal platelet aggregation was significantly greater in the presence of high concentration M.tb-secreted factors (dark green line) than 7H9 control (black line) at an ADP concentration of both 0.3µl and 1µl, and by low concentration M.tb-secreted antigens (light green line) at an ADP concentration of 0.3µl only. Graphs show pooled data from four independent experiments. Data shown are median, lines represent 95% confidence intervals; data compared using a two-way ANOVA with Šídák's correction for multiple comparisons.

There was no significant difference in maximal TRAP-6- or collagen-induced platelet aggregation in the presence of either LPS or M.tb-secreted antigens (data not shown).

In summary, these findings indicate that platelets can be functionally activated by M.tb-secreted antigens leading to both secretion of platelet factors and agonist-induced platelet aggregation. These responses are comparable to those observed in response to lipopolysaccharide (LPS). This is a novel finding, as platelet responses to M.tb have not been published in the literature. However, the concentrations of both LPS and M.tb-secreted antigens used in these experiments are not physiologically applicable, and whether this effect occurs *in vivo* remains unknown.

3.1.3 Optimisation of a flow cytometry protocol for the evaluation of platelet activation and platelet-leukocyte interactions in whole blood

3.1.3.1 Rationale

Traditional methods of evaluating platelet phenotype and function such as aggregometry and thromboelastography are limited by their complexity, requirement for large volumes of blood, and ability to only examine one aspect of platelet activity at a time. More recently, approaches employing whole blood flow cytometric analysis have been developed(170).

Flow cytometry is a tool that is able to rapidly analyse suspended single particles or cells. Basic light scatter enables quantification of particle size through forward scatter parameters (FSC) or internal complexity or granularity through 90 degree side-scatter (SSC). The incorporation of lasers enables the detection of cell surface markers or internal components using fluorescently conjugated antibodies or dyes. Flow cytometry can be applied to both pure cell populations and to mixed populations sourced from blood or tissues, and is used widely in a multitude of disciplines including immunology, infectious diseases, and cancer biology(189).

When applied specifically to platelets, flow cytometry is advantageous as it enables simultaneous and detailed evaluation of various aspects of platelet function including platelet phenotype, activation state, reactivity to agonists, and interaction with other cell types. Clinically it is used

for the evaluation of platelet reactivity in cardiovascular disease, pre-eclampsia, and the detection of inherited platelet disorders, amongst other uses(190-192). The incorporation of different platelet agonists allows each pathway to be investigated independently, and the utilisation of protocols involving minimal sample manipulation also allow avoidance of pre-activation and thus gives an accurate representation of true platelet phenotype. This can all be performed using as little as 5µl blood, and cell fixation allows storage of samples prior to evaluation on a flow cytometer, enabling batch analysis.

These characteristics made flow cytometric analysis an attractive tool for both *in vitro* exploration of platelet activity and function, and also desirable for future application to clinical studies. The flexibility of the technology enabled the optimization of the protocol detailed below. This was designed to include the minimum possible number of steps, specifically avoiding any centrifugation to prevent platelet activation or shearing through manipulation and to maximise reproducibility.

3.1.3.2 Fixation step

A combined fix-lysis buffer applied immediately after staining was found to give cleaner readouts compared with a dual strategy of either first lysing erythrocytes and then fixing the cells, or vice versa.

3.1.3.3 Determination of antibody concentrations for use in whole blood flow cytometry

Optimal antibody concentrations were determined through titration experiments performed for each antibody separately. The stain, or separation, index (SI), is the ratio of separation between the positive and negative population, divided by twice the standard deviation of the negative population(193). This was calculated as follows:

$$SI = \frac{(\text{Median positive} - \text{Median negative})}{(2 \times \text{Robust SD negative})}$$

A combination of the optimal stain index and ease of visualisation of distinct plots was used to select the antibody concentration.

3.1.3.4 Determining the lifespan of stained and fixed samples

Samples were prepared and stored at 5°C. Serial analysis demonstrated that samples were stable for 72 hours, after which cells began to degrade.

3.1.3.5 Choice of vacutainer for collection of whole blood for platelet evaluation

Platelets are widely understood to be activated when in contact with glass(194, 195) and for this reason many laboratory protocols used in the evaluation of platelets recommend avoiding glass tubes. To assess whether the material of the vacutainer tubes affected platelet activation, flow cytometric analysis was performed using blood obtained in both glass and plastic tubes.

Whole blood was taken in glass or plastic vacutainers containing 10% sodium citrate (both BD Vacutainer® sodium citrate tubes). A 500µl aliquot of whole blood was separated from each, and the remaining blood underwent platelet extraction (see section 2.3). Platelets were resuspended in platelet wash buffer to 1 x 10^8 cells/ml, and incubated with thrombin (none, 0.01U/ml, and 0.025U/ml) for 6 minutes. 1mM PGE1 was then added at a dilution of 1 in 500, and platelets were washed then resuspended in platelet buffer. Whole blood and washed platelets were then processed for flow cytometry (see methods section 2.14). Only anti-CD41b and anti-CD62P were used for this analysis. Platelets were identified according to characteristic FSC/SSC and CD41b positivity, and the percentage of platelets that expressed CD62P, and median fluorescence intensity (MFI) of CD62P on the platelet population, were calculated. No significant difference in platelet CD62P expression was observed in either whole blood or washed platelets collected in glass versus plastic tubes (Figure 3.10).

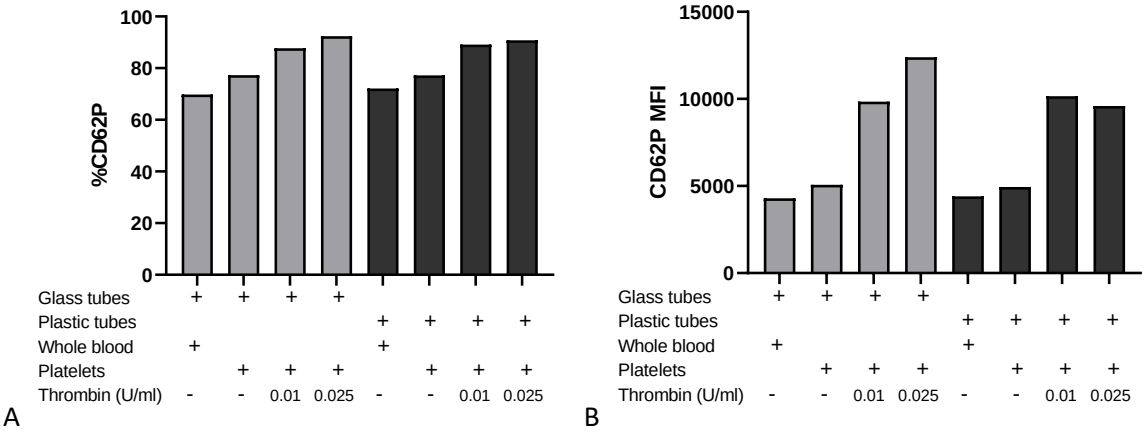

Figure 3.10 Platelet CD62P expression in thrombin-stimulated platelets isolated from whole blood taken in glass compared to plastic tubes.

There was no difference observed in the percentage of CD41+ events expressing CD62P (A) or in median fluorescence intensity (MFI) of CD62P among CD41+ events (B) in response to thrombin stimulation in whole blood isolated from glass compared to plastic tubes.

Platelet activation was also assessed by measurement of PF4 in response to thrombin stimulation. Whole blood was taken in glass or plastic vacutainers containing 10% sodium citrate (both BD Vacutainer® sodium citrate tubes). Platelets were isolated (see section 2.3), resuspended in platelet wash buffer to 1 x 10^8 cells/ml, and divided into aliquots which were incubated with thrombin (none, 0.01U/ml, 0.025U/ml, 0.05U/ml, and 0.1U/ml) for 6 minutes. Supernatants were collected and PF4 measured using a PF4 Duoset ELISA Development System (R&D Systems, Abingdon, UK) according to the manufacturer's protocol.

Platelets obtained from both glass and plastic vacutainers stimulated with 0.05 and 0.1U/ml thrombin were noted to have clotted during activation. Contrary to expectations based on the literature and common perception, PF4 concentration was higher in supernatants obtained from blood collected in plastic tubes stimulated with a thrombin concentration of 0.025U/ml and 0.05U/ml compared to blood collected in glass tubes ($p<0.0001$) (Figure 3.11).

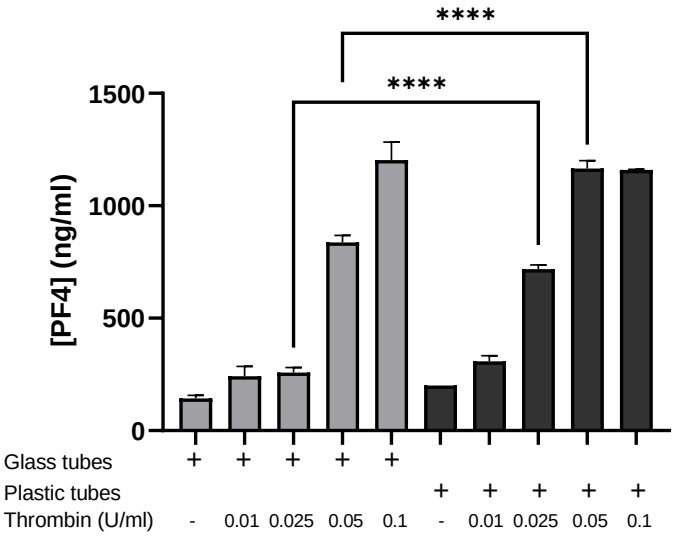

Figure 3.11 Platelet factor 4 (PF4) secretion from thrombin-stimulated platelets isolated from whole blood taken in glass or plastic tubes.

Experiment performed in duplicate. Data compared with one-way ANOVA with Šídák's correction for multiple comparisons; ****$p<0.0001$.

In summary: the material of the vacutainers used to obtain whole blood in citrate for flow cytometric analysis was not found to appreciably affect platelet activation. Glass tubes were used for all further experiments, as the volume contained in glass tubes (4.5ml, vs 2.7ml in plastic tubes) was more convenient as it required fewer tubes to be taken during venepuncture.

3.2 Investigating the effect of platelets on gene expression and secretion of matrix metalloproteinases by M.tb-stimulated monocytes

3.2.1 Optimisation of the monocyte-platelet co-culture model.

Previous published research that employed a monocyte-platelet co-culture model utilise a wide range of methodologies, including whether or not platelets are pre-activated with either thrombin(196, 197), other platelet agonists such as ADP(198), or unactivated(199, 200) prior to use. Human thrombin is the most common agent used. Generated as part of the coagulation cascade, thrombin interacts with protease-activated receptors to potently activate platelets. However, inclusion of thrombin in experimental models can be problematic for a number of reasons. The potency of the thrombin is highly batch-dependent; use of the same batch of thrombin for all experiments provides a degree of standardization, but may make the data difficult to reproduce. Platelets are highly reactive to thrombin with a tendency to clot, and as susceptibility to clotting varies between donors this can occur abruptly leading to inability to proceed with the experiment. Moreover, thrombin acts on components of the plasma including fibrinogen which may interfere with the assay. This can be avoided by using thrombin receptor activator peptide 6 (TRAP-6), a synthetic compound that selectively activates the protease-activated receptor-1 (PAR-1), the target of thrombin. Other agonists such as ADP or collagen may also have a more uniform effect on platelet activation than thrombin. However, stimulation of platelets with different agonists is known to lead to differential intracellular pathway activation and subsequently to different platelet phenotypes(201, 202). In addition, the monocyte and/or M.tb themselves may also activate platelets to a greater or lesser extent than the agonist. The impact of choice of platelet agonist on downstream effects in co-culture is unknown.

Our group has previously used thrombin-activated platelets in monocyte-platelet co-culture(103). In order to establish whether this affects downstream results, monocytes were cultured with platelets that were unstimulated or had been stimulated with a range of thrombin concentrations.

3.2.1.1 Platelets secrete platelet factor 4 in response to stimulation with thrombin in a concentration-dependent manner.

To first assess whether platelets are activated *in vitro* by thrombin, platelets were isolated from whole blood taken in 10% sodium citrate (BD Vacutainer® sodium citrate tubes) and resuspended in platelet wash buffer to 1 x 10^8 cells/ml (see methods section 2.3). The platelet suspension was then divided into aliquots which were incubated with increasing concentrations of thrombin for 6 minutes, then supernatants were collected. Platelet factor 4 (PF4) and soluble CD40 Ligand (sCD40L), both major components of platelet alpha granules, were measured using a Duoset ELISA Development System (R&D Systems, Abingdon, UK) according to the manufacturer's protocol.

Platelets secreted PF4 and sCD40L following stimulation with thrombin in a dose-dependent manner (Figure 3.12). This is consistent with co-secretion of these molecules during platelet degranulation.

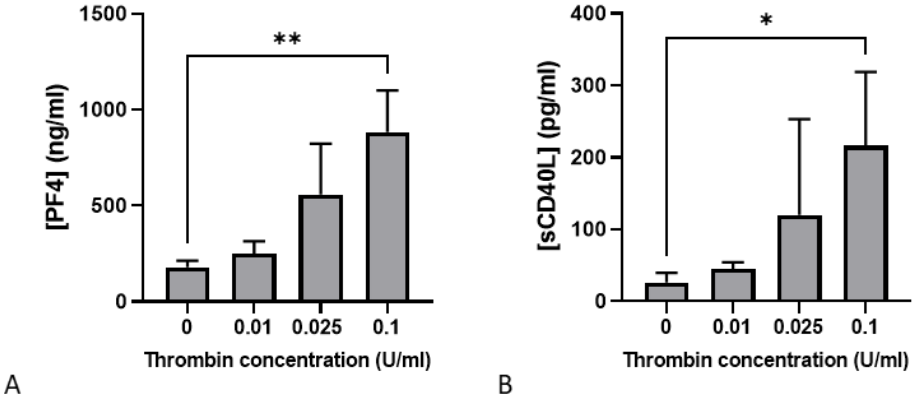

Figure 3.12 Platelet secretion of (A) platelet factor 4 (PF4) and (B) soluble CD40 ligand (sCD40L) increased in response to thrombin stimulation in a dose-dependent manner.

Bars represent mean +/-SD of three separate experiments, each performed in duplicate. Data compared with one-way ANOVA; *p<0.05, **p<0.001.

3.2.1.2 Thrombin activation of platelets prior to incorporation into a monocyte co-culture model does not affect monocyte MMP-1 or TIMP-1 secretion.

Prior to addition to monocytes, isolated platelets were divided into four aliquots and activated with 0.01U/ml, 0.025U/ml, and 0.1U/ml thrombin, or no thrombin as a control for 6 minutes at room temperature. 1mM Prostaglandin E1 (PGE1) was added at a dilution of 1 in 500, and the platelets were washed and suspended in DMEM supplemented with 10% FCS and 10µg/ml ampicillin. Suspended platelets or equal volumes of control media were added to the monocytes which were then infected with M.tb or an equal volume of 7H9 control media, and incubated for 24 hours at 37°C prior to collection of the supernatants.

Thrombin concentrations of 0.025U/ml or higher consistently caused platelets to clot, rendering them unusable for further experimentation. Therefore, platelets activated with 0.01U/ml thrombin were used in co-culture.

Platelet activation with thrombin prior to addition to monocytes did not affect monocyte secretion of either MMP-1 or TIMP-1, in the presence or absence of M.tb. (Figure 3.13).

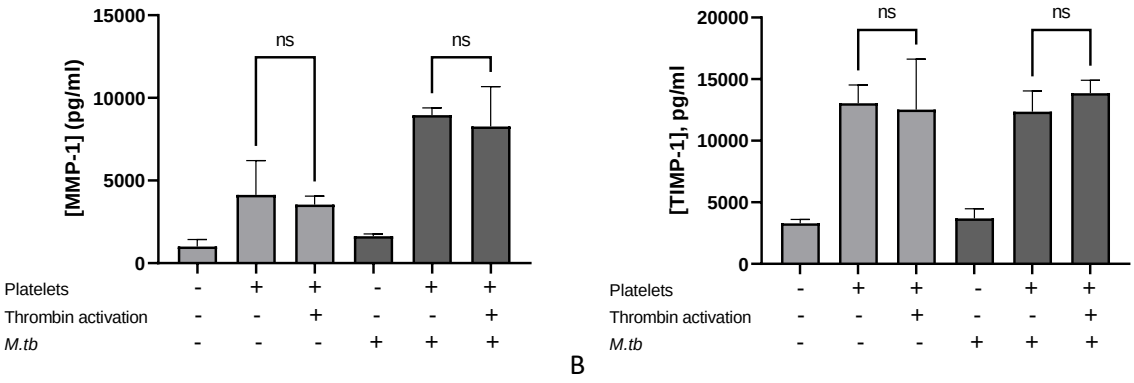

Figure 3.13 Secretion of (A) MMP-1 and (B) TIMP-1 from M.tb-infected and uninfected monocytes cultured in the presence of platelets was unaffected by prior platelet activation with thrombin.

(A) Bars represent mean +/-SD of two experiments, each performed in duplicate. (B) Bars represent mean +/-SD, single experiment performed in duplicate. Data compared with one-way ANOVA with Šídák's correction for multiple comparisons.

It is likely that any prior activation of platelets is relatively insignificant compared with activation following contact with monocytes; therefore, for subsequent experimentation, unactivated platelets were used for all co-culture experiments.

3.2.2 Co-culture with platelets increases MMP-1 secretion by M.tb-stimulated monocytes.

Monocytes and autologous platelets were isolated and co-cultured with/without M.tb for 24 hours prior to collection of supernatants for analysis by ELISA (see methods section 2.6).

The addition of M.tb to monocytes increased MMP-1 secretion from 124.8 +/- 88.3 pg/ml to 1,298 +/- 990 pg/ml (p=0.12). This was substantially increased by the additional presence of platelets to 3,479 +/- 1,720 pg/ml (p=0.0018). Platelets alone increased MMP-1 secretion by monocytes from 124.8 +/- 88.3 pg/ml to 475 +/- 293.8 pg/ml (p=0.90, Figure 3.14 A). Findings were similar for MMP-10 (Figure 3.14 B).

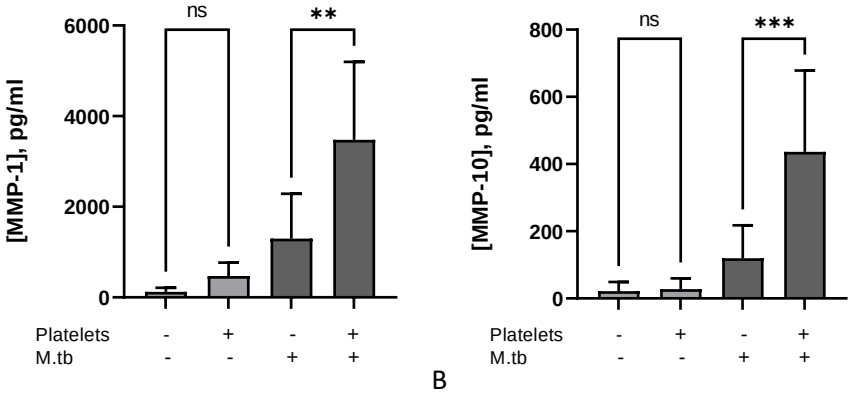

Figure 3.14 Co-culture with platelets enhances (A) MMP-1 and (B) MMP-10 secretion by M.tb-stimulated monocytes.

Platelet:monocyte ratio of 25:1. Graphs represent pooled data from seven separate experiments; each experiment performed in duplicate. Data compared with one-way ANOVA with Šídák's correction for multiple comparisons; **p<0.01, ***p<0.001.

3.2.3 Platelet augmentation of M.tb-infected monocyte MMP-1 secretion increases with an increasing platelet:monocyte ratio

M.tb-infected monocytes and platelets were co-cultured at platelet:monocyte ratios ranging from 10:1 to 100:1 for 24 hours at 37°C, before supernatants were collected for evaluation using ELISA.

MMP-1 secretion from monocytes co-cultured with platelets increased in a dose-dependent manner with an increasing platelet:monocyte ratio. This effect was further enhanced by the presence of M.tb (Figure 3.15). Contribution from platelet-only controls was negligible. Based on these data, a platelet:monocyte ratio of 25:1 was used in all subsequent experiments.

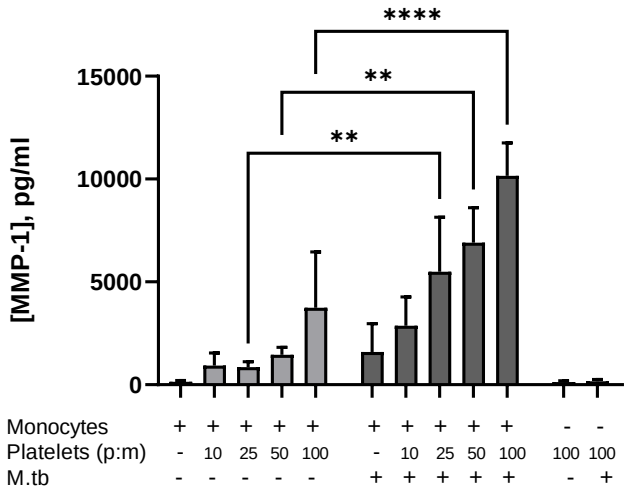

Figure 3.15 MMP-1 secretion by M.tb-infected and uninfected monocytes cultured in the presence or absence of platelets for 24 hours.

MMP-1 secretion increased with increasing platelet:monocyte ratio in a dose-dependent manner in uninfected monocytes, and this effect was further enhanced by the addition of M.tb. Bars represent mean +/- standard deviation (SD). Pooled data from four independent experiments, each experiment performed in duplicate. Data compared with one-way ANOVA with Šídák's correction for multiple comparisons; **p<0.01, ****p<0.0001.

3.2.4 MMP-1 secretion and *mmp-1* gene expression from M.tb- and platelet-stimulated monocytes increases over time

To evaluate kinetics of platelet- and M.tb-stimulated monocyte secretion and gene expression, M.tb-infected and uninfected monocytes were cultured with/without autologous platelets. Supernatants and cell lysates were collected after 4, 8, 18, and 24 hours; cultures were not extended beyond 24h in order to avoid monocyte maturation or differentiation during culture.

Both MMP-1 secretion and *mmp-1* expression were negligible after 4h incubation and increased significantly over time. By 24 hours, monocyte MMP-1 secretion had increased from 29.8 pg/ml to 192.6 pg/ml, and in the presence of platelets this increased further to 1,751 pg/ml (Figure 3.16 A), and monocyte *mmp-1* gene expression increased 17.5-fold by the addition of M.tb, and 207.2-fold by the addition of both M.tb and platelets (Figure 3.16 B).

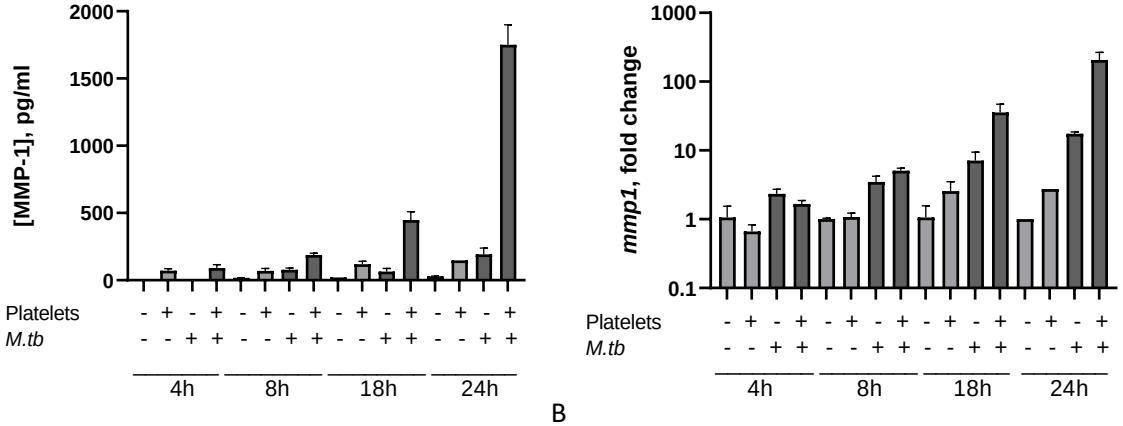

Figure 3.16 MMP-1 secretion and *mmp-1* expression from M.tb-infected monocytes over time.

Both MMP-1 (A) secretion and *mmp-1* expression (B) from M.tb-infected and uninfected monocytes cultured with or without autologous platelets progressively increased over time after incubation for 4, 8, 18, and 24 hours and were maximal after 24 hours. Experiment performed in duplicate.

3.2.5 Co-culture with platelets increases *Mmp-1* gene expression in M.tb-infected monocytes.

Monocytes and autologous platelets were isolated and co-cultured with/without infection with M.tb for 24 hours at 37°C. After collection of supernatants, cell lysates were collected and stored in Tri-Reagent for later analysis by qPCR (see methods sections 2.6 and 2.12).

Platelets alone did not significantly increase *mmp-1* secretion from uninfected monocytes. Infection of monocytes with M.tb increased *mmp-1* expression 26.6-fold, and the addition of platelets increased this further to 125.4-fold compared to monocytes alone (Figure 3.17 B).

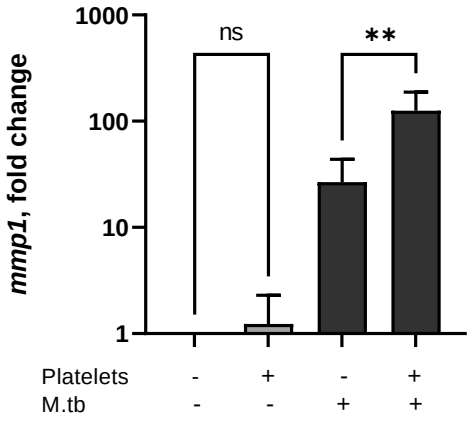

Figure 3.17 Expression of *mmp-1* from M.tb-infected monocytes co-cultured with or without platelets for 24hours.

Mmp-1 expression was significantly increased in M.tb-infected monocytes co-cultured with platelets. Graph shows pooled data from four separate experiments. Bars represent mean +/- SD, all experiments performed in duplicate. Data compared using one-way ANOVA with Šídák's correction for multiple comparisons; **p<0.01.

3.2.6 Investigation of the impact of platelets on M.tb-induced activation of monocyte signalling pathways

3.2.6.1 Phosphoinositide 3 (Pi3) Kinase pathways

Phosphoinositide 3 (Pi3) kinases signal through Akt and activate mTOR, leading to cell growth and proliferation. LY294002 is a potent inhibitor of class I Pi3Ks, by inhibiting the p110 subunit which acts on the ATP binding site of the catalytic subunit(203). This results in the induction of apoptosis and suppression of growth of tumour cells both in vitro and in vivo(204), as well as blocking autophagosome formation and thereby inhibiting autophagy(205).

Monocytes and platelets were isolated from autologous whole blood as described above (see methods sections 2.3 and 2.5). Monocytes were incubated with LY294002 (1 or 10uM) for one hour prior to addition of platelets and infection with M.tb. The cells were incubated for 8, 18, or 24 hours at 37°C, 5% CO_2. Cell supernatants were collected and sterile-filtered prior to evaluation by ELISA, and cell lysates were collected in Tri-Reagent and stored at -80 prior to evaluation by qPCR.

Secretion of MMP-1 and MMP-10 at 8h was low, and no difference in the presence of LY294002 was found (Figure 3.18 A-B). At 18h, the addition of LY294002 reduced MMP-1 secretion by M.tb-infected monocytes from 2,629 +/- 264.5 pg/ml to 506.1 +/- 55 pg/ml, and of M.tb-infected monocytes cultured with platelets from 5,533 +/- 947.9 pg/ml to 1,087 +/- 43.0 pg/ml ($p<0.0001$). Similarly, the concentration of MMP-10 secreted by M.tb-infected monocytes was reduced from 500.2 +/- 137.3 pg/ml to 136.0 +/- 4.83 pg/ml ($p=0.032$), and in the presence of platelets from 1,184 +/- 362.2 pg/ml to 216.4 +/- 43.54 pg/ml ($p<0.0001$) (Figure 3.18 C-D). Peak secretion occurred at 24h, and the presence of LY294002 reduced MMP-1 and MMP-10 secretion from M.tb-infected monocytes both with and without co-culture with platelets in a dose-dependent manner (Figure 3.18 E-F).

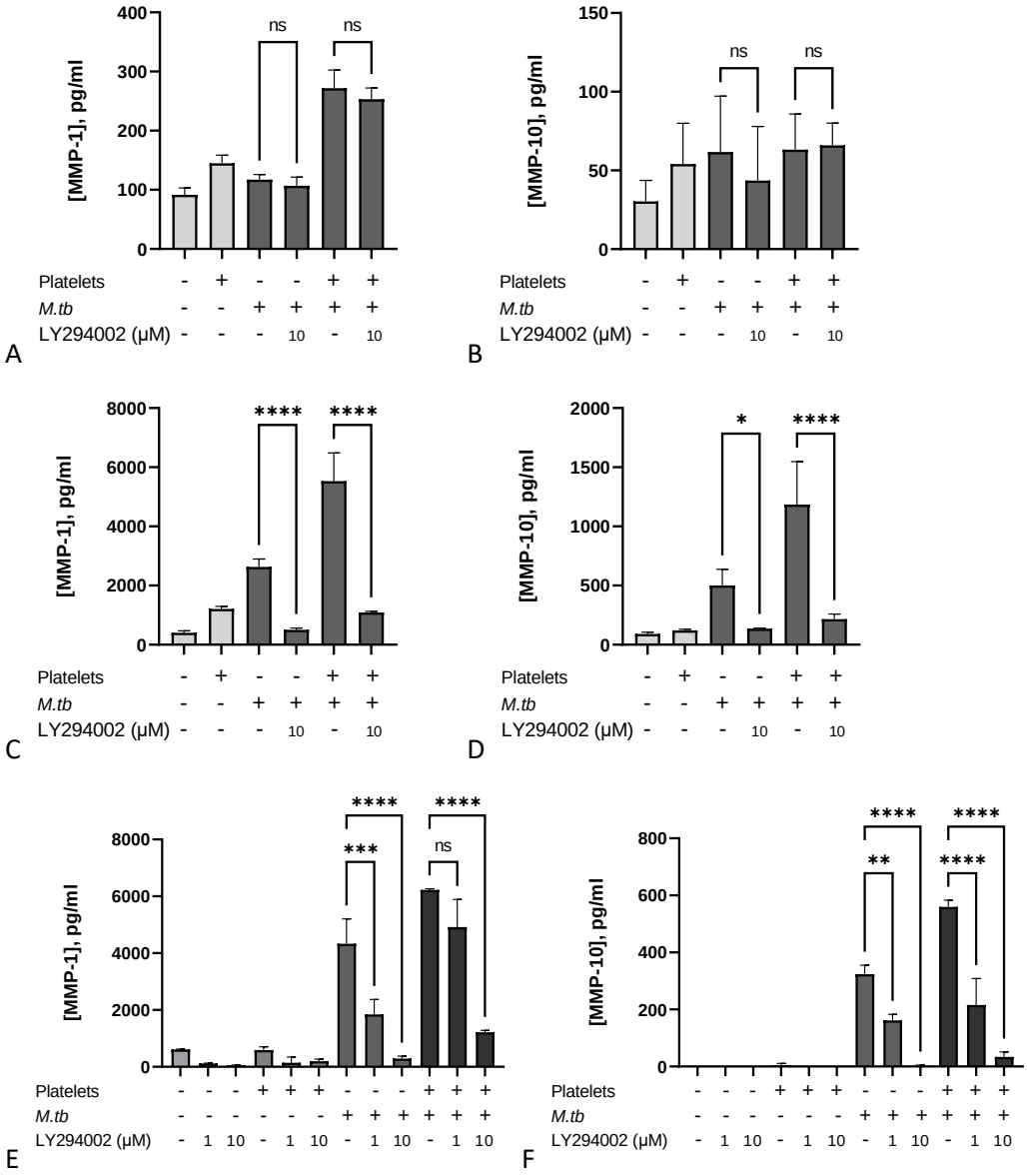

Figure 3.18 Pi3K inhibitor LY294002 downregulates MMP-1 and MMP-10 secretion by M.tb-infected monocytes in the presence or absence of autologous platelets.

LY294002 downregulated MMP-1 and MMP-10 secretion by M.tb-infected monocytes incubated with or without autologous platelets after incubation for 8h (A, B), 18h (C, D), or 24h (E, F). Graphs representative of at least three separate experiments. Data compared using one way ANOVA with Šídák's correction for multiple comparisons. *p<0.05, **p<0.01, ***p<0.001, ****p<0.0001.

To investigate monocyte gene expression, RNA was extracted from cell lysates, converted to cDNA, and expression of *mmp-1* and *mmp-10* quantified using qPCR (see methods section 2.12).

After 8h there was no effect from addition of LY294002 but by 18h expression of both *mmp-1* and *mmp-10* was downregulated by LY294002. After 24h incubation, the expression of *mmp-1* by M.tb-infected monocytes increased by 41.1 fold +/- 13.3 fold relative to monocytes alone, and with the addition of LY294002 this decreased to 21.4 fold +/- 7.5 fold ($p=0.038$). *mmp-1* expression by M.tb-infected monocytes cultured in the presence of platelets increased by 105.1 fold +/- 11.2 fold relative to monocytes alone, and this reduced to 22.04 fold +/- 1.2 fold with LY294002 ($p<0.0001$) (Figure 3.19 E). LY294002 increased *mmp-10* gene expression by M.tb-infected monocytes, and decreased expression by M.tb-infected monocytes co-cultured with platelets (Figure 3.19 F).

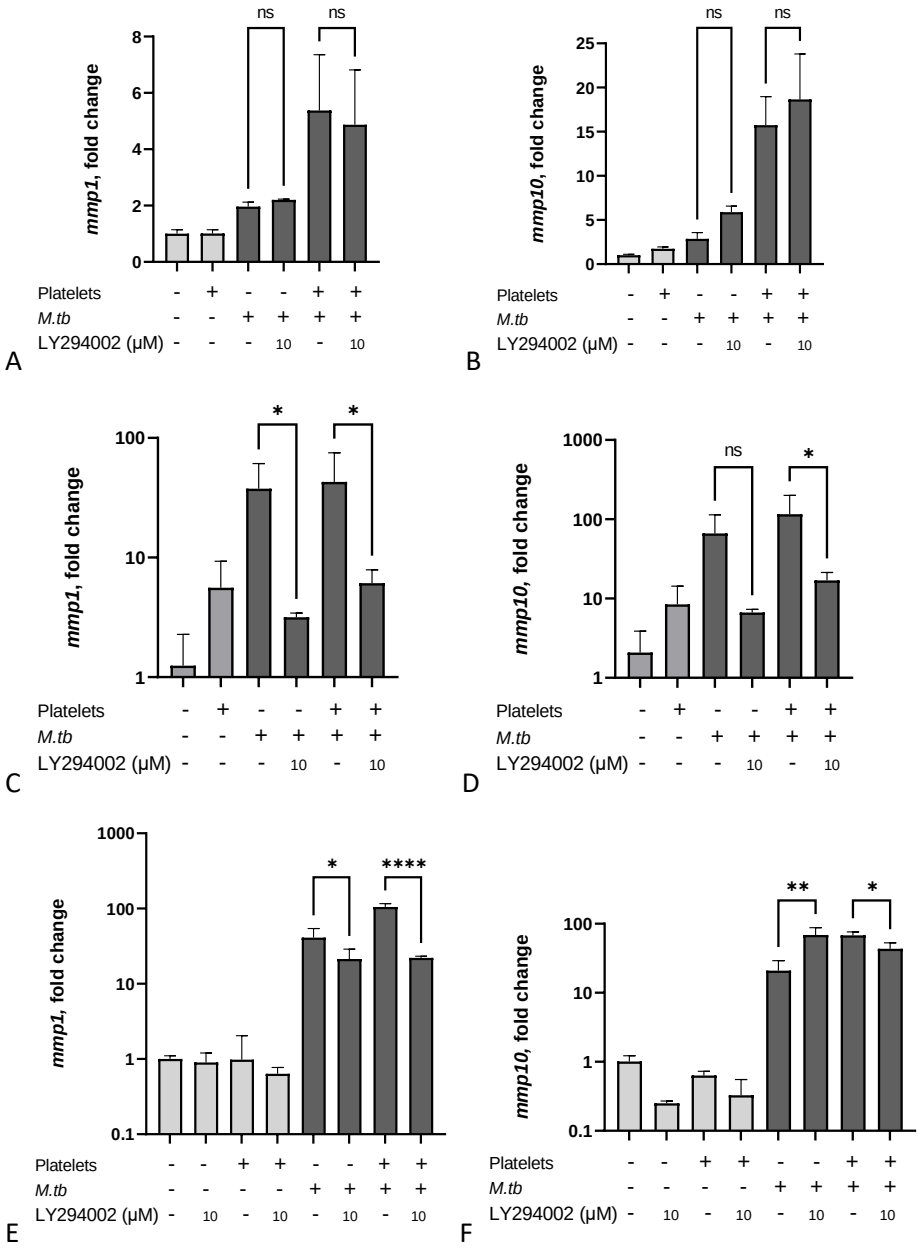

Figure 3.19 The effect of LY294002 on expression of *mmp-1* and *mmp-10* by M.tb-infected monocytes in the presence or absence of autologous platelets.

Pi3K inhibition using LY294002 did not significantly affect *mmp-1* or *mmp-10* gene expression by M.tb-infected monocytes incubated with or without platelets after incubation for 8 hours (A, B), but downregulated *mmp-1* and *mmp-10* gene expression after 18 hours (C, D) and 24 hours (E, F). Data compared using one way ANOVA with Šídák's correction for multiple comparisons. *p<0.05, ** p<0.01, ****p<0.0001.

3.2.6.2 Inhibition of the mammalian target of rapamycin (mTOR) signalling pathway

The mammalian target of rapamycin (mTOR) signalling pathway is an important regulator of cell growth and metabolism, and consists of two functionally distinct complexes, mTOR complex 1 (mTORC1) and mTOR complex 2 (mTORC2). mTORC1 responds to signals from a wide range of stimuli including soluble growth factors, cytokines, and amino acids to regulate processes integral to cellular proliferation and growth, whereas mTORC2 regulates cellular structure and survival. Rapamycin potently inhibits mTORC1, and to a lesser extent mTORC2(206).

Monocytes and platelets were isolated from autologous whole blood as described above (see methods sections 2.3 and 2.5). Monocytes were incubated with 0.5uM Rapamycin for one hour prior to addition of platelets and infection with M.tb. The cells were incubated for 24 hours at 37°C, 5% CO_2, then cell supernatants were collected and sterile-filtered prior to evaluation by ELISA.

0.5uM Rapamycin reduced MMP-1 secretion from M.tb-infected monocytes co-cultured with platelets from 3,324 +/- 888.3 pg/ml to 2,023 +/- 613.0 pg/ml (p=0.045, Figure 3.20).

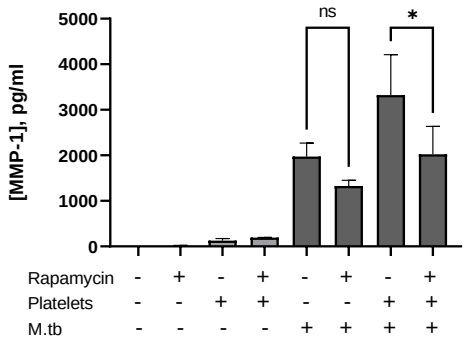

Figure 3.20 The effect of Rapamycin on MMP-1 secretion by M.tb-infected monocytes in the presence or absence of autologous platelets.

mTOR inhibition with Rapamycin downregulated MMP-1 secretion from M.tb-infected monocytes co-cultured with autologous platelets for 24 hours. Data compared using one way ANOVA with Šídák's correction for multiple comparisons. *p<0.05.

The experiment was repeated multiple times, and results were found to be very variable and difficult to reproduce. This was attributed to the many off-target effects of Rapamycin(206), and for this reason this line of experimentation was not taken any further.

3.2.6.3 Mitogen-activated protein kinase (MAPK) inhibition

PD98059 inhibits the ERK pathway by selectively binding to inactive MEK1, preventing its activation by upstream activators including c-RAF, and thereby preventing ongoing activation of the MAP kinase cascade. It also prevents MEK2 activation to a lesser extent. The inhibitor SB203580 selectively inhibits p38 MAPK.

Monocytes and platelets were isolated from autologous whole blood as described above (see methods sections 2.3 and 2.5). Monocytes were incubated with PD98059 (10µM) or SB203580 (10µM) for one hour prior to addition of platelets and infection with M.tb. The cells were incubated for 24 hours at 37°C, 5% CO_2. Cell supernatants were collected and sterile-filtered prior to evaluation by ELISA, and cell lysates were collected in Tri-Reagent and stored at -80 prior to evaluation by qPCR.

PD98059 downregulated MMP-1 secretion in M.tb-infected monocytes co-cultured with platelets at 8, 18, and 24h (Figure 3.21 A, C, E) and downregulated MMP-10 secretion at 18 and 24h (Figure 3.21 B, D, F).

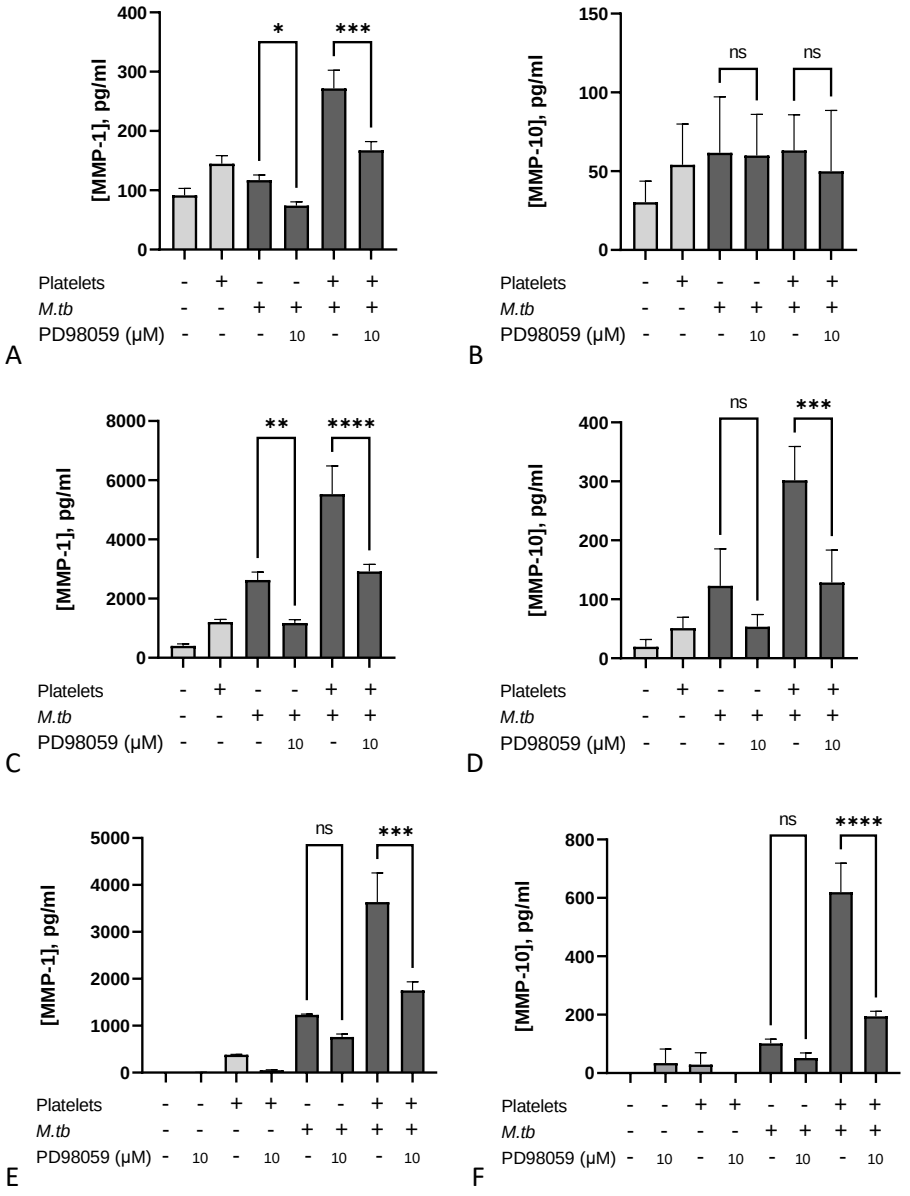

Figure 3.21 The effect of PD98059 on secretion of MMP-1 and MMP-10 by M.tb-infected monocytes in the presence or absence of autologous platelets.

PD98059 significantly downregulates MMP-1 and MMP-10 secretion by M.tb-infected monocytes co-cultured with platelets. Graphs representative of at least three separate experiments after incubation for 8h (A, B), 18h (C, D), or 24h (E, F). Data compared using one way ANOVA with Šídák's correction for multiple comparisons. *p<0.05, **p<0.01, ***p<0.001, ****p<0.0001.

Similarly, SB203580 downregulated MMP-1 secretion in M.tb-infected monocytes co-cultured with platelets at 8, 18, and 24h (Figure 3.22 A, C, E) and downregulated MMP-10 secretion at 18 and 24h (Figure 3.22 B, D, F).

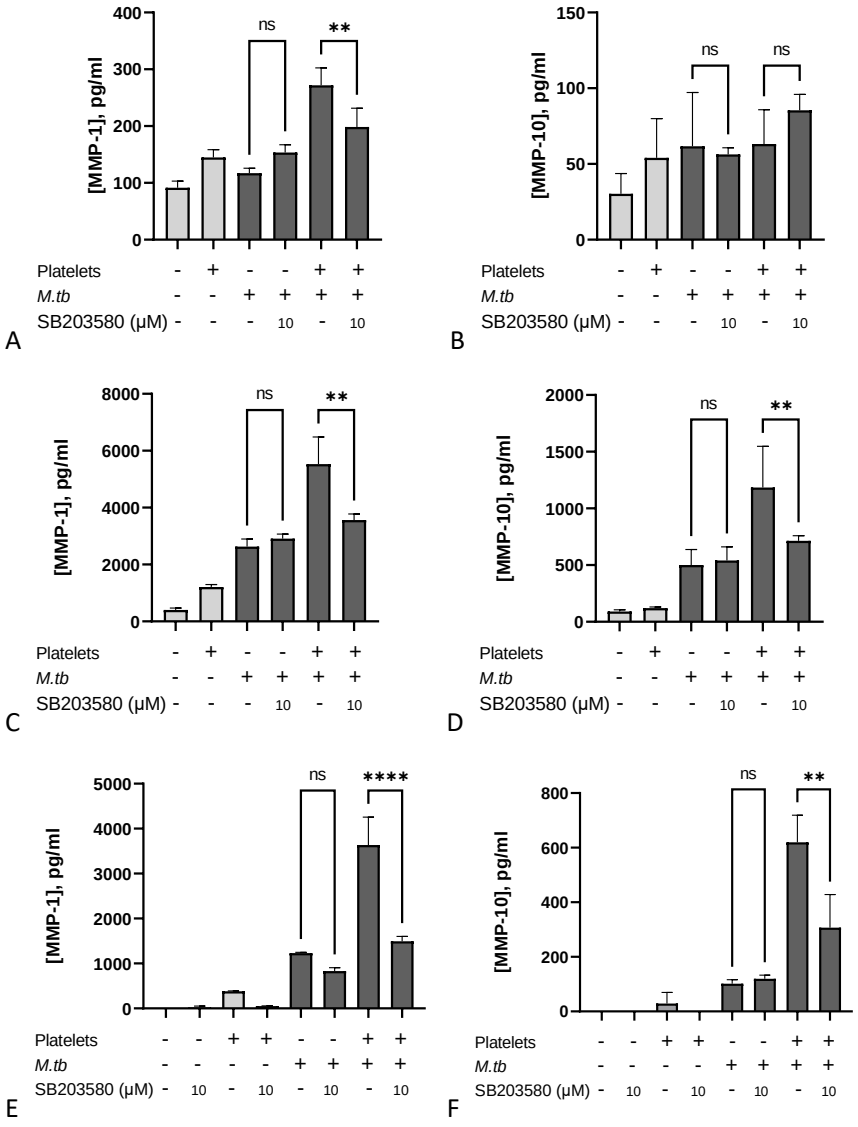

Figure 3.22 The effect of SB203580 on secretion of MMP-1 and MMP-10 by M.tb-infected monocytes in the presence or absence of autologous platelets.

SB203580 significantly downregulates MMP-1 and MMP-10 secretion by M.tb-infected monocytes co-cultured with platelets after incubation for 8h (A, B), 18h (C, D), or 24h (E, F). Graphs representative of at least three separate experiments. Data compared using one way ANOVA with Šídák's correction for multiple comparisons. **p<0.01, ****p<0.0001.

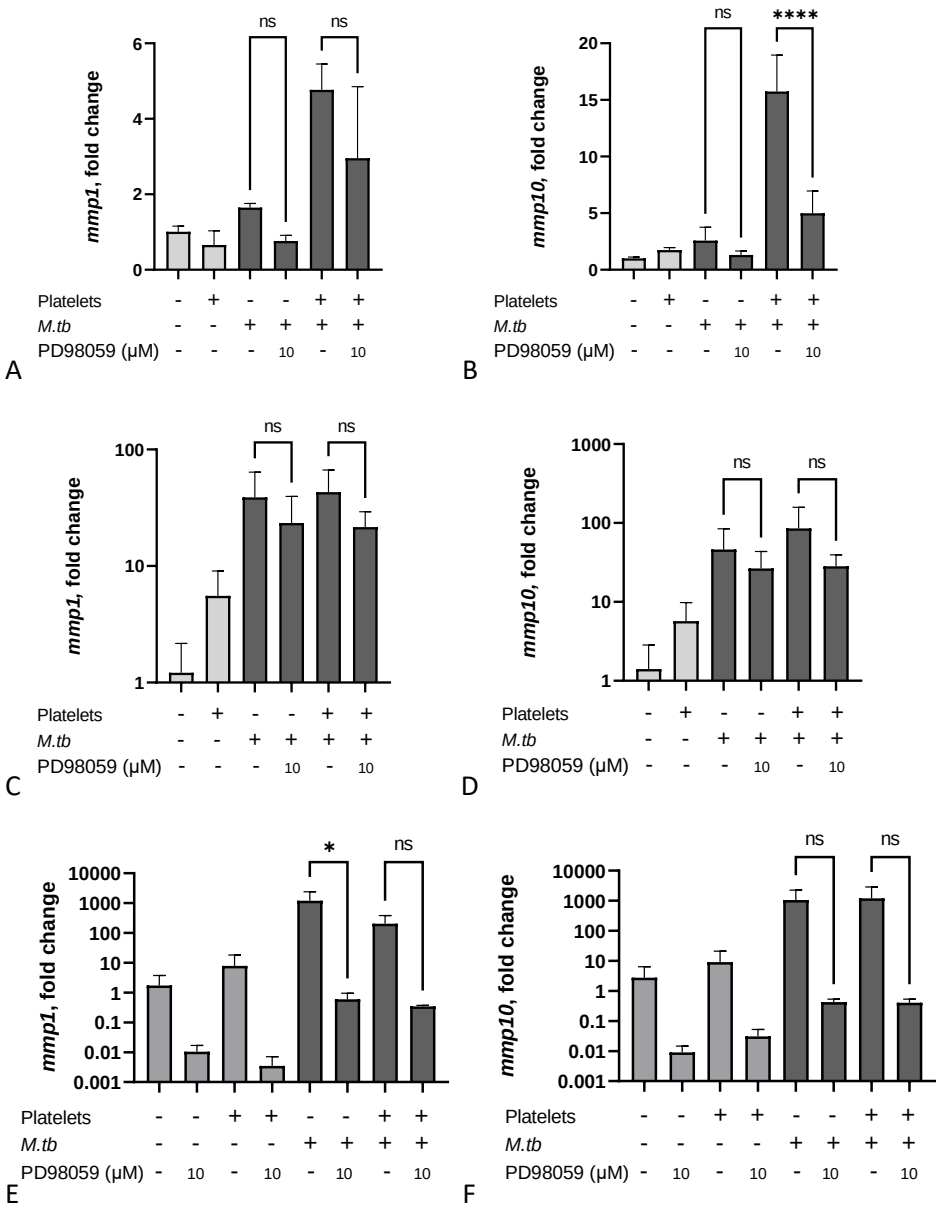

Figure 3.23 The effect of PD98059 on expression of *mmp-1* and *mmp-10* by M.tb-infected monocytes in the presence or absence of autologous platelets.

After incubation for 8h (A, B), 18h (C, D), or 24h (E, F), a trend towards downregulation by PD98059 of *mmp-1* and *mmp-10* expression by M.tb-infected monocytes cultured with or without autologous platelets was observed. Data compared using one way ANOVA with Šídák's correction for multiple comparisons. *p<0.05, **p<0.01, ****p<0.0001.

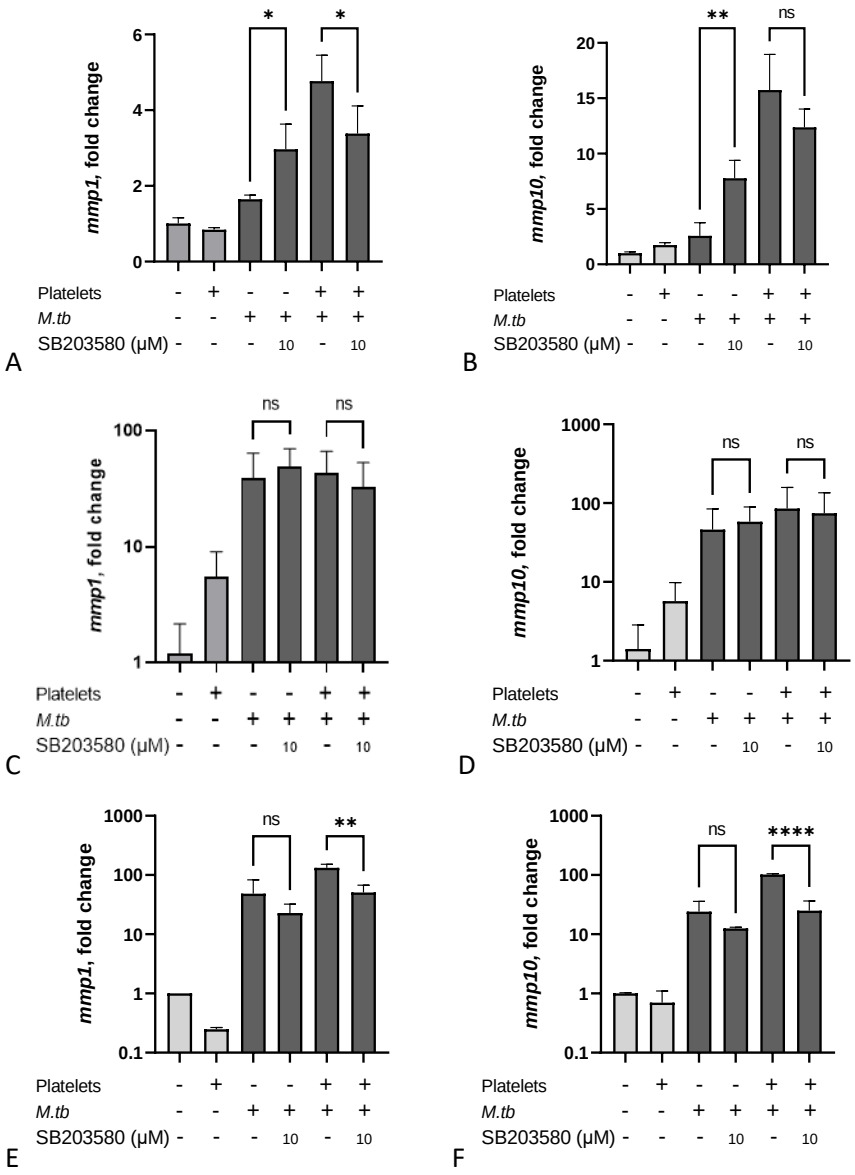

Figure 3.24 The effect of SB203580 on expression of *mmp-1* and *mmp-10* by M.tb-infected monocytes in the presence or absence of autologous platelets.

SB203580 did not significantly affect *mmp-1* or *mmp-10* gene expression by M.tb-infected monocytes +/- platelets after 8 hours (A,B) or 18 hours (C,D), but significantly downregulated *mmp-1* and *mmp-10* gene expression by M.tb-infected monocytes co-cultured with platelets for after 24 hours (E,F). Data compared using one way ANOVA with Šídák's correction for multiple comparisons. *p<0.05, **p<0.01, ****p<0.0001.

At the level of gene expression, there was a trend towards downregulation of *mmp-1* and *mmp-10* gene expression following MAP-K inhibition with PD98059 (Figure 3.23). SB203580 reduced *mmp-1* gene expression by M.tb-infected monocytes from an 132.4-fold increase compared to monocytes alone to a 50.5-fold increase compared to monocytes alone ($p=0.0078$, Figure 3.24 E), and reduced *mmp-10* gene expression from M.tb-infected monocytes from an 102.3-fold increase compared to monocytes alone to a 25.1-fold increase compared to monocytes alone ($p<0.0001$, Figure 3.24 F).

3.2.7 The contribution of P-selectin-PSGL-1 interactions to platelet-induced activation of M.tb infected monocytes

P-selectin Glycoprotein Ligand 1 (PSGL-1) is an important regulator of monocyte function. Notably, its interactions with L-selectin lead to rolling and adhesion, enabling monocyte migration in inflammation(207). It also binds with platelet P-selectin which leads to downstream signal transduction and modulation of monocyte activity(208). The following experiments were conducted to investigate the importance of PSGL-1-P-selectin interactions in the context of M.tb.

3.2.7.1 Anti-PSGL-1 antibody prevents platelet-monocyte aggregation without affecting platelet receptor activation

The specific anti-PSGL-1 monoclonal antibody KPL1 has been shown to mimic PSGL-1 stimulation with its physiological ligand, P-selectin, leading to inhibition of proliferation and induction of apoptosis in CD34+CD38- haemopoietic stem cells(209), initiation of PSGL-1-mediated neutrophil rolling(210), and enhanced leukocyte adhesion(211).

Whole blood taken in 10% sodium citrate was stimulated with 10µg/ml anti-PSGL-1 antibody, or PBS control, for 10 minutes. 25µl blood was then incubated with anti-CD14, anti-CD42b, anti-CD62P, and anti-PAC-1 antibodies, with or without 10uM TRAP-6 or 5uM ADP, and binding buffer (1% w/v BSA) to a final volume of 100µl in the dark for 20 minutes, before 500µl 1x fix/lysis solution (ThermoFisher Scientific, UK) was added for 15 minutes and a final addition of 1ml PBS. Samples were then analysed using a CytoFLEX S analyser (Beckman Coulter Life Sciences, UK) and data were entered into FlowJo™ v10 software.

ADP and TRAP-6 led to an increase in platelet-monocyte aggregation from 4.3% +/- 0.4% to 14.3% +/- 1.5% and 47.5% +/- 1.4% respectively (Figure 3.25). This effect was removed in the presence of anti-PSGL-1 antibody (platelet-monocyte aggregation 3.3% +/- 0.2% in unstimulated blood versus 3.6% +/- 0.8% and 5.5% +/- 0.2% respectively, both $p<0.0001$). Anti-PSGL-1 antibody also reduced TRAP-6 induced platelet-granulocyte aggregation from 5.91% +/- 0.5% to 2.32% +/- 0.007% ($p<0.0001$); no effect was observed in the presence of ADP. Anti-PSGL-1 antibody did not affect platelet expression of CD62P or PAC-1.

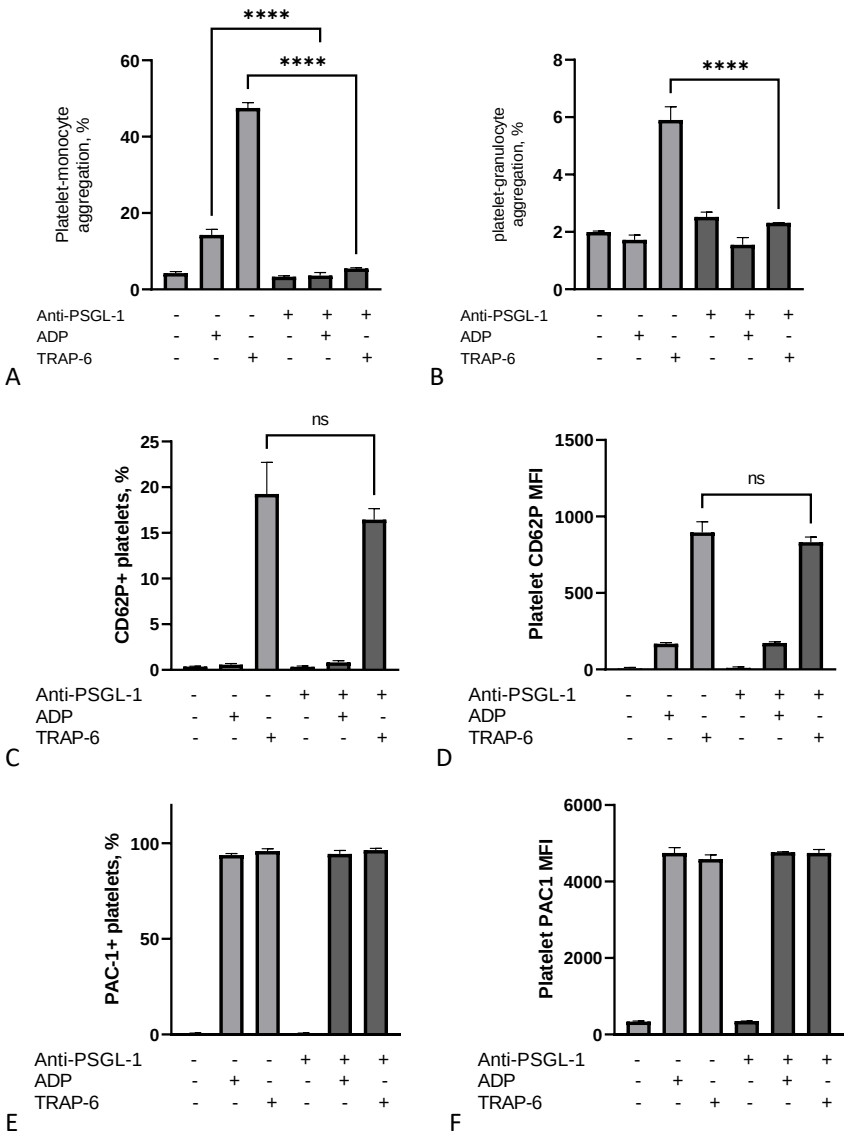

Figure 3.25 The effect of anti-PSGL-1 antibody on ADP- or TRAP-6-induced platelet-monocyte aggregation, platelet-granulocyte aggregation, and platelet activation, evaluated using flow cytometry.

Anti-PSGL-1 antibody significantly reduced ADP- and TRAP-6-induced upregulation of platelet-monocyte aggregation (A) and TRAP-6-induced platelet-granulocyte aggregation (B), but did not affect agonist-induced upregulation of CD62P (P-selectin, C-D) or PAC-1 (E-F). Bars represent mean +/- SD. Data compared using one-way ANOVA with Šídák's correction for multiple comparisons. ****p<0.0001. Graphs representative of two independent experiments.

3.2.7.2 Ligation of monocyte PSGL-1 receptors increases secretion of MMP-1

Monocytes and platelets were isolated from autologous whole blood as described above (see methods sections 2.3 and 2.5). Monocytes were incubated with the ligating anti-PSGL-1 KPL1 antibody (10µg/ml) for one hour prior to addition of platelets and infection with M.tb. The cells were incubated for 24 hours at 37°C, 5% CO_2, then cell supernatants were collected and sterile-filtered prior to evaluation by ELISA.

PSGL-1 ligation increased MMP-1 and MMP-10 secretion from M.tb infected monocytes both with and without co-culture with platelets (Figure 3.26). There was no difference in *mmp-1* or *mmp-10* gene expression (Figure 3.27).

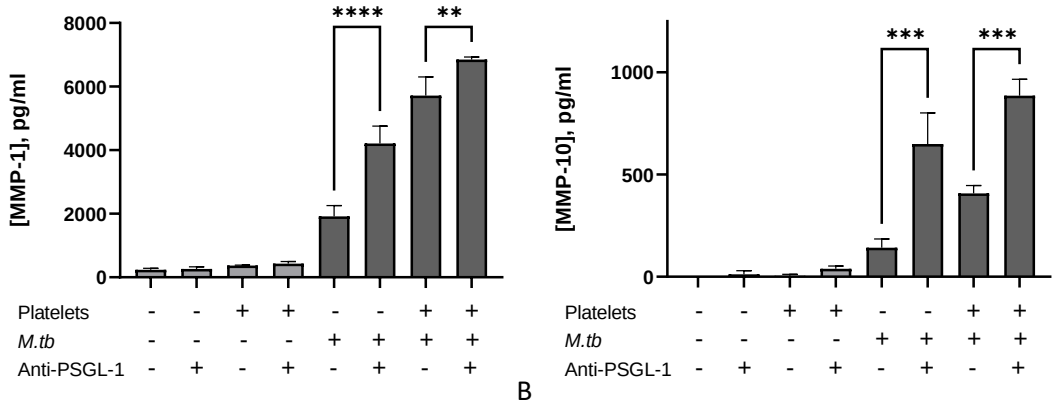

Figure 3.26 The effect of PSGL-1 ligation on MMP secretion by M.tb-infected monocytes in the presence or absence of autologous platelets.

PSGL-1 ligation significant increased secretion of MMP-1 (A) and MMP-10 (B) both in the presence and absence of platelets. Data compared using one way ANOVA with Šídák's correction for multiple comparisons. **p<0.01, ***p<0.001, ****p<0.0001.

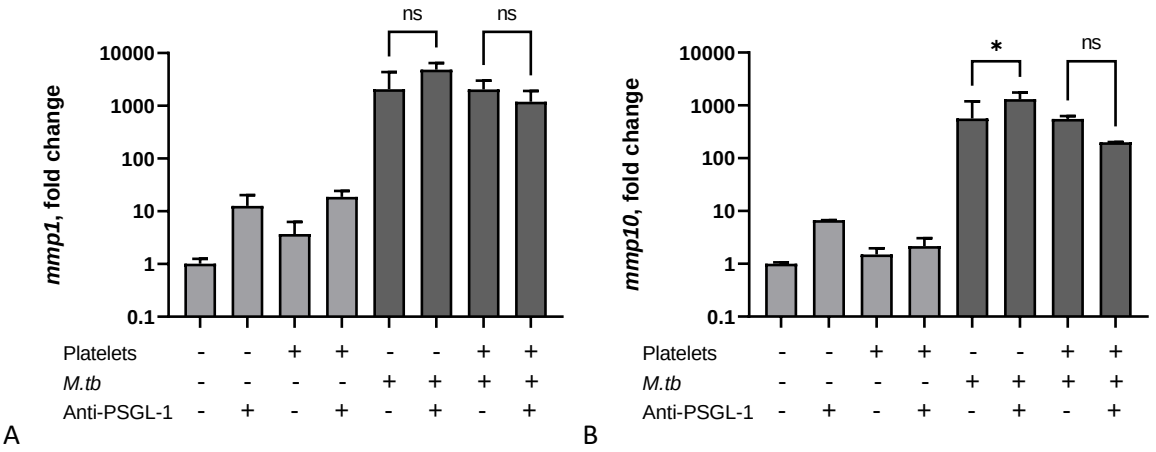

Figure 3.27 The effect of PSGL-1 ligation on expression of *mmp-1* and *mmp-10* by M.tb-infected monocytes in the presence or absence of autologous platelets.

PSGL-1 ligation did not significantly affect expression of either *mmp-1* (A) or *mmp-10* (B) by M.tb-infected monocytes cultured in the presence or absence of platelets. Data compared using one way ANOVA with Šídák's correction for multiple comparisons. *p<0.05.

-

3.2.7.3 Blockade of platelet P-selectin prevents platelets aggregating with monocytes or granulocytes without affecting platelet PAC-1 expression.

Whole blood taken in 10% sodium citrate was stimulated with 10µg/ml anti-P-selectin antibody (Human P-Selectin/CD62P Antibody Monoclonal Mouse IgG1 Clone # 9E1 Catalogue number BBA30), or control, for 10 minutes. 25µl blood was then incubated with anti-CD14, anti-CD42b, anti-CD62P, and anti-P-selectin antibodies, with or without 10uM TRAP-6 or 5uM ADP, and binding buffer (1% w/v BSA) to a final volume of 100µl in the dark for 20 minutes, before 500µl 1x fix/lysis solution (ThermoFisher Scientific, UK) was added for 15 minutes and a final addition of 1ml PBS. Samples were then analysed using a CytoFLEX S analyser (Beckman Coulter Life Sciences, UK) and data were entered into FlowJo™ v10 software.

Platelet-monocyte aggregation increased in response to stimulation with ADP and TRAP-6 from 5.2% to 11.8% and 12.0% respectively; this effect disappeared when platelets were pre-incubated

with anti-P-selectin antibody (Figure 3.28 A). Platelet-granulocyte aggregation was under 3% in all conditions and was unaffected by addition of anti-P-selectin antibody (Figure 3.28 B). Fluoroscopic detection of anti-CD62P antibody on platelets was significantly increased in response to both ADP and TRAP-6, and this was significantly diminished with addition of anti-P-selectin antibody, which is in keeping with blockade of the P-selectin receptor(Figure 3.28 C-D); there was no impact on ADP- or TRAP-6-induced PAC-1 expression indicating that this antibody did not in fact affect platelet activation (Figure 3.28 E-F).

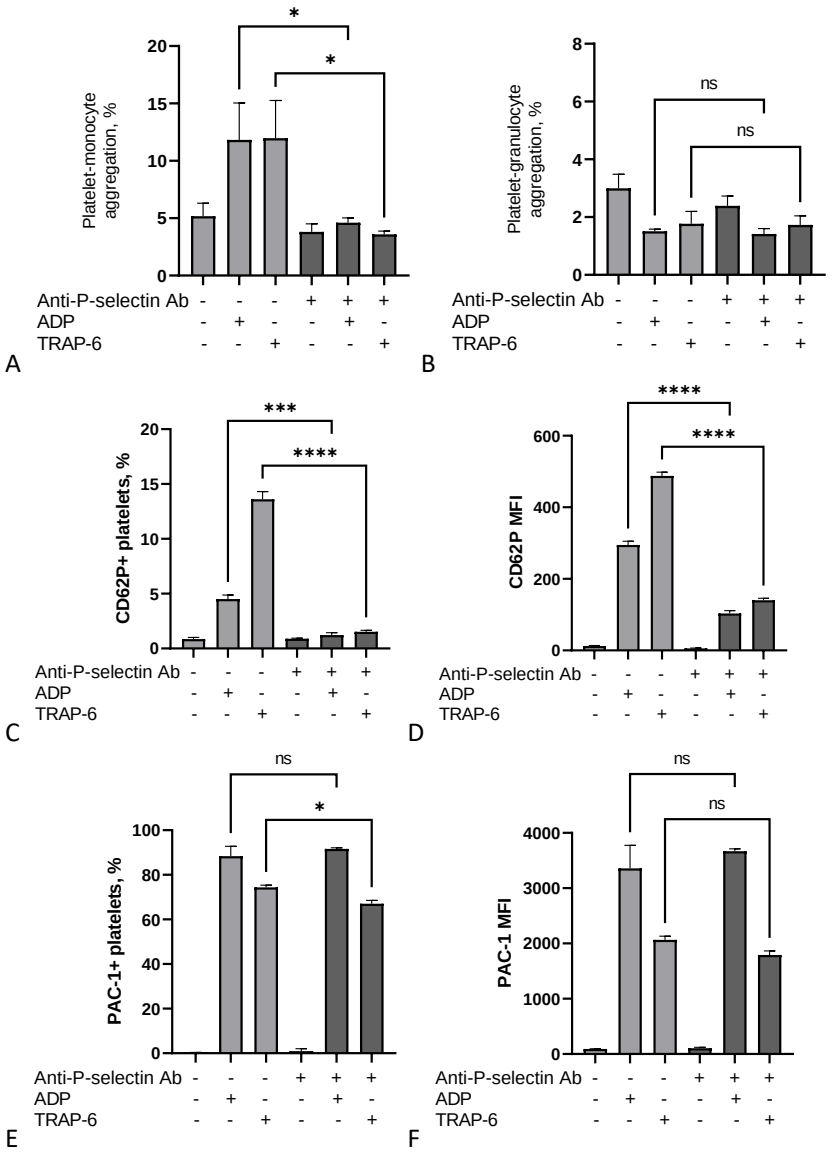

Figure 3.28 The effect of anti-P-selectin antibody on ADP- or TRAP-6-induced platelet-monocyte aggregation, platelet-granulocyte aggregation, and platelet activation, evaluated using flow cytometry.

Anti-P-selectin antibody significantly reduced ADP- and TRAP-6-induced upregulation of platelet-monocyte aggregation (A); ADP and TRAP-6 did not significantly increase platelet-granulocyte aggregation so no effect on this output caused by addition anti-P-selectin antibody was observed (B). Anti-P-selectin antibody significantly reduced agonist-induced increases in CD62P (P-selectin) detection on the surface of platelets (C-D) but did not affect agonist-induced PAC-1 upregulation (E-F). Bars represent mean +/- SD. Data compared using one-way ANOVA with Šídák's correction for multiple comparisons. *p<0.05, **p<0.01, ***p<0.001, ****p<0.0001.

3.2.7.4 Blockade of platelet P-selectin may downregulate MMP production by M.tb-infected monocytes co-cultured with platelets.

Having demonstrated that anti-P-selectin antibody prevents monocyte-platelet aggregation, the effect of blocking this interaction on M.tb-induced monocyte activation in monocyte-platelet co-culture was investigated.

Monocytes and autologous platelets were isolated as per Methods section 2.3 and 2.5. Platelets were incubated with or without anti-P-selectin antibodies at a concentration of 10µg/ml for 15mins, then added to monocytes with the respective antibody at a final concentration of 10µg/ml. These were infected with M.tb at a MOI of 1 or 7H9 control, and cultured for 24h before collection of supernatants for analysis by ELISA.

Two different antibodies were used: Human P-Selectin/CD62P Antibody Monoclonal Mouse IgG1 Clone # 9E1 (product BBA30), and Invitrogen CD62P (P-Selectin) Monoclonal Antibody (Psel.KO2.12) from eBioscience. After results were obtained using the BBA30 antibody were found to be variable, the Psel.KO2.12 antibody was acquired and data using this antibody were found to be more reliably reproducible.

The concentration of MMP-1 in supernatant collected from M.tb-infected monocytes co-cultured with platelets was 1,818 +/- 140.5 pg/ml. When platelets were pre-incubated with anti-P-selectin antibody there was a non-significant trend towards a reduction in MMP-1 concentration: pre-incubation with anti-P-selectin antibody (BBA30) gave a measured MMP-1 concentration of 1,442 +/- 511 pg/ml, and pre-incubation with anti-P-selectin antibody (Psel.KO2.12) gave an MMP-1 concentration of 1,330 +/- 20.9 pg/ml (p=0.19). Data were similar for MMP-10 (Figure 3.29).

There was no difference in *mmp-1* or *mmp-10* gene expression in the presence of either antibody (Figure 3.30).

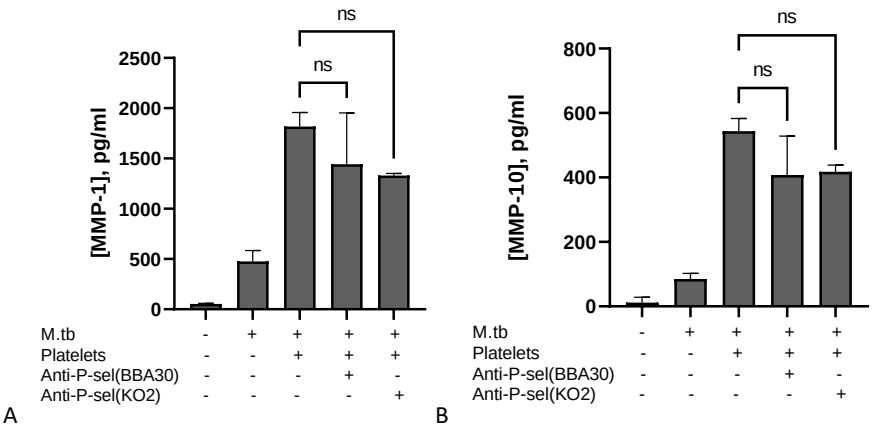

Figure 3.29 The effect of platelet P-selectin receptor inhibition on monocyte secretion of MMP-1 and MMP-10 following co-culture with platelets and M.tb.

Platelet pre-incubation with both BBA30 and Psel.KO2.12 anti-P-selectin antibodies prior to addition to monocytes, M.tb infection, and culture for 24h led to a non-significant trend towards reduced monocyte secretion of (A) MMP-1 and (B) MMP-10. Graph represents single experiment using anti-P-selectin BBA30 antibody and three separate experiments using Psel.KO2.12 antibody. Data compared using one way ANOVA with Šídák's correction for multiple comparisons.

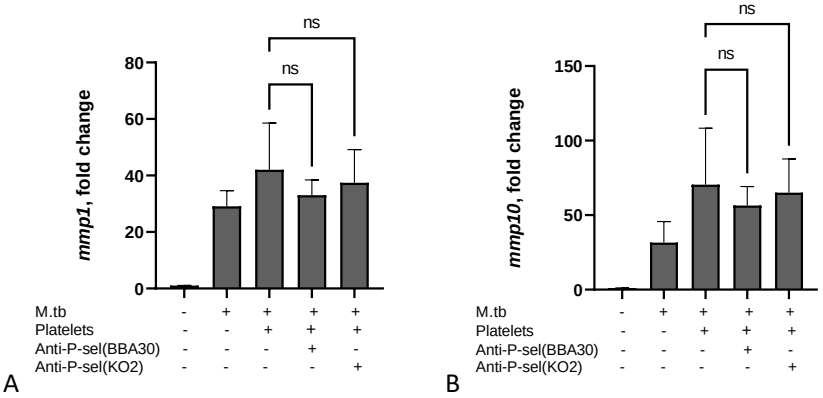

Figure 3.30 The effect of platelet P-selectin receptor inhibition on expression of *mmp-1* and *mmp-10* following co-culture with platelets and M.tb.

Pre-incubation of platelets with BBA30 or Psel.KO2.12 anti-P-selectin antibodies prior to addition to monocytes, infection with M.tb, and culture for 24 hours did not affect monocyte expression of either (A) *mmp-1* or (B) *mmp-10.* Data compared using one way ANOVA with Šídák's correction for multiple comparisons.

3.2.7.5 Recombinant P-selectin partially upregulates MMP secretion by M.tb-infected monocytes

To investigate the effect of platelet stimulation of monocyte PSGL-1 receptors, recombinant P-selectin (Bio-Techne™) was added to monocytes with or without autologous platelets. Cells were then infected with M.tb and incubated for 8, 18, or 24 hours, then supernatants and cell lysates in Tri-Reagent were collected for later analysis.

After 8h the addition of 1µg/ml recombinant P-selectin, 2µg/ml recombinant P-selectin, or platelets increased secretion of MMP-1 by similar amounts (from 462.4 pg/ml to 656.1 pg/ml, 650.0 pg/ml, and 646.9 pg/ml respectively, all $p<0.05$, Figure 3.31 A). Secretion of MMP-10 was unaffected (Figure 3.31 B). After 18h, the addition of 1µg/ml or 2µg/ml recombinant P-selectin upregulated both MMP-1 and MMP-10 secretion to a lesser extent than the addition of platelets (Figure 3.31 C-D). At 24h, the addition of 1µg/ml recombinant P-selectin to M.tb-infected monocytes upregulated MMP-1 secretion from 713.7 +/- 45.35 pg/ml to 1,346 +/- 94.6 pg/ml ($p=0.044$). The addition of recombinant P-selectin to M.tb-infected monocytes co-cultured with platelets upregulated MMP-1 secretion from 4,072 +/- 568 pg/ml to 4,919 +/- 530.1 pg/ml ($p=0.0076$). Data were similar for MMP-10 (Figure 3.31 E-F). These differences were not reflected at the level of gene expression (Figure 3.32).

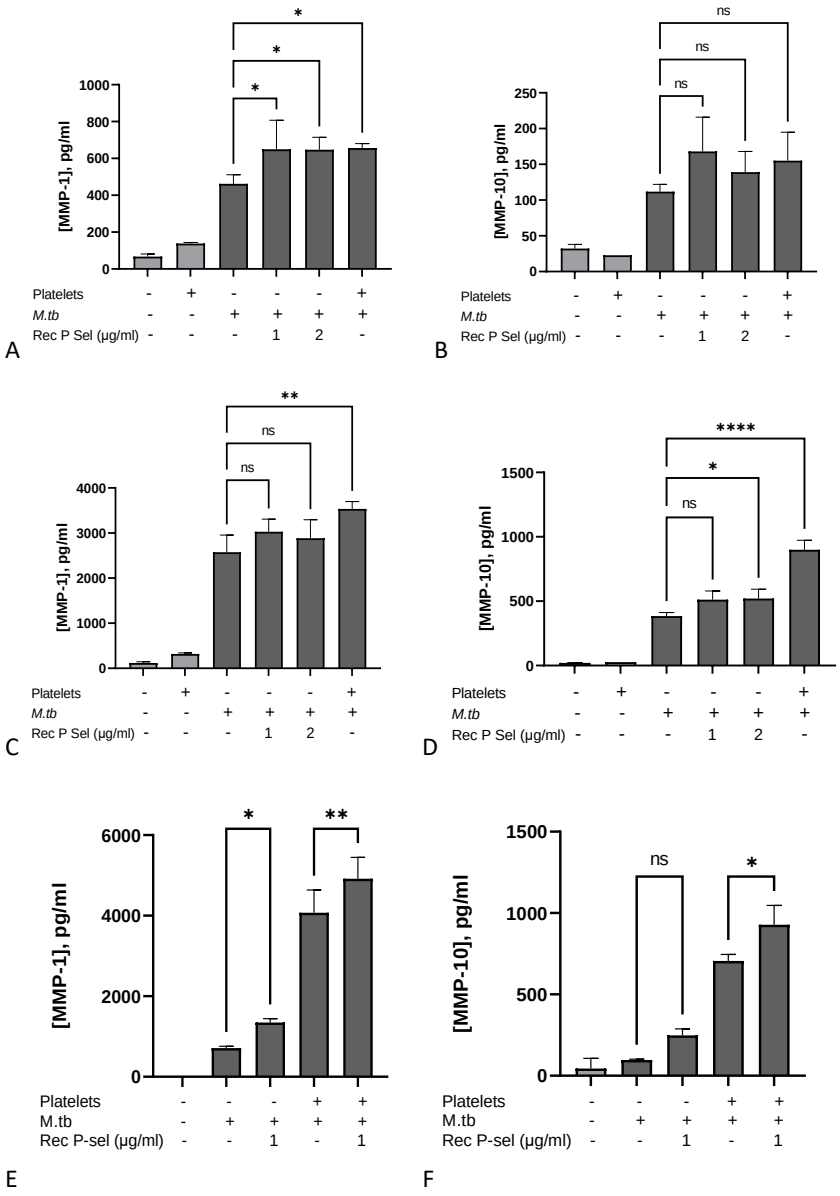

Figure 3.31 The effect of recombinant P-selectin (Rec P-sel) on secretion of MMP-1 and MMP-10 by M.tb-infected monocytes.

After incubation for 8h both platelets and recombinant P-selectin increased secretion of MMP-1 but not MMP-10 from M.tb-infected monocytes (A and B). After 18h, recombinant P-selectin upregulated MMP-1 and MMP-10 secretion to a lesser extent than platelets themselves (C and D). After 24h, the addition of recombinant P-selectin increased secretion of both MMP-1 and MMP-10 from M.tb-infected monocytes alone and in the presence of platelets (E and F). 24 hour timepoints representative of at four separate experiments. Data compared using one way ANOVA with Šídák's correction for multiple comparisons. *p<0.05, **p<0.01, ****p<0.0001.

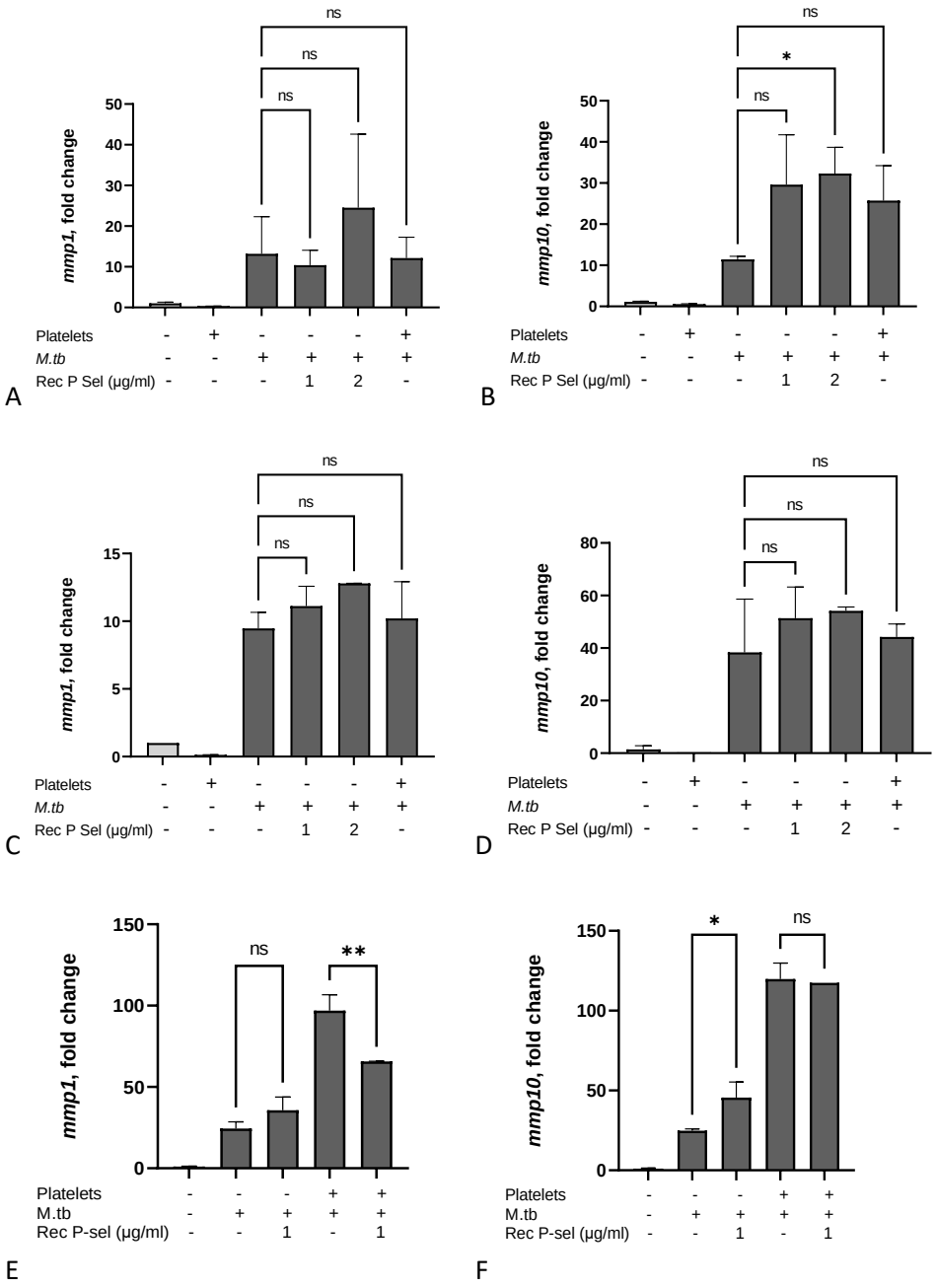

Figure 3.32 The effect of recombinant P-selectin (Rec P-sel) on expression of *mmp-1* and *mmp-10* by M.tb-infected monocytes.

The addition of recombinant P-selectin did not appreciably affect expression of *mmp-1* or *mmp-10* by M.tb-infected monocytes after 8 hours (A, B), 18 hours (C, D), or 24 hours (E, F). Data compared using one way ANOVA with Šídák's correction for multiple comparisons. *p<0.05, **p<0.01.

3.2.8 The contribution of platelet-secreted mediators to platelet-induced activation of M.tb-stimulated monocytes

Having studied the effect of contact-dependent activation of monocytes by platelets via P-selectin-PSGL-1 receptor interactions, it was pertinent to next investigate the indirect activation of monocytes via secreted mediators. One of the hallmarks of platelet activation is the rapid and substantial release of over 300 different mediators hitherto stored in granules. These are recognized to be important in a range of functions including platelet aggregation and adhesion to other cells, antimicrobial activity, clotting, thrombo-inflammation, and wound healing(212, 213).

To investigate indirect activation of monocytes by platelets via the platelet secretome, monocytes and autologous platelets were extracted from whole blood (see methods sections 2.3 and 2.5). Platelets were resuspended in DMEM supplemented with FCS and ampicillin to a concentration of 2.5 x 10^8 cells/ml and divided into three aliquots. 0.5U/ml thrombin was added to one aliquot and incubated at room temperature for 10 minutes. Thrombin-activated and control platelets were spun at 10,000 x *g* for 1 minute to pellet the platelets, then the supernatant sterile filtered to remove any residual platelets, to generate thrombin-activated platelet supernatant (SN) and unactivated platelet SN respectively. Platelets (1.25 x 10^8 cells/ml), or platelet SN or thrombin-activated platelet SN (1:4 final volume), were then added to monocytes which were infected with M.tb or inoculated with an equal volume of 7H9 control media. The cells were incubated for 24 hours at 37°C, 5% CO_2 for 24 hours before collection of supernatants, which were stored at -20°C until evaluation using ELISA.

Platelets increased MMP-1 secretion from M.tb-infected monocytes from 406.0 +/- 24.1 pg/ml to 3,301 +/- 32.7 pg/ml (p=0.0009). Platelet supernatant from unstimulated platelets also increased MMP-1 secretion to 2,554 +/- 34.7 pg/ml (p=0.0029), but the increase in MMP-1 secretion in response to platelet supernatant from thrombin-activated platelets was significantly greater (5,684 +/- 455.8 pg/ml, p<0.0001, Figure 3.33).

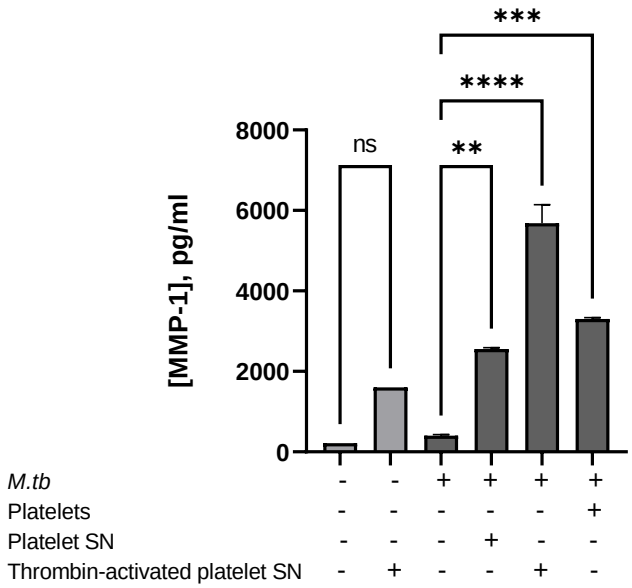

Figure 3.33 The effect of supernatant (SN) from unstimulated and thrombin-stimulated platelets on secretion of MMP-1 from M.tb-infected monocytes.

Platelets, platelet supernatant, and supernatant from thrombin-activated platelets all significantly increased MMP-1 secretion from M.tb infected monocytes. Data compared using one way ANOVA with Šídák's correction for multiple comparisons. **p<0.01, ***p<0.001, ****p<0.0001.

To investigate the effect of platelet agonists other than thrombin, platelet supernatant was obtained by incubating platelets suspended in DMEM supplemented with 10% FCS and 10µg/ml ampicillin at a concentration of 2.5 x 10^8 cells/ml with thrombin (0.1 or 0.5U/ml), ADP (5 µM or 10µM), or TRAP-6 (5 µM or 10µM) for 15 minutes. Platelets were then pelleted by centrifugation, and the supernatants filtered through a 0.22 µm filter to remove any residual platelets. Supernatants from unactivated or activated platelets, or platelets at a final concentration of 1.25 x 10^8 cells/ml, were added to M.tb-infected or uninfected monocytes which were cultured for 24 hours before collection of the cell supernatants.

MMP-1 secretion from M.tb-infected monocytes was not increased by the addition of supernatant obtained from unstimulated platelets, but was increased significantly by supernatant from platelets stimulated by each of the agonists used, with higher levels of MMP-1 secretion associated with higher concentrations of platelet agonists used (Figure 3.34 A). Platelets

themselves were included as a positive control. MMP-10 secretion followed a similar pattern although the differences were less marked (Figure 3.34 B).

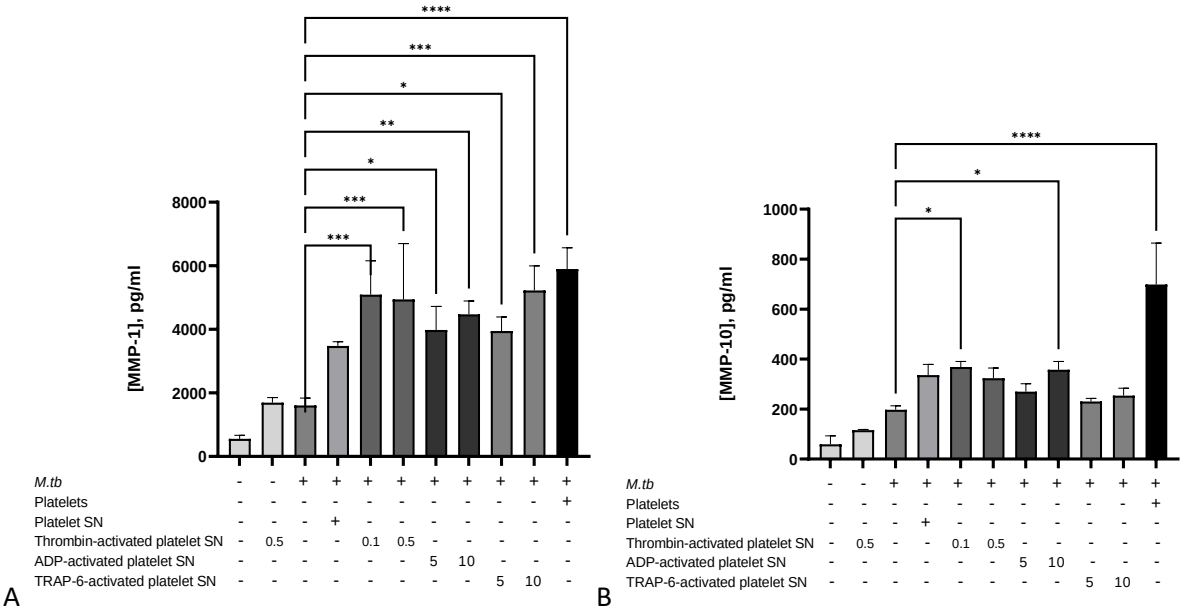

Figure 3.34 The effect of supernatant from unstimulated and stimulated platelets on secretion of MMP-1 and MMP-10 from M.tb-infected monocytes.

(A) MMP-1 secretion by M.tb-infected monocytes was not affected by incubation with supernatant from unstimulated platelets, but increased significantly after incubation with supernatant from platelets activated with thrombin, ADP, and TRAP-6. Platelets included as a positive control. (B) MMP-10 secretion followed a similar, but less pronounced, pattern. Thrombin units of concentration: U/ml. ADP and TRAP-6 units of concentration: µM. Graphs representative of two separate experiments, each performed in triplicate. Data compared using one way ANOVA with Šídák's correction for multiple comparisons. *p<0.05, **p<0.01, ***p<0.001, ****p<0.0001.

3.3 Discussion

The data presented above have demonstrated, for the first time to my knowledge, that M.tb can activate platelets. This effect was not seen following contact with the mycobacteria themselves, but rather as a result of activation by M.tb-secreted antigens. The order of magnitude of activation was similar to that observed using LPS as a positive control. This effect may be M.tb strain-dependent as the bacterial secretory profile varies, and it is not clear which of these products are important in immunogenicity or which may interact with platelets(214-217). It may also prove not to be an important effect *in vivo*, as few bacilli are generally present in infection and it is unlikely that the concentrations of M.tb antigens used in this work would be achieved in a patient.

Applying a range of techniques enabled a holistic investigation of platelet activity, encompassing surface receptor upregulation, secretion, and functional responses including aggregation and adherence to other cells. The use of multiple platelet agonists also enabled different signalling mechanisms to be explored. This approach identified that, of the agonists interrogated, ADP was the most responsive both to LPS and to M.tb. It was also found that incorporation of platelet agonists into experimental design is important and without these often no effect was seen, reflecting the frequent requirement for co-stimulation of platelets in order to exert an effect.

The platelet-monocyte co-culture model was able to reliably corroborate the finding that platelets augment M.tb-stimulated MMP secretion previously reported by our group(103) and others(108). Further refinement of the protocol to remove a step involving thrombin activation of platelets circumvented problems associated with inadvertent over-stimulation of platelets which can lead to clotting mid-experiment. Manipulation of this optimized model using specific inhibitors of monocyte signalling pathways showed that platelets enhance monocyte activation through the signalling pathways already understood to be important in M.tb infection, including PI3 Kinase(134, 218) and MAP Kinase(130, 219) pathways. Confirmation of these findings using Western Blot and/or siRNA techniques to rule out any off-target effects of the inhibitors used was not possible within the time frame of this study, but would be the next step in this analysis. In addition, the possibility of Fc receptor activation influencing these results should be investigated using targeted blocking antibodies. Moreover, further work needs to be done to develop an understanding of the role of mTOR, as the results obtained using rapamycin were not consistent;

experimentation using alternative inhibitors that have a more targeted activity would be useful. It would also be important to investigate the role of the signalling pathways described on gene expression and secretion of other MMPs and tissue inhibitors of matrix metalloproteinases (TIMPs), as these are known to be differentially regulated by different signalling mechanisms(126).

Finally, to evaluate the mechanisms involved in platelet activation of monocytes, experimentation initially focused on P-selectin-PSGL-1 interactions, known to be important in platelet-monocyte interactions in other inflammatory diseases. While this receptor interaction does contribute to monocyte activation, platelet-secreted factors were shown to have a greater impact. Further work in this area could involve generation of different phenotypic platelet supernatants following activation with different agonists, characterization of the components of theses secretomes using Luminex and/or a proteomics approach, and exploration of how these each affect monocyte activation. This may lead to the identification of specific secreted products that may be useful for the later development of therapeutic targets to tackle platelet over-activity in tuberculosis.

In summary: platelets can be activated by secreted factors from M.tb, but not by contact with the bacteria themselves, although the biological relevance of this is uncertain. Platelets enhance M.tb-induced monocyte responses, leading to upregulation of MMP secretion. This occurs through well established pathways in the monocyte. The mechanisms by which platelets are able to achieve this remain poorly defined but have been shown to involve secretion of immunologically-active mediators as well as direct cell to cell contact.

Chapter 4 Platelet activity in patients with pulmonary tuberculosis

4.1 Rationale behind the clinical study

The data presented in Chapter 3 are insightful in terms of mechanisms of cellular interactions; however, what is really of interest to clinicians is what is happening in the patient. Platelets, monocytes, and other inflammatory cells each have enormously complex and wide-ranging functions, each affected by dynamic interactions and feedback mechanisms. A simple cellular model cannot encompass the complexities of this cross-talk and as such any *in vitro* findings must be confirmed *in vivo*.

Peru presents an ideal location for the clinical component of this project for a multitude of reasons. It has a high burden of TB and therefore good access to potentially eligible participants, and our group has a good track record of completing patient-focused studies within the chosen study sites. In addition, facilities at the university are comparable to those in resource-rich settings whereas costs including staffing are lower, enabling high quality research to be conducted within a limited research budget.

4.2 Peru and Tuberculosis

4.2.1 Peru

The third largest country in South America and 21st largest country worldwide, Peru is highly biodiverse, with the climate varying from tropical in the Amazon basin of the east, temperate climate in the central Andean highlands, and arid desert on the Western pacific coast. Situated along the Pacific Ring of Fire, it is prone to natural disasters including earthquakes, tsunamis, and flooding.

In July 2021 the population of Peru was estimated at 32,201,224, making it the 45th most populated country worldwide(220). 78.3% of the total population are urban, and over ten million people, a third of the national population, live in the metropolitan coastal capital city, Lima. Ethnically, approximately 60% of the Peruvian population are classed as mestizo (mixed white and Amerindian), around 25% Amerindian, and the remaining 15% comprise white, African descended, and other ethnicities. Life expectancy at birth is 72.8 years for men and 77.2 years for women, and HIV prevalence among adults is estimated at 0.3%(220).

The 1980s saw economic instability as the country was caught up in regional waves of hyperinflation and economic volatility. Peru also suffered a violent internal conflict, which led to political, economic, and social destabilisation the effects of which are still widely felt. The capture of Shining Path leader Abimael Guzman in 1992 effectively signalled the end of the civil war. The past two decades have been characterized by greater stability and economic growth, with Peru boasting one of the fastest growing economies in Latin America. Peru is rich in natural resources and the country's economy depends largely on the exportation of metals including copper, zinc, and gold, as well as other minerals. Although the natural resources are distributed throughout the country, as is common in rapidly growing economies, wealth is centered in cities, particularly Lima. Recent governments have endeavoured to champion social inclusion and a more equitable income distribution, yet economic gains have still mostly benefited the urban and coastal populations, with little change in living standards among minority populations including Afro-Peruvians and indigenous Amerindian populations.

Such heavy dependence on the exportation of metals and other minerals leaves the country's economic position vulnerable to fluctuations in global prices. Between 2009 and 2013 the Peruvian economy grew steadily by an average of 5.6% per year. The rate of poverty (individuals living below $5.5 per day) fell from 52.2% in 2005 to 26.1% in 2015, and extreme poverty, defined as living below $3.2 per day, fell from 30.9% to 11.4%(221). This growth rate slowed between 2014 and 2017 due to a drop in the global metal market, and then recovered, and by 2019 per capita GDP was estimated at $7,028. Sadly, the COVID-19 pandemic and the strict and prolonged quarantine imposed by the government have had a devastating impact, and in 2020 the per capita GDP dropped to $6,127(222).

The SARS-CoV-2 virus struck Peru with merciless ferocity. Peru has suffered the highest rate of deaths worldwide, with 626.72 deaths per 100,000 population, and the second highest case fatality rate at 7.5%(223). Peru was quick to respond to the pandemic, implementing a strict lockdown on March 16th 2020, only ten days after the first reported case of SARS-CoV-2 infection in the country. However, this failed to contain the spread of the virus, and in addition severely affected the national economy. This experience revealed Peru's economic gains to be superficial, leaving the country exposed during a crisis such as the pandemic. With over 70% of working adults engaged in the informal economy, with no contracts, social protection, or worker benefits(224), it was impossible for the majority of the population to adhere to the strict measures. Compounded with other factors including multigenerational living and fragility of the health system, whose crumbling infrastructure and limited critical care facilities became quickly overwhelmed, this led to an inevitable but devastating crisis. It is expected that the COVID-19 pandemic has sent the economy into a deep recession which will last for years to come.

4.2.2 Tuberculosis in Peru

M. tuberculosis DNA has been identified in mummified remains dating back over 1,000 years, informing us that TB has existed in Peru since the pre-colonial era(225). Peru has continued to hold the unfortunate status of having one of the highest rates of TB in the region, and of being a hot spot for the development and transmission of drug-resistant strains. During the 1980s, neoliberal restructuring as well as terrorism, causing a flux of internally displaced persons into poor urban areas and loss of access to large areas of the country, led to the collapse of the public health system in Peru(226). Only 30% of patients diagnosed with TB between 1980 and 1985 were started on treatment, and 41% of these did not complete their course(227). This culminated in a national crisis and in 1991 Peru declared TB a widespread public health problem. Funding to the national tuberculosis programme was increased, WHO global targets were adopted, a mass training scheme for doctors was implemented, drugs were made free to the patient, and regional TB laboratories were expanded from 13 in 1991 to 57 in 1996(226). The number of cases notified peaked due to an increase in case finding, then dropped significantly, such that by 1996 the national TB programme received international recognition as a model programme(228). However,

rates remain high and, with more recent increases in transmission of drug-resistant strains, the control of TB remains a significant challenge.

In 2019 there were 32,970 cases of TB notified nationally, including 28,892 new cases, of which 16,452 were sputum smear positive. This equated to 101.4 cases per 100,000 population, including 88.8 new cases and 50.6 smear-positive cases per 100,000 population (see Figure 4.1). Among these patients were 992 with rifampicin-resistant TB, 303 patients with isoniazid-resistant TB, 1,464 patients with multi-drug resistant (MDR) TB, and 89 cases of extensively drug resistant (XDR) TB (Figure 4.2).

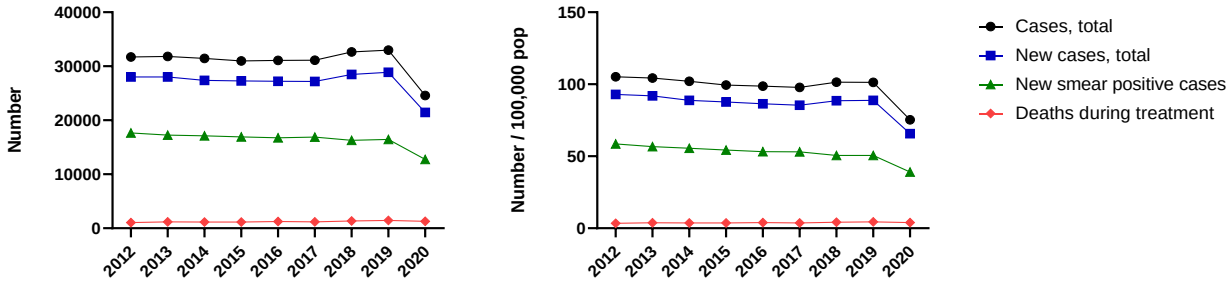

Figure 4.1 Peruvian national trends in notified tuberculosis cases.

Graphs indicating total cases (black circles), new cases (blue squares), new smear-positive cases (green triangles), and deaths during treatment (red diamonds) overall (A) and per 100,000 population (B). Data adapted from Peruvian National Ministry of Health's National Tuberculosis Programme, URL: www.tuberculosis.MINSA.gob.pe. Accessed 08th January 2022.

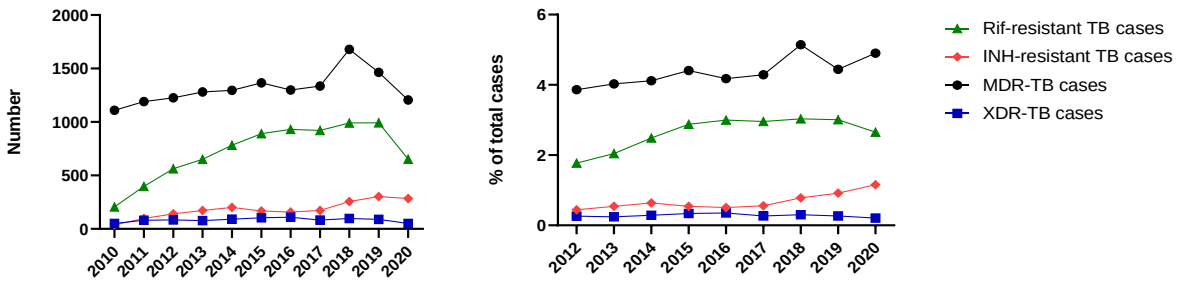

Figure 4.2 Peruvian national trends in drug resistance among notified TB cases.

Total number of cases of Rifampicin (Rif) mono-resistant TB (green triangles), Isoniazid (INH) mono-resistant TB (red diamonds), multi-drug resistant (MDR) TB (black circles), and extensively drug resistant (XDR) TB (blue squares) overall (A) and as a percentage of total notified cases (B). Data adapted from Peruvian National Ministry of Health's National Tuberculosis Programme, URL: www.tuberculosis.MINSA.gob.pe. Accessed 08th January 2022.

In 2020 the official figures presented above show a striking reduction to a total of 75.3 patients per 100,000 population being diagnosed with TB, including 65.7 new cases per 100,000 population which included 39 smear-positive cases per 100,000. Similarly, the number of patients with drug-resistant TB was also noted to have fallen in 2020 overall, although as a proportion of total cases this was unchanged or increasing. Data from the next few years will demonstrate the real effect of the COVID-19 pandemic both on TB incidence and on rates of drug resistant TB in Peru. This is thought to be due to a sharp decline in case detection and treatment enrolment due to the pandemic, and this is anticipated to have adverse long-term consequences on the burden of TB with a forthcoming increase in cases presenting with more severe pathology predicted(228).

4.3 Study Design

4.3.1 Ethical approval

The study protocol was approved by the Institutional Review Boards at the Peruvian Ministry of Health (MINSA), Universidad Peruana Cayetano Heredia (UPCH), Hospital Cayetano Heredia (HCH), and the Asociación Benéfica PRISMA, and written informed consent was obtained from all patients prior to any study-related procedures. All study staff have undergone training in Human Subjects Research prior to working with patients.

4.3.2 Study design

This was a prospective study that comprised a cross-sectional component comparing patients with TB with healthy controls and symptomatic controls (patients with respiratory disease other than TB), and a longitudinal follow-up component to assess responses in the group of TB patients.

Patients with newly diagnosed smear-positive pulmonary TB (group 1) and healthy controls (group 2) were recruited in a case-control design. In addition, patients undergoing a bronchoscopy (group 3) were recruited as a cohort that was followed up prospectively, and patients were classified as either tuberculosis or non-tuberculosis once further information was available. Patients in Group 1 and those diagnosed with TB in Group 3 were followed up at 7 days, 14 days, 28 days, 2 months, and 6 months following initiation of TB treatment. Patients in Group 2 and those not diagnosed with TB in Group 3 were followed up by telephone consultation at 2 months to review whether they had subsequently been diagnosed with TB elsewhere and, for patients in Group 3, to obtain the diagnosis of their presenting illness. A summary of inclusion and exclusion criteria, as well as a participation schedule, is shown in Figure 4.3. HIV status was self-reported by potential participants; where HIV status was not known, a test was offered to the patient, in line with national policy.

4.3.3 Study sites

Laboratory work was undertaken at the Universidad Peruana Cayetano Heredia (UPCH), and patients were recruited from the Hospital Cayetano Heredia (HCH) which is adjacent to UPCH. HCH includes the Centro de Excelencia de Neumología (CENEX), a three storey centre purpose-built in 2014 for the diagnosis and management of pulmonary TB and other respiratory diseases, and comprising an outpatient department, bronchoscopy suite, on-site laboratory for the rapid processing of diagnostic samples, and 15 bed inpatient facility.

Patients referred to the CENEX for investigation for TB undergo a clinical evaluation including a chest x-ray, and are required to submit three or more sputum samples for microscopy and culture. Patients found to have a new positive result are contacted by a TB nurse or technician and asked to return to the clinic whereupon they are given their result by one of the TB doctors and, unless there is a contra-indication or other concern, commenced on standard quadruple anti-TB treatment. The majority of patients are then referred for ongoing therapy and monitoring at their local community TB centre, depending to some extent upon patient accessibility and preference. In 2019, a total of 685 patients were diagnosed with TB at HCH, including 191 smear-positive pulmonary TB outpatients and 72 smear-positive pulmonary TB inpatients; 144 smear-negative pulmonary TB outpatients and 50 smear-negative pulmonary TB inpatients; 41 extrapulmonary TB outpatients and 187 extrapulmonary TB inpatients(229).

The CENEX was attractive as the primary site for patient recruitment as its proximity enabled the processing of blood samples as soon after venepuncture as possible, to prevent platelet activation in transit. However, its location within a large public hospital compounded by the decentralisation of TB services in Lima in the last few years has meant that a large proportion of patients who are diagnosed and treated at the CENEX have multiple co-morbidities, in particular HIV co-infection, and did not meet inclusion/exclusion criteria for this study. Recruitment was thus slower than desirable. The study sites were subsequently expanded to include TB patients attending health centres from the Lima North region and which were under 20 minutes from UPCH by taxi.

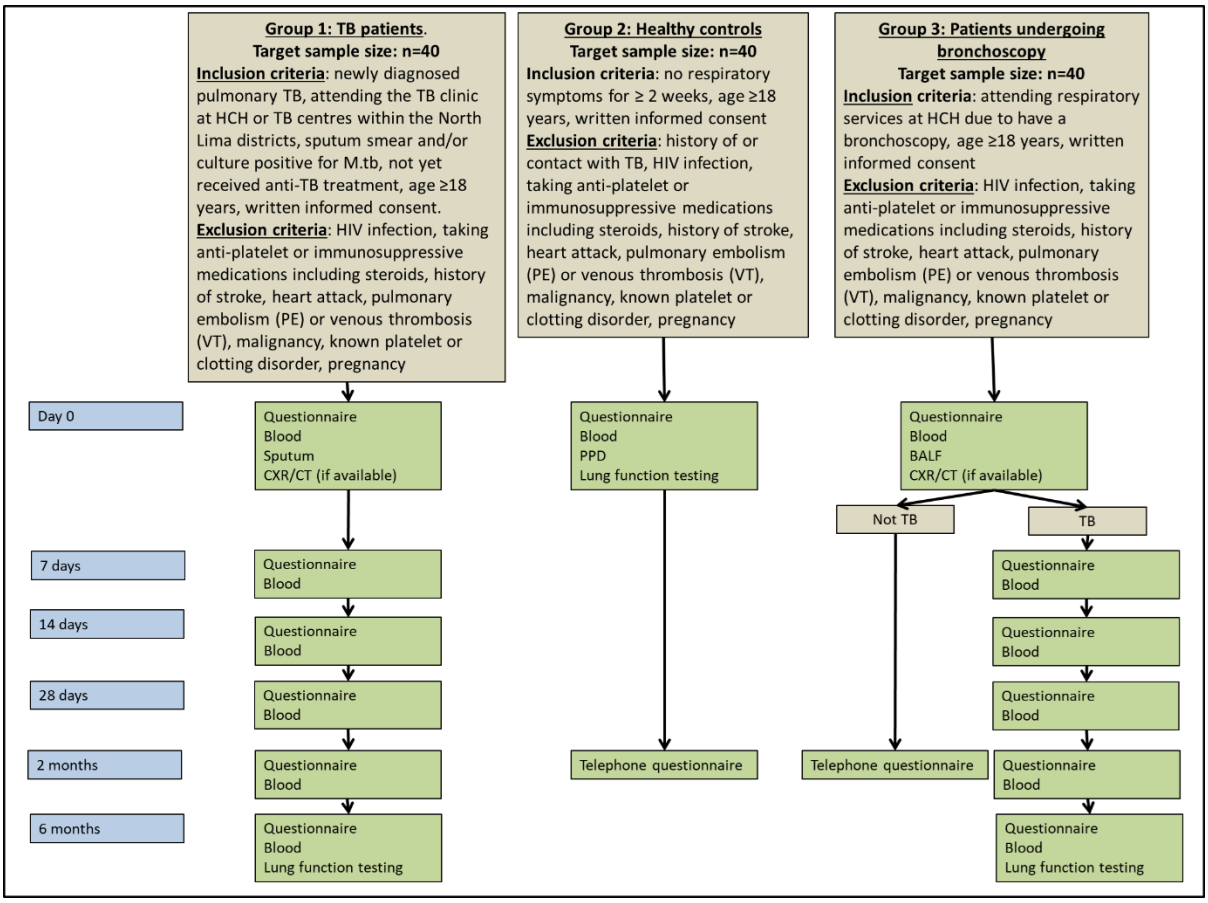

Figure 4.3 Patient participation schedule.

4.3.4 Role of Dr. Kirwan

Dr. Kirwan devised the study design, obtained the necessary permissions, and implemented and optimised all relevant laboratory techniques prior to initiation of the study. She consented patients, obtained biological samples, and processed and/or stored them in the laboratory. As the study progressed Dr. Kirwan trained four laboratory technicians in the laboratory procedures, and two study nurses to consent the patients, obtain data and biological samples, and arrange follow-up. Dr. Kirwan supervised the storage of samples and data, and compiled and analysed the data sets. After the study ended she arranged shipment of plasma and bronchoalveolar lavage fluid (BALF) samples at -80°C to London, UK where she performed further laboratory work including Luminex assays.

4.3.5 Recruitment

4.3.5.1 Group 1: pulmonary TB patients

Sputum samples from patients with suspected TB attending the pulmonology medicine department (CENEX) at the Hospital Cayetano Heredia are processed in the hospital's onsite laboratory. Microscopy results are delivered to a team of nurses and technicians who immediately contact the patient and request that they attend the centre to receive their results from one of the physicians. Sputum samples from patients presenting to their local health centres are sent to the National TB Centre's laboratory for processing. Results are communicated as soon as they become available to the health centre who then contact the patient and arrange treatment.

Our team were in daily contact with the nurses and/or technicians at the hospital and in each of the participating health centres, in person or by telephone. The clinical team (doctors, nurses, and/or technicians) identified any patients who may be eligible for the study and delivered the diagnosis as per usual procedures, and afterwards informed the patients about the study and invited them to meet the study team. If they agreed, the study team were informed immediately, and approached the patient to explain the study and invite them to participate.

4.3.5.2 Group 2: Healthy controls

Healthy controls were identified from relatives of patients attending the outpatient clinic at the CENEX with non-TB respiratory disease. At the end of the consultation, the clinician informed the relatives of the study and invited them to participate. If they agreed, the study nurses then approached the relative to explain the study and obtain informed consent.

4.3.5.3 Group 3: Bronchoscopy patients

Bronchoscopies are performed in a designated suite within the respiratory department at the Hospital Cayetano Heredia (CENEX). Patients scheduled for a bronchoscopy were approached prior to their procedure and, if inclusion/exclusion criteria were met, were invited to participate in the study.

4.3.6 Procedures

After the participant provided written informed consent, the study nurse or doctor conducted a questionnaire. Patients in Group 1 were asked to provide a sputum sample to confirm diagnosis by smear microscopy in our TB lab at UPCH. For patients undergoing a bronchoscopy, a sample of bronchoalveolar lavage fluid (BALF) was obtained from the clinical team immediately after the procedure was completed. Bloods were taken from all patients and transported immediately to the laboratory at UPCH. This was the final procedure, and the time of venepuncture was noted.

Participants from Groups 1 and those who were diagnosed with TB in group 3 were followed up prospectively, with visits scheduled to take place at 7 days, 14 days, 28 days, month 2, and month 6 of treatment, as our preliminary data are suggestive of an initial inflammatory response that peaks at Day 14 then resolves. At each visit a follow-up questionnaire was completed and blood sampling and processing repeated. In addition, participants from Group 2 were scheduled to have a purified protein derivative (PPD) test performed at the respiratory department at the Hospital Cayetano Heredia and lung function testing was also scheduled as soon as was convenient for them. Patients with TB (Groups 1 and 3) were scheduled to have lung function testing performed following their final visit at treatment completion (6 months).

4.3.6.1 Questionnaire

A questionnaire was completed at all visits and collected demographic information and clinical data, microbiology, including results of sputum smear and mycobacterial culture, and date and result of HIV test if known.

4.3.6.2 Blood samples

The following were collected at each visit: (1) 10mls (2 tubes) in EDTA for measurement of immunological markers including cytokines and MMPs, and for storage of platelet RNA, (2) 20mls (5 x 4ml tubes) in citrate to evaluate platelet activity by flow cytometry and LTA, (3) 4mls in heparin for measurement of immunological markers including cytokines and MMPs.

4.3.6.3 Measurement of secreted factors in plasma

Whole blood collected in EDTA were centrifuged and the supernatant frozen within 30mins. Samples were stored at -80°C and shipped to SGUL at the end of the study, where analysis was later performed using custom Luminex arrays (see methods section 2.11).

4.3.6.4 Flow cytometry

Whole blood was stained with monocyte and platelet markers and platelet/monocyte aggregation and platelet activation assessed (see section 2.14). 25ul aliquots of whole blood were with antibodies and/or stimulants to give a total volume of 100ul. Samples were processed both without agonists, to detect changes in resting platelet status, and with TRAP-6 or ADP to investigate platelet reactivity, and this was performed in the presence or absence of 25ul M.tb-secreted antigens (see section for preparation) or 7H9 control. Each condition was performed in duplicate. These samples were incubated in the dark for 20 minutes, after which fix-lysis solution was added. After a further 15 minutes in the dark, 1ml PBS was added. The samples were kept in the dark at 4°C until evaluation using a BD FACSCanto™ II flow cytometer, within 72h. Compensation across channels was performed for each combination of fluorophores, and slow flow rates were used to minimize false-positive aggregates. Data were analysed using FlowJo v10 operating software and GraphPad PRISM v9.1.2.

4.3.6.5 Light transmission aggregometry (LTA)

Whole blood collected from patients was transported immediately to the laboratory and was processed immediately upon arrival. The blood was centrifuged for 15 mins at 150 x *g* at room temperature to obtain platelet rich plasma (PRP) which was incubated in a ratio of 2:1 with M.tb-secreted antigens (see methods section 2.2), LPS diluted in 7H9 to give a final concentration of 100 µg/ml, or 7H9 control for 30 minutes at room temperature. 90µl of the sample was then added to a 96 well plate pre-loaded with serial dilutions of platelet agonists ADP, TRAP-6, and collagen. The plate was immediately inserted into a TECAN Sunrise™ plate reader and absorbance read at 595nm every 20 seconds at 37°C and with shaking for a total of 40 cycles. Data were downloaded in Excel format. (See methods section 2.13).

4.3.6.6 Bronchoalveolar lavage fluid (BALF)

To investigate immunopathology at the site of disease itself, bronchoalveolar lavage fluid (BALF) samples were obtained from respiratory symptomatic patients undergoing bronchoscopy (Group 3). These patients were retrospectively defined as TB or non-TB respiratory symptomatics once results became available.

BALF samples were transported into the Category 3 laboratory at UPCH and processed inside a hood. Following removal of an aliquot for culture using the MODS method(230, 231), the sample was poured through a 70µl filter into a sterile 50ml Falcon tube to remove cellular debris. It was then placed in a sealed bucket and centrifuged at 13,000 x *g* for 10 minutes, then the supernatant filtered through a 0.22µl filter to remove any M.tb(166). The sterile supernatant was then aliquoted and stored at -80°c. Samples were shipped to SGUL at the end of the study, where analysis was later performed using custom Luminex arrays (see methods section 2.11).

4.3.6.7 Spirometry

Pulmonary function testing was performed using a standard spirometer in collaboration with colleagues at a private clinic in Lima (Clínica La Luz). Our group has used this technique in both rural and urban settings in Peru. Measured parameters include forced expiratory volume-one second (FEV1), forced vital capacity (FVC), FEV1/FVC(%), and % predicted FEV1 and FVC. This was performed both without, and ten minutes after bronchodilatation with 2 puffs of salbutamol.

4.4 Results: Patient demographics and clinical data

4.4.1 Patient demographics at enrolment

Patient enrolment to the study was carried out between 30th April 2019 and 13th March 2020. The country declared a National State of Emergency due to COVID-19 with strict lock-down measures on 15th March 2020(232) at which point the study was closed abruptly. No further patients were recruited, and no further follow-up visits took place.

Patient demographic and clinical data are presented in Table 3. 11 patients with smear-positive pulmonary TB were recruited from the hospital, including one from the emergency department

and one from an inpatient ward, and 6 from local health centres. Median age was 37 years and just over half were males. We also evaluated 14 healthy controls who were older (median age 45 years) and more likely to be female (71%) although these differences did not reach significance (p=0.093 and p=0.28, respectively).

Mean age of the bronchoscopy patients was 55 years, and 44% were males. Eight bronchoscopy patients were classified as having TB and 17 were classified as TB-negative respiratory symptomatic controls (see Section 4.4.3 below). The bronchoscopy patients who were diagnosed with TB were significantly younger than those who were not (median age 23 years vs 60 years respectively, p=0.0085). Accordingly, when these patients were combined with the pulmonary TB patients from Group 1 to give a total of 25 TB patients, this group of patients was younger than both the healthy controls (median age 28 years vs 48 years, p=0.026) and also the respiratory symptomatic controls (median age 28 years vs 60 years, p=0.0004).

Body mass index (BMI) was lower for TB patients than non-TB patients (23.3 vs 25.97, p=0.028, two-tailed Mann-Whitney test).

The majority of TB patients (66.7%) reported either a family member or other known contact with TB, whereas among non-TB patients this was 35.5%.

Five pulmonary TB patients and four bronchoscopy patients were taking antibiotics at the time of enrolment. Six patients in the pulmonary TB group were already taking anti-TB medications at the time of enrolment, for a median of 2 and a maximum of 5 days. All bronchoscopy patients had their baseline evaluation and blood sample taken on the day of the bronchoscopy. Of the eight bronchoscopy patients who were diagnosed with TB, one had already started treatment 7 days prior to her bronchoscopy; her MODS culture was negative. Two patients commenced treatment the day after their bronchoscopy, three patients two days later, and one patient four days later. The final patient, a 22 year old student, was lost to follow-up to the clinic and so information on whether or not he was treated is not available. He had been made aware of his positive MODS result and his diagnosis, and may have been treated elsewhere.

11 healthy controls had PPD tests done for latent TB, of which 7 were positive, defined as a lesion measuring ≥10mm. These patients were defined as having latent TB. There was no difference in age, sex, or BMI in healthy controls with or without latent TB (median age 48 vs 45 yrs, p=0.56; males comprised 14.3% vs 42.9%, p=0.56, BMI was 27.9 vs 26.0, p=0.10).

Table 3 Demographics of all patients enrolled to the study

	Pulmonary TB (N=17)¥	Bronchoscopy, TB-positive (N=8)	Bronchoscopy, TB-negative (N=17)	Healthy controls (N=14)
Age, median (IQR)	37 (23-45)	23 (19-32)	60 (47-71)	45 (33-53)
No. of males (%)	9 (52.9%)	4 (50%)	7 (41%)	4 (28.6%)
BMI, median (IQR)*	23.3 (21.2-27.5)	20.7 (22.9-24.2)	23.9 (22.2-29.3)	27.1 (25.7-27.8)
Marital status				
Single (%)	8 (47.1%)	7 (87.5%)	7 (41.2%)	5 (35.7%)
Married or co-habiting (%)	9 (52.9%)	1 (12.5%)	6 (35.3%)	8 (57.1%)
Separated or divorced (%)	0	0	1 (5.9%)	1 (7.1%)
Widowed (%)	0	0	2 (11.8%)	0
Unknown (%)	0	0	1 (5.9%)	0
Education				
Incomplete primary education (%)	0	1 (12.5%)	1 (5.9%)	1 (7.1%)
Completed primary education (%)	3 (17.6%)	0	4 (23.5%)	1 (7.1%)
Completed secondary education (%)	6 (35.3%)	4 (50%)	3 (17.6%)	5 (35.7%)
Higher education (%)	8 (47.1%)	3 (37.5%)	9 (52.9%)	7 (50%)
Site of recruitment				
CENEX (%)	9 (52.9%)	8 (100%)	16 (94.1%)	14 (100%)
Emergency department (%)	1 (5.9%)	0	0	0
Hospital inpatient (%)	1 (5.9%)	0	1 (5.9%)	0
Health centre (%)	6 (35.3%)	0	0	0
Smoking and alcohol history				
Current smoker (%)	2 (12.5%)	1 (12.5%)	1 (5.9%)	0
Ex-smoker (%)	8 (50%)	2 (25%)	4 (23.5%)	0

Current alcohol consumption				
Never (%)	7 (43.8%)	1 (12.5%)	7 (71.2%)	5 (35.7%)
0-1 times per month (%)	7 (43.8%)	5 (62.5%)	9 (52.9%)	9 (64.3%)
2-4 times per month (%)	1 (6.3%)	2 (25%)	1 (5.9%)	0
2-4 times per week (%)	0	0	0	0
>4 times per week (%)	1 (6.3%)	0	0	0
Recent HIV test (%)	6 (37.5%)	3 (37.5%)	10 (58.8%)	8 (57.1%)
History of family member with TB (%)	8 (50%)	5 (62.5%)	5 (29.4%)	2 (14.3%)
Other known TB contact (%)	3 (18.8%)	0	1 (5.9%)	3 (21.4%)
Past medical history				
Asthma (%)	2 (12.5%)	2 (25%)	3 (17.6%)	1 (7.1%)
COPD (%)	1 (6.3%)	0	0	0
Hypertension (%)	1 (6.3%)	0	2 (11.8%)	1 (7.1%)
Hypercholesterolaemia (%)	0	0	2 (11.8%)	3 (21.4%)
Myocardial infarction (%)	0	0	0	0
Angina (%)	0	0	0	0
Heart failure (%)	0	0	0	0
Stroke (%)	0	0	0	0
TIA (%)	0	0	0	0
Vasculitis (%)	0	0	0	0
Diabetes (%)	3 (18.8%)	0	0	1 (7.1%)
Cancer (%)	0	0	1 (5.9%)	0
Chronic renal disease (%)	0	0	0	0
Current medications				
Antibiotics (%)	5 (31.3%)	2 (25%)	2 (11.8%)	0
Anti-TB treatment (%)	6 (35.3%)	1 (12.5%)	0	0
Days on anti-TB therapy, median (IQR)	2 (1.25-3.5)	7	N/A	N/A

¥*data other than basic demographics not available for one patient from the pulmonary TB group*

**data missing from 2 pulmonary TB patients and 1 healthy control*

4.4.2 Clinical features

Clinical features at diagnosis are presented in Table 4. Patients with smear-positive pulmonary TB reported a median symptom duration of 8 weeks prior to diagnosis (IQR 4-14 weeks), whilst bronchoscopy patients reported a median duration of 4 weeks (IQR 3-12 weeks). There was no difference in symptom duration between patients diagnosed with TB and TB-negative bronchoscopy patients (median 6 vs 8 weeks, p=0.95, two-tailed Mann Whitney test).

Figure 4.4 shows the distribution of symptoms across the different patient groups. This graph indicates that it is not possible to differentiate the groups based on symptoms alone. One or more of the main triad of TB symptoms of fever, cough, and weight loss was reported in all of the TB patients and 70.6% of the bronchoscopy patients who were not diagnosed with TB. All three symptoms were reported in 9 patients with pulmonary TB, 1 bronchoscopy patient with TB, and 4 bronchoscopy patients who did not have TB.

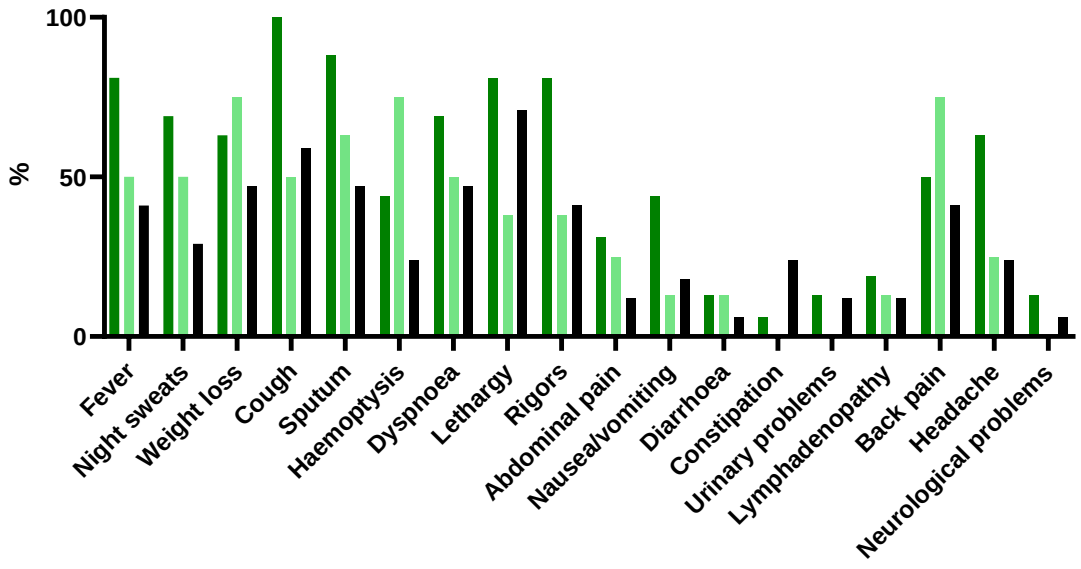

Figure 4.4 Distribution of symptoms in all participants at baseline assessment.

Percentage of patients with smear-positive pulmonary TB (dark green bars), TB diagnosed following bronchoscopy (light green bars), or non-TB bronchoscopy patients (black bars) reporting symptoms at recruitment. Graph indicates that symptoms do not cluster and it is not possible to assign patients to a group based on symptoms alone.

62.5% of patients with smear-positive pulmonary TB and 75% of TB-positive bronchoscopy patients reported weight loss in the past year, compared to 47.1% of TB-negative bronchoscopy patients (Table 4). Two TB patients reported weight loss greater than 10kg.

Appetite was assessed at recruitment using the simplified nutritional appetite questionnaire (SNAQ), which is included in the appendix (Section 7.2), and has been validated and applied in a range of populations and settings(233) including Bolivian(234) and Peruvian(103, 235) patients with TB. A SNAQ score of <14 is considered to represent poor appetite and is predictive of significant weight loss in the next six months(236). Total SNAQ scores were lower for TB patients than non-TB patients (median 13.5 vs 15.0, p=0.0008, two-tailed Mann-Whitney test) indicative of poorer appetite in this group and a risk of further weight loss.

The modified CES-D score is included in the appendix (Section 7.3) in both English and Spanish. The Spanish version of this five-item score has previously been validated in a Peruvian cohort(237). It has a minimum score of 5 and a total score of 20; a score of 6 or above has been associated with major depressive episodes(238). Total modified CES-D scores were higher for TB patients than non-TB patients (median 7.5 vs 5.0, p=0.0069), and 18 patients with TB had scores of 6 or above, compared with 10 patients without TB (75% vs 32.3%, p=0.0026, two-sided Fisher's exact test).

Table 4 Clinical data from all participants at baseline

	Pulmonary TB (N=16)	Bronchoscopy, TB-positive (N=8)	Bronchoscopy, TB-negative (N=17)	Healthy controls (N=14)
Symptoms				
Duration of symptoms, weeks. Median (IQR)	8 (4-14)	4 (3-6)	8 (4-12)	0
Weight loss in the last year (%)	10 (62.5%)	6 (75%)	8 (47.1%)	0
≤5kg (%)	3 (18.8%)	5 (62.5%)	5 (29.4%)	0
6-10kg (%)	3 (18.8%)	0	3 (17.6%)	0
11-20kg (%)	1 (6.3%)	0	0	0
>20kg (%)	1 (6.3%)	0	0	0
Unknown (%)	2 (18.8%)	1 (12.5%)	0	0
N/A (%)	6 (37.5%)	2 (25%)	9 (52.9%)	0
Malaise (%)	13 (81.3%)	3 (37.5%)	12 (70.6%)	0
Fever (%)	13 (81.3%)	4 (50%)	7 (41.2%)	0
Rigors (%)	13 (81.3%)	3 (37.5%)	7 (41.2%)	0
Night sweats (%)	11 (68.8%)	4 (50%)	5 (29.4%)	0
Cough for ≥15 days (%)	16 (100%)	4 (50%)	10 (58.8%)	0
Sputum (%)	14 (87.5%)	5 (62.5%)	8 (47.1%)	0
Haemoptysis (%)	7 (43.8%)	6 (75%)	4 (23.5%)	0
Dyspnoea (%)	11 (68.8%)	4 (50%)	8 (47.1%)	0
Abdominal pain (%)	5 (31.3%)	2 (25%)	2 (11.8%)	0
Nausea and/or vomiting (%)	7 (43.8%)	1 (12.5%)	3 (17.6%)	0
Diarrhoea (%)	2 (18.8%)	1 (12.5%)	1 (5.9%)	0
Constipation (%)	1 (6.3%)	0	4 (23.5%)	0
Urinary problems (%)	2 (18.8%)	0	2 (11.8%)	0
Enlarged lymph nodes (%)	3 (18.8%)	1 (12.5%)	2 (11.8%)	0
Back pain (%)	8 (50%)	6 (75%)	7 (41.2%)	0
Headache (%)	10 (62.5%)	2 (25%)	4 (23.5%)	0
Confusion or neurology (%)	2 (18.8%)	0	1 (5.9%)	0

Appetite: SNAQ questionnaire				
1 Appetite, median (IQR)	2 (2-3)	3 (3-4)	3 (3-4)	3 (3-4)
2 Satisfaction, median (IQR)	3 (2-4)	4 (4-4)	4 (4-4)	4 (4-4)
3 Flavour, median (IQR)	3 (2-3)	3 (3-3)	3 (3-3)	3 (3-4)
4 Meals, median (IQR)	4 (4-4)	4 (4-5)	4 (4-4)	5 (4-5)
Total SNAQ score, median (IQR)	12 (11-14)	15 (14-15)	14 (14-15)	15 (14-16)
Depression: modified CES-D score				
1 Sadness, median (IQR)	2 (1-3)	2 (1-2)	1 (1-2)	1 (1-1)
2 Depression, median (IQR)	2 (1-2)	2 (1-2)	1 (1-2)	1 (1-1)
3 Failure, median (IQR)	1 (1-2)	1 (1-1)	1 (1-1)	1 (1-1)
4 Loneliness, median (IQR)	1 (1-2)	1 (1-1)	1 (1-2)	1 (1-1)
5 Sadness, median (IQR)	2 (2-3)	1 (1-1)	1 (1-2)	1 (1-1)
Total modified CES-D score, median (IQR)	9 (6-10)	7 (5-8)	6 (5-8)	5 (5-5)
No. of patients with score ≥6 (%)	13 (81.3%)	5 (62.5%)	9 (52.9%)	1 (7.1%)

4.4.3 Microbiological data and definition of TB diagnosis

All of the patients in group 1 had been AFB-positive according to samples processed at the hospital's microbiology laboratory as per the inclusion criteria. In addition, sputum samples were obtained by the study for Auramine microscopy and MODS culture in our own laboratory at UPCH. BALF samples from all 25 bronchoscopy patients also underwent Auramine microscopy and MODS culture in the UPCH laboratory. Microbiological data are presented in Table 5.

12 of 14 sputum samples obtained from the pulmonary TB patients were positive on Auramine microscopy, and 13 were positive according to MODS culture. 11 patients had fully susceptible strains. One demonstrated rifampicin mono-resistance and one patient's isolate was resistant to both rifampicin and isoniazid. This information was relayed to the clinical team and both patients' treatment regimens were modified accordingly; they were excluded from further participation in the study.

Of the bronchoscopy patients, 6 had a positive BALF MODS culture in our laboratory, all of whom had strains sensitive to both rifampicin and isoniazid. One patient had a paucibacillary Auramine smear and an indeterminate MODS result. Results of all other TB investigations for this patient were negative; the clinicians determined that he did not have TB so he was classed as negative for the purposes of the study. 18 patients had negative MODS results. An additional two patients, females aged 19 and 22 years, were commenced on anti-TB therapy based on clinical and/or radiological findings. Therefore 8 bronchoscopy were classified as having TB and 17 were classified as not having TB (i.e. respiratory symptomatic controls).

Table 5 Results of microbiological data performed as part of study

	Pulmonary TB (N=17)	**Bronchoscopy, TB-positive (N=8)**	**Bronchoscopy, TB-negative (N=17)**
Sputum sample provided	14	0	0
BALF sample provided	0	8	17
Auramine result			
Negative (%)	2 (14.3%)	5 (62.5%)	16 (94.1%)
Paucibacillary (%)	5 (35.7%)	1 (12.5%)	1 (5.9%)
1+ (%)	5 (35.7%)	2 (25%)	0
2+ (%)	0	0	0
3+ (%)	2 (14.3%)	0	0
MODS result			
Positive, fully sensitive (%)	11 (78.6%)	6 (75%)	0
Positive, rifampicin mono-resistant (%)	1 (7.1%)	0	0
Positive, rifampicin- and isoniazid-resistant (MDR; %)	1 (7.1%)	0	0
Indeterminate (%)	0	0	1 (5.9%)
Negative (%)	1 (7.1%)	2 (25%)	16 (94.1%)

4.4.4 Longitudinal follow-up of TB patients

Follow-up dates were calculated based on the date of treatment initiation. Two of 17 patients from group 1 completed the six month follow-up period as scheduled. Of the remaining 15 patients, three completed their two month visit, three completed their 4 week visit, one completed their two week visit, and eight completed their baseline visit only. Two patients were found to have MDR-TB after their baseline visits so were excluded from further participation, one patient had a drug-induced hepatotoxicity and was admitted to hospital and did not participate further. Six patients' participation terminated because their subsequent visit was scheduled for after March 15th 2020. The remaining six patients were lost to follow-up due to lack of time to complete follow-up visits (n=1), no longer wishing to have blood taken for the study (n=1), or unspecified reasons (n=4).

Of the eight bronchoscopy patients with a diagnosis of TB, none completed the full six months. Two completed a two month visit, and one completed their four week visit; the remaining five were evaluated at baseline only. Three patients were lost from the study because their subsequent visit was scheduled for after March 15th 2020, and five were lost to follow-up, of whom two specified that this was due to a lack of time.

Pulmonary function testing was performed on one patient, after completion of their six-month treatment regimen, and ten healthy controls. As this is insufficient for analyses, these data shall not be discussed further.

4.5 Platelet aggregation

To investigate the functional activity of platelets in TB, light transmission aggregometry was performed as described in Methods Section 2.13. Whole blood collected from participants in blue-top citrate vacutainer tubes was transported promptly to the laboratory at UPCH and processed immediately. The blood was decanted into two 15ml Falcon tubes and centrifuged for 15 mins at 150 x *g* at room temperature, with slow acceleration and deceleration (centrifuge settings 3 and 1 respectively), to obtain platelet rich plasma (PRP). This was transferred to a new 15ml Falcon tube, inverted gently, and three aliquots separated. These were incubated in a ratio of 2:1 with M.tb-secreted antigen preparation (see Methods Section 2.2), LPS diluted in 7H9 to give a final concentration of 100 µg/ml, or 7H9 control, for 30 minutes at room temperature. 90µl of the sample was then added to wells of a 96 well plate that had been pre-loaded with serial dilutions of platelet agonists ADP, collagen, and TRAP-6. Control wells containing PRP and PPP (platelet poor plasma, prepared by centrifugation of 1ml PRP at max speed and separation of the plasma) were included. The plate was immediately inserted into a TECAN Sunrise™ plate reader and absorbance read at 595nm every 20 seconds at 37°C and with shaking for a total of 40 cycles. Data were downloaded in Excel format and analysed in GraphPad PRISM v9.1.2.

Platelet aggregation data are available for all patients. The time from venepuncture to sample centrifugation was consistently short: a median of 25 minutes (IQR 21 to 30 minutes) for Group 1, 17.5 minutes (IQR 15.25 to 19.75 minutes) for Group 2, and 21 minutes (IQR 17.3 to 30 minutes) for Group 3.

4.5.1 The effect of pulmonary tuberculosis on platelet aggregation

4.5.1.1 Platelets obtained from patients with tuberculosis displayed an altered tendency to aggregate in response to stimulation with platelet agonists.

Aggregation of platelets obtained from sputum smear-positive TB patients (n=17) was reduced compared to the aggregation of platelets obtained from healthy controls (n=14) in the presence of ADP at concentrations of 30µg/ml (69.0% vs 79.9%, p=0.033), 10µg/ml (59.7% vs 75.6%, p=0.0005), and 3µg/ml (44.8% vs 57.5%, p=0.0079), but not at the three lower concentrations used (Figure 4.5 A). In response to collagen, platelet aggregation was reduced at a concentration

of 3µg/ml only in patients with smear-positive pulmonary TB versus healthy controls (54.8% vs 40.2%, p=0.0044, (Figure 4.5 B); there was no difference in response to stimulation with TRAP-6 (Figure 4.5 C).

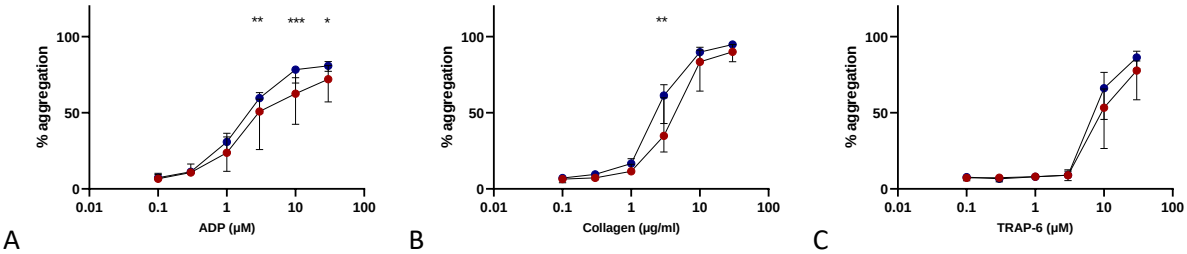

Figure 4.5 Maximum agonist-induced platelet aggregation in patients with smear-positive pulmonary TB versus healthy controls.

Data show maximal platelet aggregation in response to stimulation with increasing concentrations of ADP (A), collagen (B), or TRAP-6 (C), in patients with newly diagnosed smear-positive pulmonary TB (red circles, n=17) compared to healthy controls (navy circles, n=14). Agonist-induced maximal platelet aggregation was reduced in patients with smear-positive pulmonary TB compared to healthy controls, particularly in response to ADP. Data points represent median value and error bars show interquartile ranges. Data compared using a two-way ANOVA with Šídák's correction for multiple comparisons. * $p<0.05$, ** $p<0.01$, *** $p<0.001$.

Similarly, platelet aggregation was reduced in bronchoscopy patients who were diagnosed with TB following their procedure (n=8) compared to those who were not (n=17) in the presence of ADP at concentrations of 1µg/ml (22.2% vs 33.4%, p=0.049) and 0.3µg/ml (11.7% vs 15.3%, p=0.051, Figure 4.6 A). There was a trend towards reduced collagen- and TRAP-6-induced aggregation of platelets from bronchoscopy patients with TB versus those without, although these did not reach statistical significance (Figure 4.6 B and C).

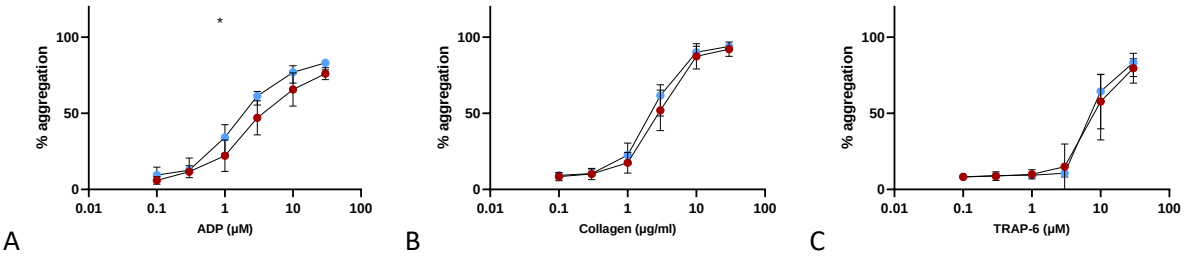

A B C

Figure 4.6 Maximum agonist-induced platelet aggregation in patients who underwent bronchoscopy and were diagnosed with TB compared to those who were not.

Graphs show platelet aggregation in response to stimulation with increasing concentrations of ADP (A), collagen (B), or TRAP-6 (C), in patients who underwent bronchoscopy and were subsequently diagnosed with TB (red circles, n=8) compared to bronchoscopy patients who were not diagnosed with TB (light blue, n=17). There was a trend towards reduced agonist-induced maximal platelet aggregation in patients who underwent a bronchoscopy and were subsequently diagnosed with TB compared to those who were not. Data points represent median value and error bars show interquartile ranges. Data compared using a two-way ANOVA with Šídák's correction for multiple comparisons. * $p<0.05$.

Findings were similar when these patient groups were combined to represent all TB patients (n=25) compared against healthy controls (Figure 4.7 A-C). More strikingly, when all TB patients were compared against all non-TB participants (n=31) there was a notable decrease in platelet aggregation in the TB patient group compared to the non-TB group, particularly in response to ADP (30µg/ml 71.1% vs 80.0%, $p=0.0087$; 10µg/ml 61.5% vs 74.9%, $p<0.0001$; 3µg/ml 45.5% vs 57.9%, $p<0.0001$; 1µg/ml 24.1% vs 32.0%, $p=0.031$, Figure 4.7 D-F).

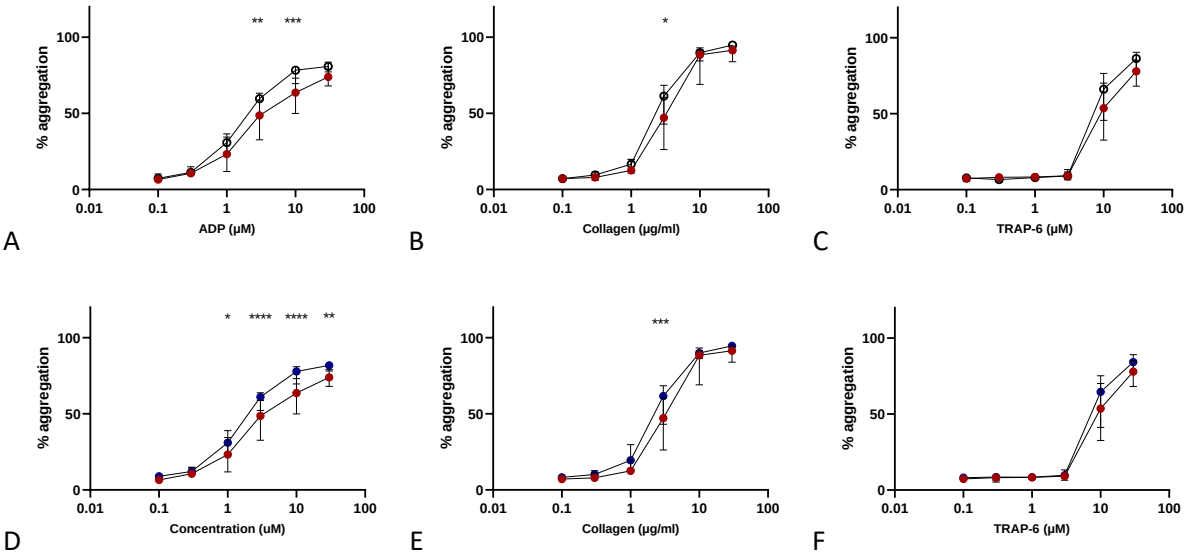

Figure 4.7 Maximum agonist-induced platelet aggregation in TB patients compared to TB-negative controls.

Maximum platelet aggregation in response to stimulation with increasing concentrations of ADP (A,D), collagen (B,E), or TRAP-6 (C,F). Graphs show data from all patients with a diagnosis of TB (red circles, n=25) compared healthy controls (open circles, n=14, A-C) and also compared to all TB-negative patients, i.e. healthy controls plus bronchoscopy patients who were not diagnosed with TB (navy circles, n=31, D-F). Agonist-induced maximal platelet aggregation was lower in patients with TB compared to patients without TB, particularly in response to ADP; a lesser difference was seen following stimulation with collagen, and there was no significant difference in maximal aggregation following stimulation with TRAP-6. Data points represent median value and error bars show interquartile ranges. Data compared using a two-way ANOVA with Šídák's correction for multiple comparisons. $p<0.05$, ** $p<0.01$, *** $p<0.001$, **** $p<0.0001$.

Of note, there was no difference between platelet aggregation in samples from healthy controls and non-TB bronchoscopy patients in response to any of the three agonists used (Figure 4.8).

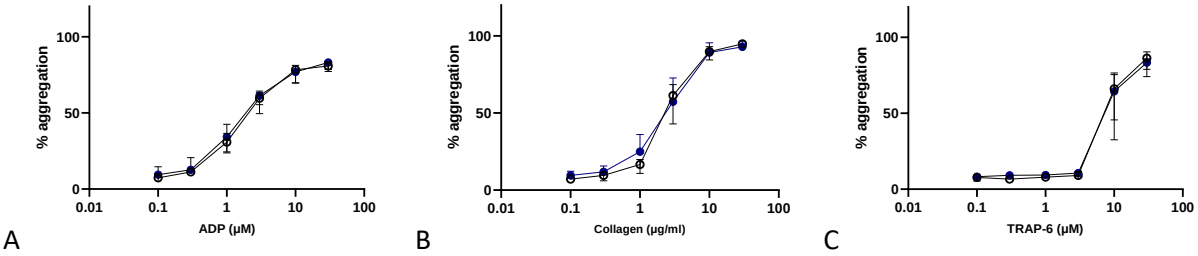

A B C

Figure 4.8 Maximal agonist-induced platelet aggregation in participants without TB.

Maximum platelet aggregation in response to stimulation with increasing concentrations of ADP (A), collagen (B), or TRAP-6 (C). Graphs show data from healthy controls (open circles, n=14) compared to plus bronchoscopy patients who were not diagnosed with TB (navy circles, n=17). There was no difference in aggregation in response to any of the agonists used in these two groups of participants. Data points represent median value and error bars show interquartile ranges. Data compared using a two-way ANOVA with Šídák's correction for multiple comparisons.

Taken together, these data indicate that pulmonary TB, but not other pulmonary disease, leads to a reduced tendency of platelets to aggregate in response to stimulation with platelet agonists, in particular ADP.

4.5.1.2 Platelet aggregation in response to stimulation with LPS was not affected by a diagnosis of tuberculosis or by non-TB respiratory disease.

The addition of LPS and M.tb-secreted antigens enabled evaluation of whether *ex vivo* platelets from patients with tuberculosis had altered responsiveness to these antigens compared to platelets obtained from participants without tuberculosis.

Aggregation responses were compared in PRP incubated with or without 100µg/ml LPS prior to addition to a 96-well plate pre-loaded with agonists.

There was a trend towards increased platelet aggregation in PRP pre-incubated with LPS compared to addition of PRP pre-incubated with 7H9 control. However, this did not reach statistical significance for any of the three agonists used in either patients with smear-positive

pulmonary TB or bronchoscopy patients diagnosed with TB (not shown), or when these two groups were combined (Figure 4.9). In TB-negative patients, a difference was only observed in response to 10µM TRAP-6; this difference was observed in healthy controls but not TB-negative bronchoscopy patients (not shown), and persisted these two groups were combined (maximal aggregation 57.2% without LPS vs 66.3% with LPS, p=0.011, Figure 4.10 C).

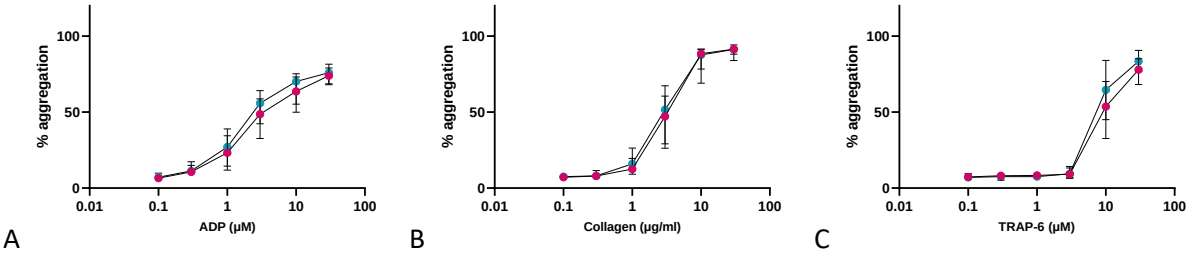

Figure 4.9 The effect of LPS on maximal agonist-induced platelet aggregation in TB patients.

There was no difference in maximal platelet aggregation in PRP incubated with (turquoise circles) compared to PRP incubated without (red circles) LPS in response to stimulation with platelet agonists (A) ADP, (B) collagen, or (C) TRAP-6. Data from all patients diagnosed with TB, n=25. Data points represent median value and error bars show interquartile ranges. Data compared using a two-way ANOVA with Šídák's correction for multiple comparisons.

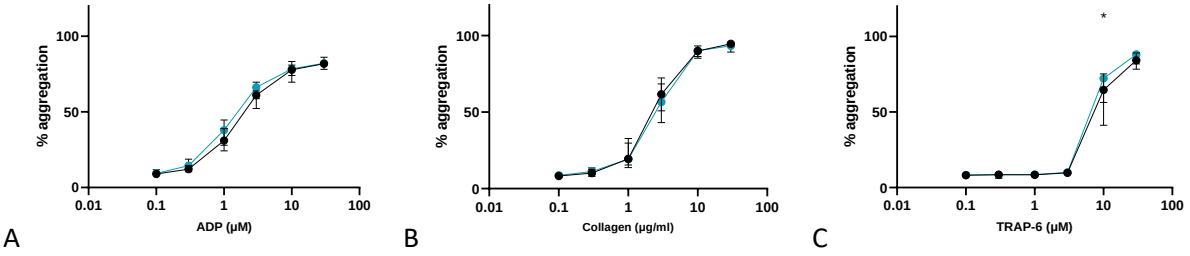

Figure 4.10 The effect of LPS on maximal agonist-induced platelet aggregation in TB-negative patients.

Maximal platelet aggregation in PRP incubated with LPS (turquoise circles) compared to PRP incubated with 7H9 control media (black circles) in response to stimulation with platelet agonists (A) ADP, (B) collagen, or (C) TRAP-6. LPS-stimulated maximal platelet aggregation was only

significantly higher in the presence of 10µM TRAP-6. Data from all patients without TB (healthy controls plus respiratory symptomatic controls), n=31. Data points represent median value and error bars show interquartile ranges. Data compared using a two-way ANOVA with Šídák's correction for multiple comparisons. *p<0.05.

Differences observed in platelet responses in TB vs non-TB patients were preserved, albeit less obvious, when LPS was added (Figure 4.11).

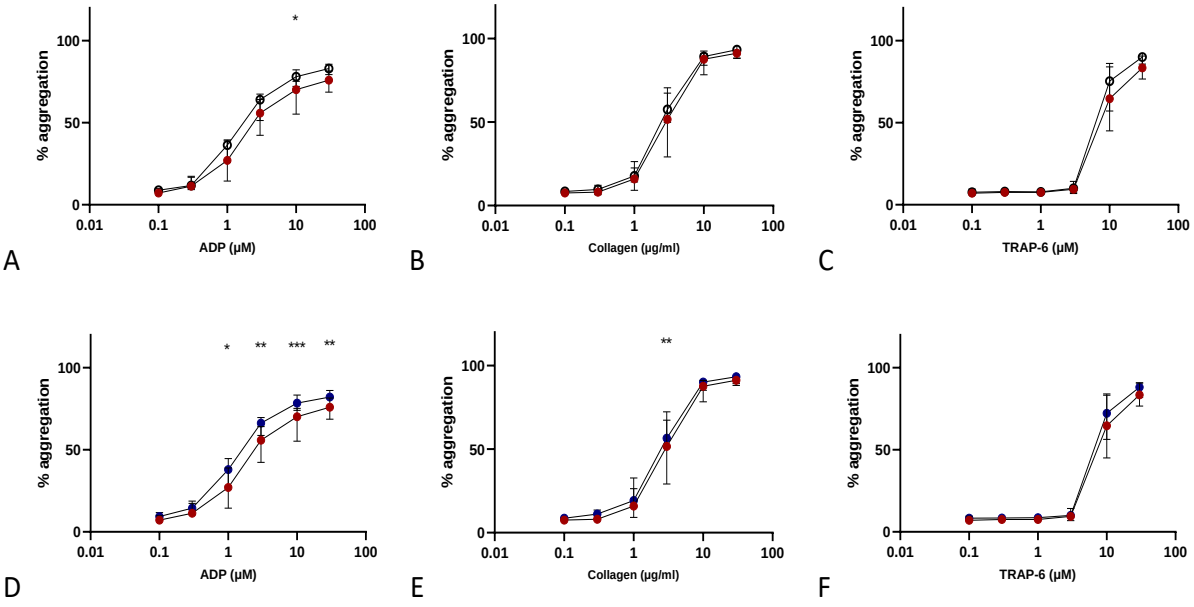

Figure 4.11 Maximum aggregation of platelets pre-incubated with 100µg/ml LPS in response to stimulation with increasing concentrations of ADP (A,D), collagen (B,E), or TRAP-6 (C,F).

Graphs show data from all patients with a diagnosis of TB (red circles, n=25) compared healthy controls (open circles, n=14, A-C) and also compared to all TB-negative patients, i.e. healthy controls plus bronchoscopy patients who were not diagnosed with TB (navy circles, n=31, D-F). Agonist-induced maximal platelet aggregation was lower in patients with TB compared to patients without TB, particularly in response to ADP; a lesser difference was seen following stimulation with collagen, and there was no significant difference in maximal aggregation following stimulation with TRAP-6. Data points represent median value and error bars show interquartile ranges. Data compared using a two-way ANOVA with Šídák's correction for multiple comparisons. * p<0.05 , ** p<0.01, *** p<0.001, **** p<0.0001.

There was no difference when TB-negative bronchoscopy patients were compared with healthy controls (Figure 4.12).

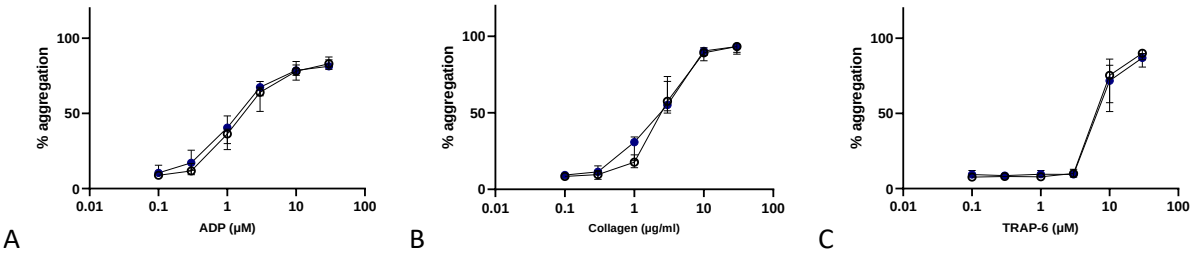

A B C

Figure 4.12 Maximum aggregation of platelets pre-incubated with 100µg/ml LPS in participants without TB.

There was no difference in aggregation responses to stimulation with increasing concentrations of ADP (A), collagen (B), or TRAP-6 (C) in healthy controls (open circles, n=14) compared to bronchoscopy patients who were not diagnosed with TB (navy circles, n=17). Data points represent median value and error bars show interquartile ranges. Data compared using a two-way ANOVA with Šídák's correction for multiple comparisons.

4.5.1.3 Platelet aggregation in response to stimulation with M.tb-secreted antigens was not affected by a diagnosis of tuberculosis or by non-TB respiratory disease.

Aggregation responses were next compared in PRP incubated with M.tb-secreted antigens, compared to addition of PRP incubated with 7H9 control media, prior to addition to a 96-well plate pre-loaded with platelet agonists ADP, collagen, and TRAP-6.

There was no difference in platelet aggregation in PRP pre-incubated with M.tb-secreted antigens compared to addition of PRP pre-incubated with 7H9 control in TB-positive patients (Figure 4.13). In TB-negative patients, maximal platelet aggregation was only reduced when PRP was pre-incubated with M.tb-antigen then stimulated with 10µM TRAP-6 (maximal aggregation 46.2% vs 57.2% respectively, p=0.0018, Figure 4.14 C), otherwise no difference was observed. There was

no difference observed between healthy controls and TB-negative bronchoscopy patients (Figure 4.16).

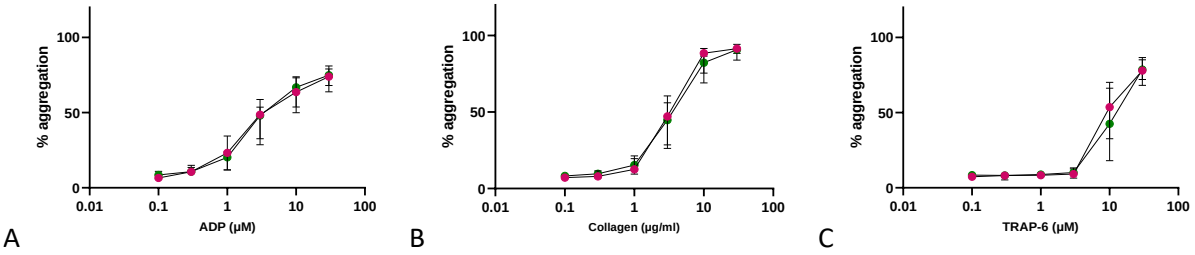

Figure 4.13 The effect of M.tb-secreted antigens on maximal agonist-induced platelet aggregation in TB patients.

There was no difference in maximal platelet aggregation in PRP incubated with M.tb-secreted antigen (green circles) compared to PRP incubated with 7H9 control media (red circles) in response to stimulation with platelet agonists (A) ADP, (B) collagen, or (C) TRAP-6. Data from all patients diagnosed with TB, n=25. Data points represent median value and error bars show interquartile ranges. Data compared using a two-way ANOVA with Šídák's correction for multiple comparisons.

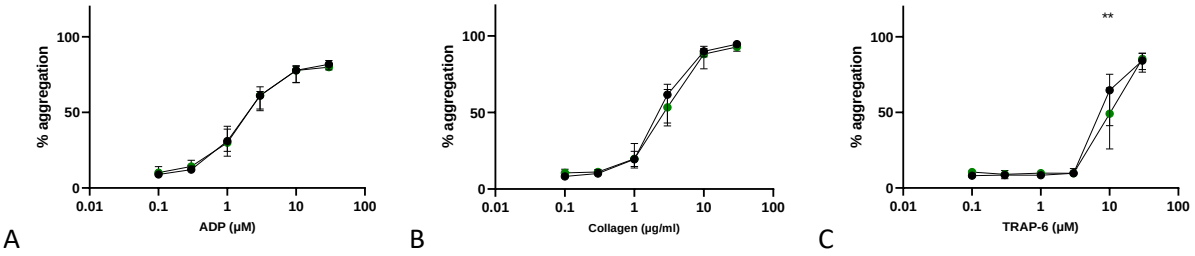

Figure 4.14 The effect of M.tb-secreted antigens on maximal agonist-induced platelet aggregation in TB-negative patients.

Maximal platelet aggregation in PRP incubated with M.tb-secreted antigens (green circles) compared to PRP incubated with 7H9 control media (black circles) in response to stimulation with platelet agonists (A) ADP, (B) collagen, or (C) TRAP-6. Maximal platelet aggregation was

significantly higher in the presence of M.tb-secreted antigens compared to 7H9 control only when stimulated with 10µM TRAP-6; no other significant difference was found. Data from all patients without TB (healthy controls plus respiratory symptomatic controls), n=31. Data points represent median value and error bars show interquartile ranges. Data compared using a two-way ANOVA with Šídák's correction for multiple comparisons. **p<0.01.

Differences observed in platelet responses in patients with versus those without TB were largely unchanged following incubation with M.tb-secreted antigens (Figure 4.15). There was no difference in platelet aggregation in healthy controls compared to TB-negative respiratory symptomatic controls following exposure to M.tb-secreted antigens (Figure 4.16).

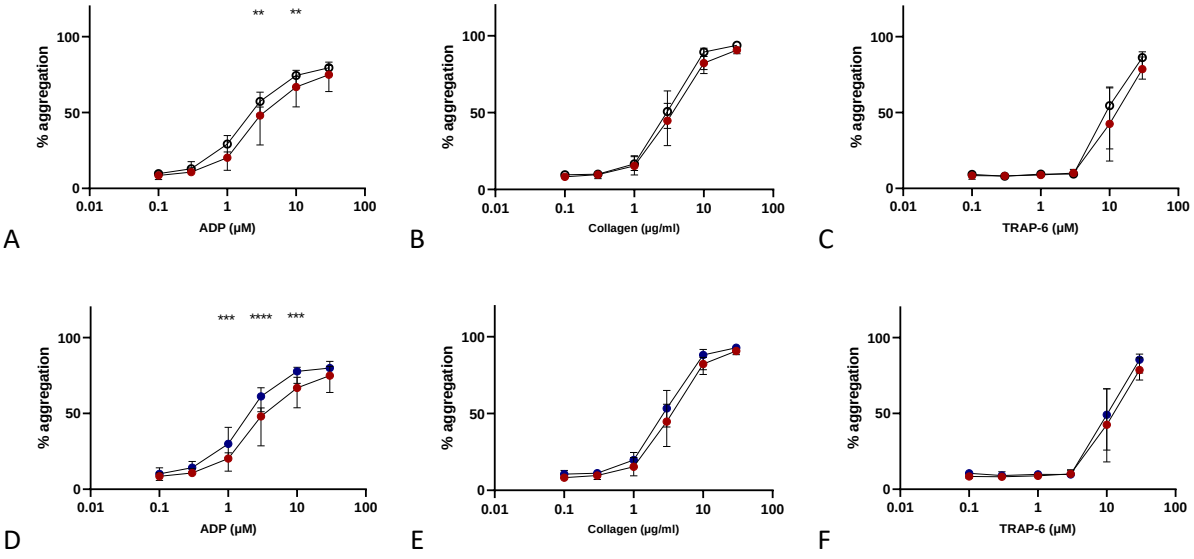

Figure 4.15 Maximum aggregation of platelets pre-incubated with M.tb-secreted antigens in response to stimulation with increasing concentrations of ADP (A,D), collagen (B,E), or TRAP-6 (C,F).

Graphs show data from all patients with a diagnosis of TB (red circles, n=25) compared healthy controls (open circles, n=14, A-C) and also compared to all TB-negative patients (navy circles, n=31, D-F). Agonist-induced maximal platelet aggregation in the presence of M.tb-secreted antigens was lower in patients with TB compared to patients without TB only in response to ADP. A non-significant trend towards a reduction in aggregation was observed following stimulation

with collagen and TRAP-6. Data points represent median value and error bars show interquartile ranges. Data compared using a two-way ANOVA with Šídák's correction for multiple comparisons. ** p<0.01, *** p<0.001, **** p<0.0001.

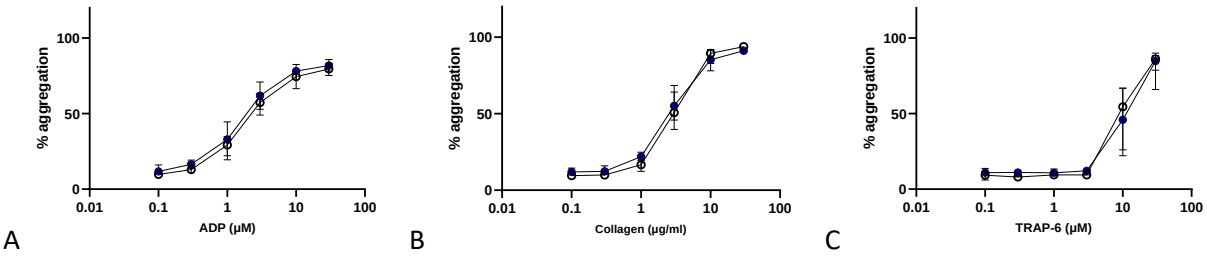

A B C

Figure 4.16 Maximum aggregation of platelets pre-incubated with M.tb-secreted antigens in participants without TB.

When PRP was pre-incubated with M.tb-secreted antigens, there was no difference in aggregation responses to stimulation with increasing concentrations of ADP (A), collagen (B), or TRAP-6 (C) in healthy controls (open circles, n=14) compared to bronchoscopy patients who were not diagnosed with TB (navy circles, n=17). Data points represent median value and error bars show interquartile ranges. Data compared using a two-way ANOVA with Šídák's correction for multiple comparisons.

4.5.1.4 Longitudinal analysis of aggregometry data

Due to interruptions to recruitment owing to the COVID-19 pandemic and/or patient loss to follow-up, three or more longitudinal samples were only available for nine of 25 TB patients, and thus a comprehensive analysis has not been possible.

For these nine patients, maximum platelet aggregation was plotted over time. A tendency towards reduced aggregation at weeks 2 and 4 was seen, with a return to normalisation by 6 months. Responses to ADP were more consistent than responses to collagen or to TRAP-6, as was also seen in the data above. An example for one of the patients with a full data set is shown in

Figure 4.17. For this patient, maximal percentage aggregation in response to ADP decreased from baseline to 2 weeks, and further from 2 weeks to 4 weeks, before increasing again at 2 months and then at six months. A similar pattern occurred in response to TRAP-6, and also to collagen, although the latter was less clearly defined.

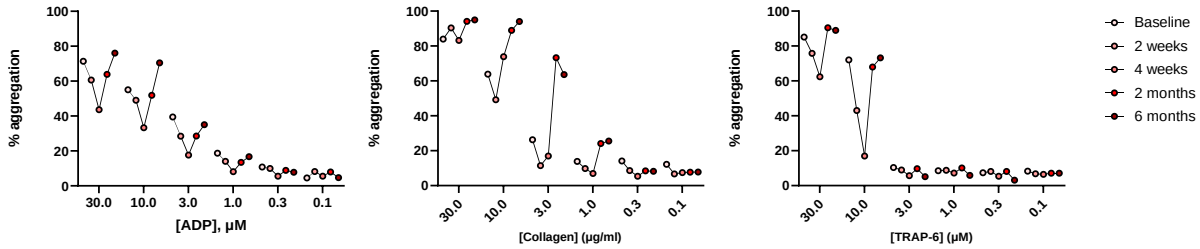

Figure 4.17 Changes in ADP-, Collagen-, and TRAP-6 induced platelet aggregation in a single patient with smear-positive pulmonary tuberculosis TB over time.

Maximal agonist-induced aggregation is presented at diagnosis (baseline, pale circles) and after 2 weeks, 4 weeks, 2 months, and 6 months of treatment (increasingly dark red circles).

When all available patient data were cumulated, a similar pattern is perceptible in the data although the small sample size and substantial variations in individual patients' responses meant statistical comparison difficult (Figure 4.18). Nevertheless, a mixed effects analysis was performed to compare changes in platelet aggregation over time, during anti-TB treatment. ADP-induced maximal platelet aggregation was significantly different in TB patients compared to healthy controls when stimulated with 30µm, 10µm, 3µm, 1µm, and 0.1µm ADP but not 0.3µm ADP. When stimulated with 0.3µm ADP, maximal platelet aggregation was reduced after 2 weeks treatment compared to baseline (median 9.3% vs 10.7% respectively, p-0.033). No such differences were found when platelet aggregation was induced by stimulation with collagen or with TRAP-6.

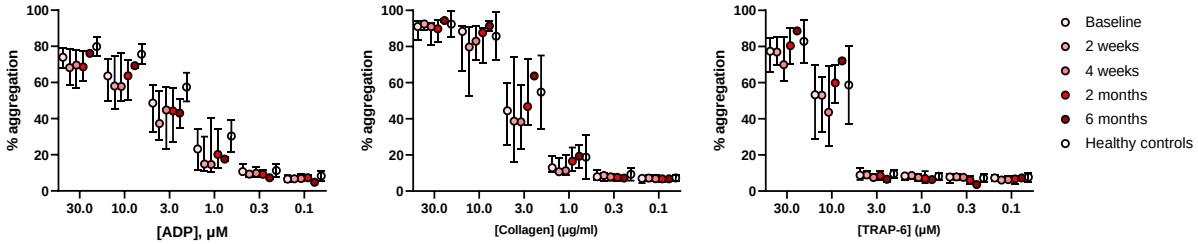

Figure 4.18 Changes in ADP-, Collagen-, and TRAP-6 induced platelet aggregation in serial blood samples obtained from patients with TB over time.

Maximal agonist-induced aggregation is presented at diagnosis (baseline, pale circles, n=24) and after 2 weeks (n=10), 4 weeks (n=10), 2 months (n=6), and 6 months of treatment (n=2); later timepoints indicated by increasingly dark red circles. Healthy controls are included for comparison (n=14, open circles).

Similar patterns were preserved when the assays were performed in the presence of M.tb-secreted antigens (Figure 4.19) and LPS (Figure 4.20).

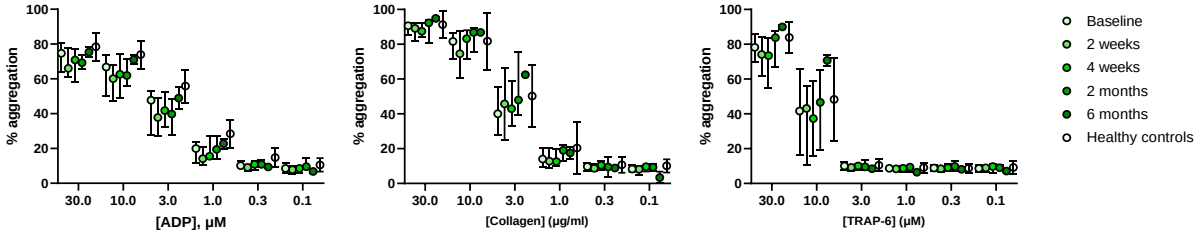

Figure 4.19 Changes in ADP-, Collagen-, and TRAP-6 induced platelet aggregation in serial blood samples obtained from patients with TB over time and stimulated with M.tb-secreted antigens.

Maximal agonist-induced aggregation is presented at diagnosis (baseline, pale circles, n=24) and after 2 weeks (n=10), 4 weeks (n=10), 2 months (n=6), and 6 months of treatment (n=2); later timepoints indicated by increasingly dark green circles. Healthy controls are included for comparison (n=14, open circles).

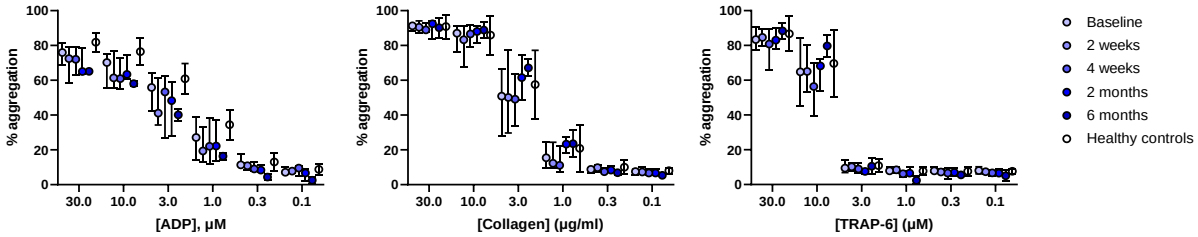

Figure 4.20 Changes in ADP-, Collagen-, and TRAP-6 induced platelet aggregation in serial blood samples obtained from patients with TB over time and stimulated with lipopolysaccharide (LPS).

Maximal agonist-induced aggregation is presented at diagnosis (baseline, pale circles, n=24) and after 2 weeks (n=10), 4 weeks (n=10), 2 months (n=6), and 6 months of treatment (n=2); later timepoints indicated by increasingly dark blue circles. Healthy controls are included for comparison (n=14, open circles).

4.5.2 Discussion

Maximal agonist-induced platelet aggregation was consistently reduced in patients with newly diagnosed TB in two distinct cohorts: those with sputum smear positive pulmonary TB versus healthy controls; as well as bronchoscopy patients who were diagnosed with TB and commenced on anti-TB therapy compared to those who were not. As these were independent cohorts, this is likely to represent a genuine finding. All patient groups were recruited in parallel, which controls for any drift in the protocol or flow cytometer settings. Although the sample sizes were smaller than the planned study, the difference was sufficient to reach statistical significance. This effect was most pronounced in the presence of the platelet agonist ADP, and was also present in the presence of collagen, but no statistical difference was found with the addition of TRAP-6. Of note, there was no difference in maximal aggregation between healthy controls and symptomatic controls (patients who underwent a bronchoscopy, without a diagnosis of TB).

The addition of LPS led to a non-significant increase in aggregation responses in the presence of ADP and TRAP-6, but not collagen; this is surprising as the literature shows a significant increase with LPS, even at much lower doses(175). M.tb-secreted antigens made no discernible difference. In the presence of both of these additional stimuli the responses to agonists were preserved.

On longitudinal follow-up there was a trend towards an initial dip in maximal platelet aggregation at weeks 2 and 4, with a normalisation by the end of treatment; however, the small number of patients who underwent follow-up combined with the large inter-individual variation means that this infrequently reached statistical significance.

4.6 Evaluation of patient activity in patients using flow cytometry

Flow cytometric analysis was performed using samples of whole blood collected from patients in 10% citrate, as described in section 2.14 and section 4.3.6.4 as above: whole blood was stained with monocyte and platelet markers, and platelet/monocyte aggregation and platelet activation were assessed. This was performed in the presence of M.tb-secreted antigens or 7H9 control, and in the presence or absence of platelet agonists TRAP-6 and ADP. Data were acquired using a BD FACSCanto flow cytometer at UPCH. Due to a fault in the equipment at the start of the project, data are only available for samples processed after 27th August 2019. Results were analysed using FlowJo v10 operating software and GraphPad PRISM v9.1.2.

Data from flow cytometric analysis are available for 10 patients with newly diagnosed smear-positive pulmonary TB at diagnosis, 6 patients who underwent bronchoscopy and were later diagnosed with TB, 14 healthy controls, and 14 patients who underwent bronchoscopy and were not diagnosed with TB (respiratory symptomatic controls). The 16 TB cases were considered as a single group for the purposes of analysis. Data were also available from 7 TB patients at 2 weeks post treatment initiation, from 8 TB patients at 8 weeks, from 4 at 2 months, and from 2 at 6 months post treatment initiation.

4.6.1 Platelet activation

Platelet activation was assessed by comparing the presence of platelet activation markers CD62P (P-selectin) and PAC-1 on the surface of platelets. The most commonly studied platelet activation markers are P-selectin, activated alpha2b-beta3 complex, and lysosomal associated membrane protein (CD63). As there was only space for two in the panel, two were selected. These two receptors behave differently: CD62P is present in the membranes of granules and is externalised during degranulation as the granule becomes incorporated into the outer cellular membrane. The alpha2b-beta3 complex is already present on the surface of the platelet and undergoes conformational change upon platelet activation. It can be detected using PAC-1, a mouse monoclonal antibody that detects the active form only(239).

Platelets were defined as events that fell within the characteristic region of the FSC/SSC plot, and upon which CD42b, a ubiquitous platelet marker, could be detected, and platelet activation was assessed through the quantification of anti-CD62P antibody or anti-PAC-1 antibody among this population. An example showing the gating strategy is presented in Figure 4.21.

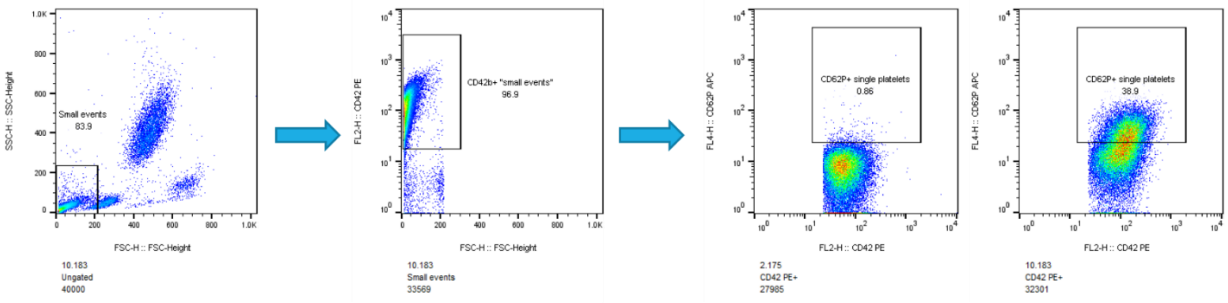

Figure 4.21 Example of gating strategy used to evaluate platelet activation.

Flow cytometric analysis of whole blood reveals characteristic distribution of cells based on forward scatter (FSC, indicating size) and side scatter (SSC, indicating cellular complexity) as shown in the first box. Events falling within the population in the left lower region of the plot indicate small cells, including platelets. These are selected and assessed for staining of CD42b, as shown in the second box; CD42b positive events within this population are defined as 'platelets'. This population is then evaluated based on detection of fluorophores against platelet activation markers CD62P and PAC-1. The example presented here shows CD62 positivity in platelets in the absence (third box) or presence (fourth box) of platelet agonist ADP. Both the percentage of platelets that are positive for CD62P, and the median fluorescence intensity (MFI) of CD62P among the platelet population, can then be calculated.

CD62P expression, defined as the percentage of platelets that were positive for CD62P, was 8.34% in patients with TB compared to 8.13% in healthy controls and 8.07% in symptomatic controls (Figure 4.22 A). Similarly, there was no difference in median fluorescence intensity (MFI) of CD62P among CD42b positive platelets in the three groups (Figure 4.22 B). In the presence of ADP and TRAP-6 there was a dose dependent increase in both the percentage of platelets expressing CD62P as well as the CD62P MFI, as expected; in the presence of 1uM TRAP-6 this was greater in TB patients compared to healthy controls; no other difference was observed (Figure 4.22 C-F).

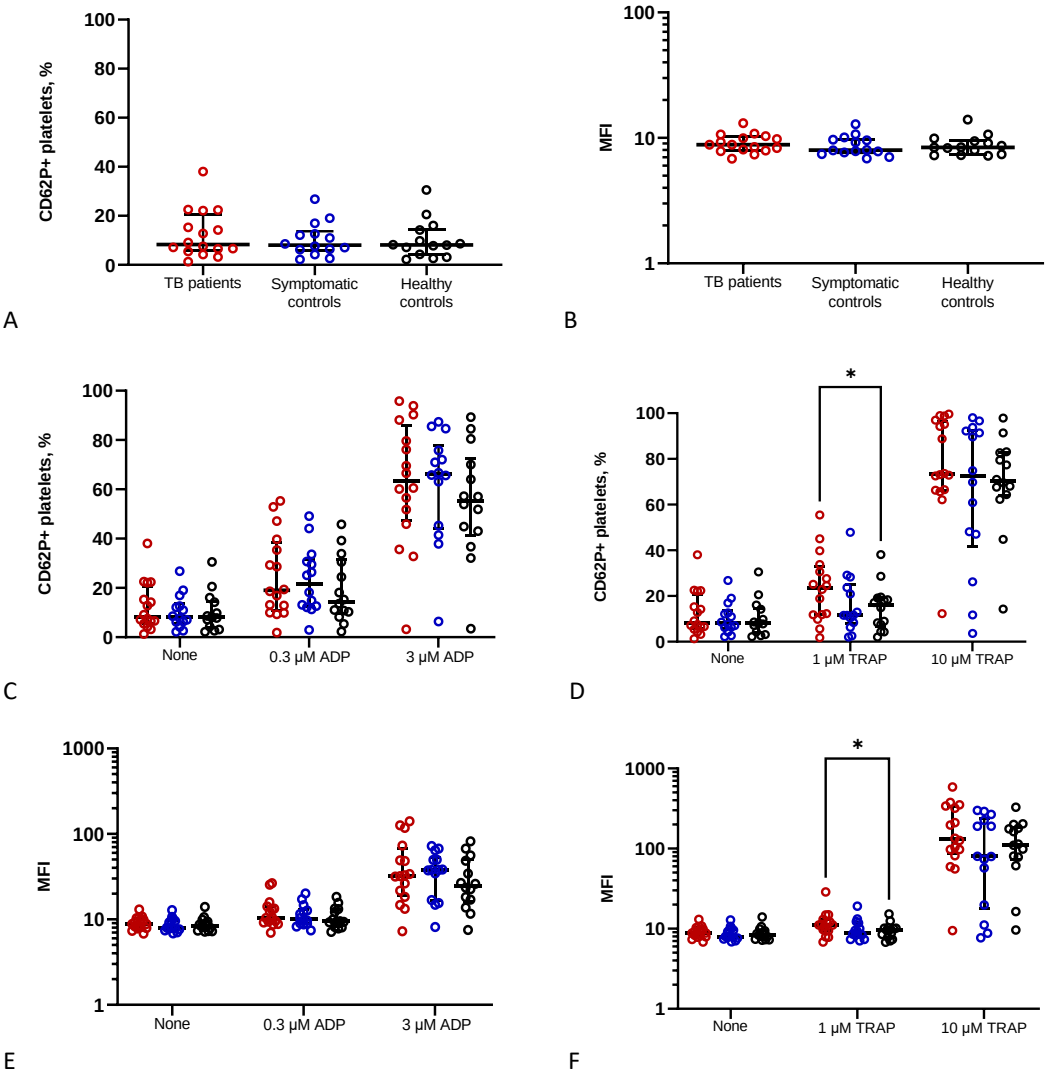

Figure 4.22 CD62P expression by CD42b+ platelets in the whole blood of patients with TB, symptomatic controls, and healthy controls.

Graphs represent the percentage of CD42b+ platelets that were positive for CD62P (A) and median fluorescence intensity (MFI) of CD62P in CD42b+ platelets (B) in unstimulated whole blood, and in the presence of ADP (C-D) and TRAP-6 (E-F) from patients with TB (red circles), symptomatic controls (blue circles), and healthy controls (black circles). Data presented as median +/- interquartile range. Comparisons with one-tailed Mann-Whitney U test. *p<0.05.

Similarly, there was no difference in rates of positivity for PAC1 in unstimulated platelets, or in PAC1 MFI (Figure 4.23 A and B). In the presence of 0.3µM ADP both the percentage of platelets that were positive for PAC1, and the PAC1 MFI in CD42b+ platelets, were higher in symptomatic controls than in patients with TB; there was no difference between patients with TB and healthy controls in the presence of ADP or TRAP-6 (Figure 4.23 C-F).

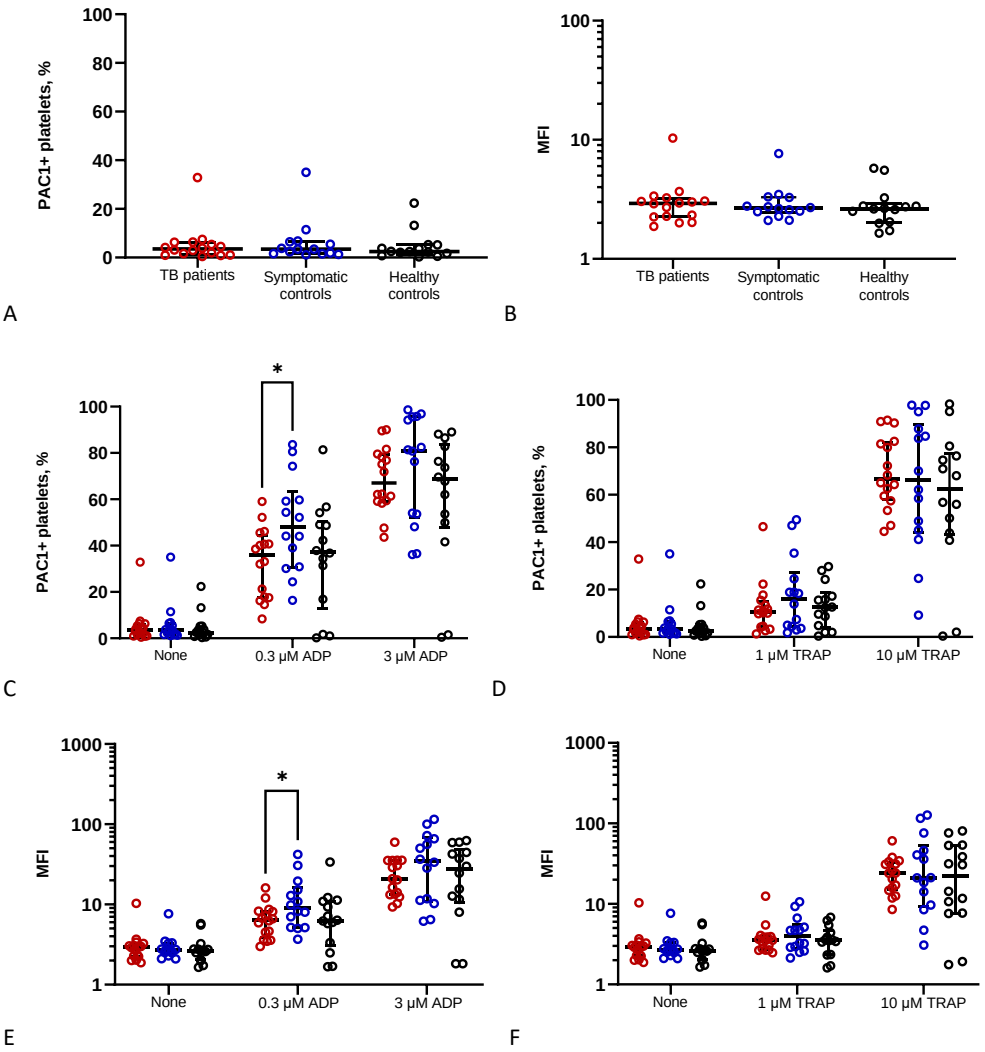

Figure 4.23 PAC1 expression by CD42b+ platelets in the whole blood of patients with TB, symptomatic controls, and healthy controls.

Graphs represent the percentage of CD42b+ platelets that were positive for PAC1 (A) and median fluorescence intensity (MFI) of PAC1 in CD42b+ platelets (B) in unstimulated whole blood, and in

the presence of ADP (C-D) and TRAP-6 (E-F) from patients with TB (red circles), symptomatic controls (blue circles), and healthy controls (black circles). Data presented as median +/- interquartile range. Comparisons with one-tailed Mann-Whitney U test. *p<0.05.

4.6.2 Platelet-monocyte aggregation

Monocytes were identified by first selecting events that fell within the characteristic region of the FSC/SSC plot, and among which CD14, a ubiquitous monocyte marker, could be detected. The percentage of monocytes which were positive for platelet marker CD42b was taken to indicate platelet-monocyte aggregation (PMA). An example is shown in Figure 4.24.

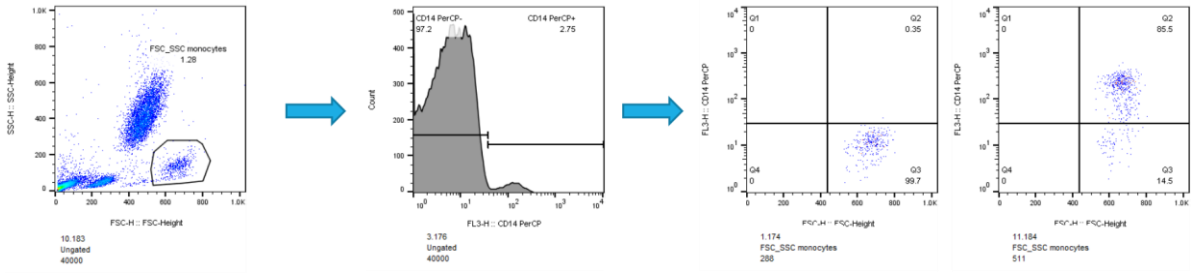

Figure 4.24 Example of gating strategy used to evaluate platelet-monocyte aggregation.

Events falling within the characteristic region in the FSC/SSC plot associated with monocytes were selected: these are relatively large cells, as indicated by the relatively high value on the *x* axis, with relatively low complexity, as indicated by the low position on the *y* axis. Events within this region that were positive for CD14, defined using a histogram as indicated in the second box, were defined as 'monocytes'. This population is then evaluated based on detection of fluorophores against platelet marker CD42b. The example presented here shows detection of CD42b in the monocyte population in the absence (third box) or presence (fourth box) of platelet activation marker ADP. The addition of a platelet activation marker has caused a significant proportion of monocytes to express CD42b, indicating the presence of platelets adhered to the monocyte surface. The detection of CD42b did not significantly change the size or complexity of the monocytes, in keeping with the much smaller size of platelets compared to monocytes.

In peripheral blood from patients with TB at diagnosis, the percentage of PMA was 26.1%, which was significantly higher than the percentage of PMA in peripheral blood from healthy controls (12.4%, p=0.035) but no different from the rate among symptomatic controls (32.0%, p=0.48; Figure 4.25 A). There was no difference in median fluorescence intensity (MFI) of the platelet marker CD42b among CD14+ monocytes between the three groups (17.3, 18.4, and 14.1, respectively; Figure 4.25 B).

In the presence of low and high doses of ADP and TRAP-6, both PMA and CD42b MFI were higher in samples from patients with TB than from healthy controls (Figure 4.25 C-F).

Percentage PMA was found to correlate positively with P-selectin expression on platelets, consistent with both being measures of platelet activation (Figure 4.26).

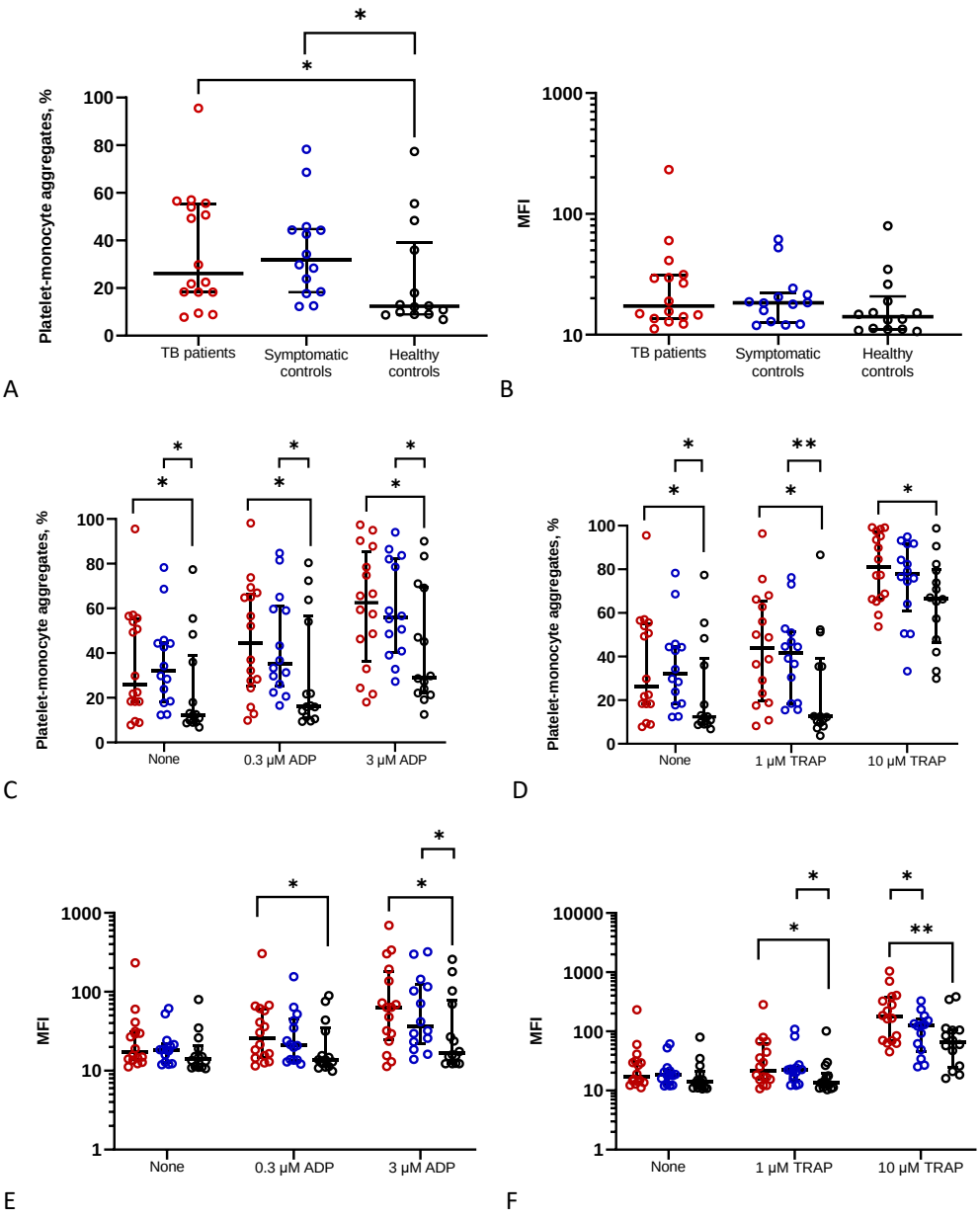

Figure 4.25 Platelet-monocyte aggregation in patients with TB (red circles) compared to symptomatic controls (blue circles) or healthy controls (black circles).

(A) The percentage of monocytes that were positive for platelet marker CD42b (platelet-monocyte aggregates, PMA). (B) Median fluorescence intensity (MFI) of platelet marker CD42b among CD14+ monocytes. The percentage of PMA in the presence of ADP (C) or TRAP-6 (D). Median fluorescence intensity (MFI) of platelet marker CD42b among CD14+ monocytes in the presence of ADP (E) or TRAP-6 (F). Data presented as median +/- IQR. Results compared using one-tailed Mann-Whitney U test. *p<0.05, **p<0.01.

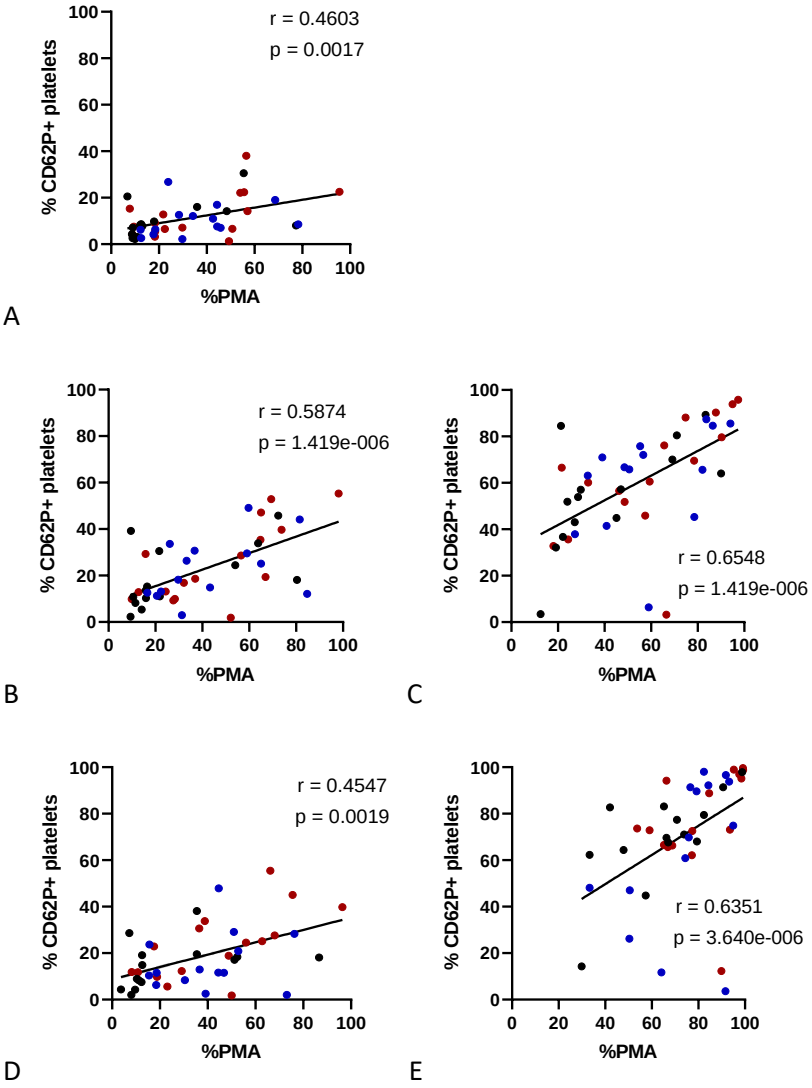

Figure 4.26 Correlation between platelet-monocyte aggregation (PMA) and CD62P positivity on platelets.

The percentage of monocytes that were positive for platelet marker CD42b (platelet-monocyte aggregates, PMA, *x* axis) plotted against the percentage of free platelets that were CD62P+ (*y* axis) for samples that were unstimulated (A) or in the presence of 0.3uM or 3uM ADP (B-C) or 1uM or 10uM TRAP-6(D-E). Data from patients with TB (red circles), symptomatic controls (blue circles), and healthy controls (black circles). *r* calculated using Spearman's non-parametric coefficient of correlation.

4.6.3 Platelet-granulocyte aggregation

Platelet-granulocyte aggregation was evaluated using the gating strategy presented in Figure 4.27. Although it is not possible to categorically state that this represents a pure neutrophil population, gating strategies incorporating anti-CD45 antibody (a pan-leukocyte marker) and/or anti-CD16 antibody (a neutrophil-specific marker) did not significantly change the outcome of this analysis (data not shown).

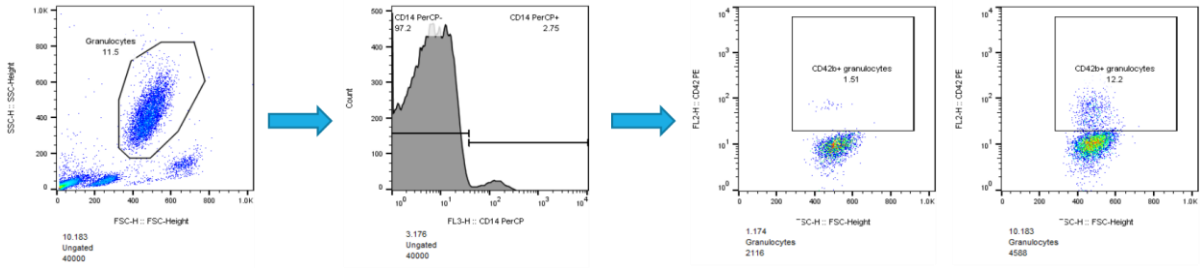

Figure 4.27 Example of gating strategy used to evaluate platelet-granulocyte aggregation.

As cells that are abundant, large, and containing numerous granules and intracellular structures, granulocytes typically fall within the region on a FSC/SSC plot indicated in the first box. To exclude CD14 positive granulocytes such as eosinophils, any events that expressed CD14 were removed, and the remaining population was defined as 'granulocytes'. Granulocytes that were positive for the platelet marker CD42b were taken to represent platelet-granulocyte aggregates. The example presented here shows detection of CD42b in the granulocyte population in the absence (third box) or presence (fourth box) of platelet activation marker ADP. The addition of a platelet activation marker has caused a significant proportion of granulocytes to show detectable CD42b, increasing from 1.51% to 12.2%, and indicative of the presence of platelets adhered to the granulocyte surface.

The percentage of CD14-negative granulocytes that expressed platelet marker CD42b was greater in TB patients than in healthy controls (11.7% versus 7.12%, p=0.032, Figure 4.28 A) and was 6.27% in symptomatic controls (p=0.051). There was no difference in CD42b MFI across the three groups (Figure 4.28 B). The increased rate of platelet-granulocyte aggregates in TB patients compared to healthy controls was maintained in the presence of ADP and of 1µM TRAP-6; in the presence of

10µM TRAP-6 the rate of platelet granulocyte aggregates was significantly higher in TB patients than in symptomatic controls (Figure 4.28 C-D). There was no difference in CD42b MFI, apart from in the presence of 10µM TRAP-6 where it was higher in patients with TB than in symptomatic controls (Figure 4.28 E-F).

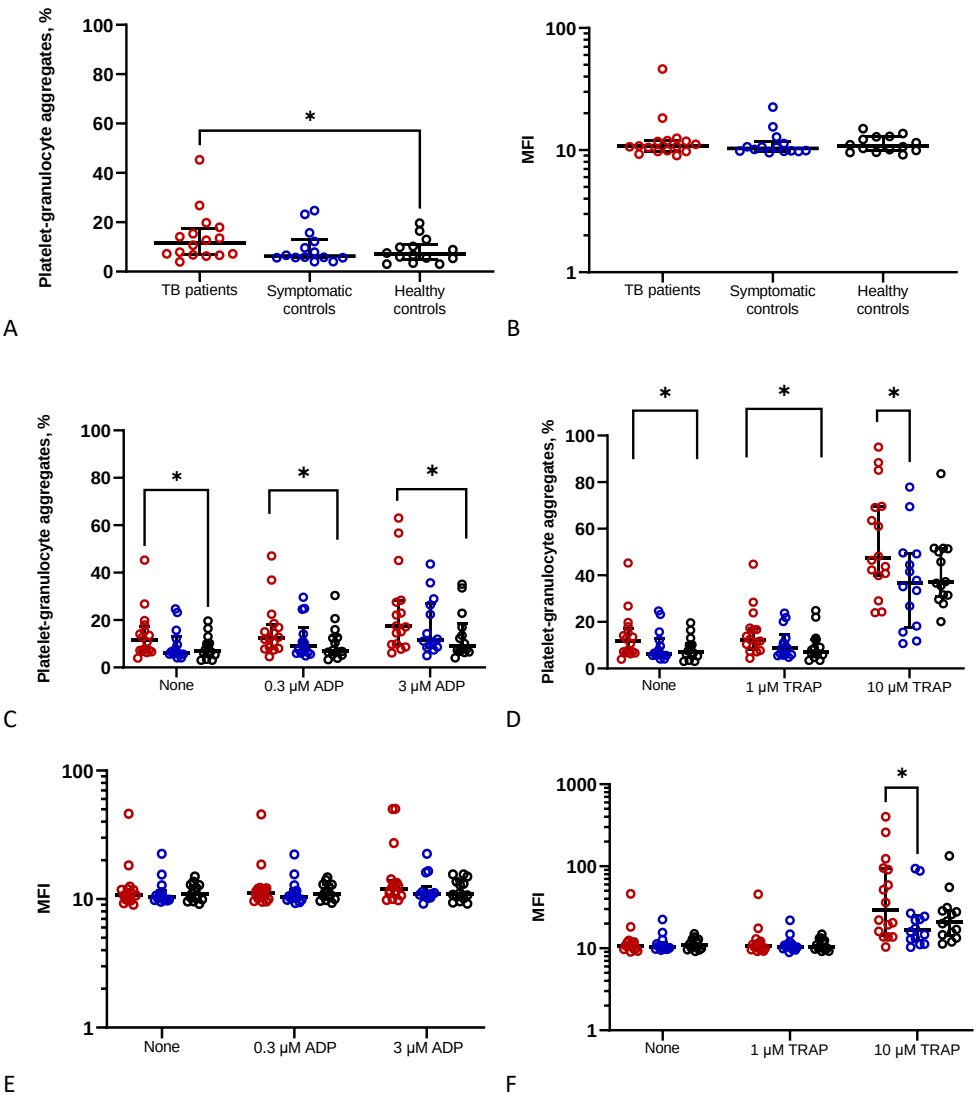

Figure 4.28 Platelet-granulocyte aggregation in patients with TB (red circles) compared to symptomatic controls (blue circles) or healthy controls (black circles).

A) The percentage of CD14- granulocytes that were positive for platelet marker CD42b (platelet-granulocyte aggregates). B) Median fluorescence intensity (MFI) of platelet marker CD42b among CD14- granulocytes. The percentage of platelet-granulocyte aggregates in the presence of ADP

(C) or TRAP-6 (D). Median fluorescence intensity (MFI) of platelet marker CD42b among CD14- granulocytes in the presence of ADP (E) or TRAP-6 (F). Data presented as median +/- IQR. Results compared using one-tailed Mann-Whitney U test. *p<0.05.

4.6.4 Longitudinal evaluation of platelet activity by flow cytometry

Longitudinal flow cytometric data were available from 16 TB patients at baseline, 7 patients after 2 weeks of initiation of anti-TB treatment, 8 patients after 4 weeks, 4 patients after 2 months, and 2 patients after completion of treatment at six months. Data are presented in Figure 4.29 to Figure 4.32. Although numbers were too small to permit a rigorous statistical analysis, it can be clearly seen from the graphs that there is a trend towards reductions in platelet-monocyte aggregation and in CD62P positivity of platelets over time.

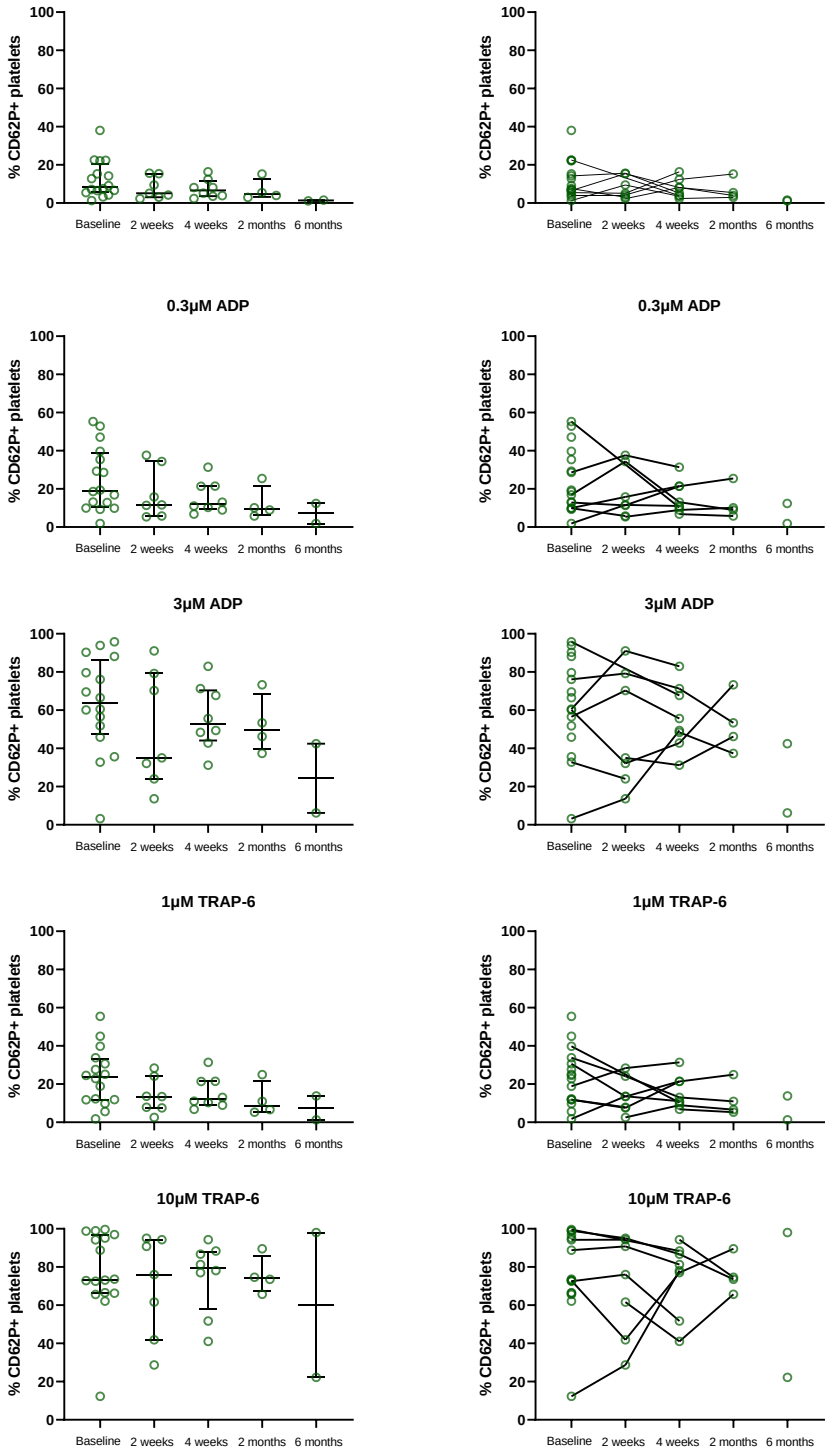

Figure 4.29 Longitudinal evaluation of percentage of CD62+ platelets in unstimulated whole blood, and in blood stimulated with 0.3µM and 3µM ADP, and with 1µM and 10µM TRAP-6.

Data show median and interquartile range (left), and lines linking individual patients over time (right).

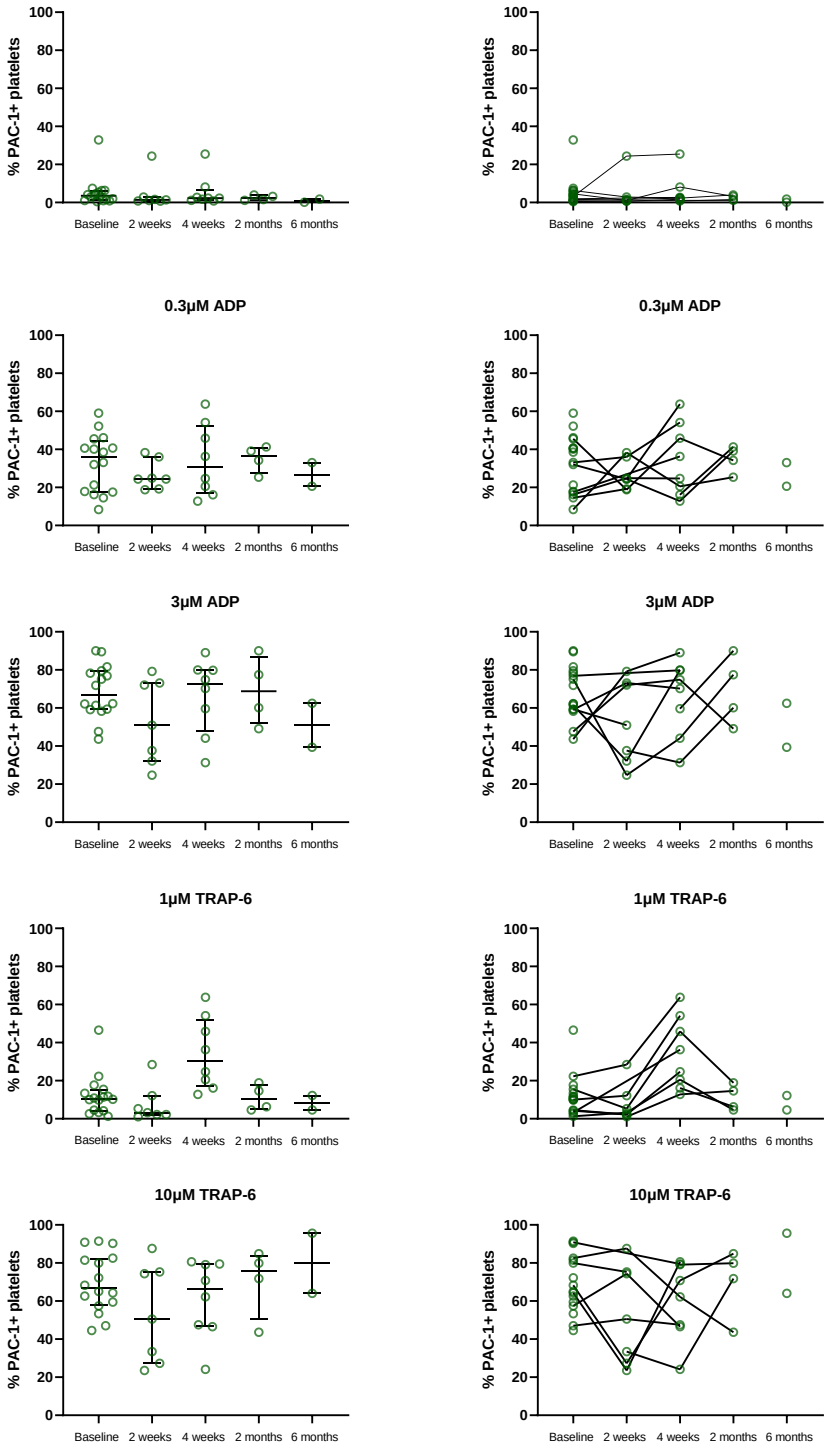

Figure 4.30 Longitudinal evaluation of percentage of PAC-1+ platelets in unstimulated whole blood, and in blood stimulated with 0.3µM and 3µM ADP, and with 1µM and 10µM TRAP-6.

Data show median and interquartile range (left), and lines linking individual patients over time (right).

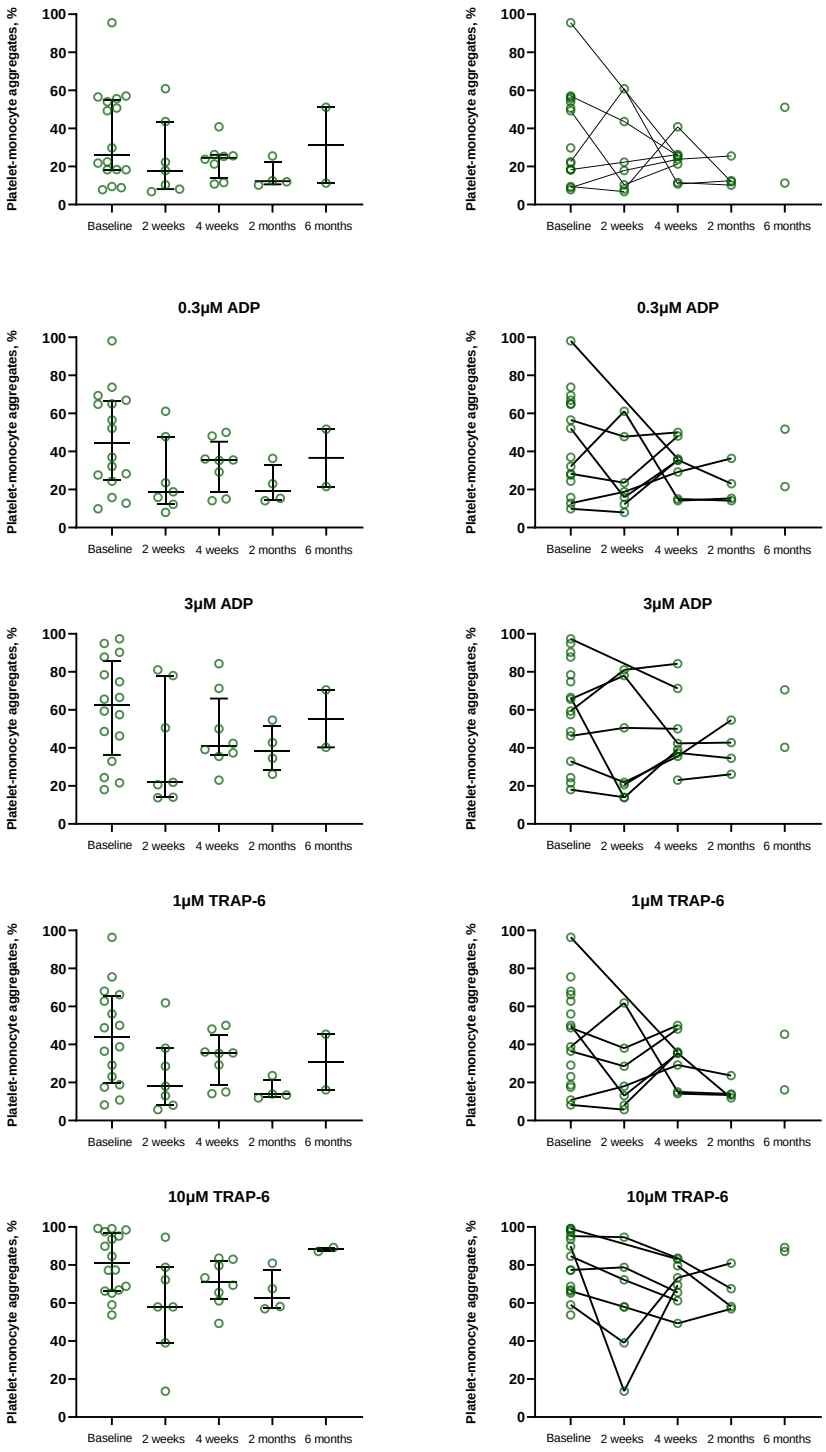

Figure 4.31 Longitudinal evaluation of platelet-monocyte aggregation (PMA) in unstimulated whole blood, and in blood stimulated with 0.3µM and 3µM ADP, and 1µM and 10µM TRAP-6.

Data show median and interquartile range (left), and lines linking individual patients over time (right).

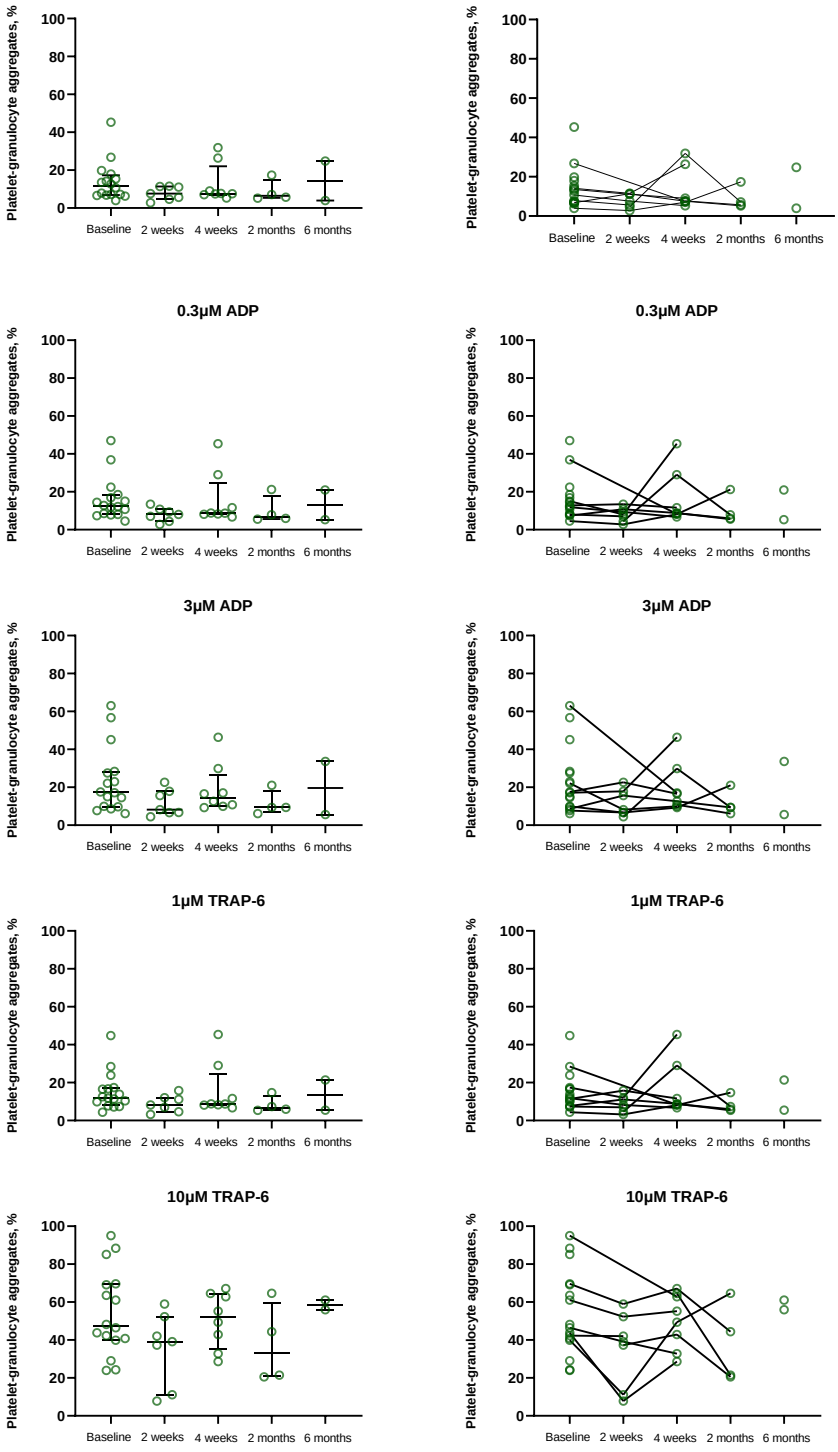

Figure 4.32 Longitudinal evaluation of platelet-granulocyte aggregation in unstimulated whole blood, and in whole blood stimulated with 0.3µM and 3µM ADP, and 1µM and 10µM TRAP-6.

Data show median and interquartile range (left), and lines linking individual patients over time (right).

4.6.5 Discussion

The data presented here showed an increase in platelet-monocyte aggregates in TB patients compared to healthy controls. This is in keeping with other studies which have shown increased platelet-monocyte or platelet-leukocyte aggregates in patients with other inflammatory disorders including heart disease(240), rheumatological disorders(241), and dengue(242). Platelet-monocyte aggregation was also found to be elevated in patients with non-TB lung disease suggesting that this effect may be part of a generalised lung inflammatory process. Conversely, platelet-granulocyte activation was elevated in TB patients but not in the respiratory symptomatic group, which indicates that this may be a more TB-specific effect. The longitudinal analysis also gave an indication that these findings normalised over time while patients took their anti-TB medication.

Although there was no observed difference in CD62P or PAC-1 expression between TB patients and either healthy or symptomatic controls, we found strong correlation between CD62P expression and PMA indicating that any difference in CD62P expression may have been too small to detect with our sample size but may in fact have been detectable with the original planned sample size of 40 in each group. Future studies will be needed to determine whether increased platelet activation in the form of increased surface receptor expression can in fact be demonstrated in patients with TB.

Platelet-leukocyte aggregations are recognized markers of inflammation, and there are some data from the literature that shed light on possible implications. In COVID-19, both monocyte-platelet aggregates and neutrophil-platelet aggregates were found to be elevated in patients compared to healthy donors; these markers were higher in patients with severe disease, and also correlated with markers of inflammation C-reactive protein and IL-6, and the authors postulated that these aggregates may have mechanistic roles in pathological lung inflammation(243). Hottz *et al* showed that in Dengue infection, formation of platelet-monocyte aggregates modulates monocyte activation and cytokine release(244). In this study, the binding of activated and apoptotic platelets from patients with dengue increased monocyte secretion of IL-1β, IL-8, IL-10, and MCP-1, whereas platelets from healthy volunteers increased secretion of MCP-1 only.

Cytokine release was shown to be dependent on P-selectin-mediated adhesion, as well as recognition of apoptotic platelets.

The data presented in this chapter are limited by the small sample size of the patients, and also by the lack of follow-up data on the participants evaluated at baseline. A larger study with robust measures to enable longitudinal monitoring of patients would be useful to confirm and strengthen the findings presented above.

4.7 Soluble mediators of inflammation, tissue destruction, and platelet activity in the lungs and blood of patients with and without TB.

The next analysis sought to investigate evidence of inflammation and platelet activity both in the blood and at the site of disease in the lung itself. Nineteen soluble mediators were measured in plasma and bronchoalveolar lavage fluid (BALF) samples from all patients at baseline. These mediators were divided into three panels: markers associated with inflammation, lung tissue destruction (matrix metalloproteinases), and platelet activity (see Table 6).

Table 6 Soluble factors measured in clinical samples

Inflammatory markers	Matrix metalloproteinases	Platelet associated factors
Interleukin (IL) 1 alpha (IL-1 α)	MMP-1	Soluble CD40 Ligand (sCD40-L)
IL-1 beta (IL-1 β)	MMP-3	Soluble P-selectin (sP-selectin)
IL-6	MMP-7	Von Willebrand factor A2 (vWF-A2)
IL-8	MMP-8	Vascular epithelial growth factor (VEGF)
IL-10	MMP-10	Phospholipase A2 Group 7 (PLA2G7)
IL-12		
Tumour necrosis factor alpha (TNF-α)		
MCP-1 (CCL-2)		
Interferon inducible protein 10 (IP-10)		

Concentrations were measured using custom-designed Luminex multiplex arrays (see methods section 2.11). Data were downloaded in Excel and analysed in GraphPad PRISM v9.1.2 software. A coefficient of variation (CV) of <30% was considered acceptable. The CV of one measurement (0.0005%) was over 30% and was excluded. 4 (0.002%) measurements were in the range of 20-30% and 26 (0.013%) measurements had a CV of 15-20%.

Values that fell below the lower limit of detection were substituted with a value equal to half of the lower limit of detection, taking into consideration the dilution factor of the sample. No values were above the limit of detection.

4.7.1 Correlation between concentrations of soluble mediators in bronchoalveolar lavage fluid (BALF)

To evaluate the relationship between markers of inflammation and platelet activity measured in the BALF, a Spearman's correlation matrix was constructed (Figure 4.33). Soluble mediators measured in all BALF samples were found to correlate strongly, with the exception of vascular endothelial growth factor (VEGF) which correlated negatively with CCL-2 (r = -0.14) and with PLA2G7 (r = -0.22) and weakly or not at all with all others.

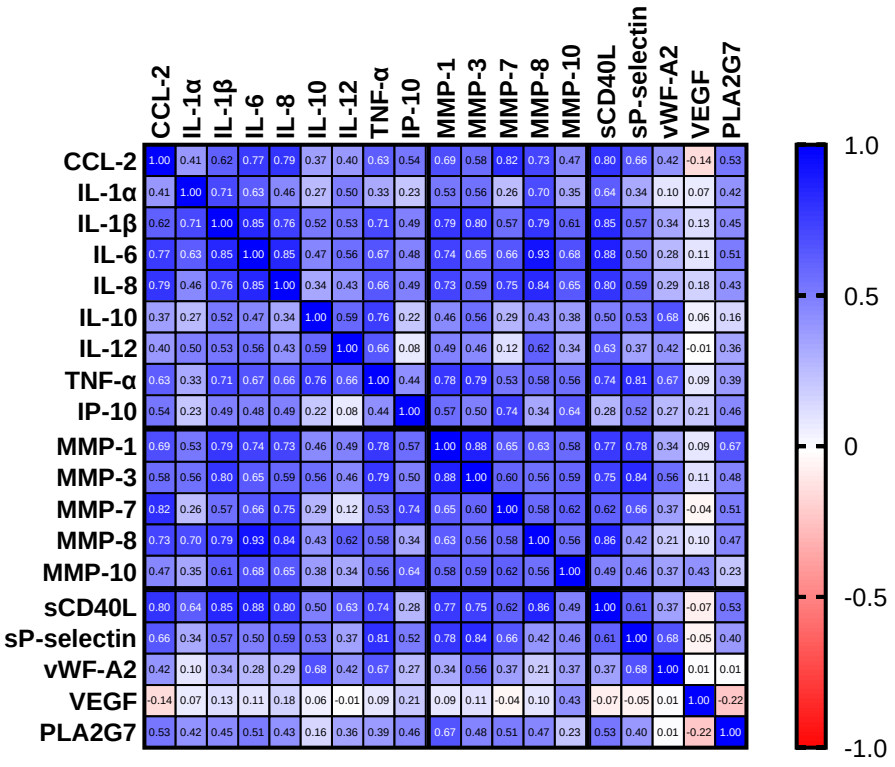

Figure 4.33 Spearman's nonparametric correlation matrix of soluble markers measured in bronchoalveolar lavage fluid (BALF) samples from all patients who underwent bronchoscopy.

Data show correlation between concentrations of inflammatory markers, matrix metalloproteinases (MMPs), and platelet associated factors in all patients who underwent bronchoscopy (n=25). Significant correlation was observed between all markers apart from VEGF which correlated negatively with CCL-2 and with PLA2G7 and weakly or not at all with all others. Values indicate Spearman's r co-efficient of correlation.

When these data were disaggregated according to whether or not the patient was diagnosed with TB, it was observed that among patients with TB, concentrations of all soluble markers measured in BALF showed a very strong positive correlation, with the exception of VEGF which showed a strong negative correlation with all other markers (Figure 4.34). Non-TB patients, on the other hand, demonstrated a much more variable picture (Figure 4.35).

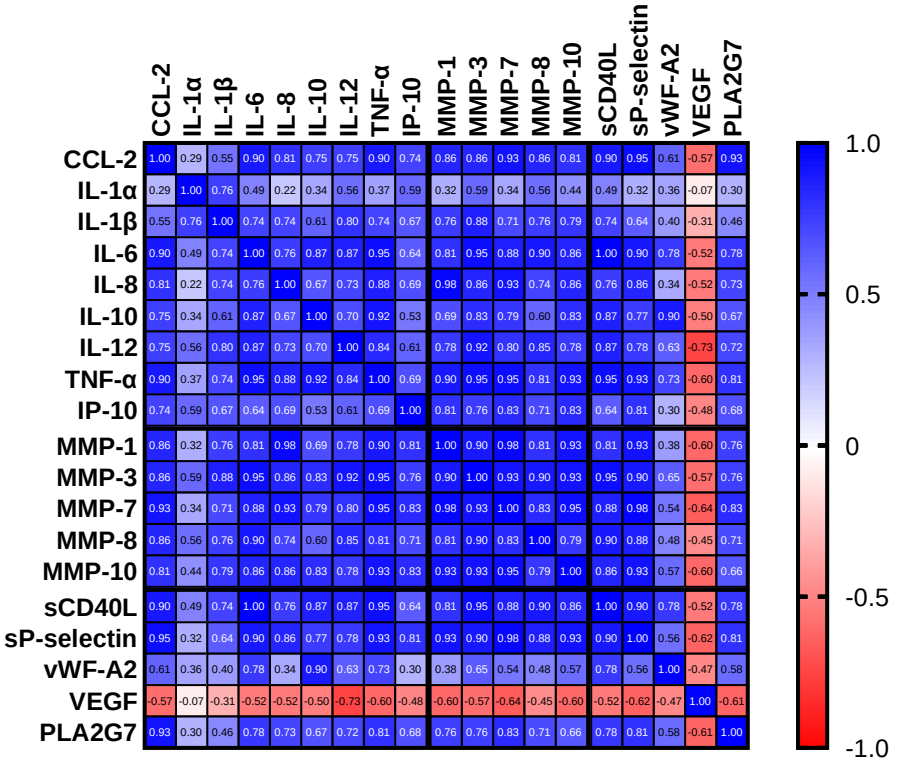

Figure 4.34 Spearman's nonparametric correlation matrix of soluble markers measured in bronchoalveolar lavage fluid (BALF) samples from bronchoscopy patients with tuberculosis.

Data show correlation between concentrations of inflammatory markers, matrix metalloproteinases (MMPs), and platelet associated factors in patients who underwent bronchoscopy and were subsequently diagnosed with TB (n=8). Significant correlation was observed between all markers apart from VEGF which demonstrated strong negative correlation with other markers. Values indicate Spearman's *r* co-efficient of correlation.

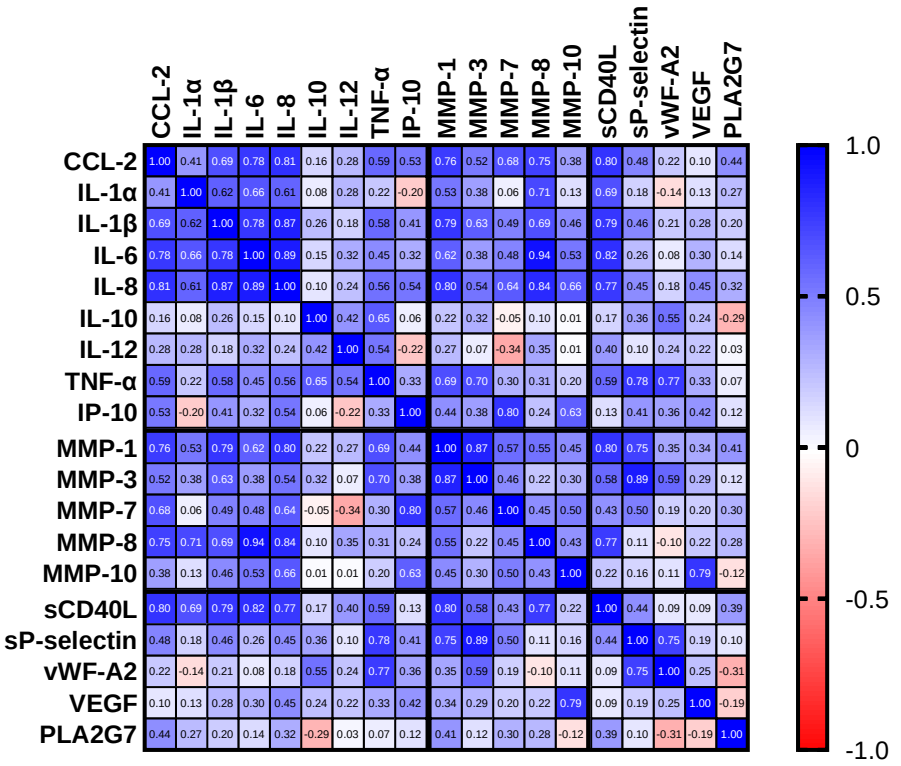

Figure 4.35 Spearman's nonparametric correlation matrix of soluble markers measured in bronchoalveolar lavage fluid (BALF) samples from bronchoscopy patients without tuberculosis.

Data show correlation between concentrations of inflammatory markers, matrix metalloproteinases (MMPs), and platelet associated factors in patients who underwent bronchoscopy who were not diagnosed with tuberculosis (n=17). Correlation was found to be variable. Strong correlation was observed between many of the pro-inflammatory markers and MMPs. Values indicate Spearman's *r* co-efficient of correlation.

4.7.2 Characterisation of soluble mediators in bronchoalveolar lavage fluid (BALF) in patients with and without TB

Concentrations of mediators measured in the BALF were compared in patients who underwent bronchoscopy and were subsequently diagnosed with TB versus those who were not. Levels of IL-1α were significantly higher in patients with TB than in those with other respiratory diseases

(median concentration 9.47 pg/µl [IQR 0.5-36.0 pg/µl] vs 0.47 pg/µl [IQR 0.47-2.02 pg/µl] respectively, p=0.035). There was a trend towards higher levels in TB patients in many of the other pro-inflammatory mediators measured but these did not reach statistical significance (Figure 4.36).

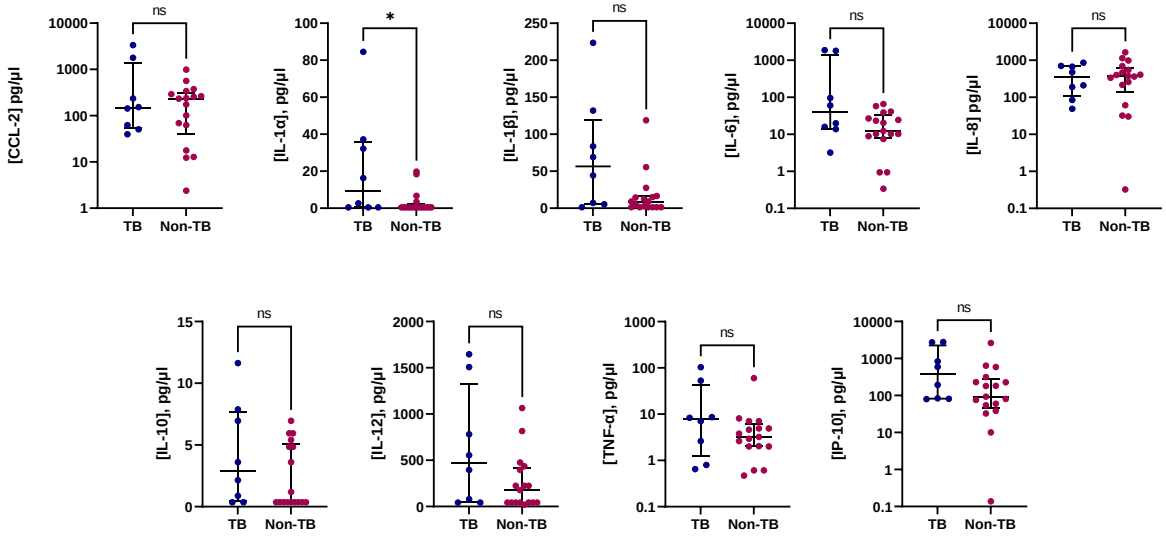

Figure 4.36 Soluble inflammation-related mediators measured in bronchoalveolar lavage fluid (BALF) in patients who underwent bronchoscopy and were diagnosed with TB (n=8) versus those who were not (n=17).

Although a trend towards higher concentrations of measured pro-inflammatory markers was observed in the majority of markers evaluated, a significant difference was only seen for IL-1α. Data compared using Kruskall-Wallace test, *p<0.05.

Concentrations of MMPs were found to be elevated in the BALF of patients with TB versus those without (Figure 4.37). This was significant for MMP-1 (median 1,328 pg/µl [IQR 67.3-5,523 pg/µl] vs 67.4 pg/µl [IQR 10.2-254.9 pg/µl], p=0.027) and MMP-3 (median 549.8 pg/µl [IQR 75.1-1,845 pg/µl] vs 82.0 pg/µl [IQR 37.0-161.9 pg/µl], p=0.028) but not for MMP-7, MMP-8, or MMP-10.

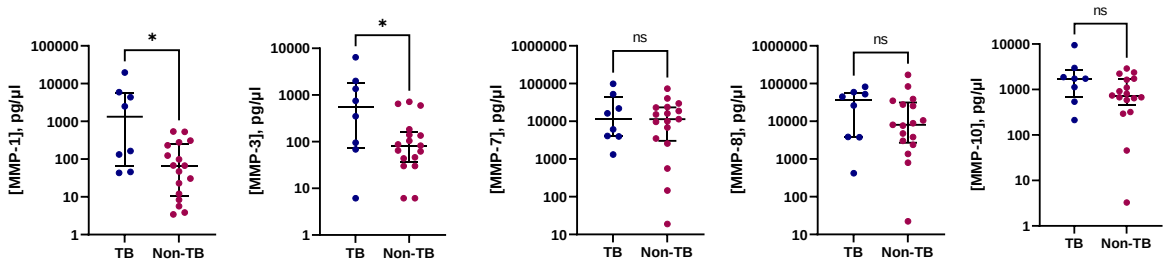

Figure 4.37 Soluble matrix metalloproteinases (MMPs) measured in bronchoalveolar lavage fluid (BALF) from bronchoscopy patients who were diagnosed with TB (n=8) versus those who were not (n=17).

Concentrations of MMP-1 and MMP-3 were significantly elevated in BALF samples from patients with TB compared to samples from those with other respiratory diseases. Data compared using Kruskall-Wallace test, *p<0.05.

Finally, platelet-associated factors were evaluated in the lung (Figure 4.38). Only PLA2G7 had significantly higher levels in BALF from TB patients compared to respiratory symptomatic controls (median 5,888 pg/µl [IQR 278-21,238 pg/µl] vs 278.0 pg/µl [IQR 278-3,044 pg/µl] respectively, p=0.031). VEGF, which had been found to display a strong negative correlation with all of the other markers measured in the BALF, was no different in patients with TB versus those without.

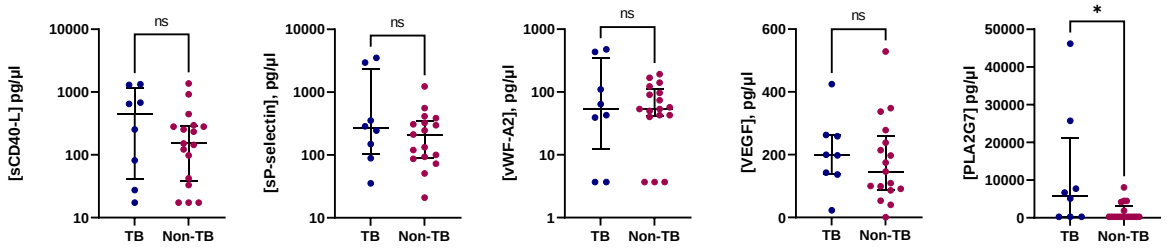

Figure 4.38 Soluble platelet-related mediators measured in bronchoalveolar lavage fluid (BALF) in patients who underwent bronchoscopy and were diagnosed with TB (n=8) versus those who were not (n=17).

Concentrations of PLA2G7 in BALF samples were significantly elevated in patients with TB compared to samples from those with other respiratory diseases. Data compared using Kruskall-Wallace test, *p<0.05.

4.7.3 Correlation between plasma concentrations of soluble mediators

The same three panels of soluble mediators were measured in plasma taken from patients at their baseline evaluation. Correlation between concentrations of the mediators in all patients was evaluated using a Spearman's correlation matrix (Figure 4.39). Many of the mediators were found to correlate strongly, particularly those associated with an inflammatory response. sCD40L and sP-selectin were found to correlate strongly with IL-1α (r = 0.69 and 0.77 respectively) and IL-6 (r = 0.77 and 0.79 respectively). Conversely, PLA2G7 correlated negatively with both IL-1α and IL-6 (r = -0.12 and r = -0.38, respectively).

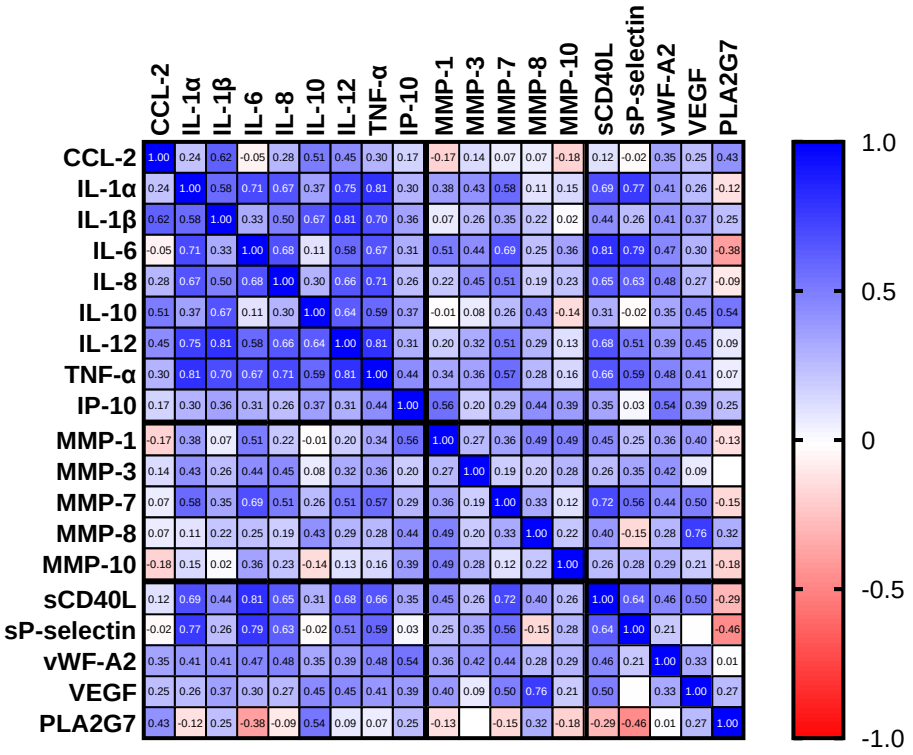

Figure 4.39 Spearman's nonparametric correlation matrix of soluble markers measured in plasma samples from all patients.

Data show correlation between concentrations of inflammatory markers, matrix metalloproteinases (MMPs), and platelet associated factors in all patients recruited to the study (n=56). Correlation was strongest between pro-inflammatory markers. Values indicate Spearman's r co-efficient of correlation.

Correlation between plasma concentrations of soluble mediators followed quite distinct patterns when evaluated separately for patients with TB, respiratory symptomatic controls, and healthy controls. In TB patients, strong correlations were preserved between pro-inflammatory mediators (Figure 4.40). Strong correlations were also present within platelet-associated mediators and also between these and pro-inflammatory markers. MMP-1 was found to correlate weakly with a number of mediators and negatively with some, including CCL-2 (r = -0.29), IL-1β (r = -0.17), and IL-10 (r = -0.15).

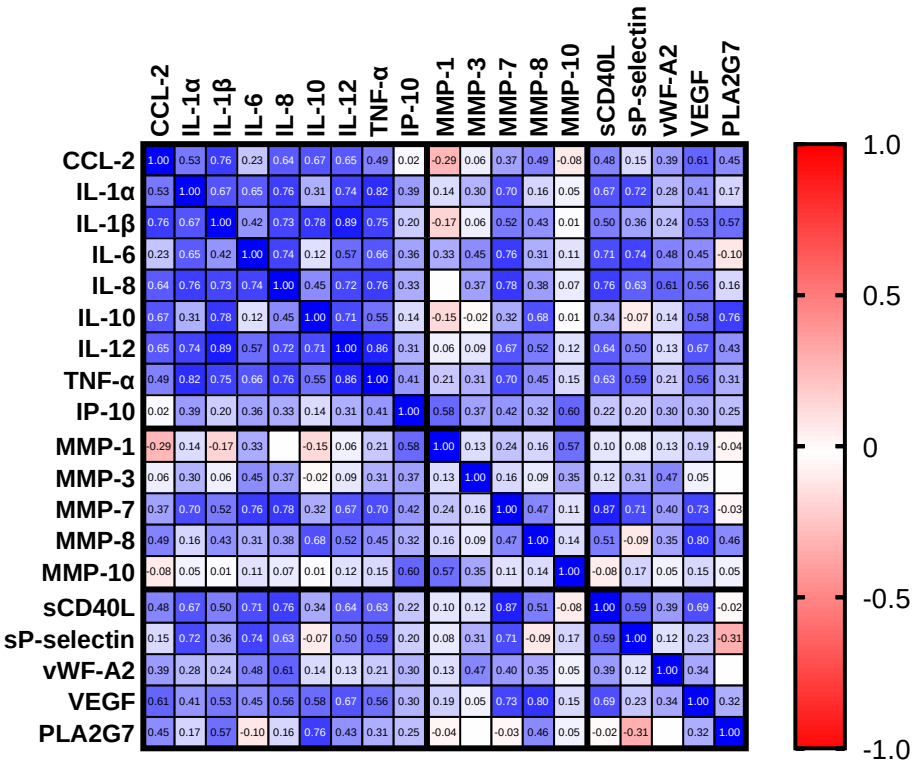

Figure 4.40 Spearman's nonparametric correlation matrix of soluble markers measured in plasma samples from patients with tuberculosis (n=25).

Data show correlation between concentrations of inflammatory markers, matrix metalloproteinases (MMPs), and platelet associated factors in patients with tuberculosis (n=25). Values indicate Spearman's r co-efficient of correlation.

Correlation matrices for plasma concentrations of soluble mediators in samples obtained from respiratory symptomatic controls showed a much broader range of correlations, including many strong negative associations (Figure 4.41). This was even more pronounced in healthy controls (Figure 4.42).

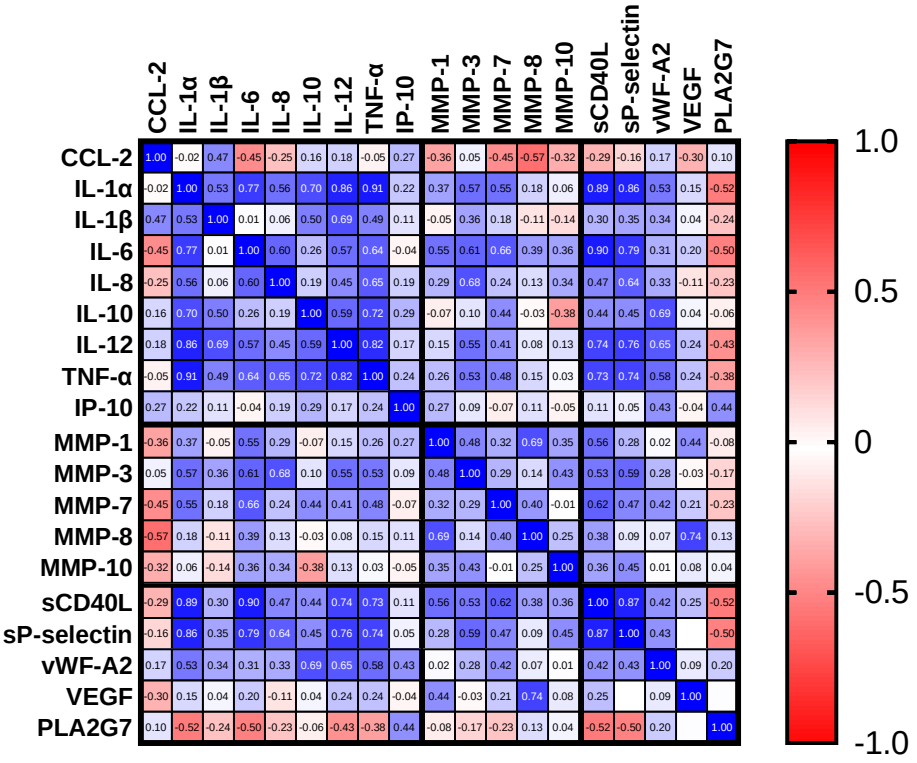

Figure 4.41 Spearman's nonparametric correlation matrix of soluble markers measured in plasma samples from respiratory symptomatic controls.

Data show correlation between concentrations of inflammatory markers, matrix metalloproteinases (MMPs), and platelet associated factors in patients with non-tuberculosis lung disease (n=17). Values indicate Spearman's *r* co-efficient of correlation.

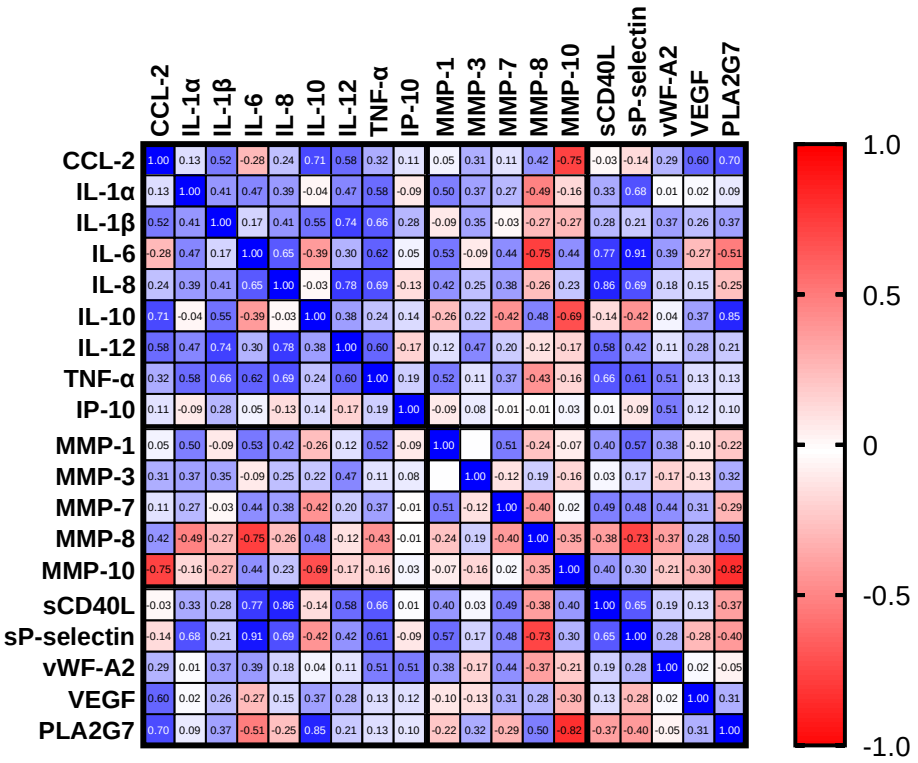

Figure 4.42 Spearman's nonparametric correlation matrix of soluble markers measured in plasma samples from healthy controls.

Data show correlation between concentrations of inflammatory markers, matrix metalloproteinases (MMPs), and platelet associated factors in healthy controls (n=14). Values indicate Spearman's *r* co-efficient of correlation.

4.7.4 Characterisation of soluble mediators in plasma obtained from patients with TB compared to healthy controls and patients with non-TB respiratory disease.

Concentrations of inflammation-associated mediators in all patients are presented in Figure 4.43. Concentration of IP-10 was significantly elevated in patients with TB compared to healthy controls (median 468.9 pg/µl [IQR 164.5-781.4 pg/µl] vs 82.1 pg/µl [IQR 69.1-112.2 pg/µl] respectively, p<0.0001). IP-10 concentrations were also significantly higher in patients with TB compared to

respiratory symptomatic controls (median 468.9 pg/µl [IQR 164.5-781.4 pg/µl] vs 139.1 pg/µl [IQR 27.4-196.5 pg/µl], p=0.029). No other differences were identified.

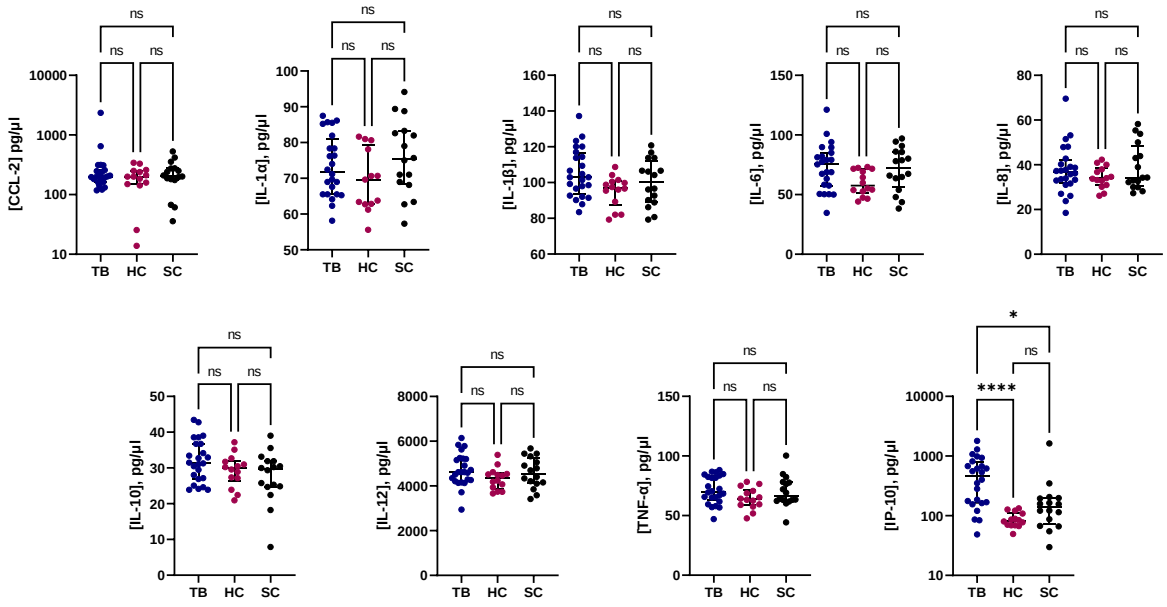

Figure 4.43 Soluble inflammation-related mediators measured in plasma samples from patients with TB (blue circles, n=25), healthy controls (HC, red circles, n=25), and respiratory symptomatic controls (SC, black circles, n=17).

A trend towards elevated plasma concentrations of measured pro-inflammatory markers in patients with TB compared to healthy controls was observed. Plasma levels of IP-10 were significantly higher in TB patients than in both healthy controls and respiratory symptomatic controls. Data compared using Kruskall-Wallace test with Dunn's correction for multiple comparisons, *p<0.05, ****p<0.0001.

When plasma levels of MMPs were evaluated, patients with TB were found to have significantly elevated levels of MMP-1, MMP-8, and MMP-10 compared to healthy controls (Figure 4.44). Concentrations of MMP-10 were also elevated in respiratory symptomatic patients compared to healthy controls, with no difference between patients with TB and respiratory symptomatic

patients, indicating that this marker may be elevated in all patients with lung disease regardless of aetiology.

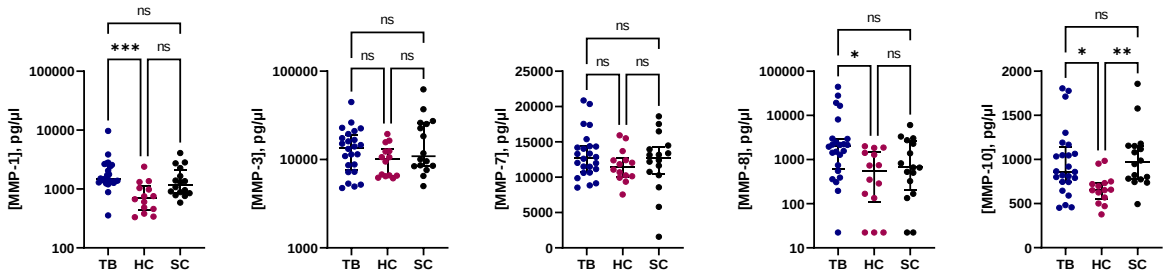

Figure 4.44 Concentrations of matrix metalloproteinases (MMPs) in plasma samples from patients with TB (blue circles, n=25), healthy controls (HC, red circles, n=25), and respiratory symptomatic controls (SC, black circles, n=17).

Plasma concentrations of MMP-1, MMP-8, and MMP-10 were elevated in patients with TB compared to healthy controls. Plasma levels of MMP-10 were also higher in respiratory symptomatic controls compared to healthy controls. Data compared using Kruskall-Wallace test with Dunn's correction for multiple comparisons, *p<0.05, **p<0.01, ***p<0.001.

Finally, evaluation of plasma concentrations of platelet mediators identified elevated levels of sCD40L, vWF-A2, and VEGF in plasma from patients with TB compared to healthy controls; vWF-A2 was also elevated in patients with non-TB lung disease compared to healthy controls with no difference between patients with TB and those with other causes of lung disease (Figure 4.45).

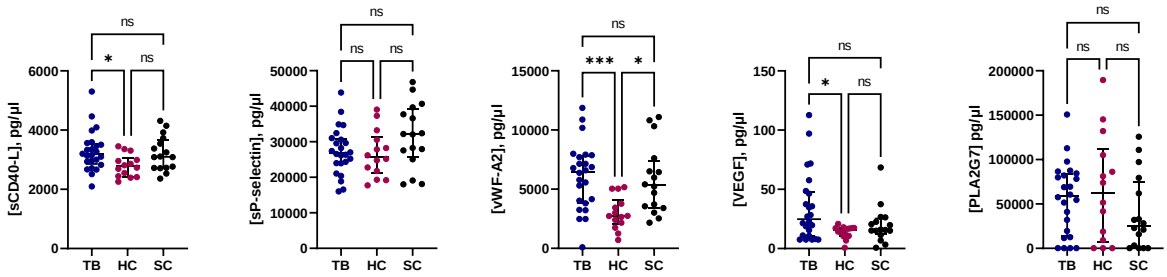

Figure 4.45 Concentrations of platelet-related factors in plasma samples from patients with TB (blue circles, n=25), healthy controls (HC, red circles, n=25), and respiratory symptomatic controls (SC, black circles, n=17).

Plasma concentrations of sCD40L, vWF-A2, and VEGF were elevated in patients with TB compared to healthy controls. Plasma levels of vWF-A2 were also higher in respiratory symptomatic controls compared to healthy controls. Data compared using Kruskall-Wallace test with Dunn's correction for multiple comparisons, *p<0.05, ***p<0.001.

4.7.5 Discussion

In summary, these data indicate some important differences in characteristics between patients with TB and both healthy and symptomatic controls. Correlation between concentrations of soluble mediators in BALF was strong, and this was particularly striking when evaluated only in patients with TB, which is indicative of strong inflammatory responses in the lungs. Despite the relatively small sample size and the broad range of measured concentrations between individuals, these data identified that concentrations of IL-1α, MMP-1, MMP-3, and PLA2G7 were significantly elevated in patients with TB, with an overall trend towards a pro-inflammatory response in the TB patients.

It is interesting that there was such a strongly negative correlation between BALF levels of VEGF and all other markers in the bronchoscopy patients with TB. BALF concentrations of VEGF were not higher in TB patients than those without TB overall, and this negative correlation was not seen in the plasma, where it correlated positively with a number of markers and plasma concentrations were in fact higher in TB patients than in healthy controls. VEGF, as its name implies, is important in angiogenesis and mainly targets endothelial cells. With fibroblast growth factor (FGF) and

hepatocyte growth factor (HGF) it is considered one of the direct proangiogenic markers, with transforming growth factor-beta (TGF-β), IL-6, IL-8, and platelet-derived growth factor (PDGF) acting as indirect proangiogenic markers(245). VEGF-mediated pathogenic effects in cancers and other diseases have been attributed to its effect on permeability and neoangiogenesis(246). In the lung, VEGF is released in response to hypoxia and causes inflammation and remodelling of the airways(245). Data from cellular studies suggest that VEGF secreted from M.tb-infected macrophages may facilitate spread from the primary site of infection, and in animal studies M.tb dissemination was reduced following anti-VEGF treatment(247). In patients with pulmonary TB it has been associated with fibrous remodelling in cavities (248), and in pleural TB with fibrosis (249). Unfortunately, radiological data are not available for the patients in our cohort so it has not been possible to assess whether levels were higher in patients who had evidence of radiological changes including cavitation. It is possible that reduced concentrations of VEGF may help to limit dissemination and this could be a protective response to pulmonary M.tb infection, and treatment of TB patients with anti-VEGF agents such as bevacizumab has been suggested(250).

A recent meta-analysis identified significant heterogeneity of VEGF levels across different clinical presentations of TB, as well as compartmentalisation(251). A single study was identified that measured VEGF in BALF, in which VEGF levels were elevated in BALF from patients with pleural TB compared to healthy controls(252). No studies comparing BALF levels in pulmonary TB compared to non-TB lung disease were found. Further investigation is needed in this area, specifically quantification of VEGF levels at different anatomical sites in patients with TB, and evaluation of changes in VEGF concentrations over time during anti-tuberculous treatment and how this relates to other processes in the lung.

Concentrations of MMPs were significantly higher in the lung in patients with TB compared to those without. This is in keeping with findings reported previously(46).

In the plasma, correlations were less strong than in the BALF. Nevertheless, correlations were much more skewed towards positivity among TB patients than in respiratory symptomatic controls and healthy controls. This is significant particularly if we view the data from the healthy control groups as the ‘normal’, and in whom correlations were highly variable and with a broader

distribution between positive and negative correlations. Notably, MMPs were found to correlate negatively with many of the pro-inflammatory mediators, notably IL-6 and IL-10.

It is interesting that MMPs correlated weakly even with one another, and in fact correlations between MMPs were stronger in patients with non-TB respiratory symptomatic disease than in those with TB. When concentrations were compared across the groups, however, there were significantly higher levels of MMPs in plasma from TB patients compared to both healthy controls and symptomatic controls. This was significant for MMPs 1, 8, and 10, and also reflects findings in the BALF. These findings were expected. MMP-1 is known to be highly important in pulmonary TB: it degrades type 1 collagen leading to inflammation and pathological processes including cavitation, and MMP-1 concentrations have been found previously to correlate with the extent of disease in pulmonary TB(54). Similarly, MMP-8 has been mechanistically linked with neutrophil-associated tissue destructive processes in the M.tb-infected lung(253).

Finally, the data showed that levels of platelet-associated markers were also higher in the plasma of patients with TB compared to healthy controls and to respiratory symptomatic controls. Von Willebrand factor was also elevated in the plasma of patients with non-TB lung disease. To our knowledge, this study represents the first time that von Willebrand factor has been evaluated in patients with pulmonary TB. In pleural disease, vWF has been found to be elevated in patients with an empyema caused by tuberculosis than in patients with cancer or heart failure(254), and in a study of contacts of Ugandan patients with TB, vWF was identified as a blood-based biomarker of early M.tb infection(255). vWF is involved in a wide variety of processes in addition to coagulation, including angiogenesis, cellular proliferation, and inflammation; it assists the adhesion of platelets to sites of vascular injury, playing a role in modulating inflammatory responses to vascular insults and in tissue repair(256). It may provide an important link between leukocytes and platelets in pulmonary inflammation, and this may be an effect that is not specific to TB.

Chapter 5 Clinical features and inflammation in a cohort of SARS-CoV-2 infected patients in 2020

5.1 Introduction

The clinical spectrum of disease associated with SARS-CoV-2 infection ranges from entirely asymptomatic to acute respiratory distress syndrome (ARDS) and septic shock, which can lead to multi-organ dysfunction (MOD) and death. Epidemiological data have highlighted that some groups are particularly at risk of poor outcomes, including the elderly, male sex, deprivation, those with pre-existing health conditions, and individuals from certain ethnic groups(257, 258). However, the specific mechanisms involved in progression to ARDS or MOD, and why some individuals are more at risk than others, remain poorly understood.

Early in the pandemic excessive inflammation including uncontrolled cytokine release was identified as a key component of the immunopathological damage and subsequent clinical deterioration occurring in some patients with SARS-CoV-2 infection. Cytokines are released in response to infection, whereupon they effect a multitude of functions including activation and coordination of immune responses that are useful in clearing pathogens from the site of infection. In addition, they concurrently initiate compensatory-repair processes that restore tissue and organ function. However, cytokine release can sometimes be disproportionate to the insult, leading to a “cytokine storm” that is detrimental to the host and can lead to significant and even fatal end organ damage.

This study aimed to characterise a cohort of patients with SARS-CoV-2 infection, and to explore patient factors relating to immune responses, levels of serum inflammation-associated biomarkers, and disease severity and outcomes.

5.2 Methods

5.2.1 Participants

The study population comprised patients with RT-PCR-confirmed SARS-CoV-2 infection and a blood sample sent for biochemistry analysis at the South West London Pathology (SWLP) laboratory. The SWLP laboratory provides a regional service for microbial diagnostics and is located within St. George's Hospital NHS Foundation Trust, a tertiary teaching hospital in London, UK. RT-PCR testing was performed on nasopharyngeal swab samples using Roche RNA extraction kits (Magnapure, West Sussex, UK) followed by Altona Diagnostics RealStar® SARS-CoV-2 RT-PCR Kit (S and E genes, Hamburg, Germany) or Roche cobas® SARS-CoV-2 Test (E and ORF targets).

5.2.2 Procedures

Each weekday a list of patients with positive SARS-CoV-2 RT-PCR tests and a blood sample in the last 72 hours was generated. Excess diagnostic material (EDM), comprising surplus serum from samples taken for clinical management, was obtained from the laboratory. Once included in the cohort, patients were sampled longitudinally; if samples became unavailable from one patient, a new patient was added to the cohort. A maximum of 30 samples per day were collected due to limitations in processing capacity. This thus represents a convenience sample. In addition, clinical and demographic information were collected from the patients' electronic medical records.

Aliquots of serum were anonymised and stored at 4°C. They were then used to measure antibody levels using the OMEGA IgG ELISA and Mologic Lateral Flow Assay, before being stored at -80°C.

Stored aliquots were batch tested for cytokine levels using high performance electrochemiluminescence multiplex immunoassay kits (Meso Scale Discovery (MSD), Rockville, MD, USA) as per the manufacturer's instructions. Samples with sufficient volume remaining after antibody testing had been completed were selected chronologically until the capacity of the multiplex kits was reached.

5.2.3 Scoring of severity of illness

A variety of different scoring systems have been developed to help stratify patients with SARS-CoV-2 infection according to severity and to predict outcome. The large number of scores available, the poor definition of variables and outcomes, and applicability in specific settings such as emergency departments or intensive care units, have made it difficult to compare severity across studies (259, 260). Moreover, many available severity indexes include markers that are not readily available or routinely gathered from patients(261-264) or use an unmanageably large number of variables(265, 266). Some severity scores, including the 4C Mortality Score which was developed based on data from the ISARIC study(267) aim to stratify patients according clinical information at initial presentation, which for the purposes of this study may be misleading as they depend upon the stage in their illness that the patient presents to hospital.

We opted for a simple score of 0 to 5 based on maximal oxygen requirements during the patient's illness, shown in Box 1 below. These data could easily and reliably be obtained from the patient's clinical record. This is similar to scores used elsewhere(268).

Box 1 Severity scoring system applied to patients with PCR-confirmed SARS-CoV-2 infection

0	Asymptomatic, no oxygen requirement
1	Symptomatic at time of swab, no oxygen requirement
2	Received oxygen via nasal cannulae for ≥12h
3	Received oxygen via face mask for ≥12h
4	Received non-invasive ventilation for ≥12h
5	Intubated and ventilated for ≥12h

5.2.4 Laboratory assays

5.2.4.1 Enzyme-linked immunosorbent assay (ELISA) for human IgG against SARS-CoV-2

The COVID-19 IgG ELISA assay, developed by Mologic (Bedford, UK) and manufactured by Omega (Omega Diagnostics, Cambridge UK), was used according to the manufacturer's instructions and contained spike 2 and nucleoprotein SARS-CoV-2 antigens.

5.2.4.2 Lateral flow test for human IgA, IgM, and IgG against SARS-CoV-2

The lateral flow assay was also developed by Mologic (Bedford, UK) and samples were processed according to the manufacturer's instructions. Briefly, 5ul of patient serum was loaded onto the sample pad, followed by 80ul chase buffer. After ten minutes, the presence or absence of three lines, indicating presence of IgA, IgM, and IgG, was noted, and for each line, a score was given on a scale of 0-10 with 0 being negative and 10 a strong positive. The presence of a red control line indicated that the test was successful. All tests were read by two independently trained readers and average scores were obtained.

5.2.4.3 Multiplex assays

Bespoke MSD V-plex, R-plex and U-plex assays were used to measure serum concentrations of cytokines interleukin (IL) -6 (IL-6), Il-7, IL-8, IL-10, interferon gamma-induced protein 10 (IP-10), and tumour necrosis factor alpha (TNF-α); eosinophil chemotactic protein Eotaxin; marker of inflammation C-reactive protein (CRP); platelet-associated factors platelet-derived growth factor B (PDGF-B) and von Willebrand factor (vWF); and matrix metalloproteinases 8 and 9 (MMP-8 and MMP-9 respectively). Assays were performed in accordance with the manufacturer's instructions. Briefly, electrochemiluminescence plates were pre-coated with a capture antibody and incubated with shaking at 700 rpm for 1 hour or at 500 rpm overnight. The plates were washed, then loaded with samples or standards prepared in a 1:4 dilution series. Sample dilutions ranged from 1:2 to 1:10,000 depending on the analyte, as per the manufacturer's instructions. The plates were incubated with shaking at room temperature then washed, prior to addition of a detection antibody. After a final incubation step the plates were washed, read buffer was added to each well, and the plates were placed on the MSD platform and read according to a standard protocol. Data were downloaded in Excel and analysed in GraphPad PRISM v9.1.2 and *R* statistical software package version 4.0.5..

5.2.5 Multiple logistic regression modelling

To assess the effect of clinical and demographic features at diagnosis on outcome, multiple logistic regression was performed. For this analysis, data were restricted to patients who had been admitted to hospital (n=288).

5.2.5.1 Variable selection

Outcomes

The following outcomes were evaluated:

Oxygen requirement defined as a severity score ≥ 2

Administration of non-invasive or invasive ventilation defined as a severity score ≥ 4

Admission to intensive care (ITU)

28-day mortality defined as death within 28 days of a first positive SARS-CoV-2 PCR test

Explanatory variables

Explanatory variables were selected based on *a priori* knowledge or evidence of a likely association with the outcome under investigation. Variables that were included are described below.

Age was converted into a binary category of either below or equal to or above the median age of participants (63.5 years).

Obesity was defined as a body mass index (BMI) of 30 or greater. This was calculated from each patient's height and weight documentation in their electronic patient record on the date that was closest to the result of their first positive swab.

Ethnicity data are collected routinely by the NHS and classified according to values set by the Office for National Statistics as per the 2001 census. Ethnic category is defined as the ethnicity of a person as specified by the person(269). Categories were grouped into White, which included categories A (White – British), B (White – Irish), and C (White – Any

other White background); Non-White (categories D-R), and Other or unknown, which comprised categories S (Other ethnic groups – any other ethnic group) or Z (not stated).

Co-morbidity data were collected from each participant's electronic patient record. Any illness listed in their past medical history on admission to hospital and/or subsequent clinical entries was included. Co-morbidities deemed important based on reports in the literature and clinical opinion were defined as listed in Figure 5.2. For the purposes of this analysis, an additional category of 'any other significant co-morbidity' category was generated. This was subjective, based on whether any concurrent illnesses may have affected a patient's immune response to an infection, and as defined by two physicians. 36 participants (12.5%) had an illness that was considered significant but did not fall into one of the pre-specified groups.

Wave was defined as first or second wave depending on whether the patient's first positive PCR test was taken prior to or after 1st August 2020 (see Figure 5.1). This was considered important because of the likelihood that the virus itself, its associated clinical features, the management of patients with SARS-CoV-2 infection, and hospital capacity including availability of ITU beds will have changed over time.

Oxygen requirement was defined as no oxygen received by the patient (none), oxygen delivered via a nasal cannula or simple face mask for a minimum of 12 hours (non-invasive), or oxygen delivered via non-invasive ventilation (NIV) or mechanical ventilation for a minimum of 12 hours (invasive).

It is not possible to exclude the possibility of important co-variates for which data are were not available, such as receipt of corticosteroids or other medications.

5.2.5.2 Model Selection

Interactions between the explanatory variables were evaluated based on their scientific plausibility. To maintain model interpretability, only a single interaction term was allowed in a model at any one time. The Akaike information criterion (AIC) value was used to evaluate model fit and the model with the lowest AIC was selected. To give an objective measure of fit,

McFadden's adjusted pseudo-R^2 was calculated(270). This was selected as a summary measure of predictive power as a true R^2 cannot be calculated from logistic regression models(271).

5.2.6 Statistical analyses

Acute outcomes were defined as: severity of illness; Intensive Therapy Unit (ITU) stay; death within 28 days of the first positive swab (28-day mortality); and a composite outcome of death within 28 days and/or ITU admission. Data were analysed using GraphPad PRISM version 9.2.1 and *R* statistical software package version 4.0.5. Two-tailed parametric and non-parametric tests were used as appropriate. Multiple logistic regression was performed to determine the relationship between demographic characteristics and clinical outcomes. Correlation between concentrations of serum biomarkers was evaluated using Spearman's analysis, and associations between serum biomarker levels and outcomes were explored using Mann-Whitney tests, or Kruskall-Wallis test with Dunn's *post hoc* correction for multiple comparisons.

5.2.7 Ethics

Ethical approval was obtained from the NHS Health Research Authority (Development and Assessment of Rapid Testing for SARS-CoV-2 Outbreak, DARTS - IRAS project ID: 282104; REC reference: 20/SC/0171) and the trial is registered at clinicaltrials.gov (NCT04351646).

5.3 Results

5.3.1 Clinical cohort

We evaluated data from 312 patients. Dates of first positive swabs ranged from 3rd March to 30th December 2020; distribution over time is indicated in Figure 5.1.

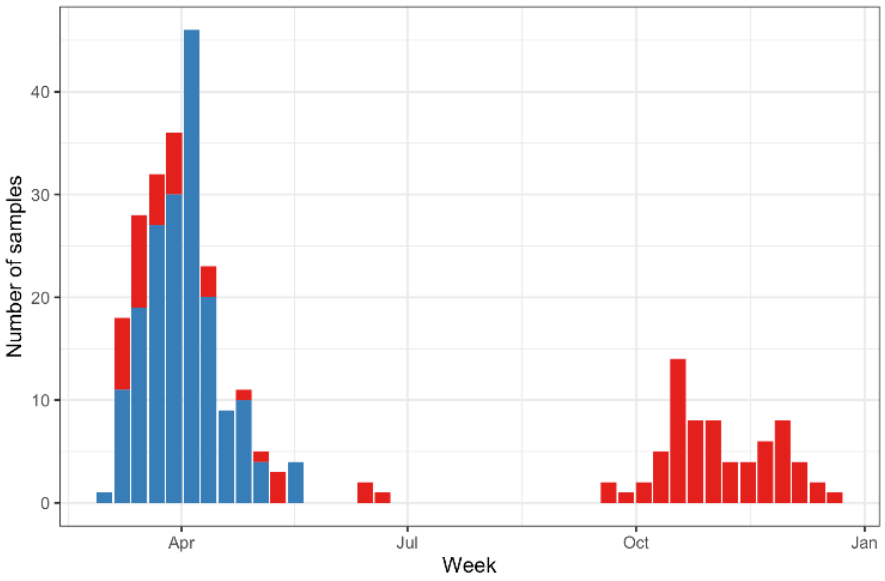

Figure 5.1 Histogram showing distribution cases over time.

Participants were recruited between 3rd March and 30th December 2020. Individual participants were classified as pertaining to the first or second wave of the pandemic depending on whether their first positive SARS-CoV-2 result was before or after 1st August 2020. Blue denotes patients for whom biomarker data are available (n=194); patients for whom red denotes biomarker data are not available (n=118). All samples that underwent biomarker analysis were taken from patients in the first wave, but some samples were omitted because there was insufficient volume available for complete analysis.

Demographics are presented in Table 7. Median age was 64 years (IQR 49-76) and 177 (56.7%) were males. 107 (34.3%) were white, 105 (33.7%) were non-white, and 100 (32.1%) were of unknown or other ethnicity. Height and weight at the time of the swab were available for 300/312 patients; median BMI was 25.2 (IQR 22.1-30.4), and 44 patients had a BMI greater than 30.

Data on whether individuals were symptomatic at the time of the swab were available for 302 patients (97.1%), of whom 267 patients (88.4%) were symptomatic at the time of their swab. We were able to establish the approximate date of symptom onset for 261 patients, among whom the median number of days from onset of symptoms to the first positive swab was 5 days (IQR 2-8 days).

Table 7 Demographic and clinical characteristics of study participants.

	Total N = 312	Biomarker data available N=194	Biomarker data not available N=118	p-value
Age, years, median (IQR)	64 (49-76)	64 (52-77)	62.5 (44.75-72.25)	0.29
No. of males (%)	177 (56.7%)	108 (55.7%)	69 (58.5%)	0.64
BMI, median (IQR) (N = 287)*	25.2 (22.1-30.4)	25.1 (21.9-29.8)	22.6 (25.3-31.1)	0.36
Ethnicity				
White	107 (34.3%)	64 (33%)	43 (36.4%)	0.76
Non-white	105 (33.7%)	68 (35.1%)	37 (31.4%)	
Other/not known	100 (32.1%)	62 (32%)	38 (32.2%)	
Relevant co-morbidities¥				
None	92 (29.5%)	66 (34%)	26 (22%)	**0.0063**
1 co-morbidity	92 (29.5%)	52 (26.8%)	40 (33.9%)	
2 co-morbidities	79 (25.3%)	54 (27.8%)	25 (21.2%)	
3 or more co-morbidities	49 (15.7%)	22 (11.3%)	27 (22.9%)	
Date of diagnosis				
Median date of diagnosis (range)	10/04/2020 (03/03/2020 – 30/12/2020)	06/04/2020 (03/03/2020 – 18/10/2020)	18/10/2020 (10/03/2020 – 30/12/2020)	
Symptoms				
Symptomatic (N=302)*	267 (88.4%)	176/190 (92.6%)	91/112 (81.3%)	**0.0028**
Median time from symptoms to RT-PCR swab, days (IQR)	5 (2-8)	5 (2-8)	4 (1-8)	0.16
Severity				
0 (asymptomatic, no oxygen requirement)	41 (13.1%)	18 (9.3%)	23 (19.5%)	**0.0019**
1 (symptomatic at time of swab, no oxygen requirement)	68 (21.8%)	41 (21.1%)	27 (22.9%)	
2 (received oxygen via nasal cannulae for ≥12h)	57 (18.3%)	36 (18.6%)	21 (17.8%)	
3 (received oxygen via face mask for ≥12h)	54 (17.3%)	36 (18.6%)	18 (15.3%)	
4 (received non-invasive ventilation for ≥12h)	12 (3.8%)	3 (1.5%)	9 (7.6%)	
5 (intubated and ventilated for ≥12h)	80 (25.6%)	60 (30.9%)	20 (16.9%)	

Serological testing for SARS-CoV-2 infection				
IgG ELISA positive (%)	275/308 (89.3%)	181/194 (93.3%)	94/114 (82.5%)	**0.004**
Peak normalised optical density (NOD), median (IQR)	1.25 (0.62-1.6)	1.28 (0.73-1.6)	1.05 (0.34-1.6)	**0.049**
No. of samples per patient, median (IQR)	3 (1-6)	4 (2-8)	1 (1-2)	**<0.0001**
Days post swab of first positive ELISA, median (IQR)	14 (9-24)	13 (9-23)	15 (8-36.5)	0.27
Days post swab of peak NOD, median (IQR)	20 (12-46.75)	23 (14-48)	16.5 (10-41.25)	0.052
LFA positive (%)	271/301 (90%)	190/194 (97.9%)	81/107 (75.7%)	**<0.0001**
IgA positive on LFA (%)	188/301 (62.5%)	146/194 (75.3%)	42/107 (43.9%)	**<0.0001**
IgM positive on LFA (%)	159/301 (52.8%)	129/194 (66.5%)	30/107 (28%)	**<0.0001**
IgG positive on LFA (%)	270/301 (89.7%)	189/194 (97.4%)	81/107 (75.7%)	**<0.0001**
No. of samples per patient, median (IQR)	3 (1-6)	4 (2-8)	1 (1-2)	**<0.0001**
Days post swab of first positive LFA, median (IQR)	14 (9-27)	15 (8.5-39)	14 (9-24.25)	0.18
Treatment location and Outcome				
Occupational health	9 (2.9%)	4 (2.1%)	5 (4.2%)	0.31
Outpatient	7 (2.2%)	5 (2.6%)	2 (1.7%)	0.71
Seen in ED only	8 (2.6%)	4 (2.1%)	4 (3.4%)	0.48
Hospitalised (%)	288 (92.3%)	181 (93.3%)	107 (90.7%)	0.39
Admitted to ITU (%)	105/288 (36.5%)	68/181 (37.6%)	37/107 (38.3%)	0.70
28-day mortality (%)	29/105 (27.6%)	20/68 (29.4%)	13/37 (35.1%)	0.66
Discharged (%)	203/288 (70.5%)	125/181 (69.1%)	78/107 (72.9%)	0.51
Length of stay, days, median (IQR)	19.9 (10.1-40.0)	19.7 (10.9-39.9)	21.5 (8.6-40.3)	0.44
Deceased (%)	87/288 (30.2%)	56/181 (30.9%)	31/107 (29%)	0.79
Length of stay, days, median (IQR)	19.3 (14.6-31)	21 (15.3-75.3)	23 (16-37)	0.61
28-day mortality (%)	46/288 (16.0%)	29/181 (16.0%)	17/107 (15.9%)	>0.99
Deceased ≤28 days after first positive swab and/or ITU admission (%)	123/288 (42.7%)	78/181 (43.1%)	45/107 (42.1%)	0.90

* Height unavailable for 25 patients and symptom data unavailable for 10 patients

¥ Relevant co-morbidities defined as: Hypertension, diabetes, chronic kidney disease, chronic lung disease, and malignancy.

P-values calculated using two-tailed Mann Whitney test for continuous data, two-tailed Fisher's exact test for categorical data, and Chi squared for multiple categories data.

Patient co-morbidities are shown in Figure 5.2. Hypertension, diabetes, chronic kidney disease, chronic lung disease, and malignancy were selected *a priori* as relevant co-morbidities for this study, as they have been associated with worse outcomes in SARS-CoV-2 infection(272-276). Of the co-morbidities listed, the median number was 1 (IQR 0-2); 92 patients had none of the co-morbidities listed, 92 had one, 79 had two, and 49 had three or more (Table 7).

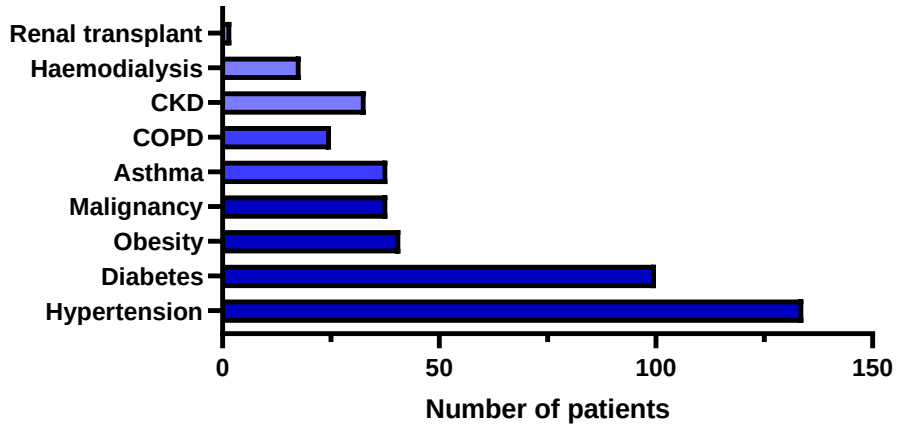

Figure 5.2 Frequency of patient co-morbidities.

CKD = chronic kidney disease, COPD = chronic obstructive pulmonary disease.

Data on clinical features at the time of the swab were available for 262/267 symptomatic patients (98.1%). Three patients had been transferred from elsewhere and details of their illness prior to transfer were absent, one was seen as part of a vaccine study and notes were stored elsewhere, and the fifth was seen in ED but documentation was minimal.

Symptomatic patients presented with a median of 3 different symptoms (IQR 2-5 symptoms). Frequencies of individual symptoms are shown in Figure 5.3. The most common presenting symptom was fever (72.9%) followed by cough (71.8%), dyspnoea (56.9%) and lethargy (41.6%). 75 patients (28.6%) presented with gastrointestinal symptoms, including 50 with diarrhoea, 32 with vomiting, and 20 with abdominal pain. 246 patients (93.9%) presented with one or more of the classic triad of cough, fever, or dyspnoea, with 93 patients reporting all three. 28 patients (9.0%) were found to be positive on incidental testing, for example on a swab performed upon admission for an unrelated presentation, or performed prior to discharge to a rehabilitation or

care-providing institution. 11 patients (3.5%) were swabbed due to contact with a positive patient in the hospital.

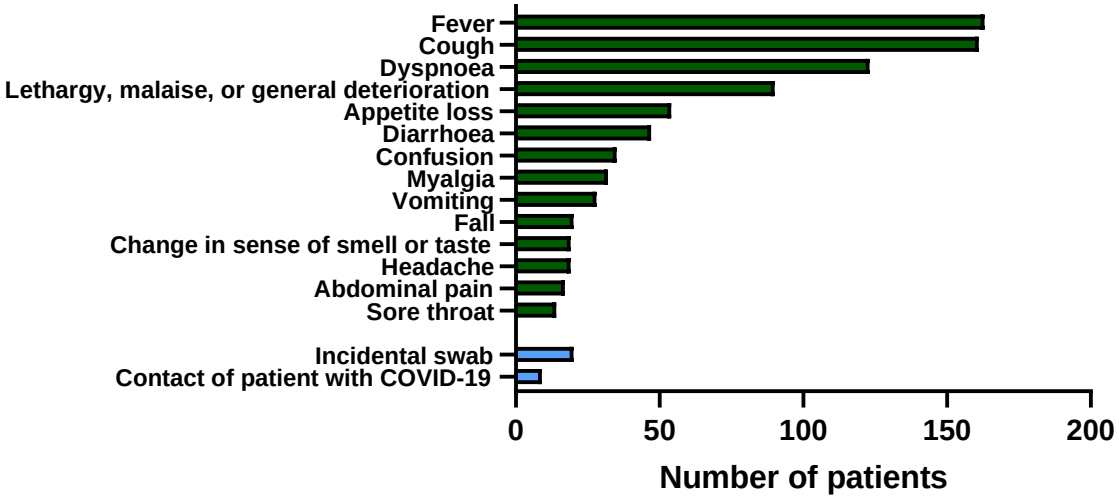

Figure 5.3 Symptoms at presentation.

Patients were classified by severity depending on their maximal oxygen requirements, according to a scale of 0-5 (Table 7). 109 (34.9%) patients did not require any oxygen at all (severity 0-1, mild), 111 (35.6%) patients required oxygen supplementation via nasal cannulae or a face mask for at least 12 hours (severity 2-3, moderate), and 92 (29.5%) patients received either NIV or mechanical ventilation for at least 12 hours (severity 4-5, severe).

Serological testing was performed for 308 patients using ELISA and 301 patients using LFA. 275 (89.3%) of patients were positive for IgG according to ELISA, and 271 (90%) were positive according to the LFA. 13 patients were positive according to LFA and negative according to ELISA, all of whom had a positive score for IgG on the LFA, and ten patients were positive according to ELISA and negative according to the LFA.

In our cohort, the majority of patients (92.3%) were hospitalised; 8 were seen in ED and not admitted, 7 were seen as outpatients, and 9 were tested through occupational health services. Of the patients who were hospitalised, 105 (36.5%) were admitted to the intensive therapy unit during their admission, including 39 patients who eventually died (29 who died within 28 days of their first positive swab). 203 patients were ultimately discharged from hospital after a median

length of stay of 19.4 days (IQR 10.6-36.1 days). 87 patients (27.9%) died during the follow-up period, after a median length of stay of 19.3 days (IQR 14.6-31 days). The median duration from the date of the first positive swab to death was 21 days (IQR 16-47 days), and this included 46 patients who died within 28 days of their first positive swab. Two patients died soon after being discharged from hospital.

There was no difference in age, sex, BMI, or ethnicity between the 194 patients for whom cytokine data are available, and the 118 patients for whom these measurements were not taken (Table 7). Those with cytokine data had more co-morbidities, were more likely to be symptomatic, and had more severe disease. They were also more likely to be positive according to ELISA (93.3% vs 82.5%, p=0.004), with higher median peak NOD values (1.3 vs 1.05 respectively, p=0.049), and also more likely to be positive according to LFA (97.9% vs 75.7%, p<0.0001). There was no difference in rates of hospitalisation, admission to intensive care, death, or length of stay.

5.3.2 Associations between explanatory variables and outcomes

Multiple logistic regression models were generated to assess whether clinical and demographic features at diagnosis were associated with outcomes among hospitalised participants (n=288) as described above.

Explanatory variables associated with receiving any oxygen therapy are presented in Table 8. Obesity was found to be associated with an odds ratio of 2.05 (95% CI 1.06 – 4.15) of requiring any oxygen therapy compared to having a BMI <30. No other factors were found to be significant, although it is worth noting that the presence of significant co-morbidities was associated with a trend towards a lower likelihood of receiving oxygen therapy compared to not having any co-morbidities (odds ratio 0.40, 95% CI 0.14-0.98).

Table 8 Output of logistic regression model exploring associations between explanatory variables and oxygen requirement among hospitalised participants.

Characteristic	Odds Ratio	95% CI	p-value
Age			
<63.5 years	—	—	
≥63.5 years	0.71	0.41, 1.23	0.2
Obesity			
No	—	—	
Yes	2.05	1.06, 4.15	**0.039**
Gender			
Female	—	—	
Male	1.03	0.60, 1.77	>0.9
Ethnicity			
White	—	—	
Non-white	1.75	0.92, 3.36	0.088
Other/unknown	1.34	0.71, 2.55	0.4
Significant co-morbidities	0.40	0.14, 0.98	0.060
Wave			
First	—	—	
Second	0.83	0.44, 1.56	0.6
Adjusted McFadden's R^2 value			0.068

CI = Confidence Interval

Factors associated with receiving non-invasive ventilation (NIV) or intubation and mechanical ventilation are presented in Table 9. Older adults were less likely to be ventilated (odds ratio 0.4, 95% CI 0.22-0.71) compared to adults whose age was below the median age of 63.5 years. Significant co-morbidities were also associated with a lower likelihood of receiving non-invasive or invasive ventilation (odds ratio 0.26, 95% CI 0.12-0.55).

Table 9 Output of logistic regression model exploring associations between explanatory variables and receiving non-invasive or invasive ventilation among hospitalised participants.

Characteristic	Odds Ratio	95% CI	p-value
Age			
<63.5 years	—	—	
≥63.5 years	0.40	0.22, 0.71	**0.002**
Obesity			
No	—	—	
Yes	1.73	0.93, 3.21	0.081
Gender			
Female	—	—	
Male	1.14	0.64, 2.03	0.7
Ethnicity			
White	—	—	
Non-white	1.71	0.86, 3.45	0.13
Other/unknown	1.69	0.84, 3.45	0.14
Significant co-morbidities	0.26	0.12, 0.55	**<0.001**
Wave			
First	—	—	
Second	1.49	0.79, 2.78	0.2
Adjusted McFadden's R^2 value			0.159

CI = Confidence Interval

Similarly, factors associated with admission to ITU, presented in

Table 10, indicate a lower likelihood of admission to ITU in older people (odds ratio 0.36, 95% CI 0.20-0.64) and in those with significant co-morbidities (odds ratio 0.16, 95% CI 0.06-0.39). Non-white ethnicity was associated with higher likelihood of admission to ITU compared to white ethnicity (odds ratio 2.02, 95% CI 1.02-4.08). Obesity was again borderline associated with a trend towards greater likelihood of admission to ITU although this did not reach statistical significance (odds ratio 1.73, 95% CI 0.92-3.23).

Whether the patient was admitted to hospital with SARS-CoV-2 infection in the first or the second wave did not affect their likelihood of admission to ITU. However, a significant interaction was identified between having one or more significant co-morbidities and wave, with an odds ratio of 7.95 (95% CI 1.17-58.2) for patients with significant co-morbidities admitted in the second wave versus patients without co-morbidities admitted in the first wave. The inclusion of this interaction in the model improved the AIC from 321.49 to 319.02. None of the other interactions that were considered affected the AIC or were deemed to be of interest.

Table 10 Output of logistic regression model exploring associations between explanatory variables admission to intensive care among hospitalised participants.

Characteristic	Odds Ratio	95% CI	p-value
Age			
<63.5 years	—	—	
≥63.5 years	0.36	0.20, 0.64	**<0.001**
Obesity			
No	—	—	
Yes	1.73	0.92, 3.23	0.084
Gender			
Female	—	—	
Male	1.09	0.61, 1.93	0.8
Ethnicity			
White	—	—	
Non-white	2.02	1.02, 4.08	**0.046**
Other/unknown	1.98	0.98, 4.05	0.058
Significant co-morbidities	0.16	0.06, 0.39	**<0.001**
Wave			
First	—	—	
Second	0.28	0.04, 1.72	0.2
Interactions			
Significant co-morbidities and Second wave	7.95	1.17, 58.2	**0.034**
Adjusted McFadden's R^2 value			0.198

CI = Confidence Interval

Finally, likelihood of death within 28 days of a first positive SARS-CoV-2 PCR result is presented in Table 11. The likelihood of death within 28 days was positively associated with age over 63.5 years (odds ratio 3.69, 95% CI 1.65-8.73). It was also associated with having received non-invasive or invasive forms of oxygen delivery (odds ratio 6.99, 95% CI 1.85-45.8, and odds ratio 31.1, 95%

CI 7.95-209, respectively), as expected. Notably, the presence of significant co-morbidities was not associated with likelihood of death within 28 days, and neither was whether the patient was unwell during the first or the second wave.

Table 11 Output of logistic regression model exploring associations between explanatory variables and 28-day mortality among hospitalised participants.

Characteristic	Odds Ratio	95% CI	p-value
Age			
<63.5 years	—	—	
≥63.5 years	3.69	1.65, 8.73	**0.002**
Obesity			
No	—	—	
Yes	1.13	0.49, 2.51	0.8
Gender			
Female	—	—	
Male	1.29	0.62, 2.77	0.5
Ethnicity			
White	—	—	
Non-white	1.33	0.55, 3.27	0.5
Other/unknown	0.89	0.35, 2.26	0.8
Significant co-morbidities	2.15	0.72, 7.45	0.2
Oxygen requirement			
None	—	—	
Non-invasive	6.99	1.85, 45.8	**0.012**
Invasive	31.1	7.95,209	**<0.001**
Wave			
First	—	—	
Second	0.90	0.36, 2.14	0.8
Adjusted McFadden's R^2 value			0.219

CI = Confidence Interval

5.3.2.1 Interpretation of findings

This analysis shows clearly that younger age was associated with receipt of oxygen therapy and admission to ITU, whereas older age was associated with 28 day mortality. Obesity was identified as associated with poor outcomes, and similarly, a trend towards being male and of non-white ethnicity being associated with negative outcomes was observed. Although these did not always reach statistical significance, this is a biologically plausible result and is in keeping with findings published elsewhere in the literature(277, 278).

The unexpected lack of a positive association between co-morbidities and likelihood of death within 28 days may be accounted for by the lack of granularity within these data. Patients with any co-morbidities were grouped together in this binary classification, masking any difference in outcomes between patients with simple co-morbidities such as tablet-controlled hypertension versus multimorbidity.

It is important that these findings are interpreted in the context of clinical reasoning, as well as the lived experience during the pandemic. The negative association between age and presence of co-morbidities and negative outcomes, including receipt of oxygen therapy and admission to ITU, may be explained by a multitude of factors leading to a difference in the management of patients with SARS-CoV-2 infection over time. It is notable that an association was found between presence of co-morbidities and whether the patient was admitted to hospital during the first or the second wave of the pandemic. The second wave may have been characterized by different prevalent strains of the virus, with associated different clinical phenotypic effects. Although vaccines were not yet available, immunity from past infection may have contributed to changes in clinical severity over time. We certainly saw an improvement in the management of patients arising from greater collective experience of the disease, as well as the rapid and immense emergence of available resources including observational studies and clinical trials leading to the routine use of medications such as corticosteroids and Remdesivir which have been shown to be highly effective(279, 280). It is lamentable that information on medication use from this cohort of patients is not available as it would be of interest to evaluate whether we could demonstrate improved outcomes associated with receipt of specific medications. Moreover, hospital capacity, including availability of ITU beds, may have influenced decisions on which patients were eligible for, and/or received, high level support(281, 282).

Other limitations of the data include the large proportion of patients for whom data on ethnicity were not available. Moreover, the retrospective nature of this study meant that the collection of data on clinical features was dependent on the quality of the medical notes, which was affected by multiple factors including mode of presentation to the hospital, time of day, and grade of the doctor admitting the patient. Data on co-morbidities in particular was often minimal or absent; for example, if a patient was transferred from another hospital a detailed list of past medical history may not have been available on our records.

5.3.3 Serum biomarkers in patients with SARS-CoV-2 infection

Serum biomarkers were measured in stored serum samples from study participants as detailed above. Patients whose samples underwent evaluation were all pertaining to wave 1, as represented by the blue bars in Figure 5.1.

5.3.3.1 Correlation between concentrations of serum biomarkers in SARS-CoV-2 infection

Crude correlation between all of the measured markers is shown in Figure 5.4. MMP-8 correlated strongly with MMP-9 (0.79), IL-6 (0.54), IL-8 (0.54), and CRP (0.45). IP-10 correlated strongly with IL-6 (0.51), CRP (0.46), and vWF (0.47). A strong correlation was also observed between CRP and IL-6 (0.52), as expected, and also with IP-10 (0.46).

PDGF-B, TNFα, IL-7, and Eotaxin were noted to have correlated negatively or weakly positive with some of the other markers evaluated. PDGF-B correlated strongly with IL-7 (0.50) but none of these other markers correlated well with each other.

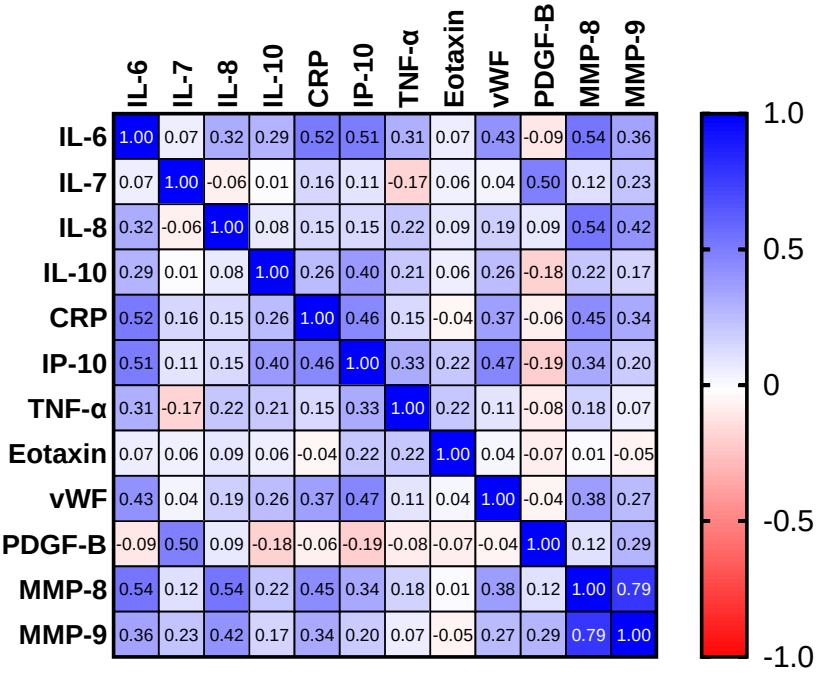

Figure 5.4 Correlation between serum biomarkers measured in all samples.

Correlation matrix computed using Spearman's analysis. N=720. Values indicate Spearman correlation coefficients (*r*).

Correlation between peak values is presented in Figure 5.5. Different values may have peaked at different times in the patient's clinical trajectory. All of the markers were positively correlated, with weak correlations between IL-7 and PDGF-B and the other markers; none were negatively correlated. This is in keeping with COVID-19 being associated with a strong inflammatory response.

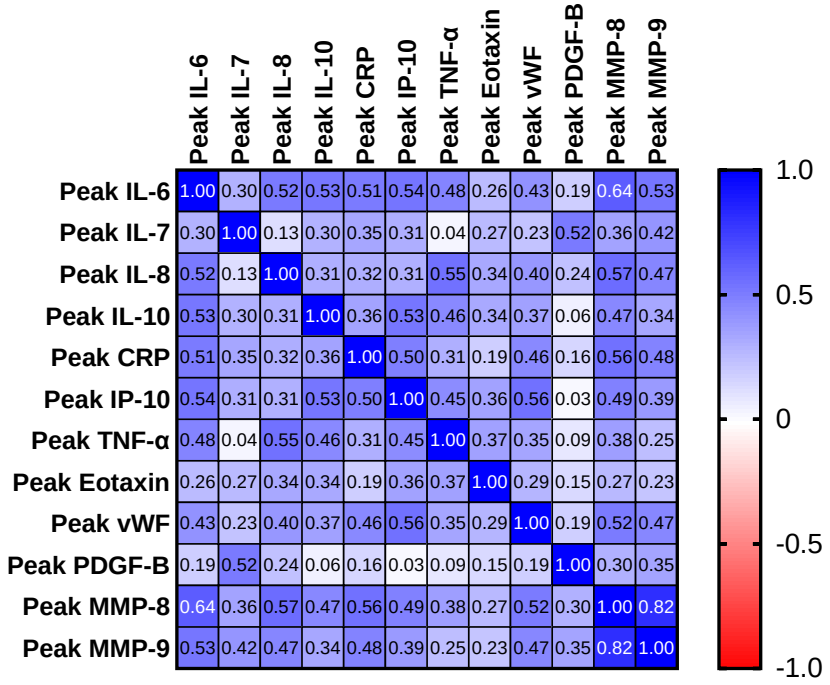

Figure 5.5 Correlation between peak serum biomarker concentrations for each participant.

Correlation matrix computed using Spearman's analysis. N=194. Values indicate Spearman correlation coefficients (*r*).

5.3.3.2 Association between levels of serum biomarkers and disease severity in SARS-CoV-2 infection.

Peak concentrations of serum biomarkers according to severity on the scale of 0 to 5 described above are presented in Figure 5.6 and Figure 5.7. There was a positive association between maximal severity of illness and concentration of the majority of the markers; there was no difference in concentrations of eotaxin, IL-10, or PDGF-B. None of the markers were negatively

correlated. Differences were predominantly observed between categories 0 (asymptomatic, no oxygen requirement) and 5 (receiving invasive ventilation).

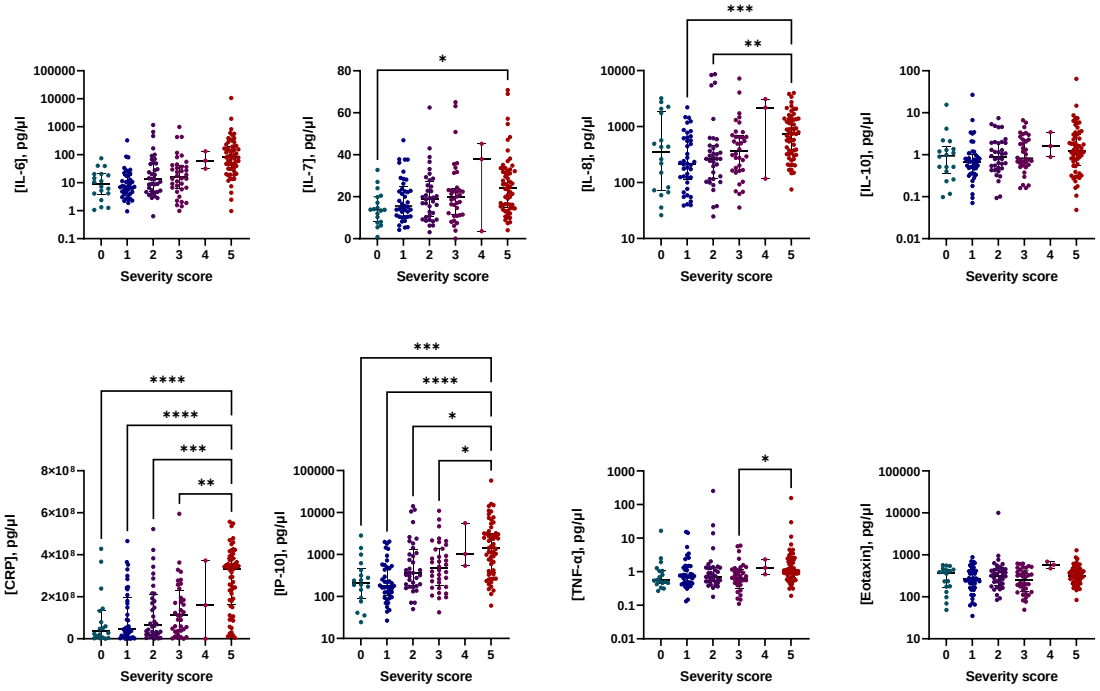

Figure 5.6 Maximal serum cytokine and chemokine levels according to severity score.

A positive relationship can be observed between severity score and peak serum concentrations of cytokines and chemokines. This was most prominently seen for IL-8, CRP, and IP-10. Data compared using Kruskall-Wallis test with Dunn's *post hoc* correction for multiple comparisons. *p<0.05, **p<0.01, ***p<0.001, ****p<0.0001.

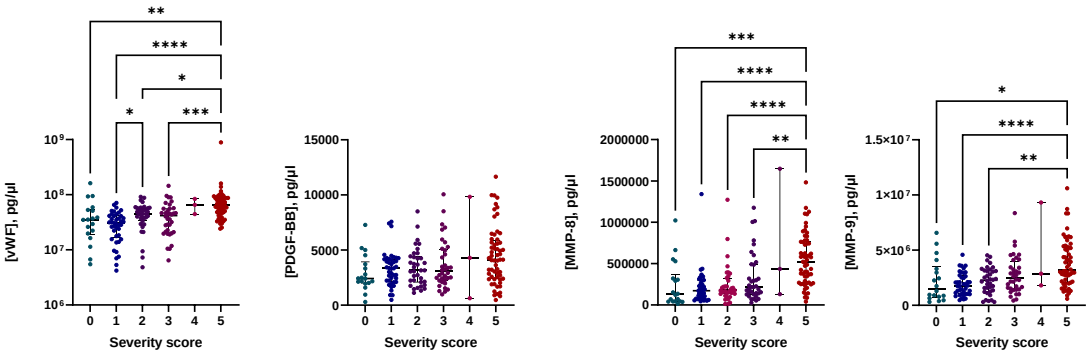

Figure 5.7 Maximal serum levels of platelet-associated factors platelet derived growth factor B (PDGF-B) and von Willebrand factor (vWF), Matrix metalloproteinase (MMP) -8 (MMP-8), and MMP-9, according to severity score.

Serum concentrations of vWF, MMP-8, and MMP-9, but not PDGF-B, increased with increasing severity score. Data compared using Kruskall-Wallis test with Dunn's *post hoc* correction for multiple comparisons. *p<0.05, **p<0.01, ***p<0.001, ****p<0.0001.

When severity scores were grouped into three categories of mild disease (severity scores of 0 and 1, i.e. asymptomatic or symptomatic but not requiring oxygen); moderate disease (severity scores of 2 and 3, i.e. requiring oxygen delivery via nasal cannulae or a simple face mask); and severe disease (severity scores of 4 and 5, i.e. requiring oxygen delivery via non-invasive or invasive ventilation), the positive associations could again be clearly seen (Figure 5.8 and Figure 5.9). A positive association between severity of illness and concentration of the biomarker was found in all of the markers measured apart from eotaxin. Again, differences were more pronounced between mild and severe disease, or moderate and severe disease, with few markers being significantly different in mild versus moderate disease.

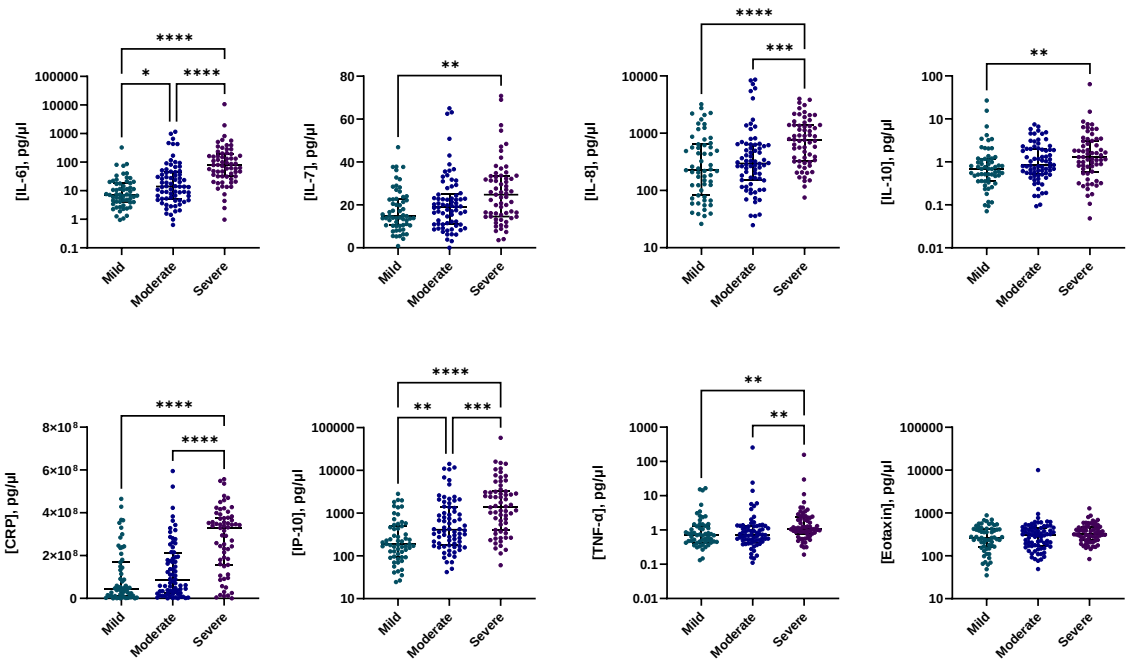

Figure 5.8 Maximal serum cytokine and chemokine levels according to severity category.

Serum concentrations of all markers of inflammation, apart from eosinophil chemokine eotaxin, increased with severity category. Data compared using Kruskall-Wallis test with Dunn's *post hoc* correction for multiple comparisons. *p<0.05, **p<0.01, ***p<0.001, ****p<0.0001.

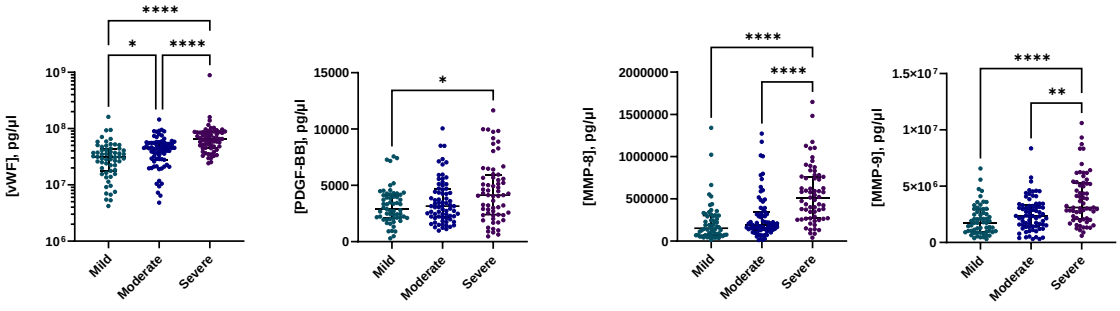

Figure 5.9 Maximal serum levels of platelet-associated factors platelet derived growth factor B (PDGF-B) and von Willebrand factor (vWF), Matrix metalloproteinase (MMP) -8 (MMP-8), and MMP-9, according to severity category.

Serum concentrations of vWF, PDGF-B, MMP-8, and MMP-9 increased with increasing severity category. Data compared using Kruskall-Wallis test with Dunn's *post hoc* correction for multiple comparisons. *p<0.05, **p<0.01, ****p<0.0001.

5.3.3.3 Association between levels of serum biomarkers and outcome in SARS-CoV-2 infection

To assess any association between levels of serum biomarkers and outcome, concentrations of measured markers were compared in patients who died within 28 days of their first positive SARS-CoV-2 PCR result (28-day mortality) versus those who did not. Of the cytokines that were evaluated, serum concentrations of IL-6, IL-10, CRP, and IP-10 were significantly higher in patients who died, whereas there was no difference in concentrations of IL-7, IL-8, TNF-α, or Eotaxin (Figure 5.10). The most striking difference was found in concentrations of IL-6 (109.8 pg/ml vs 14.1 pg/ml respectively, p<0.0001) and CRP (344 µg/ml vs 87.5 µg/ml respectively, p<0.0001).

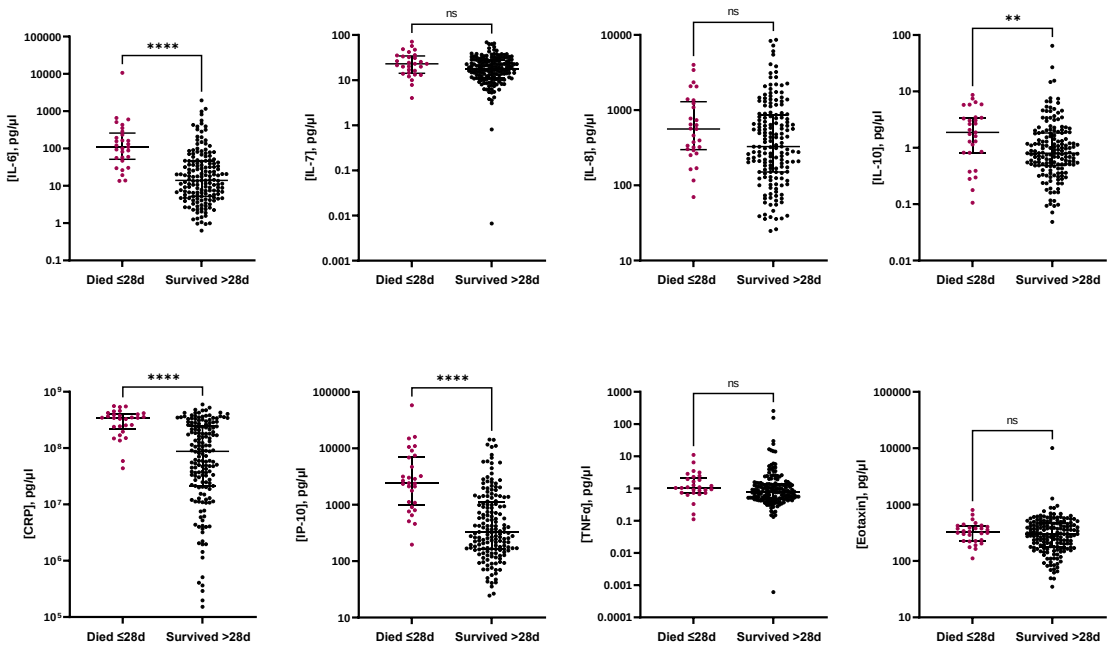

Figure 5.10 Associations between maximal serum cytokine and chemokine levels and 28-day mortality.

Serum concentrations of IL-6, IL-10, CRP, and IP-10 were significantly higher in patients who died within 28 days of a first positive SARS-CoV-2 PCR test (red circles) compared to those who did not (black circles). There was no difference in concentrations of IL-7, IL-8, TNF-α, or Eotaxin. Data compared using Mann-Whitney test, error bars show median +/- interquartile range. **p<0.01, ****p<0.0001.

When associations between platelet-associated factors and 28-day mortality were evaluated, intriguingly, PDGF-B was lower in the patients who died (2.48 pg/ml vs 3.44 pg/ml respectively, p=0.03) whereas vWF was higher in this group (61.1 µg/ml vs 41.3 µg/ml respectively, p=0.0007, Figure 5.11). Concentrations of both MMP-8 and MMP-9 were higher in the patients who died than in those who survived the first 28 days (Figure 5.11).

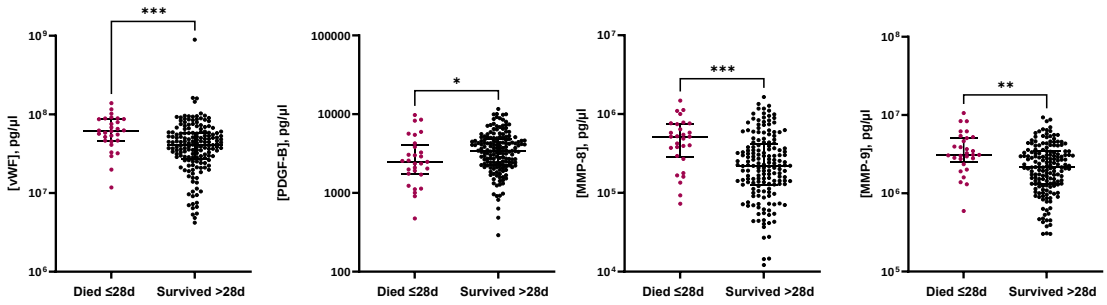

Figure 5.11 Association between maximal serum levels of platelet-associated factors platelet derived growth factor B (PDGF-B) and von Willebrand factor (vWF), Matrix metalloproteinase (MMP) -8 (MMP-8), and MMP-9 and 28-day mortality.

Serum concentrations of vWF, MMP-8, and MMP-9 were higher, and PDGF-B was lower, in patients who died within 28 days of their first positive SARS-CoV-2 PCR result (red circles) compared to those who did not (black circles). Data compared using Mann-Whitney test**,** error bars show median +/- interquartile range. *p<0.05, **p<0.01, ***p<0.001, ****p<0.0001.

A composite outcome of death within 28 days of a first positive PCR test and/or ITU admission was next evaluated. This was considered to be a more useful outcome than admission to ITU alone, as it accounts for any bias arising from selection of patients who are considered to be suitable for admission to ITU. The observed associations between levels of biomarkers and crude 28-day mortality were found to be enhanced when this composite outcome was used. Seven of the eight markers within the cytokine/inflammatory profile were positively associated with death within 28 days and/or ITU admission; there was no difference found in concentrations of eotaxin (Figure 5.12). Concentrations of vWF, MMP-8 and MMP-9 were also elevated in patients who died within 28 days and/or were admitted to ITU; there was no difference found in levels of PDGF-B (Figure 5.13).

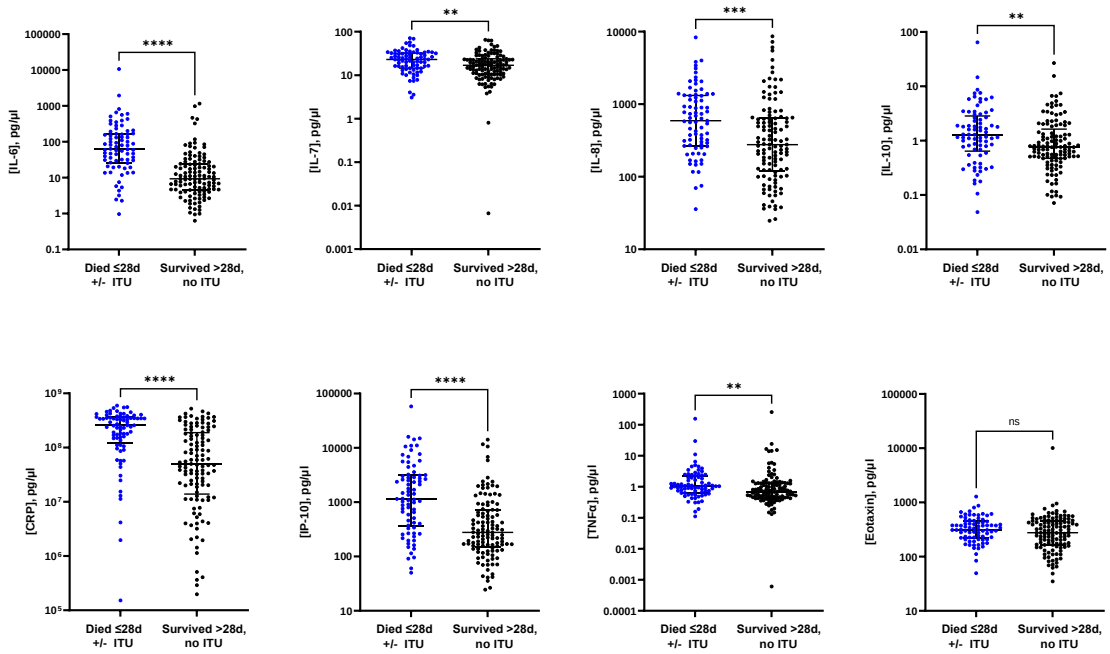

Figure 5.12 Association between maximal serum cytokine and chemokine levels and death within 28 days of a first positive SARS-CoV-2 PCR test and/or admission to ITU.

Serum concentrations of all markers apart from eotaxin were significantly higher in patients who died within 28 days of a first positive SARS-CoV-2 PCR test and/or were admitted to ITU (blue circles) compared to those who survived 28 days and did not go to ITU during their illness (black circles). Data compared using Mann-Whitney test, error bars show median +/- interquartile range. **p<0.01, ***p<0.001, ****p<0.0001.

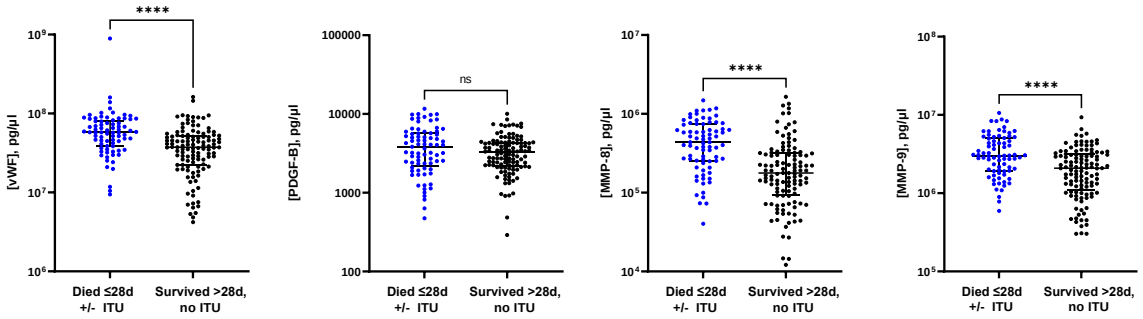

Figure 5.13 Association between maximal serum levels of platelet-associated factors platelet derived growth factor B (PDGF-B) and von Willebrand factor (vWF), Matrix metalloproteinase (MMP) -8 (MMP-8), and MMP-9 and death within 28 days of a first positive SARS-CoV-2 PCR test and/or admission to ITU.

Serum concentrations of vWF, MMP-8, and MMP-9 but not PDGF-B were higher in patients who died within 28 days of a first positive SARS-CoV-2 PCR test and/or were admitted to ITU (blue circles) compared to those who survived 28 days and did not go to ITU during their illness (black circles). Data compared using Mann-Whitney test, error bars show median +/- interquartile range. *p<0.05, **p<0.01, ***p<0.001, ****p<0.0001.

5.4 Discussion

This work presents an in depth look at a prospective cohort of patients evaluated in the first eight months of the pandemic, and from which many valuable insights can be gained. The demographics of our patient cohort, with just over half being males, a broad age range with a median age of 63 years, and a heterogenous ethnic make-up is reflective of the population served by a large teaching hospital in a highly diverse area of London.

Clinical features showing a predominance of fever, cough, and shortness of breath were typical of the presenting features of COVID-19 at the time of the study(283). The clinical presentation of infected individuals has changed significantly over time, with variation in both the genetics of the circulating virus, including changes in trophism towards cells of the upper versus lower respiratory tract(284), and host immunity in the post vaccination era leading to differing clinical features and outcomes in the second and subsequent waves(285, 286). In the UK whilst the prevalent strain

Omicron is spreading widely through the population at the time of writing, the risk of hospitalisation is approximately half for patients infected with the Omicron variant compared to the Delta variant (hazard ratio 0.53, 95% confidence intervals 0.50 to 0.57)(287). As such, a similar study carried out today would be expected to identify a much higher rate of incidental positive testing.

Serial testing for the presence of anti-SARS-CoV-2 antibodies found that the majority of patients in this cohort had detectable antibodies according to IgG ELISA and/or lateral flow testing for IgA, IgM, and IgG. This patient cohort was ideal for this type of study as it enabled collection of serum samples from almost the very start of the pandemic in the UK, meaning that prior infection rates would have been low. Moreover, the intense follow-up of the study protocol enabled detailed examination of antibody-based immune responses over time. These data have been invaluable for both the development of diagnostic tools, which we have seen have been key to control and management of the pandemic, as well as an understanding of immune responses to the virus(258).

The longitudinal nature of the study also enabled correlation of immune responses with acute clinical outcomes. A multivariate logistic regression model allowed the identification of risk factors for adverse outcomes including obesity, older age, male sex, and non-white ethnicity, all of which have been reported elsewhere(275, 277, 278). We also identified a number of associations that are of interest as part of the narrative of the evolution of the pandemic and in particular of our capacity and ability to manage infected patients. Older people and those with co-morbidities were found to be less likely to be admitted to ITU, and an interaction between presence of co-morbidities and whether the patient was admitted to hospital during the first or the second wave was identified. It is notable that the presence of co-morbidities did not affect 28-day mortality. As discussed above, the first and second waves differed in terms of relative infectivity and pathogenicity of prevalent circulating viral strains, varying rates of immunity from past infection, changes in our understanding of optimal patient management, as well as hospital capacity. Our understanding of the prognosis of COVID-19 as well as the availability and effectiveness of therapeutic interventions is likely to have affected decision making with respect to admission to ITU over time(281, 282). A more in-depth evaluation of how these variables affected outcomes individually as well as how they interacted with each other is needed.

Evaluation of serum markers of inflammation and immune activity found that many of the markers measured correlated strongly with each other. When correlations of peak concentrations of the different markers were evaluated, these were found to be much stronger. These data must be interpreted with caution as these markers did not necessarily reach their maximum concentrations at the same time, and each of the markers may have peaked at different times during the disease process depending upon the dynamics of the various pathological processes that follow infection.

All of the markers evaluated apart from eotaxin were found to correlate positively with increasing disease severity. It is plausible that a bias may be present in these data, as patients with more severe disease are likely to have been in hospital for longer and therefore to have had more serum samples evaluated; however, the association between disease severity and increases in inflammatory mediators is so extensively documented in the literature that such a bias is not likely to be responsible for the differences observed.

Strong associations were also found between peak concentrations of these markers and clinical outcomes, notably 28-day mortality and a composite variable comprising 28-day mortality and/or ITU admission. It is notable that the markers of inflammation that most strongly correlated with 28 day mortality were IL-6, IL-10, IP-10, and CRP, confirming these as highly implicated in SARS-CoV-2 infection (288-290) and predictive of severity (290-295) and outcome (273, 274, 288, 296) as reported previously. These markers remained highly significant when the composite outcome of 28-day mortality and/or ITU admission was considered.

The early recognition of the prominence of elevated pro-inflammatory cytokines such as IL-6 in patients with severe COVID-19 led to the use of specific anti-cytokine agents as therapeutics. Tocilizumab is a humanised anti-IL-6 receptor antibody that effectively blocks IL-6 signalling and is used in other inflammatory diseases including rheumatoid arthritis, Castleman's disease, and in cytokine release syndromes occurring in chimeric antigen receptor (CAR) T-cell therapy, a phenomenon that closely resembles cytokine storms in COVID-19. One of the earlier drugs to be employed against IL-6 in COVID-19, Tocilizumab is associated with lower 28-day all-cause mortality(297). Other approaches targeting cytokine activity, including anti-TNFα (infliximab, adalimumab, etanercept), anti-IFN-γ (emapalumab), anti-IL-17 (secukinumab, ixekizumab), and anti-IL-1 (canakinumab, anakinra) have also been considered(298).

It is notable that IL-8 was also found to be significantly elevated in this group, but not in the pure 28-day mortality analysis. The association between IL-8 and SARS-CoV-2 infection itself as well as increased severity of infection has been previously reported (288, 290). IL-8 is a cytokine that activates neutrophils, which are phagocytic innate immune cells more commonly associated with bacterial than with viral infections. Elevated neutrophil count has been reported in COVID-19(290, 299) and has been associated with severity and ITU admission(292), and neutrophil activation, including formation of neutrophil extracellular traps (NETs), has been implicated in the immunopathology of severe COVID-19(300, 301). It is plausible that elevated IL-8 levels may be indicative of a protective innate immune response in patients who survived an ITU admission.

The evaluation of longer-term outcomes was outside the scope of this study, yet some key insights can be gained from the findings presented above. The long-term impact of prior SARS-CoV-2 infection on the health and quality of life of survivors will become increasingly important over time as the nature of infection changes towards endemnicity and we begin to move towards looking at the societal impact of the virus on the surviving population rather than focusing on acute disease and deaths.

A proportion of patients who survive the acute illness do not recover fully, in a condition known as long COVID, or post-COVID-19 syndrome. According to guidelines jointly produced by the National Institute for Health and Care Excellence (NICE), Scottish Intercollegiate Guidelines Network (SIGN), and Royal College of General Practitioners (RCGP), post-COVID-19 syndrome can be defined as “signs and symptoms that develop during or after an infection consistent with COVID-19, continue for more than 12 weeks, and are not explained by an alternative diagnosis”(302). Symptoms are variable and can fluctuate, and in addition to respiratory and generalised symptoms, radiological changes(303, 304) as well as abnormalities in lung function testing(304) have been reported in survivors.

Extensive lung inflammation often involving both lungs is a key feature of COVID pneumonitis(305) and, as in other lung infections, aberrant healing processes can result in fibrosis(306, 307) which may explain some of the clinical features of post-COVID-19 syndrome. A series of 81 COVID-19 patients with serial cross-sectional imaging from Wuhan showed an evolution of changes from focal unilateral to bilateral ground glass opacities as patients became

symptomatic, at 2 weeks post symptom onset 9 of 28 patients had radiological evidence of organizing pneumonia, and reticulation suggesting established fibrosis was present by 3 weeks in 5 of 15 patients(308). However, it is difficult to predict how inflammatory changes seen in acute infection will resolve, whether inflammation will give way to fibrosis, and whether such fibrosis will be progressive once the initial insult, SARS-CoV-2, has been removed.

Much COVID-19 related research has focused on B- and T-lymphocyte mediated immune responses, but the often-overlooked innate immune system is of importance in the control and resolution of lung inflammation. Activation of monocytes and macrophages occurs in COVID-19 patients with poor outcomes: an Italian study identified increased levels of monocyte activation associated biomarkers such as MCP-1/CCL2, MIP-1B/CCL4 in patients who died, as well as phenotypic cellular changes including extensive vacuolisation of peripheral blood monocytes(274). The authors also found elevation of neutrophil associated biomarkers. In other pulmonary infections such as tuberculosis it is well established that lung inflammation can be extensive and aberrant healing can lead to pulmonary fibrosis. This process is understood to be driven by matrix metalloproteinases (MMPs)(309), enzymes which can degrade components of the extracellular matrix, in particular collagen, and are involved in remodelling and repair of inflammation-damaged tissues(42). In pulmonary tuberculosis, concentrations of MMPs in the blood and the lung have been shown to correlate with clinical and radiological measures of disease(46).

In COVID-19, increased concentrations of MMPs have also been identified in patients. Concentrations of MMP-9 have been shown to correlate both with mortality(274) and with progression to post-COVID-19 syndrome(310). A study that undertook the challenging task of differentiating a broad systemic inflammatory response from inflammatory processes related specifically to respiratory failure found that, after evaluation of multiple markers of inflammation initially found to be elevated, MMP-9 was the only marker that was convincingly able to distinguish patients with and without respiratory failure(311). Additionally, there are cellular and animal studies to support a role for MMP-driven disease in SARS-CoV-2 infection: a 2007 study of Cov-229E-infected monocytes found that monocytes may be reservoirs of this less pathogenic coronavirus, and that infection triggered secretion of a number of mediators including MMP-9(312). More recently, a Mexican group found that the administration of MMP inhibitors in a

mouse model of COVID-19 ameliorated SARS-CoV-2 induced lung inflammation and progression to severe disease(313). Our data showed that MMP-8 and MMP-9 concentrations were highly associated with disease severity as well as clinical outcomes, in keeping with these findings; it remains to be seen whether elevated MMP levels in acute disease also relate to poorer long-term outcomes.

Since early in the pandemic a case has been made for the use of anti-fibrotics in COVID-19 to prevent progression to pulmonary fibrosis in the future(306). More research is needed in this field: mechanisms leading to fibrosis are not fully understood in lung diseases that have been extensively studied, let alone in an illness as novel as COVID-19 for which there are no follow-up data beyond two years. Experience from other diseases may offer an opportunity to repurpose existing antifibrotic agents such as Nintedanib, a tyrosine kinase inhibitor of PDGF, VEGF and FGF, or Pirfenidone, whose precise mechanism of action is unclear but is thought to be an inhibitor of TGFβ-induced fibrosis, both of which are licensed for use in idiopathic pulmonary fibrosis. However, there is currently no certainty that pulmonary fibrosis post COVID-19 is either progressive or likely to benefit from such treatments. The administration of antifibrotic drugs in COVID-19 would be greatly facilitated by the identification of biomarkers early in the disease that could predict patients who are likely to progress to pulmonary fibrosis. Extensive studies into post-COVID-19 syndrome are underway in the UK and elsewhere(314-316).

In summary: this study characterised a prospective cohort of 312 patients with SARS-CoV-2 infection during the first eight months of the pandemic. Clinical and demographic patient factors that were associated with poorer outcomes were identified and immune responses were characterised, with potentially important implications on our understanding of the pathophysiology of COVID-19.

Chapter 6 Discussion and Future Work

6.1 Discussion

6.1.1 Platelet activity and phenotype in TB

This research project was designed to investigate the importance of platelets in innate immune responses to pulmonary tuberculosis, combining *in vitro* experimentation with a patient-centric clinical component. Evaluating a spectrum of platelet characteristics has enabled a comprehensive picture to be assembled. The data presented in this thesis demonstrate that platelets are capable of responding to M.tb-secreted antigens, adhere to and interact with leukocytes including monocytes to drive tissue-damaging inflammatory responses, while showing a reduced tendency to aggregate. This leads to a conclusion that platelets adopt a pro-inflammatory phenotype in pulmonary tuberculosis.

The *in vitro* component of this study presents novel findings that antigens secreted by M.tb are capable of activating platelets. Signalling mechanisms within the platelet identified as of potential importance include those induced by ADP-$P2Y_{12}$ interactions. Adenosine diphosphate (ADP) is stored within platelet dense granules and is released during activation, particularly following contact with the sub-endothelial layer of damaged blood vessel walls. Acting upon Gq-coupled $P2Y_1$ and Gi-coupled $P2Y_{12}$ receptors, ADP potentiates further dense granule release and recruitment of additional platelets, and $P2Y_{12}$ receptor signalling amplifies platelet activation via PI3 Kinase, Akt, ERK, Rap1b, and Src family kinases(317). PI3Kβ activity results in activation of the αIIbβ3 integrin (fibrinogen receptor) causing fibrinogen to bind and cross-link platelets in the formation of a platelet plug(318). This receptor is the target of antithrombotic thienopyridine agents such as clopidogrel(319), and patients with defects in the gene encoding the $P2Y_{12}$ receptor have been found to show impaired ADP-induced platelet aggregation(320). These same pathways are also involved in inflammatory activation of the platelet; $P2Y_{12}$ receptor antagonism reduces inflammation as well as thrombosis in animal models(321).

The work presented in Chapter 3 also confirms prior studies showing that the combination of platelets and M.tb when added to cultured monocytes exceeds the effect of either of these alone(103, 108), and advances our understanding of the mechanisms underlying this effect. Interactions between platelet P-selectin and monocyte P-selectin glycoprotein ligand-1 (PSGL-1) receptors were shown to be indispensable to cellular attachment using a whole blood flow cytometry assay in which blocking either of these receptors prevented platelet-leukocyte aggregation. Yet, in the cell culture model, the effect of inhibiting this interaction on monocyte activation was modest compared to the effect of adding platelet-secreted factors to the monocytes. The juxtaposition between platelets and monocytes in the co-culture model does not reflect that which occurs *in vivo*, and it is plausible that in the circulation and/or infected tissues the binding of platelets to monocytes facilitates reach of platelet-secreted mediators to the monocytes by proximity. P-selectin-PSGL-1 interactions lead to initial tethering between platelets and monocytes, and this is followed by integrin-mediated binding to strengthen the cellular bond(322). Meanwhile, PSGL-1 associates inside the cell with cytoskeletal proteins as well as the tyrosine kinase Syk, leading to Src family kinase phosphorylation and PI3K activation, which in turn results in upregulation of gene transcription and secretion of pro-inflammatory cytokines and chemokines(196). Use of inhibitors in my cell co-culture model showed that platelets do indeed augment M.tb-induced monocyte activation via pathways including PI3Kinase and MAP Kinases, which have previously been shown to be upregulated by M.tb(130, 134, 218, 219).

The clinical component of this study was highly insightful, despite interruption by the COVID-19 pandemic resulting in a smaller than anticipated sample size and a paucity of follow-up data. The demographics were representative of the population, and the predominance of young adult males in the TB patient group was similar to the demographics observed in other studies of pulmonary TB(46, 55, 103). Clinical features were varied, and the lack of clustering of symptoms across the different patient groups serves to underline the impossibility of diagnosing TB by history alone and to highlight the need for accurate diagnostic tests and for active case finding.

TB was associated with significant weight loss. A well-documented feature of the disease, weight loss in TB is multifactorial, and reduced appetite associated with deranged appetite hormones such as ghrelin and peptide YY (PYY) have been previously reported(234). The inclusion in the baseline data collection form of the simplified nutritional appetite questionnaire (SNAQ),

designed to assess appetite as a risk factor for weight loss, identified that appetite was significantly affected in the TB patients compared to controls. Assessment for depression using the modified CES-D score was also performed, and patients with TB were shown to have higher scores than patients without TB (median 7.5 vs 5.0, p=0.0069) indicating a higher risk of a major depressive episode(238). Increased rates of depression and other mental health problems have been found in TB patients(323), although surprisingly little research has focused on this area; it is not known whether there may be a biological basis for this finding, similar to the identification of deranged gut hormones associated with poor appetite, rather than merely a result of illness as has been largely assumed in the past.

An inflammatory platelet response in patients with TB was indicated by both the flow cytometry and secretion data. Evaluation of platelet activation and platelet-leukocyte aggregation by flow cytometry identified a divergent response in patients with TB compared to respiratory symptomatic controls and to healthy controls: platelet-monocyte aggregation increased in both patients with TB and respiratory controls compared to healthy controls, whereas the increase in platelet-granulocyte aggregates occurred in TB patients only, suggesting that the former may be a non-specific feature of lung inflammation whereas the latter may be TB-specific. Longitudinal data are suggestive of a normalisation over the six month follow-up period, although the small sample size did not permit a meaningful quantitative analysis.

The incorporation of bronchoalveolar lavage fluid (BALF) analysis into this study enabled evaluation of inflammatory and platelet activity at the site of disease itself; this is important as there may be compartmentalisation of immune responses to infection. The majority of the soluble mediators measured in BALF correlated strongly, which may reflect varying dilutions of the samples; however, correlation coefficients among the TB positive patients were strikingly high compared to those among the TB-negative group which cannot be solely explained by this effect. Vascular endothelial growth factor (VEGF) was unique in its negative correlation with the other measured markers among the TB patients. The reason for this remains unknown and warrants careful consideration: as was discussed in Section 4.7.5 above, lower concentrations of VEGF may be associated with protective responses to pulmonary M.tb infection. The group of patients with non-TB respiratory lung disease also demonstrated a strong correlation between pro-

inflammatory markers, which also correlated well with MMP-1 and MMP-8, as well as sCD40L which may indicate platelet activity as part of a generalised inflammatory response in the lungs.

The comparative analyses were again limited by the sample size and high variability. Nonetheless, a convincing increase in pro-inflammatory markers was seen in BALF samples obtained from TB patients compared to those with non-TB respiratory disease. Concentrations of MMPs were also elevated, most notably MMP-1 and -3, in keeping with other studies. Concentrations of MMP-1, -2, -3, -8 and -9, but not MMP-7, have been shown to be significantly elevated in induced sputum from patients with pulmonary TB compared to healthy controls and normalised during treatment(46). A study of 73 Indian patients with pulmonary TB found elevated neutrophils in BALF from patients with cavities compared to those without, and identified an association between BALF concentrations of IP-10 and IL-6 and non-cavitary lung disease(324), which is interesting given that elsewhere IP-10 has been associated with protection against the development of lung cavities in pulmonary TB in HIV co-infected patients(325). IL-10 was significantly raised in TB patients in my cohort, but it is not known which patients, if any, had cavitating lung disease. Elsewhere, analysis of lung biopsies from patients with pulmonary TB identified neutrophils in the inner walls of lung cavities, and these cells co-localised with MMP-8 (neutrophil collagenase), particularly in central necrotic areas of granulomas, suggesting that MMP-8 may be pathogenically implicated in necrosis(253).

The evaluation of platelet-associated mediators in the lungs of TB patients showed significantly higher levels of PLA2G7 and a trend towards increased concentrations of sCD40L and vascular endothelial growth factor (VEGF) compared to non-TB respiratory symptomatic patients. This provides evidence that platelets are active in the lungs of TB patients. Our group has previously shown increased concentrations of P-selectin, PDGF-BB, and RANTES, but not PF4 in BALF from patients with pulmonary TB compared to respiratory controls, and that P-selectin levels correlated well with MMP concentrations(103). These findings would be strengthened by identification of platelets themselves within the BALF, perhaps using flow cytometry.

Plasma levels of pro-inflammatory markers correlated less well than in the lung. sCD40L and P-selectin showed similar patterns of correlation with pro-inflammatory cytokines and good

correlation with each other, consistent with co-secretion from alpha granules. In TB, pro-inflammatory markers again correlated well with one another.

Aggregation responses were reduced in patients with TB compared to both healthy and respiratory symptomatic controls. This was a surprise finding, and is indicative of a divergence of platelet functional responses perhaps caused by differential usage of specific signalling pathways. This effect was seen in two independent cohorts, in smear-positive pulmonary TB patients compared to healthy controls and also in bronchoscopy patients with and without TB, which strengthens the validity of the finding. It is interesting that the symptomatic controls did not show altered aggregation responses, suggesting that this may be reduced or absent in other pulmonary diseases.

Clinically, this unexpected finding does not fit well with what we know about TB. Pulmonary haemorrhage is a recognized complication of TB, and has been called "the most appalling manifestation of pulmonary tuberculosis"(326). Prevalence varies with setting: in Indian study of patients with haemoptysis found tuberculosis to be the most common cause, responsible for 39% of cases(327), and a Turkish study of 203 patients admitted to hospital with haemoptysis found that TB was the cause in 89 (43.8%)(328), although in industrialised countries other causes such as malignancy and bronchiectasis tend to predominate. Haemoptysis in pulmonary TB can be catastrophic, and associated risk factors include male sex, younger age, first episode of TB, sputum smear positive disease, and presence of cavities(329). Mechanistically, however, it is usually associated with erosion of blood vessels in or adjacent to inflammatory lesions rather than disorders of coagulation(330).

Conversely, an increased risk of thromboembolism associated with tuberculosis has been repeatedly reported(331-333). A multivariate analysis of over 27.5 million admissions identified venous thromboembolism (VTE) in 2.07% of patients with active tuberculosis (95% CI 1.62%-2.59%), and the odds ratio of developing VTE was 1.55 (95% CI 1.23-1.97) in adults with active TB compared to those without(334). A systematic review and meta-analysis of 16,190 patients with active TB identified a similar prevalence of VTE of 3.5% (95% CI 2.2-5.2%) and of pulmonary embolism of 5.8% and deep vein thrombosis of 1.3%, also with raised odds ratios compared to adults without TB(335). These rates are similar to the risk of VTE associated with malignancy and

are suggestive of a hypercoagulable state in TB. Thromboembolism may occur at any point in the disease process(336) and recognized risk factors include raised plasma concentrations of fibrinogen and Factor VIII, endothelial dysfunction, and external compression of the vasculature by tissue enlargement such as lymphadenopathy(84, 86). Additionally, anti-TB drugs such as rifampicin may also play a role in inducing a hypercoagulable state(336). Cerebral thrombosis is a well-recognized complication of TB affecting the central nervous system, and will not be discussed further as the inflammatory environment in the brain differs substantially from that in the lung leading to quite distinct pathology.

There are several possible explanations for the apparent discrepancy between my findings of reduced agonist-induced platelet aggregation, suggestive of a hypocoagulable state, and published reports of hypercoagulability. In TB a spectrum of abnormalities in thrombotic pathways may exist, and multiple mechanisms may interact to produce a disordered coagulopathy. Shear-mediated platelet activation, as occurs in patients on mechanical circulatory support, has been shown to reduce surface expression of the αIIbβ3 integrin alongside a reduction in ADP- and TRAP-6 induced aggregation, which may explain why these patients can exhibit both thrombosis and bleeding(337); a less extreme effect may be seen in patients with TB. The presenting phenotype may depend upon factors such as patient genetics, relevant co-morbidities, and severity of disease. Variations in the soluble components of the coagulation pathway may contribute, although my experimental design used PRP rather than washed platelets precisely to include soluble mediators in the plasma and thus be as representative of *in vivo* effects as possible. Timing may also be important: more numerous alpha granules, with largely pro-inflammatory contents, have been found in patients with both acute and chronic disease whereas increased numbers of dense granules, which contain mediators involved in the coagulation cascade, were seen only in patients with chronic TB(97) suggestive of a predominantly pro-inflammatory phenotype in acute manifestations of disease transitioning towards a mixed inflammatory-thrombotic state in chronicity. A clearer understanding of coagulation parameters alongside inflammatory platelet activity in patients with TB is necessary for the consideration of potential targets for platelet modulation. The complexity of multiple stimuli, some activating and others inhibitory, affecting the platelet is recognized and a sophisticated model of platelet activity which allows for crosstalk between different signalling pathways would be useful for the development of antiplatelet therapies and assessment of their effect(338).

There may be confounders such as age and sex(339), both known to affect platelet aggregation, particularly as the demographics across my clinical groups were not well matched in this study. The predominance of women among the healthy controls could be explained by men being more likely to attend clinic with their wives, and/or by greater uptake of the study by women. There had been a plan to review the age and gender composition of the pulmonary TB and healthy control patients after recruitment had reached 50% to endeavour to correct differences between the groups; however, the study was interrupted before this could happen. The surprisingly low age of the TB-positive bronchoscopy patients contributed to the skewed age distribution; it is not clear whether this trend would have continued with a larger sample size. The possibility of a bias in the data caused by differences in age and sex cannot be excluded without repeating the study with a larger sample size (as originally planned) and with better matching between cases and controls.

The data in my study were also limited by lack of routine laboratory bloodwork including a full blood count and clotting profile at baseline, and these parameters must be included in any future project further exploring platelet activity. A lack of radiological data also precluded any correlation between measured parameters and radiological severity of disease, and imaging should also be included. In addition, my study was performed in a primarily outpatient population, and I may have found markedly different effects had I recruited patients with disease sufficiently severe to require hospitalisation.

6.1.2 SARS-CoV-2 versus Mycobacterium tuberculosis

Although it is not possible to perform a comprehensive analysis comparing findings in the TB and COVID-19 data sets presented in this thesis as the study designs differed, as summarized in Table 12, some useful comparisons can be drawn.

Table 12 Differences between TB and COVID-19 study designs

	TB study	**COVID-19 study**
Study location	Lima, Peru	London, UK
Median age of participants	28 years (TB), 51 years (non-TB)	64 years
Setting	Primarily outpatient	Primarily inpatient
Analyses	Cases vs control groups	Cohort; stratified according to severity and clinical outcome
Samples	Plasma	Serum
Sample processing	Luminex platform	MSD platform

Glancing at the correlation matrices in the pulmonary TB group compared to the COVID-19 cohort, it is apparent that correlation between pro-inflammatory markers was overall stronger among the TB patients than in the COVID-19 cohort. Surprisingly, MMPs correlated poorly in TB, with the exception of MMP-1 and MMP-10 for which Spearman's coefficient of correlation r was 0.57. In the COVID-19 cohort, correlation between MMP-8 and MMP-9 was excellent (r = 0.79 overall, and r = 0.82 among peak values).

Review of the pro-inflammatory mediators evaluated in the two studies identifies IP-10 as highly significant in both: plasma concentrations in TB patients were significantly higher than in healthy controls and also compared to respiratory symptomatic controls, and of the inflammation panel assessed in the TB patient group this was the only marker that differed between the groups. In the COVID-19 study, IP-10 concentrations were highly associated with increasing severity and with adverse outcomes including 28-day mortality. In TB, elevated IP-10 levels have been well

described and it has been evaluated as a marker for diagnosis(340), discrimination between active and latent disease, and prognosis(341). IP-10 (interferon gamma-induced protein 10, CXCL-10) is a chemokine that is released by M.tb-infected alveolar macrophages and attracts Th1 cells to the site of infection(342), and interestingly has been associated with non-cavitating rather than cavitating TB(324). In SARS-CoV-2 infection IP-10 has been associated with increasing severity(290). Elevated IP-10 may represent a non-specific inflammatory response to pulmonary infection or disease.

In COVID-19 a triad of IP-10, IL-10, and IL-6 was shown to predict progression and adverse outcomes(290). In our data IL-6 was highly associated with disease severity and outcome, and IL-10 less markedly so. Correlation between concentrations of IL-6 and IP-10 were stronger ($r = 0.51$) than correlations between IL-6 and IL-10 or between IL-10 and IP-10 ($r = 0.29$ and $r = 0.40$ respectively). Although IL-6 was not significantly associated with pulmonary TB in the Kruskall-Wallis analysis when the Dunn's test was adjusted for multiple comparisons, in an unadjusted analysis levels were significantly higher in patients with TB than in healthy controls (median concentrations 75.3 pg/µl (IQR 57.5-85.0 pg/µl) vs 57.6 pg/µl (IQR 51.3-71.7 pg/µl) respectively, p=0.034). A statistically important difference may have been attained had a larger sample size been used, as was initially planned for this analysis.

In contrast, IL-8 responses were different in patients with TB compared to those with COVID-19. In the TB study there was no difference in IL-8 concentrations between the groups, but in COVID-19 it was strongly associated with disease severity, and with the composite outcome variable of 28-day mortality and/or ITU, but not with 28-day mortality alone. As discussed earlier, IL-8 is strongly linked with neutrophil activity and this may indicate a strong, and protective, inflammatory response in the lung that associates with survival rather than mortality. It would be interesting to evaluate IL-8 responses in TB patients with severe disease requiring hospitalisation.

MMPs emerged as highly significant in both data sets. As aforementioned, MMPs are well known to be related to disease severity in TB. The predominant MMP both in the literature and in the data presented above was MMP-1, a collagenase that degrades Type 1 collagen, the main structural component of the lung. MMP-8 and MMP-10 were also higher in TB patients than in controls, but the differences were less marked. Only MMP-8 and MMP-9 were evaluated in the

COVID-19 cohort; both were strongly associated with severity and with 28-day mortality, and this difference was more marked for MMP-8 than for MMP-9.

vWF was found to be elevated in patients with both TB infection and with non-TB lung disease and was also strongly associated with increasing severity and outcome in COVID-19. A search of the literature yields no information on vWF in pulmonary TB, although it has been associated with pleural TB(254) and as a biomarker of early M.tb infection in contacts of TB patients(255). In contrast, despite having emerged only two years ago, there is a body of literature describing vWF in COVID-19. Early in the pandemic SARS-CoV-2 infection was linked with coagulopathies(343-345) and an increased risk of venous thromboembolism(346), and recommendations were made for venous thromboprophylaxis in hospitalised patients(347). Platelet activity is increased in COVID-19, as evidenced by increased serum concentrations of P-selectin(348) and biomarkers for coagulation including D-dimers, fibrinogen(349), and vWF(350) have been found in large concentrations and associated with COVID-19 severity.

vWF is a multimeric glycoprotein that is stored in endothelial Weibel-Palade bodies and platelet alpha granules, from which it is secreted during inflammation. Following cleavage and activation by the metalloproteinase ADAMTS-13, exposed sites bind to platelet GP1bα or integrin αIIbβ3 surface receptors initiating thrombogenesis(351). vWF binding to GP1bα causes activation of tyrosine protein kinases belonging to the Src kinase family, causing tyrosine phosphorylation of FcRγ or FcγRIIa receptors which associate physically with GPIb(352) whilst αIIbβ3 receptors are involved in platelet aggregation and interact with fibrinogen leading to clot formation(353). In COVID-19, the vWF:ADAMTS-13 axis is tilted towards hypercoagulability and an increased risk of thrombosis(354).

Taking this together, it is unsurprising that vWF levels were elevated in the patients with severe disease and/or adverse clinical outcomes in our cohort, and it is of interest that these levels were also significantly elevated in patients with pulmonary TB given the weaker association of this latter infection with coagulopathies and thrombosis. It would be interesting to perform a quantitative comparison of vWF levels in the two patient groups.

In many of the markers assessed in the COVID-19 cohort, including MMP-8 and MMP-9, statistical significance was most pronounced between patients with a severity score of 5, i.e. those who were intubated and mechanically ventilated, compared to those with severity scores of 0-4. This

warrants caution due to the potential confounder of ventilator-induced lung injury (VILI), whereby mechanical ventilation leads to a proinflammatory response. This is characterized by increases in mediators such as TNF-α and IFN-γ, which normalise during healing, and other mediators including MMP-2, MMP-9, and macrophage inflammatory protein-2 (MIP-2) which remained elevated(355-357). This persistence of high concentrations of MMPs is associated with improved recovery, indicating that inflammatory responses and extracellular matrix remodelling are necessary. In my data, the analysis grouping severity scores into mild, moderate, and severe identified that there were also significant differences between both the mild and moderate and the moderate and severe groups, indicating that VILI-related inflammation cannot be solely responsible for these findings.

Neither study enabled the collection of long-term outcome data including residual symptoms or deficits in lung function following resolution of the infective insult. It would be interesting to see how markers of platelet activity and of inflammation, including MMP levels, relate to the development of fibrosis and/or symptomatic long COVID following SARS-CoV-2 infection, and fibrosis and impaired lung function following TB, and how this compares in the two diseases.

6.2 Future work

The *in vitro* model used in this study is effective for the interrogation of signalling pathways and mechanisms underpinning intercellular interactions. Having shown that platelets enhance utilisation of signalling pathways upregulated by M.tb infection, the next step would be to confirm this using Western Blot and/or siRNA techniques. However, the real challenge lies in identifying the mechanisms of platelet-leucocyte communication, and how modulation of these cellular interactions may influence monocyte phenotype.

My experiments crudely showed that pre-activation of platelets with thrombin did not grossly impact monocyte output, suggesting that activation may occur during co-culture on a much larger scale that would overwhelm any effect of a platelet agonist. However, other studies indicate that the platelet stimulus is important in defining its response. For example, Rex *et al* showed that thrombotic versus inflammatory stimuli affect different platelet pathways: the PI3K/Akt signalling pathway is known to be involved in Pam_4CSK_4-induced platelet stimulation via toll-like receptors,

but not in thrombin-induced platelet activation(202). This line of investigation could be pursued by conducting a more finely tuned series of experiments to investigate the effect of different agonists on platelet phenotype, and how this affects monocyte activation. The aim would be to first define the platelet secretome generated by activation with different agonists by incubating platelets with ADP, TRAP-6, and collagen, collecting the supernatant, and characterizing its contents using Luminex. This would then be added to M.tb-infected monocytes and, similarly, the monocyte supernatant would be characterised to assess whether distinctive effects upon the monocyte can be detected. If so, the important components of the platelet secretome could be identified through a proteomics approach and confirmation with recombinant proteins. One would also wish to characterize cellular interactions in more detail by exploring integrins and other receptors as co-receptors in P-selectin-PSGL-1 signalling and also in their own right.

This study did not take into consideration the contribution of microparticles to the cell processes investigated. Microparticles are small vesicles between 0.1 and 1µm that are formed during cellular processes including activation and apoptosis. They are important in intercellular communication both in physiological processes and notably in inflammatory(358, 359) and infectious(360, 361) diseases; circulating microparticles have been associated with COVID-19 associated coagulopathy(362, 363). Microparticles originate from most, if not all, cell types, with their contents and consequently effects depending upon the cell from which they are derived(364). Most microparticles found in the circulation originate from platelets, and there has been increasing interest in their role in disease processes and even for therapeutic purposes(360). Microparticles can be isolated using centrifugation and characterized according to characteristics acquired from the parent cell e.g. expression of cell surface receptors using flow cytometry(365). Whilst this was outside the scope of this project, the quantification and characterization of circulating platelet-derived microparticles in patients with TB, as well as their incorporation into cell culture assays, would add a novel dimension to this study.

The clinical study presented here represents an exploration of platelet activity in patients with TB, and these findings are useful in the design and refinement of a follow-up study. I intend to return to Peru and implement a more robust and targeted study design.

Having observed trends towards reduced platelet aggregation despite the literature pointing towards a pro-thrombotic phenotype in TB, it is important to firstly confirm this observation, and then to probe more deeply into why this may be the case. I am curious about the inverse correlation between vWF and the other markers measured in the patients' BALF. A complete assessment should include quantification of soluble markers of thrombosis and haemostasis as well as a full clotting profile.

The practical experience of recruiting patients in a busy public hospital within a fragmented healthcare system and serving a chaotic population has taught me valuable lessons. It is not possible to assume that, even if patients have had baseline blood and radiological investigations during investigations for TB, it will be easy to access this information. In Peru patients are the custodians of their medical records, and paper copies of laboratory results as well as physical x-rays can get lost, damaged, or left at home during appointments. It would be advantageous for any follow-up study to support the patients to have these investigations done, thereby guaranteeing a copy of the data for the study as well as benefitting the patients themselves. Radiological data in particular would be of value in terms of associating platelet and MMP activity with the presence or absence of cavities and/or fibrosis.

Another important question that needs answering is whether a characteristic platelet phenotype occurs in pulmonary TB as a result of changes at the level of the pre-platelet and megakaryocyte. Megakaryocytes are highly polyploid cells that reside primarily in the marrow from where they release thousands of platelets into the circulation(366). Each platelet contains an abundance of granules as well as pre-mRNA, mRNA, and miRNA which are used for protein synthesis and regulation of platelet function(367). The platelet transcriptome is altered in inflammatory diseases including myocardial infarction, systemic lupus erythematosus, and cancer(96, 368-370). To test the hypothesis that TB is associated with a specific platelet transcriptomic signature, platelet RNA collected from patients with and without TB could be sequenced to define a platelet transcriptome for TB.

The ultimate aim of clinical research is to benefit patients. This work is building towards the development and evaluation of a host directed therapy aiming to limit lung damage in TB survivors. I anticipate that through the work described above we shall arrive at a detailed

understanding of platelet activity in TB patients. This knowledge will be invaluable in the development of animal studies followed by clinical trials of anti-platelet agents, guiding parameters for evaluation including measures of inflammation, risk of bleeding and thrombosis, and outcomes.

6.3 Final conclusions

In summary, this thesis has done much to elucidate the role of platelets in the pro-inflammatory response to TB, and has indicated clear lines for further research.

Chapter 7 Appendices

7.1 Published evidence for benefits of anti-platelet agents in TB.

Table 13 Animal and human studies investigating the effects of anti-platelet agents in tuberculosis.

Reference	Anti-platelet agent(s) tested	Host species /patients studied	Intervention	Summary of findings
Animal studies				
Shroff *et al*, 1990 (371)	Indomethacin	Swiss white mice	Six intraperitoneal injections of indomethacin, 50µg per mouse, given at 12 hour intervals; immunization with intraperitoneal *M. vaccae* 12 hours after the last dose	Indomethacin-treated mice showed a delayed type hypersensitivity response, whereas non-treated mice did not.
Hernández-Pando *et al*, 1995 (152)	Indomethacin	Male 6-8 week old BALB/c mice immunized with culture filtrate proteins (CFP) from H37Rv M.tb delivered via endotracheal route	20mg/kg cyclophosphamide or 5mg/kg indomethacin given by intraperitoneal injection one day prior to endotracheal challenge with CFP	Induction of granulomas with sepharose beads coated with CFP reduced antibody production and delayed-type hypersensitivity responses to mycobacterial antigens; this was reversed with the administration of cyclophosphamide and indomethacin.
Rangel Moreno *et al*, 2002 (372)	Niflumic acid	Male 6-8 week old BALB/c mice infected with H37Rv M.tb via endotracheal route	500µg/ml niflumic acid given by intragastric cannula twice per day	Mice treated with niflumic acid early in infection produced greater expression of TNF-α, IL-1α, and IFN-γ, with a reduction in inhaled nitric oxide synthase (iNOS) expression and an increased bacterial load. Mice treated after 60 days of infection showed increased pro-inflammatory cytokine concentrations, a striking increment of iNOS expression, and reduced bacillary load.
Dutta *et al*, 2004 (145)	Diclofenac sodium	45 mycobacterial strains including drug-sensitive and -resistant strains in Kirchner's liquid culture medium; male Swiss Albino mice infected via intraperitoneal route with M.tb H37Rv102	Mycobacteria were tested with increasing concentrations of diclofenac sodium. Infected mice were injected with 10mg/kg diclofenac sodium daily for 6 weeks	Diclofenac sodium exhibited bactericidal activity in most mycobacterial strains at a range of 15-25µg/ml. Diclofenac sodium treatment of infected mice resulted in reduced macroscopic lesions and a reduction in mycobacterial load.

Hernández-Pando *et al*, 2006 (373)	Niflumic acid (a COX-2 inhibitor) and soluble betaglycan (an anti-TGF-β agent)	Male 6-8 week old BALB/c mice infected with H37Rv M.tb	30µg soluble betaglycan administered twice a week by intraperitoneal route from 30 days post infection, with/without 500µg niflumic acid administered twice a day by intragastric cannulation, or pan-specific TGF-β antibodies. Mice euthanised at 15, 30, 45, and 60 days	Compared to control animals, treatment produced higher expression of TNF-α, IFN-γ, IL-2, iNOS and lower expression of IL-4, with decreased lung fibrosis and bacillary load; there was a higher inflammatory response manifested as a greater area of lung affected by pneumonia. The addition of niflumic acid was synergistic, with reduced bacillary load and increased TNF-α.
Byrne *et al*, 2007 (151)	Aspirin and ibuprofen	BALB/c mice infected with M.tb H37Rv by aerosol administration	Oral treatment of aspirin (10, 20, 40 mg/kg) and ibuprofen (10, 20, 40 mg/kg) +/- pyrazinamide (150 mg/kg) daily for 1 month	Aspirin and ibuprofen had no effect alone, but increased bactericidal activity of pyrazinamide when given in combination.
Byrne *et al*, 2007 (374)	Aspirin and ibuprofen	Four week old BALB/c mice infected with M.tb H37Rv by aerosol administration	Aspirin or ibuprofen (10-40mg/kg) with or without isoniazid (25mg/kg) administered by oral gavage five times per week for one month. Mice were euthanized one day after treatment completion	Co-administration of aspirin and isoniazid antagonized the antimycobacterial activity of isoniazid. Ibuprofen had no interaction with isoniazid.
Dutta *et al*, 2007 (146)	Diclofenac	Male Swiss Albino mice infected via intraperitoneal route with M.tb H37Rv	Infected mice treated with diclofenac 10µg/g or streptomycin 150µg/g, alone or in combination, daily for 4 weeks	Diclofenac and streptomycin both resulted in improved survival, reduced bacillary count, and reduced splenic weight. The two drugs acted synergistically
Peres-Buzalaf *et al*, 2011 (375)	Celecoxib and MK-886 (5-LO activation protein inhibitor)	Male 5-8 week old BALB/c mice infected intratracheally with M.tb H37Rv strain	Oral treatment with celecoxib 5mg/kg/0.5ml, and/or MK-886 5mg/kg/0.5ml, 1h prior to infection with M.tb and again every 24h for 60 days	Celecoxib enhanced 60-day survival from 86% to 100% and reduced lung bacterial burden; conversely, MK-886 reduced 60-day survival from 86% to 43% and increased lung bacterial load.

Vilaplana *et al*, 2013 (153)	Ibuprofen	C3HeB/FeJ pathogen-free mice infected intravenously with M.tb H37Rv	Ibuprofen 80mg/kg given orally 3 or 4 weeks post infection.	Ibuprofen treated animals had a reduction in size and number of lung lesions, bacillary load, and improved survival.
Marzo *et al*, 2014 (144)	Aspirin and ibuprofen	C3HeB/FeJ and C3H/HeN pathogen-free mice infected intravenously with M.tb H37Rv	Aspirin 3mg/kg, sodium heparin 20 UI/kg, ibuprofen 80mg/kg orally	Aspirin administration reduced bacterial load, attenuated the severity of histopathological changes, and improved survival. Aspirin and ibuprofen-treated C3HeB/FeJ and C3H/HeN mice had lower levels of pro-inflammatory mediators including TNF-a, IL-6, IL-17 and CXCL5 than untreated C3HeB/FeJ mice.
Kroesen *et al*, 2018 (142)	Aspirin	C3HeB/FeJ infected with M.tb H37Rv Pasteur strain	Aspirin 3mg/kg given alone or in combination with anti-TB treatment	Low-dose aspirin reduced bacterial load and increased survival, reduced lung pathology, decreased production of pro-inflammatory cytokines and delayed neutrophil recruitment and T cell responses. In combination with anti-TB treatment aspirin enhanced survival and reduced lung pathology.
Hortle *et al*, 2019 (150)	Aspirin, and tirofiban and eptifibatide (specific inhibitors of glycoprotein IIb/IIIa–fibrinogen binding)	Zebrafish infected with *M. marinum*	Infected zebrafish treated with 10µg/ml aspirin, 20µg/ml tirofiban, 10uM eptifibatide, or 5uM warfarin, or control	Mycobacterial burden correlated with thrombocyte density. Aspirin, tirofiban, and eptifibatide reduced mycobacterial burden by inhibiting thrombocyte-granuloma interactions.
Mortensen *et al*, 2019 (376)	Celecoxib and ibuprofen	CB6F1 mice infected with M.tb Erdman strain via aerosol or intravenous (IV) routes	Celecoxib or ibuprofen administered orally in mouse feed 4-12 weeks post infection	Aerosol-infected mice treated with celecoxib or ibuprofen had higher bacillary burdens in lung and spleen and there was no difference in pulmonary immune cell infiltration or cytokine levels measured in plasma or lung homogenates. Celecoxib led to increased bacterial burden and altered function/differentiation of Type 1 helper T cells in mice re-infected following antibiotic treatment. IV-infected mice had reduced inflammation and bacterial burden following ibuprofen treatment.

Human Studies				
Misra *et al*, 2010 (157)	Aspirin	Patients with TB meningitis diagnosed based on clinical, magnetic resonance imaging (MRI), and cerebrospinal fluid (CSF) criteria	118 patients randomized to receive 150mg aspirin per day or placebo. All patients received standard treatment with rifampicin, isoniazid, pyrazinamide and ethambutol with/without corticosteroids	Aspirin resulted in insignificantly fewer strokes (24.2% versus 43.3%, OR 0.42, 95%CI 0.121-1.39) and significantly reduced mortality (21.7% versus 43.4%, p=0.02) compared to placebo. Aspirin was well tolerated.
Schoeman *et al*, 2011 (377)	Aspirin	Children with TB meningitis	146 children randomized to placebo, low-dose aspirin (75mg/day), and high-dose (100mg/kg/day) aspirin, alongside standard treatment plus prednisolone for the first month of treatment	There was no benefit in morbidity or mortality.
Mai *et al*, 2018 (156)	Aspirin	HIV-uninfected adults with TB meningitis	120 patients randomized to aspirin (81mg/day or 1000mg/day) or placebo added to the first 60 days of anti-tuberculosis drugs plus dexamethasone	There was no difference in rates of gastro-intestinal or cerebral bleeding, new brain infarction, or death by 60 days. There was a reduction in new infarcts and deaths by day 60 in aspirin-treated participants with microbiologically confirmed TBM compared to placebo.
Lee *et al*, 2019 (154)	Antiplatelet agents including aspirin	Retrospective cohort study of incident TB cases in the Taiwan National Tuberculosis Registry between 2008 and 2014	9,497 antiplatelet users (including 7,764 aspirin users) compared to 8,864 non-users	After 1:1 propensity score matching, antiplatelet use was associated with longer survival (adjusted hazard ratio (HR): 0.91, 95% confidence interval (CI): 0.88-0.95, $p < 0.0001$) but no increase in major bleeding risk (p=0.604).
Wang *et al*, 2020 (155)	Aspirin	Patients with pulmonary TB and type 2 diabetes mellitus	348 patients randomized to aspirin (100mg/day) or placebo. 168 patients completed the trial and were included in analysis	Erythrocyte sedimentation rate and C-reactive protein levels were lower (p=0.000), the sputum-negative conversion rate was higher (86.7% versus 53.8%, p=0.031), and the number and size of cavities was smaller in the aspirin-treated than the placebo-treated group.

7.2 Simplified nutritional appetite questionnaire (SNAQ)

Administration Instructions: Ask the subject to complete the questionnaire by circling the correct answers and then tally the results based upon the following numerical scale: a 1, b 2, c 3, d 4, e 5. The sum of the scores for the individual items constitutes the SNAQ score. SNAQ score 14 indicates significant risk of at least 5% weight loss within six months.

1. My appetite is:
    a. very poor
    b. poor
    c. average
    d. good
    e. very good

2. When I eat
    a. I feel full after eating only a few mouthfuls
    b. I feel full after eating about a third of a meal
    c. I feel full after eating over half a meal
    d. I feel full after eating most of the meal
    e. I hardly ever feel full

3. Food tastes
    a. very bad
    b. bad
    c. average
    d. good
    e. very good

4. Normally I eat
    a. less than one meal a day
    b. one meal a day
    c. two meals a day
    d. three meals a day
    e. more than three meals a day

7.3 Modified CES-D questionnaire

(To be filled out by the patient)

You are going to read some sentences that describe how you might have felt. Please tell me how often you have felt this way, in the last week, that is, in the last 7 days:

1. I felt like I couldn't get rid of the sadness even with the help of my family or friends.
    a. Rarely or not at all (less than a day)
    b. Sometimes or a few times. (1-2 days)
    c. Occasionally or a good part of the time (3-4 days)
    d. Most of the time or all of the time (5-7 days)

2. I was feeling depressed.
    a. Rarely or not at all (less than a day)
    b. Sometimes or a few times. (1-2 days)
    c. Occasionally or a good part of the time (3-4 days)
    d. Most of the time or all of the time (5-7 days)

3. I thought my life had been a failure.
    a. Rarely or not at all (less than a day)
    b. Sometimes or a few times. (1-2 days)
    c. Occasionally or a good part of the time (3-4 days)
    d. Most of the time or all of the time (5-7 days)

4. I was lonely.
    a. Rarely or not at all (less than a day)
    b. Sometimes or a few times. (1-2 days)
    c. Occasionally or a good part of the time (3-4 days)
    d. Most of the time or all of the time (5-7 days)

5. I felt sad.
    a. Rarely or not at all (less than a day)
    b. Sometimes or a few times. (1-2 days)
    c. Occasionally or a good part of the time (3-4 days)
    d. Most of the time or all of the time (5-7 days)

Cuestionario CES-D en Español

(Para ser llenado por el paciente)

Va a leer unas frases que describen como usted se podría haber sentido. Por favor dígame con qué frecuencia se ha sentido de esta manera, durante la última semana, o sea, en los últimos 7 días:

1. Sentía que no podía quitarme de encima la tristeza aún con la ayuda de mi familia o amigos.

    a. Rara vez o ninguna vez (menos de un día)
    b. Alguna vez o pocas veces.(1-2 días)
    c. Ocasionalmente o una buena parte del tiempo (3-4 días)
    d. La mayor parte del tiempo o todo el tiempo (5-7 días)

2. Me sentía deprimido.

    a. Rara vez o ninguna vez (menos de un día)
    b. Alguna vez o pocas veces.(1-2 días)
    c. Ocasionalmente o una buena parte del tiempo (3-4 días)
    d. La mayor parte del tiempo o todo el tiempo (5-7 días)

3. Pensaba que mi vida había sido un fracaso.

    a. Rara vez o ninguna vez (menos de un día)
    b. Alguna vez o pocas veces.(1-2 días)
    c. Ocasionalmente o una buena parte del tiempo (3-4 días)
    d. La mayor parte del tiempo o todo el tiempo (5-7 días)

4. Me sentía solo.

    a. Rara vez o ninguna vez (menos de un día)
    b. Alguna vez o pocas veces.(1-2 días)
    c. Ocasionalmente o una buena parte del tiempo (3-4 días)
    d. La mayor parte del tiempo o todo el tiempo (5-7 días)

5. Me sentía triste.

    a. Rara vez o ninguna vez (menos de un día)
    b. Alguna vez o pocas veces.(1-2 días)
    c. Ocasionalmente o una buena parte del tiempo (3-4 días)
    d. La mayor parte del tiempo o todo el tiempo (5-7 días)

7.4 Conference Proceedings

Platelets regulate monocyte collagenase-driven morbidity in tuberculosis through diverse signalling pathways. Kirwan DE, Gilman RH, Friedland JH. Abstract 03409 European Congress of Clinical Microbiology and Infectious Diseases (ECCMID) 2022, Lisbon, Portugal, 25th April 2022. (Accepted for oral presentation.)

El rol de las plaquetas en la respuesta inmunológica a la tuberculosis pulmonar. Kirwan DE. VII Jornada Científica Internacional "Investigación Peruana para el Control de la Tuberculosis en el Perú", MINSA (Ministry of Health), Lima, Peru. 11th October 2019. (Oral presentation.)

Direct contact with platelets modulates monocyte responses to *Mycobacterium tuberculosis*. Kirwan DE, Fox K, Whittington A, Porter JC, Gilman RH, Friedland JS. 21st BIA Annual Scientific Meeting, London, UK. 17th May 2018. (Oral presentation. First Prize)

The role of platelets in modulating innate inflammatory responses in tuberculosis. Imperial College Wellcome Centre for Global Health Annual Scientific Meeting, London, UK. 20th November 2017. (Oral presentation.)

Platelets drive pro-inflammatory platelet-leukocyte interactions in patients with pulmonary tuberculosis. Kirwan DE, Ugarte-Gil C, Gayoso O, Gilman RH, Friedland JS. European Congress of Clinical Microbiology and Infectious Diseases (ECCMID) 2021, Virtual only. 9th July 2021 (ePoster 3776.)

IgG antibody dynamics in a cohort of SARS-CoV-2 positive patients in London, UK. Staines H, Kirwan DE, Clark D, Augustin Y, Eckersley N, Davies B, Hadcocks L, Monahan I, Fitchett J, Krishna S, Planche T. ESCMID Conference on Coronavirus Disease (ECCVID) 2020. Virtual only. 23rd September 2020. (ePoster P103.)

TB-secreted antigens drive platelet-controlled tissue destruction in pulmonary tuberculosis. Kirwan DE, Whittington AM, Fox K, Gilman RH, Taylor K, Emerson M, Friedland JS. EUPLAN 2018 (European Platelet Network Meeting), Bruges, Belgium. 19-21 September 2018. (Poster.)

Platelets and the regulation of tissue destruction in tuberculosis. Kirwan DE, Whittington A, Fox K, Gilman RH, Taylor K, Emerson M, Friedland JS. European Congress of Immunology, Amsterdam, The Netherlands. 2-5 September 2018. (Poster.)

Platelets drive inflammatory mediator gene expression, secretion, and activity in tuberculosis. Fox K, Kirwan DE, Whittington A, Brilha S, Lopez JW, Porter JC, Gilman RH, Friedland JS. British Society of Immunology annual conference, Brighton, UK. 4-7 December 2017. (Poster.)

7.5 Publications

7.5.1 Publications related to PhD

Kirwan DE, Chong DLW, Friedland JS. "Platelet activation and the immune response to tuberculosis." *Front Immunol.* 2021; 12:631696. eCollection 2021. DOI: 10.3389/fimmu.2021.631696

Staines HM, **Kirwan DE**, Clark DJ, Adams ER, Augustin Y, Byrne RL, Cocozza M, Cubas-Atienzar AI, Cuevas LE, Cusinato M, Davies BMO, Davis M, Davis P, Duvoix A, Eckersley NM, Forton D, Fraser AJ, Garrod G, Hadcocks L, Hu Q, Johnson M, Kay GA, Klekotko K, Lewis Z, Macallan DC, Mensah-Kane J, Menzies S, Monahan I, Moore CM, Nebe-von-Caron G, Owen SI, Sainter C, Sall AA, Schouten J, Williams CT, Wilkins J, Woolston K, Fitchett JRA, Krishna S, Planche T. "IgG Seroconversion and Pathophysiology in Severe Acute Respiratory Syndrome Coronavirus 2 Infection." *Emerg Infect Dis*. 2021 Jan;27(1):85-91. DOI: 10.3201/eid2701.203074

Savage HR, Santos VS, Edwards T, Giorgi E, Krishna S, Planche TD, Staines HM, Fitchett JRA, **Kirwan DE,** Cubas Atienzar AI, Clark DJ, Adams ER, Cuevas LE. "Prevalence of neutralising antibodies against SARS-CoV-2 in acute infection and convalescence: A systematic review and meta-analysis." *PLoS Negl Trop Dis.* 2021 Jul 8;15(7):e0009551. DOI: 10.1371/journal.pntd.0009551

Carter J, Friedland JS, **Kirwan DE**, Nathavitharana RR. "Translating scientific discoveries during pandemics: ensuring equity for people affected by COVID-19 and tuberculosis." *ERJ Open Res.* 2020 Oct 19;6(4):00562-2020. DOI: 10.1183/23120541.00562-2020

Fox KA, **Kirwan DE**, Whittington AM, Krishnan N, Robertson BD, Gilman RH, López JW, Singh S, Porter JC, Friedland JS. "Platelets regulate pulmonary inflammation and tissue destruction in tuberculosis." *Am J Respir Crit Care Med* 2018; 198(2): 245-55. DOI: 10.1164/rccm.201710-2102OC

7.5.2 Publications unrelated to PhD

Florentini EA, Angulo N, Gilman RH, Alcántara R, Roncal E, Antiparra R, Toscano E, Vallejos K, **Kirwan D**, Zimic M, Sheen P. "Immunological detection of pyrazine-2-carboxylic acid for the detection of pyrazinamide resistance in Mycobacterium tuberculosis." *PLoS One.* 2020 Nov 5;15(11):e0241600.

Vallejos-Sánchez K, Lopez JM, Antiparra R, Toscano E, Saavedra H, **Kirwan DE**, Amzel LM, Gilman RH, Maruenda H, Sheen P, Zimic M. "Mycobacterium tuberculosis ribosomal protein S1 (RpsA) and variants with truncated C-terminal end show absence of interaction with pyrazinoic acid." *Sci Rep.* 2020 May 20;10(1):8356.

Alcántara R, Fuentes P, Marin L, **Kirwan DE**, Gilman RH, Zimic M, Sheen P. "Direct Determination of Pyrazinamide (PZA) Susceptibility by Sputum Microscopic Observation Drug Susceptibility (MODS) Culture at Neutral pH: the MODS-PZA Assay." *J Clin Microbiol.* 2020 Apr 23;58(5):e01165-19.

Vargas AP, Rios AA, Grandjean L, **Kirwan DE**, Gilman RH, Sheen P, Zimic MJ. "Determination of potentially novel compensatory mutations in rpoc associated with rifampin resistance and rpob mutations in *Mycobacterium tuberculosis* Clinical isolates from Peru." *Int J Mycobacteriol.* 2020 Apr-Jun;9(2):121-137.

Sheen P, Monsalve A, Campos J, Huerta R, Antiparra R, Arteaga H, Duran P, Bueno C, **Kirwan DE**, Gilman RH, Zimic M. "Metallochaperones Are Needed for Mycobacterium tuberculosis and Escherichia coli Nicotinamidase-Pyrazinamidase Activity." *J Bacteriol.* 2020 Jan 2;202(2):e00331-19.

Petersen E, Rao M, Ippolito G, Gualano G, Chakaya J, Ntoumi F, Moore D, Allen R, Gaskell K, Öhd JN, Hergens MP, Krishnamoorthy S, Ugarte-Gil C, **Kirwan DE**, Honeyborne I, McHugh TD, Köser CU, Kranzer K, Tiberi S, Migliori GB, Mao Q, Yang Y, Oliveira SP, Cardoso RF, Detjen A, Marais B, de Gijsel D, von Reyn CF, Goscé L, Abubakar I, Maeurer M, Zumla A. "World Tuberculosis Day March 24th 2019 Theme: "It's TIME" - International Journal of Infectious Diseases Tuberculosis Theme Series." *Int J Infect Dis.* 2019 Mar;80S:S1-S5.

Ugarte-Gil C, Carrillo-Larco RM, **Kirwan DE**. "Latent tuberculosis infection and non-infectious co-morbidities: Diabetes mellitus type 2, chronic kidney disease and rheumatoid arthritis." *Int J Infect Dis.* 2019 Mar; 80S:S29-S31.

Alcántara R, Fuentes P, Antiparra R, Santos M, Gilman RH, **Kirwan DE**, Zimic M, Sheen P. "MODS-Wayne, a Colorimetric Adaptation of the Microscopic-Observation Drug Susceptibility (MODS) Assay for Detection of *Mycobacterium tuberculosis* Pyrazinamide Resistance from Sputum Samples." *J Clin Microbiol.* 2019 Jan 30;57(2):e01162-18.

Kirwan DE, Gilman RH. "A false economy: we cannot afford to be complacent when it comes to tuberculosis control." *Lancet Public Health* 2018; 3(3):e105-e106.

Montalvo R, Bernabe-Ortiz A, **Kirwan DE**, Gilman RH. "Bioimpedance markers and tuberculosis outcome among HIV-infected patients" *Afr. J. Infect. Dis* 2018; 12(2): 47-54

Chapter 8 Bibliography

1. WHO. Global Tuberculosis Report 2020. World Health Organization; 2020.
2. Tuberculosis in England: 2019 report. London, UK Public Health England; 2019.
3. Kaufmann SH, Dorhoi A. Inflammation in tuberculosis: interactions, imbalances and interventions. Curr Opin Immunol. 2013;25(4):441-9.
4. Ehrt S, Schnappinger D, Rhee KY. Metabolic principles of persistence and pathogenicity in Mycobacterium tuberculosis. Nature Reviews Microbiology. 2018;16(8):496-507.
5. Dhar R, Singh S, Talwar D, Mohan M, Tripathi SK, Swarnakar R, et al. Bronchiectasis in India: results from the European Multicentre Bronchiectasis Audit and Research Collaboration (EMBARC) and Respiratory Research Network of India Registry. Lancet Glob Health. 2019;7(9):e1269-e79.
6. Maguire GP, Anstey NM, Ardian M, Waramori G, Tjitra E, Kenangalem E, et al. Pulmonary tuberculosis, impaired lung function, disability and quality of life in a high-burden setting. Int J Tuberc Lung Dis. 2009;13(12):1500-6.
7. Byrne AL, Marais BJ, Mitnick CD, Lecca L, Marks GB. Tuberculosis and chronic respiratory disease: a systematic review. Int J Infect Dis. 2015;32:138-46.
8. Amaral AF, Coton S, Kato B, Tan WC, Studnicka M, Janson C, et al. Tuberculosis associates with both airflow obstruction and low lung function: BOLD results. Eur Respir J. 2015;46(4):1104-12.
9. Miller TL, McNabb SJ, Hilsenrath P, Pasipanodya J, Weis SE. Personal and societal health quality lost to tuberculosis. PLoS One. 2009;4(4):e5080.
10. Daniels KJ, Irusen E, Pharaoh H, Hanekom S. Post-tuberculosis health-related quality of life, lung function and exercise capacity in a cured pulmonary tuberculosis population in the Breede Valley District, South Africa. S Afr J Physiother. 2019;75(1):1319.
11. Motta I, Centis R, D'Ambrosio L, García-García JM, Goletti D, Gualano G, et al. Tuberculosis, COVID-19 and migrants: Preliminary analysis of deaths occurring in 69 patients from two cohorts. Pulmonology. 2020;26(4):233-40.
12. Hoger S, Lykens K, Beavers SF, Katz D, Miller TL. Longevity loss among cured tuberculosis patients and the potential value of prevention. The International Journal of Tuberculosis and Lung Disease. 2014;18(11):1347-52.
13. Snider GL, Doctor L, Demas TA, Shaw AR. Obstructive airway disease in patients with treated pulmonary tuberculosis. Am Rev Respir Dis. 1971;103(5):625-40.
14. Birath G, Caro J, Malmberg R, Simonsson BG. Airways obstruction in pulmonary tuberculosis. Scand J Respir Dis. 1966;47(1):27-36.
15. Lancaster JF, Tomashefski JF. Tuberculosis--a cause of emphysema. Am Rev Respir Dis. 1963;87:435-7.
16. Simpson DG, Uschner M, Mc CJ. Respiratory function in pulmonary tuberculosis. Am Rev Respir Dis. 1963;87:1-16.
17. Garvin A, Lundsgaard C, Van Slyke DD. STUDIES OF LUNG VOLUME : II. TUBERCULOUS MEN. J Exp Med. 1918;27(1):87-94.
18. Garvin A, Lundsgaard C, Van Slyke DD. STUDIES OF LUNG VOLUME : III. TUBERCULOUS WOMEN. J Exp Med. 1918;27(1):129-42.
19. Hnizdo E, Singh T, Churchyard G. Chronic pulmonary function impairment caused by initial and recurrent pulmonary tuberculosis following treatment. Thorax. 2000;55(1):32-8.

20. Caballero A, Torres-Duque CA, Jaramillo C, Bolívar F, Sanabria F, Osorio P, et al. Prevalence of COPD in five Colombian cities situated at low, medium, and high altitude (PREPOCOL study). Chest. 2008;133(2):343-9.
21. Salvi SS, Barnes PJ. Chronic obstructive pulmonary disease in non-smokers. Lancet. 2009;374(9691):733-43.
22. Allwood BW, Myer L, Bateman ED. A systematic review of the association between pulmonary tuberculosis and the development of chronic airflow obstruction in adults. Respiration. 2013;86(1):76-85.
23. Ehrlich RI, White N, Norman R, Laubscher R, Steyn K, Lombard C, et al. Predictors of chronic bronchitis in South African adults. Int J Tuberc Lung Dis. 2004;8(3):369-76.
24. Pasipanodya JG, Miller TL, Vecino M, Munguia G, Garmon R, Bae S, et al. Pulmonary impairment after tuberculosis. Chest. 2007;131(6):1817-24.
25. Baig IM, Saeed W, Khalil KF. Post-tuberculous chronic obstructive pulmonary disease. J Coll Physicians Surg Pak. 2010;20(8):542-4.
26. Menezes AM, Hallal PC, Perez-Padilla R, Jardim JR, Muiño A, Lopez MV, et al. Tuberculosis and airflow obstruction: evidence from the PLATINO study in Latin America. Eur Respir J. 2007;30(6):1180-5.
27. Ross J, Ehrlich RI, Hnizdo E, White N, Churchyard GJ. Excess lung function decline in gold miners following pulmonary tuberculosis. Thorax. 2010;65(11):1010-5.
28. Willcox PA, Ferguson AD. Chronic obstructive airways disease following treated pulmonary tuberculosis. Respir Med. 1989;83(3):195-8.
29. Plit ML, Anderson R, Van Rensburg CE, Page-Shipp L, Blott JA, Fresen JL, et al. Influence of antimicrobial chemotherapy on spirometric parameters and pro-inflammatory indices in severe pulmonary tuberculosis. Eur Respir J. 1998;12(2):351-6.
30. Ando M, Mori A, Esaki H, Shiraki T, Uemura H, Okazawa M, et al. The effect of pulmonary rehabilitation in patients with post-tuberculosis lung disorder. Chest. 2003;123(6):1988-95.
31. Ferrero E, Biswas P, Vettoretto K, Ferrarini M, Uguccioni M, Piali L, et al. Macrophages exposed to Mycobacterium tuberculosis release chemokines able to recruit selected leucocyte subpopulations: focus on gammadelta cells. Immunology. 2003;108(3):365-74.
32. Hilda JN, Das S, Tripathy SP, Hanna LE. Role of neutrophils in tuberculosis: A bird's eye view. Innate Immun. 2020;26(4):240-7.
33. Hinchey J, Lee S, Jeon BY, Basaraba RJ, Venkataswamy MM, Chen B, et al. Enhanced priming of adaptive immunity by a proapoptotic mutant of Mycobacterium tuberculosis. J Clin Invest. 2007;117(8):2279-88.
34. Chatterjee A, D'Souza D, Vira T, Bamne A, Ambe GT, Nicol MP, et al. Strains of Mycobacterium tuberculosis from western Maharashtra, India, exhibit a high degree of diversity and strain-specific associations with drug resistance, cavitary disease, and treatment failure. J Clin Microbiol. 2010;48(10):3593-9.
35. Kempker RR, Rabin AS, Nikolaishvili K, Kalandadze I, Gogishvili S, Blumberg HM, et al. Additional drug resistance in Mycobacterium tuberculosis isolates from resected cavities among patients with multidrug-resistant or extensively drug-resistant pulmonary tuberculosis. Clin Infect Dis. 2012;54(6):e51-4.
36. Dye C, Williams BG. The population dynamics and control of tuberculosis. Science. 2010;328(5980):856-61.
37. Saravayskaya Y, Zilberstein G, Zilberstein R, Zilberstein S, Maor U, D'Amato A, et al. "1984": What Orwell could not predict. Proteomic analysis of his scripts. Electrophoresis. 2020.

38. Price NM, J. Farrar, T. T. Tran, T. H. Nguyen, T. H. Tran, J. S. Friedland. Identification of a matrix-degrading phenotype in human tuberculosis in vitro and in vivo. J Immunol. 2001;166:4223–30.
39. Ong CW, Elkington PT, Friedland JS. Tuberculosis, pulmonary cavitation, and matrix metalloproteinases. Am J Respir Crit Care Med. 2014;190(1):9-18.
40. Parks WC, Wilson CL, López-Boado YS. Matrix metalloproteinases as modulators of inflammation and innate immunity. Nat Rev Immunol. 2004;4(8):617-29.
41. Boire A, Covic L, Agarwal A, Jacques S, Sherifi S, Kuliopulos A. PAR1 is a matrix metalloprotease-1 receptor that promotes invasion and tumorigenesis of breast cancer cells. Cell. 2005;120(3):303-13.
42. Elkington PT, D'Armiento JM, Friedland JS. Tuberculosis Immunopathology: The Neglected Role of Extracellular Matrix Destruction Science Translational Medicine. 2011;3(71):71ps6.
43. Elkington PT, Green JA, Emerson JE, Lopez-Pascua LD, Boyle JJ, O'Kane CM, et al. Synergistic Up-Regulation of Epithelial Cell Matrix Metalloproteinase-9 Secretion in Tuberculosis. Am J Respir Cell Mol Biol. 2007;37(4):431-7.
44. Elkington PT, Ugarte-Gil CA, Friedland JS. Matrix metalloproteinases in tuberculosis. Eur Respir J. 2011;38(2):456-64.
45. Welgus HG, Jeffrey JJ, Stricklin GP, Roswit WT, Eisen AZ. Characteristics of the action of human skin fibroblast collagenase on fibrillar collagen. J Biol Chem. 1980;255(14):6806-13.
46. Ugarte-Gil CA, Elkington P, Gilman RH, Coronel J, Tezera LB, Bernabe-Ortiz A, et al. Induced sputum MMP-1, -3 & -8 concentrations during treatment of tuberculosis. PLoS One. 2013;8(4):e61333.
47. D'Armiento J, Dalal SS, Okada Y, Berg RA, Chada K. Collagenase expression in the lungs of transgenic mice causes pulmonary emphysema. Cell. 1992;71(6):955-61.
48. Finlay GA, O'Driscoll LR, Russell KJ, D'Arcy EM, Masterson JB, FitzGerald MX, et al. Matrix metalloproteinase expression and production by alveolar macrophages in emphysema. Am J Respir Crit Care Med. 1997;156(1):240-7.
49. Zhou L, Le Y, Tian J, Yang X, Jin R, Gai X, et al. Cigarette smoke-induced RANKL expression enhances MMP-9 production by alveolar macrophages. Int J Chron Obstruct Pulmon Dis. 2019;14:81-91.
50. Eum SY, Kong JH, Hong MS, Lee YJ, Kim JH, Hwang SH, et al. Neutrophils are the predominant infected phagocytic cells in the airways of patients with active pulmonary TB. Chest. 2010;137(1):122-8.
51. Taylor JL, Hattle JM, Dreitz SA, Troudt JM, Izzo LS, Basaraba RJ, et al. Role for matrix metalloproteinase 9 in granuloma formation during pulmonary Mycobacterium tuberculosis infection. Infect Immun. 2006;74(11):6135-44.
52. Thwaites GE, Simmons CP, Than Ha Quyen N, Thi Hong Chau T, Phuong Mai P, Thi Dung N, et al. Pathophysiology and prognosis in vietnamese adults with tuberculous meningitis. J Infect Dis. 2003;188(8):1105-15.
53. Singh S, Kubler A, Singh UK, Singh A, Gardiner H, Prasad R, et al. Antimycobacterial drugs modulate immunopathogenic matrix metalloproteinases in a cellular model of pulmonary tuberculosis. Antimicrob Agents Chemother. 2014;58(8):4657-65.
54. Elkington P, Shiomi T, Breen R, Nuttall RK, Ugarte-Gil CA, Walker NF, et al. MMP-1 drives immunopathology in human tuberculosis and transgenic mice. J Clin Invest. 2011;121(5):1827-33.

55. Walker NF, Clark SO, Oni T, Andreu N, Tezera L, Singh S, et al. Doxycycline and HIV infection suppress tuberculosis-induced matrix metalloproteinases. Am J Respir Crit Care Med. 2012;185(9):989-97.
56. Sundararajan S, Babu S, Das SD. Comparison of localized versus systemic levels of Matrix metalloproteinases (MMPs), its tissue inhibitors (TIMPs) and cytokines in tuberculous and non-tuberculous pleuritis patients. Hum Immunol. 2012;73(10):985-91.
57. Elkington P, Nuttall R, Boyle J, O'Kane C, Horncastle D, Edwards D, et al. Mycobacterium tuberculosis but not vaccine BCG specifically up-regulates matrix metalloproteinase-1. Am J Respir Crit Care Med. 2006;172:1596-604.
58. Price N, Gilman R, Uddin J, Recavarren S, Friedland J. Unopposed Matrix Metalloproteinase-9 Expression in Human Tuberculous Granuloma and the Role of TNF-alpha-Dependent Monocyte Networks. J Immunol. 2003;171(10):5579-86.
59. Thuong NT, Dunstan SJ, Chau TT, Thorsson V, Simmons CP, Quyen NT, et al. Identification of tuberculosis susceptibility genes with human macrophage gene expression profiles. PLoS Pathog. 2008;4(12):e1000229.
60. Wang CH, Lin HC, Lin SM, Huang CD, Liu CY, Huang KH, et al. MMP-1(-1607G) polymorphism as a risk factor for fibrosis after pulmonary tuberculosis in Taiwan. Int J Tuberc Lung Dis. 2010;14(5):627-34.
61. Schwertz Hr, Tolley ND, Foulks JM, Denis MM, Risenmay BW, Buerke M, et al. Signal-dependent splicing of tissue factor pre-mRNA modulates the thrombogenecity of human platelets. Journal of Experimental Medicine. 2006;203(11):2433-40.
62. Neu CT, Gutschner T, Haemmerle M. Post-Transcriptional Expression Control in Platelet Biogenesis and Function. Int J Mol Sci. 2020;21(20).
63. Gerstberger S, Hafner M, Tuschl T. A census of human RNA-binding proteins. Nat Rev Genet. 2014;15(12):829-45.
64. Senzel L, Gnatenko DV, Bahou WF. The platelet proteome. Curr Opin Hematol. 2009;16(5):329-33.
65. Youssefian T, Massé JM, Rendu F, Guichard J, Cramer EM. Platelet and megakaryocyte dense granules contain glycoproteins Ib and IIb-IIIa. Blood. 1997;89(11):4047-57.
66. Semple JW, Italiano JE, Jr., Freedman J. Platelets and the immune continuum. Nat Rev Immunol. 2011;11(4):264-74.
67. Cognasse F, Garraud O. Human platelets exhibit infectious-pathogen-binding ligands and participate to inflammation (and more?). Exp Hematol. 2005;33(10):1081-2.
68. Antoniades C, Bakogiannis C, Tousoulis D, Antonopoulos AS, Stefanadis C. The CD40/CD40 ligand system: linking inflammation with atherothrombosis. J Am Coll Cardiol. 2009;54(8):669-77.
69. Kapur R, Semple JW. Platelets as immune-sensing cells. Blood Advances. 2016;1(1):10-4.
70. Kraemer BF, Campbell RA, Schwertz H, Franks ZG, Vieira de Abreu A, Grundler K, et al. Bacteria differentially induce degradation of Bcl-xL, a survival protein, by human platelets. Blood. 2012;120(25):5014-20.
71. Garraud O, Cognasse F. Are Platelets Cells? And if Yes, are They Immune Cells? Front Immunol. 2015;6.
72. Cognasse F, Hamzeh H, Chavarin P, Acquart S, Genin C, Garraud O. Evidence of Toll-like receptor molecules on human platelets. Immunol Cell Biol. 2005;83(2):196-8.
73. Andonegui G, Kerfoot SM, McNagny K, Ebbert KV, Patel KD, Kubes P. Platelets express functional Toll-like receptor-4. Blood. 2005;106(7):2417-23.

74. Blair P, Rex S, Vitseva O, Beaulieu L, Tanriverdi K, Chakrabarti S, et al. Stimulation of Toll-like receptor 2 in human platelets induces a thromboinflammatory response through activation of phosphoinositide 3-kinase. Circ Res. 2009;104(3):346-54.
75. Aslam R, Speck ER, Kim M, Crow AR, Bang KW, Nestel FP, et al. Platelet Toll-like receptor expression modulates lipopolysaccharide-induced thrombocytopenia and tumor necrosis factor-alpha production in vivo. Blood. 2006;107(2):637-41.
76. Berthet J, Damien P, Hamzeh-Cognasse H, Arthaud CA, Eyraud MA, Zeni F, et al. Human platelets can discriminate between various bacterial LPS isoforms via TLR4 signaling and differential cytokine secretion. Clin Immunol. 2012;145(3):189-200.
77. Banerjee M, Huang Y, Joshi S, Popa GJ, Mendenhall MD, Wang QJ, et al. Platelets Endocytose Viral Particles and Are Activated via TLR (Toll-Like Receptor) Signaling. Arterioscler Thromb Vasc Biol. 2020;40(7):1635-50.
78. McDonald B, Davis RP, Kim SJ, Tse M, Esmon CT, Kolaczkowska E, et al. Platelets and neutrophil extracellular traps collaborate to promote intravascular coagulation during sepsis in mice. Blood. 2017;129(10):1357-67.
79. Clark SR, Ma AC, Tavener SA, McDonald B, Goodarzi Z, Kelly MM, et al. Platelet TLR4 activates neutrophil extracellular traps to ensnare bacteria in septic blood. Nature Medicine. 2007;13(4):463-9.
80. Levi M, van der Poll T. Coagulation and sepsis. Thromb Res. 2017;149:38-44.
81. Tang D, Wang H, Billiar TR, Kroemer G, Kang R. Emerging mechanisms of immunocoagulation in sepsis and septic shock. Trends Immunol. 2021;42(6):508-22.
82. Middleton EA, Rowley JW, Campbell RA, Grissom CK, Brown SM, Beesley SJ, et al. Sepsis alters the transcriptional and translational landscape of human and murine platelets. Blood. 2019;134(12):911-23.
83. van Gils JM, Zwaginga JJ, Hordijk PL. Molecular and functional interactions among monocytes, platelets, and endothelial cells and their relevance for cardiovascular diseases. J Leukoc Biol. 2009;85(2):195-204.
84. Robson SC, White NW, Aronson I, Woollgar R, Goodman H, Jacobs P. Acute-phase response and the hypercoagulable state in pulmonary tuberculosis. Br J Haematol. 1996;93(4):943-9.
85. Feng Y, Yin H, Mai G, Mao L, Yue J, Xiao H, et al. Elevated serum levels of CCL17 correlate with increased peripheral blood platelet count in patients with active tuberculosis in China. Clin Vaccine Immunol. 2011;18(4):629-32.
86. Turken O, Kunter E, Sezer M, Solmazgul E, Cerrahoglu K, Bozkanat E, et al. Hemostatic changes in active pulmonary tuberculosis. Int J Tuberc Lung Dis. 2002;6(10):927-32.
87. Bozóky G, Ruby E, Góhér I, Tóth J, Mohos A. [Hematologic abnormalities in pulmonary tuberculosiss]. Orv Hetil. 1997;138(17):1053-6.
88. Morris CD, Bird AR, Nell H. The haematological and biochemical changes in severe pulmonary tuberculosis. Q J Med. 1989;73(272):1151-9.
89. Unsal E, Aksaray S, Köksal D, Sipit T. Potential role of interleukin 6 in reactive thrombocytosis and acute phase response in pulmonary tuberculosis. Postgrad Med J. 2005;81(959):604-7.
90. Tozkoparan E, Deniz O, Ucar E, Bilgic H, Ekiz K. Changes in platelet count and indices in pulmonary tuberculosis. Clin Chem Lab Med. 2007;45(8):1009-13.
91. Baynes RD, Bothwell TH, Flax H, McDonald TP, Atkinson P, Chetty N, et al. Reactive thrombocytosis in pulmonary tuberculosis. J Clin Pathol. 1987;40(6):676-9.
92. Lee MY, Kim YJ, Lee HJ, Cho SY, Park TS. Mean Platelet Volume in Mycobacterium tuberculosis Infection. Biomed Res Int. 2016;2016:7508763.

93. Sahin F, Yazar E, Yildiz P. Prominent features of platelet count, plateletcrit, mean platelet volume and platelet distribution width in pulmonary tuberculosis. Multidiscip Respir Med. 2012;7(1):38.
94. Kutiyal AS. A Study of Haematological and Haemostasis Parameters and Hypercoagulable State in Tuberculosis Patients in Northern India and the Outcome with Anti Tubercular Therapy. Journal of Clinical and Diagnostic Research. 2017.
95. Berry MP, Graham CM, McNab FW, Xu Z, Bloch SA, Oni T, et al. An interferon-inducible neutrophil-driven blood transcriptional signature in human tuberculosis. Nature. 2010;466(7309):973-7.
96. Best MG, Sol N, Kooi I, Tannous J, Westerman BA, Rustenburg F, et al. RNA-Seq of Tumor-Educated Platelets Enables Blood-Based Pan-Cancer, Multiclass, and Molecular Pathway Cancer Diagnostics. Cancer Cell. 2015;28(5):666-76.
97. Khechinashvili GN, Khvitiya NG. Protective characteristics of platelets in tuberculosis. Bull Exp Biol Med. 2004;138(5):513-4.
98. Law K, Weiden M, Harkin T, Tchou-Wong K, Chi C, Rom WN. Increased release of interleukin-1 beta, interleukin-6, and tumor necrosis factor-alpha by bronchoalveolar cells lavaged from involved sites in pulmonary tuberculosis. Am J Respir Crit Care Med. 1996;153(2):799-804.
99. Schoeman J, Mansvelt E, Springer P, van Rensburg AJ, Carlini S, Fourie E. Coagulant and fibrinolytic status in tuberculous meningitis. Pediatr Infect Dis J. 2007;26(5):428-31.
100. Janssen S, Schutz C, Ward AM, Huson MA, Wilkinson RJ, Burton R, et al. Hemostatic Changes Associated With Increased Mortality Rates in Hospitalized Patients With HIV-Associated Tuberculosis: A Prospective Cohort Study. J Infect Dis. 2017;215(2):247-58.
101. Fugate JE, Lyons JL, Thakur KT, Smith BR, Hedley-Whyte ET, Mateen FJ. Infectious causes of stroke. Lancet Infect Dis. 2014;14(9):869-80.
102. Buyukasik Y, Soylu B, Soylu AR, Ozcebe OI, Canbakan S, Haznedaroglu IC, et al. In vivo platelet and T-lymphocyte activities during pulmonary tuberculosis. Eur Respir J. 1998;12(6):1375-9.
103. Fox KA, Kirwan DE, Whittington AM, Krishnan N, Robertson BD, Gilman RH, et al. Platelets Regulate Pulmonary Inflammation and Tissue Destruction in Tuberculosis. Am J Respir Crit Care Med. 2018;198(2):245-55.
104. Ye L, Zhang Y-P, Yu N, Jia Y-X, Wan S-J, Wang F-Y. Serum platelet factor 4 is a reliable activity parameter in adult patients with inflammatory bowel disease: A pilot study. Medicine. 2017;96(11):e6323-e.
105. Domschke G, Gleissner CA. CXCL4-induced macrophages in human atherosclerosis. Cytokine. 2019;122:154141.
106. Yeo L, Adlard N, Biehl M, Juarez M, Smallie T, Snow M, et al. Expression of chemokines CXCL4 and CXCL7 by synovial macrophages defines an early stage of rheumatoid arthritis. Ann Rheum Dis. 2016;75(4):763-71.
107. Lefrançais E, Ortiz-Muñoz G, Caudrillier A, Mallavia B, Liu F, Sayah DM, et al. The lung is a site of platelet biogenesis and a reservoir for haematopoietic progenitors. Nature. 2017;544(7648):105-9.
108. Feng Y, Dorhoi A, Mollenkopf HJ, Yin H, Dong Z, Mao L, et al. Platelets direct monocyte differentiation into epithelioid-like multinucleated giant foam cells with suppressive capacity upon mycobacterial stimulation. J Infect Dis. 2014;210(11):1700-10.
109. Kuhn C, Askin F. Lung and mediastinum. In: Kissane J, editor. Anderson's pathology. 8th ed. St. Louis: CV Mosby; 1985. p. 838–54.

110. Rossaint J, Margraf A, Zarbock A. Role of Platelets in Leukocyte Recruitment and Resolution of Inflammation. Front Immunol. 2018;9:2712.
111. Zucoloto AZ, Jenne CN. Platelet-Neutrophil Interplay: Insights Into Neutrophil Extracellular Trap (NET)-Driven Coagulation in Infection. Front Cardiovasc Med. 2019;6(85).
112. van der Meer AJ, Zeerleder S, Blok DC, Kager LM, Lede IO, Rahman W, et al. Neutrophil extracellular traps in patients with pulmonary tuberculosis. Respir Res. 2017;18(1):181.
113. Muefong CN, Sutherland JS. Neutrophils in Tuberculosis-Associated Inflammation and Lung Pathology. Front Immunol. 2020;11(962).
114. Nourshargh S, Alon R. Leukocyte migration into inflamed tissues. Immunity. 2014;41(5):694-707.
115. Théorêt JF, Yacoub D, Hachem A, Gillis MA, Merhi Y. P-selectin ligation induces platelet activation and enhances microaggregate and thrombus formation. Thromb Res. 2011;128(3):243-50.
116. Eini P, Shirvani M, Hajilooi M, Esna-Ashari F. Comparison of L-selectin blood level and gene polymorphism in tuberculosis patients with healthy individuals. J Clin Lab Anal. 2018;32(6):e22409.
117. Martins P, van Gils JM, Mol A, Hordijk PL, Zwaginga JJ. Platelet binding to monocytes increases the adhesive properties of monocytes by up-regulating the expression and functionality of β(1) and β(2) integrins. J Leukoc Biol. 2006;79(3):499-507.
118. Linden MD, Jackson DE. Platelets: pleiotropic roles in atherogenesis and atherothrombosis. Int J Biochem Cell Biol. 2010;42(11):1762-6.
119. Linden MD, Furman MI, Frelinger AL, 3rd, Fox ML, Barnard MR, Li Y, et al. Indices of platelet activation and the stability of coronary artery disease. J Thromb Haemost. 2007;5(4):761-5.
120. Kullaya V, van der Ven A, Mpagama S, Mmbaga BT, de Groot P, Kibiki G, et al. Platelet-monocyte interaction in Mycobacterium tuberculosis infection. Tuberculosis (Edinb). 2018;111:86-93.
121. Jennings LK, Phillips DR. Purification of glycoproteins IIb and III from human platelet plasma membranes and characterization of a calcium-dependent glycoprotein IIb-III complex. J Biol Chem. 1982;257(17):10458-66.
122. Litvinov RI, Farrell DH, Weisel JW, Bennett JS. The Platelet Integrin αIIbβ3 Differentially Interacts with Fibrin Versus Fibrinogen. J Biol Chem. 2016;291(15):7858-67.
123. Vilahur G, Gutiérrez M, Arzanauskaite M, Mendieta G, Ben-Aicha S, Badimon L. Intracellular platelet signalling as a target for drug development. Vascul Pharmacol. 2018;111:22-5.
124. Simon DI, Chen Z, Xu H, Li CQ, Dong J, McIntire LV, et al. Platelet glycoprotein ibalpha is a counterreceptor for the leukocyte integrin Mac-1 (CD11b/CD18). J Exp Med. 2000;192(2):193-204.
125. Gerdes N, Seijkens T, Lievens D, Kuijpers MJ, Winkels H, Projahn D, et al. Platelet CD40 Exacerbates Atherosclerosis by Transcellular Activation of Endothelial Cells and Leukocytes. Arterioscler Thromb Vasc Biol. 2016;36(3):482-90.
126. Sabir N, Hussain T, Mangi MH, Zhao D, Zhou X. Matrix metalloproteinases: Expression, regulation and role in the immunopathology of tuberculosis. Cell Prolif. 2019;52(4):e12649.
127. Hidari KI, Weyrich AS, Zimmerman GA, McEver RP. Engagement of P-selectin glycoprotein ligand-1 enhances tyrosine phosphorylation and activates mitogen-activated protein kinases in human neutrophils. J Biol Chem. 1997;272(45):28750-6.
128. Johnson GL, Lapadat R. Mitogen-activated protein kinase pathways mediated by ERK, JNK, and p38 protein kinases. Science. 2002;298(5600):1911-2.

129. O'Kane C, Elkington P, Jones M, Caviedes L, Tovar M, Gilman R, et al. STAT3, p38 MAPK, and NF-kappaB drive unopposed monocyte-dependent fibroblast MMP-1 secretion in tuberculosis. Am J Respir Cell Mol Biol. 2010;43(4):465-74.
130. Rand L, Green J, Saraiva L, Friedland J, Elkington P. Matrix metalloproteinase-1 is regulated in tuberculosis by a p38 MAPK-dependent, p-aminosalicylic acid-sensitive signaling cascade. J Immunol. 2009;182(9):5865-72.
131. Elkington P, Emerson J, Lopez-Pascua L, O'Kane C, Horncastle D, Boyle J, et al. Mycobacterium tuberculosis up-regulates matrix metalloproteinase-1 secretion from human airway epithelial cells via a p38 MAPK switch. J Immunol. 2005;175(8):5333-40.
132. Mercer BA, Kolesnikova N, Sonett J, D'Armiento J. Extracellular regulated kinase/mitogen activated protein kinase is up-regulated in pulmonary emphysema and mediates matrix metalloproteinase-1 induction by cigarette smoke. J Biol Chem. 2004;279(17):17690-6.
133. Reiling N, Blumenthal A, Flad HD, Ernst M, Ehlers S. Mycobacteria-induced TNF-alpha and IL-10 formation by human macrophages is differentially regulated at the level of mitogen-activated protein kinase activity. J Immunol. 2001;167(6):3339-45.
134. Brace PT, Tezera LB, Bielecka MK, Mellows T, Garay D, Tian S, et al. Mycobacterium tuberculosis subverts negative regulatory pathways in human macrophages to drive immunopathology. PLoS pathogens. 2017;13(6):e1006367.
135. George AL, Bangalore-Prakash P, Rajoria S, Suriano R, Shanmugam A, Mittelman A, et al. Endothelial progenitor cell biology in disease and tissue regeneration. J Hematol Oncol. 2011;4:24.
136. Fox R, Nhan TQ, Law GL, Morris DR, Liles WC, Schwartz SM. PSGL-1 and mTOR regulate translation of ROCK-1 and physiological functions of macrophages. Embo j. 2007;26(2):505-15.
137. Kirwan DE, Chong DLW, Friedland JS. Platelet Activation and the Immune Response to Tuberculosis. Front Immunol. 2021;12:631696.
138. Mayer-Barber KD, Andrade BB, Oland SD, Amaral EP, Barber DL, Gonzales J, et al. Host-directed therapy of tuberculosis based on interleukin-1 and type I interferon crosstalk. Nature. 2014;511(7507):99-103.
139. Colas RA, Nhat LTH, Thuong NTT, Gómez EA, Ly L, Thanh HH, et al. Proresolving mediator profiles in cerebrospinal fluid are linked with disease severity and outcome in adults with tuberculous meningitis. Faseb j. 2019;33(11):13028-39.
140. Yao C, Narumiya S. Prostaglandin-cytokine crosstalk in chronic inflammation. British journal of pharmacology. 2019;176(3):337-54.
141. Ivanyi J, Zumla A. Nonsteroidal antiinflammatory drugs for adjunctive tuberculosis treatment. J Infect Dis. 2013;208(2):185-8.
142. Kroesen VM, Rodríguez-Martínez P, García E, Rosales Y, Díaz J, Martín-Céspedes M, et al. A Beneficial Effect of Low-Dose Aspirin in a Murine Model of Active Tuberculosis. Front Immunol. 2018;9:798.
143. Kroesen VM, Groschel MI, Martinson N, Zumla A, Maeurer M, van der Werf TS, et al. Non-Steroidal Anti-inflammatory Drugs As Host-Directed Therapy for Tuberculosis: A Systematic Review. Front Immunol. 2017;8:772.
144. Marzo E, Vilaplana C, Tapia G, Diaz J, Garcia V, Cardona PJ. Damaging role of neutrophilic infiltration in a mouse model of progressive tuberculosis. Tuberculosis (Edinb). 2014;94(1):55-64.
145. Dutta NK, Kumar KA, Mazumdar K, Dastidar SG. In vitro and in vivo antimycobacterial activity of antiinflammatory drug, diclofenac sodium. Indian J Exp Biol. 2004;42(9):922-7.

146. Dutta NK, Mazumdar K, Dastidar SG, Park JH. Activity of diclofenac used alone and in combination with streptomycin against Mycobacterium tuberculosis in mice. Int J Antimicrob Agents. 2007;30(4):336-40.
147. Maitra A, Bates S, Shaik M, Evangelopoulos D, Abubakar I, McHugh TD, et al. Repurposing drugs for treatment of tuberculosis: a role for non-steroidal anti-inflammatory drugs. Br Med Bull. 2016;118(1):138-48.
148. Schaller A, Sun Z, Yang Y, Somoskovi A, Zhang Y. Salicylate reduces susceptibility of Mycobacterium tuberculosis to multiple antituberculosis drugs. Antimicrob Agents Chemother. 2002;46(8):2636-9.
149. Denkin S, Byrne S, Jie C, Zhang Y. Gene expression profiling analysis of Mycobacterium tuberculosis genes in response to salicylate. Arch Microbiol. 2005;184(3):152-7.
150. Hortle E, Johnson KE, Johansen MD, Nguyen T, Shavit JA, Britton WJ, et al. Thrombocyte inhibition restores protective immunity to mycobacterial infection in zebrafish. J Infect Dis. 2019.
151. Byrne ST, Denkin SM, Zhang Y. Aspirin and ibuprofen enhance pyrazinamide treatment of murine tuberculosis. J Antimicrob Chemother. 2007;59(2):313-6.
152. Hernández-Pando R, Orozco H, Mancilla R. T-cell lung granulomas induced by sepharose-coupled Mycobacterium tuberculosis protein antigens: immunosuppressive phenomena reversed with cyclophosphamide and indomethacin. Immunology. 1995;86(4):506-11.
153. Vilaplana C, Marzo E, Tapia G, Diaz J, Garcia V, Cardona PJ. Ibuprofen therapy resulted in significantly decreased tissue bacillary loads and increased survival in a new murine experimental model of active tuberculosis. J Infect Dis. 2013;208(2):199-202.
154. Lee MR, Lee MC, Chang CH, Liu CJ, Chang LY, Zhang JF, et al. Use of Antiplatelet Agents and Survival of Tuberculosis Patients: A Population-Based Cohort Study. J Clin Med. 2019;8(7).
155. Wang W, Du Z, Ni M, Wang Z, Liang M, Sheng H, et al. Aspirin enhances the clinical efficacy of anti-tuberculosis therapy in pulmonary tuberculosis in patients with type 2 diabetes mellitus. Infectious Diseases. 2020;52(10):721-9.
156. Mai NT, Dobbs N, Phu NH, Colas RA, Thao LT, Thuong NT, et al. A randomised double blind placebo controlled phase 2 trial of adjunctive aspirin for tuberculous meningitis in HIV-uninfected adults. Elife. 2018;7.
157. Misra UK, Kalita J, Nair PP. Role of aspirin in tuberculous meningitis: a randomized open label placebo controlled trial. J Neurol Sci. 2010;293(1-2):12-7.
158. University of Stellenbosch. TB-IRIS NSAID Cox-2 Inhibitor Prevention Trial (ClinicalTrials.gov Identifier: NCT02060006) 2014 [Available from: https://clinicaltrials.gov/ct2/show/NCT02060006
159. Fundació Institut Germans Trias i Pujol. Potential Efficacy and Safety of Using Adjunctive Ibuprofen for XDR-TB Tuberculosis (NSAIDS-XDRTB) (Clinicaltrials.gov Identifier NCT02781909) 2016 [Available from: https://clinicaltrials.gov/ct2/show/NCT02781909.
160. Anne Margarita Dyrhol Riise Therapeutic Vaccination and Immune Modulation - New Treatment Strategies for the MDR Tuberculosis Pandemic (TBCOX2) (Clinicaltrials.gov Identifier NCT02503839) 2015 [Available from: https://clinicaltrials.gov/ct2/show/NCT02503839.
161. Zhang X, Qin J, Zou J, Lv Z, Tan B, Shi J, et al. Extracellular ADP facilitates monocyte recruitment in bacterial infection via ERK signaling. Cellular & molecular immunology. 2018;15(1):58-73.
162. Thomas MR, Outteridge SN, Ajjan RA, Phoenix F, Sangha GK, Faulkner RE, et al. Platelet P2Y12 Inhibitors Reduce Systemic Inflammation and Its Prothrombotic Effects in an Experimental Human Model. Arterioscler Thromb Vasc Biol. 2015;35(12):2562-70.

163. Tunjungputri RN, van der Ven AJ, Riksen N, Rongen G, Tacke S, van den Berg TN, et al. Differential effects of platelets and platelet inhibition by ticagrelor on TLR2- and TLR4-mediated inflammatory responses. Thromb Haemost. 2015;113(5):1035-45.
164. Adcock DM. Collection, transport, and processing of blood specimes for testing plasma-based coagulation assays and molecular hemostasis assays: approved guideline: CLSI; 2008.
165. Favaloro EJ, Lippi G. Discard Tubes Are Sometimes Necessary When Drawing Samples for Hemostasis. American Journal of Clinical Pathology. 2010;134(5):851-2.
166. Elkington PT, Green JA, Friedland JS. Filter sterilization of highly infectious samples to prevent false negative analysis of matrix metalloproteinase activity. J Immunol Methods. 2006;309(1-2):115-9.
167. Elkington PTG. Matrix metalloproteinases and tissue destruction in pulmonary tuberculosis. [PhD]: Imperial College London; 2005.
168. Sun P, McMillan-Ward E, Mian R, Israels SJ. Comparison of light transmission aggregometry and multiple electrode aggregometry for the evaluation of patients with mucocutaneous bleeding. International Journal of Laboratory Hematology. 2019;41(1):133-40.
169. Armstrong PC, Leadbeater PD, Chan MV, Kirkby NS, Jakubowski JA, Mitchell JA, et al. In the presence of strong P2Y12 receptor blockade, aspirin provides little additional inhibition of platelet aggregation. J Thromb Haemost. 2011;9(3):552-61.
170. Yaw HP, Van Den Helm S, Linden M, Monagle P, Ignjatovic V. Whole blood flow cytometry protocol for the assessment of platelet phenotype, function, and cellular interactions. Platelets. 2021;32(6):786-93.
171. Suzuki-Inoue K, Fuller GLJ, García An, Eble JA, Pöhlmann S, Inoue O, et al. A novel Syk-dependent mechanism of platelet activation by the C-type lectin receptor CLEC-2. Blood. 2006;107(2):542-9.
172. Kawai T, Akira S. Toll-like receptors and their crosstalk with other innate receptors in infection and immunity. Immunity. 2011;34(5):637-50.
173. Keane C, Tilley D, Cunningham A, Smolenski A, Kadioglu A, Cox D, et al. Invasive Streptococcus pneumoniae trigger platelet activation via Toll-like receptor 2. J Thromb Haemost. 2010;8(12):2757-65.
174. Cognasse F, Hamzeh-Cognasse H, Lafarge S, Delezay O, Pozzetto B, McNicol A, et al. Toll-like receptor 4 ligand can differentially modulate the release of cytokines by human platelets. Br J Haematol. 2008;141(1):84-91.
175. Zhang G, Han J, Welch EJ, Ye RD, Voyno-Yasenetskaya TA, Malik AB, et al. Lipopolysaccharide stimulates platelet secretion and potentiates platelet aggregation via TLR4/MyD88 and the cGMP-dependent protein kinase pathway. J Immunol. 2009;182(12):7997-8004.
176. Claushuis TAM, Van Der Veen AIP, Horn J, Schultz MJ, Houtkooper RH, Van 't Veer C, et al. Platelet Toll-like receptor expression and activation induced by lipopolysaccharide and sepsis. Platelets. 2019;30(3):296-304.
177. Hally K, Fauteux-Daniel S, Hamzeh-Cognasse H, Larsen P, Cognasse F. Revisiting Platelets and Toll-Like Receptors (TLRs): At the Interface of Vascular Immunity and Thrombosis. International journal of molecular sciences. 2020;21(17):6150.
178. Carestia A, Kaufman T, Rivadeneyra L, Landoni VI, Pozner RG, Negrotto S, et al. Mediators and molecular pathways involved in the regulation of neutrophil extracellular trap formation mediated by activated platelets. J Leukoc Biol. 2016;99(1):153-62.
179. Matus V, Valenzuela JG, Hidalgo P, Pozo LM, Panes O, Wozniak A, et al. Human platelet interaction with E. coli O111 promotes tissue-factor-dependent procoagulant activity, involving Toll like receptor 4. PLoS One. 2017;12(9):e0185431.

180. Ståhl AL, Svensson M, Mörgelin M, Svanborg C, Tarr PI, Mooney JC, et al. Lipopolysaccharide from enterohemorrhagic Escherichia coli binds to platelets through TLR4 and CD62 and is detected on circulating platelets in patients with hemolytic uremic syndrome. Blood. 2006;108(1):167-76.
181. Maouia A, Rebetz J, Kapur R, Semple JW. The Immune Nature of Platelets Revisited. Transfus Med Rev. 2020;34(4):209-20.
182. Vallance TM, Ravishankar D, Albadawi DAI, Layfield H, Sheard J, Vaiyapuri R, et al. Effect of ultrapure lipopolysaccharides derived from diverse bacterial species on the modulation of platelet activation. Sci Rep. 2019;9(1):18258.
183. Semple JW, Aslam R, Kim M, Speck ER, Freedman J. Platelet-bound lipopolysaccharide enhances Fc receptor-mediated phagocytosis of IgG-opsonized platelets. Blood. 2007;109(11):4803-5.
184. Shashkin PN, Brown GT, Ghosh A, Marathe GK, McIntyre TM. Lipopolysaccharide is a direct agonist for platelet RNA splicing. J Immunol. 2008;181(5):3495-502.
185. Kleinnijenhuis J, Oosting M, Joosten LAB, Netea MG, Van Crevel R. Innate Immune Recognition of Mycobacterium tuberculosis. Clinical and Developmental Immunology. 2011;2011:405310.
186. Mitrugno A, Rigg RA, Laschober NB, Ngo ATP, Pang J, Williams CD, et al. Potentiation of TRAP-6-induced platelet dense granule release by blockade of P2Y12 signaling with MRS2395. Platelets. 2018;29(4):383-94.
187. Zhou L, Schmaier AH. Platelet aggregation testing in platelet-rich plasma: description of procedures with the aim to develop standards in the field. Am J Clin Pathol. 2005;123(2):172-83.
188. Henriksen RA, Samokhin GP, Tracy PB. Thrombin-Induced Thromboxane Synthesis by Human Platelets. Arteriosclerosis, Thrombosis, and Vascular Biology. 1997;17(12):3519-26.
189. McKinnon KM. Flow Cytometry: An Overview. Current protocols in immunology. 2018;120:5.1.-5.1.11.
190. Frossard M, Fuchs I, Leitner JM, Hsieh K, Vlcek M, Losert H, et al. Platelet function predicts myocardial damage in patients with acute myocardial infarction. Circulation. 2004;110(11):1392-7.
191. Kaur R, Kaur M, Singh J. Endothelial dysfunction and platelet hyperactivity in type 2 diabetes mellitus: molecular insights and therapeutic strategies. Cardiovasc Diabetol. 2018;17(1):121.
192. Jakobsen C, Larsen JB, Fuglsang J, Hvas AM. Platelet function in preeclampsia - a systematic review and meta-analysis. Platelets. 2019;30(5):549-62.
193. Bio-Rad. Flow Cytometry Workbook [Available from: https://www.bio-rad-antibodies.com/flow-cytometry-antibody-titration.html Accessed June 2019.
194. Donati A, Gupta S, Reviakine I. Subpopulations in purified platelets adhering on glass. Biointerphases. 2016;11(2):029811.
195. Margolis J. Glass Surface and Blood Coagulation. Nature. 1956;178(4537):805-6.
196. Stephen J, Emerson B, Fox KA, Dransfield I. The uncoupling of monocyte-platelet interactions from the induction of proinflammatory signaling in monocytes. J Immunol. 2013;191(11):5677-83.
197. Singh MV, Suwunnakorn S, Simpson SR, Weber EA, Singh VB, Kalinski P, et al. Monocytes complexed to platelets differentiate into functionally deficient dendritic cells. Journal of Leukocyte Biology. 2021;109(4):807-20.
198. Lee SJ, Yoon BR, Kim HY, Yoo S-J, Kang SW, Lee W-W. Activated Platelets Convert CD14+CD16- Into CD14+CD16+ Monocytes With Enhanced FcγR-Mediated Phagocytosis and Skewed M2 Polarization. Front Immunol. 2021;11(3363).

199. Rong M-y, Wang C-h, Wu Z-b, Zeng W, Zheng Z-h, Han Q, et al. Platelets induce a proinflammatory phenotype in monocytes via the CD147 pathway in rheumatoid arthritis. Arthritis Research & Therapy. 2014;16(6):478.
200. Passacquale G, Vamadevan P, Pereira L, Hamid C, Corrigall V, Ferro A. Monocyte-platelet interaction induces a pro-inflammatory phenotype in circulating monocytes. PLoS One. 2011;6(10):e25595.
201. Zhou Y, Yasumoto A, Lei C, Huang CJ, Kobayashi H, Wu Y, et al. Intelligent classification of platelet aggregates by agonist type. Elife. 2020;9.
202. Rex S, Beaulieu LM, Perlman DH, Vitseva O, Blair PS, McComb ME, et al. Immune versus thrombotic stimulation of platelets differentially regulates signalling pathways, intracellular protein-protein interactions, and alpha-granule release. Thromb Haemost. 2009;102(1):97-110.
203. Vlahos CJ, Matter WF, Hui KY, Brown RF. A specific inhibitor of phosphatidylinositol 3-kinase, 2-(4-morpholinyl)-8-phenyl-4H-1-benzopyran-4-one (LY294002). J Biol Chem. 1994;269(7):5241-8.
204. Hu L, Zaloudek C, Mills GB, Gray J, Jaffe RB. In vivo and in vitro ovarian carcinoma growth inhibition by a phosphatidylinositol 3-kinase inhibitor (LY294002). Clin Cancer Res. 2000;6(3):880-6.
205. Dittmann A, Werner T, Chung CW, Savitski MM, Fälth Savitski M, Grandi P, et al. The commonly used PI3-kinase probe LY294002 is an inhibitor of BET bromodomains. ACS Chem Biol. 2014;9(2):495-502.
206. Li J, Kim SG, Blenis J. Rapamycin: one drug, many effects. Cell metabolism. 2014;19(3):373-9.
207. León B, Ardavín C. Monocyte migration to inflamed skin and lymph nodes is differentially controlled by L-selectin and PSGL-1. Blood. 2008;111(6):3126-30.
208. Piccardoni P, Sideri R, Manarini S, Piccoli A, Martelli N, de Gaetano G, et al. Platelet/polymorphonuclear leukocyte adhesion: a new role for SRC kinases in Mac-1 adhesive function triggered by P-selectin. Blood. 2001;98(1):108-16.
209. Lévesque J-P, Zannettino ACW, Pudney M, Niutta S, Haylock DN, Snapp KR, et al. PSGL-1-Mediated Adhesion of Human Hematopoietic Progenitors to P-Selectin Results in Suppression of Hematopoiesis. Immunity. 1999;11(3):369-78.
210. Xu T, Liu W, Yang C, Ba X, Wang X, Jiang Y, et al. Lipid raft-associated β-adducin is required for PSGL-1-mediated neutrophil rolling on P-selectin. Journal of Leukocyte Biology. 2015;97(2):297-306.
211. Xu T, Zhang L, Geng ZH, Wang H-B, Wang J-T, Chen M, et al. P-selectin Cross-links PSGL-1 and Enhances Neutrophil Adhesion to Fibrinogen and ICAM-1 in a Src Kinase-Dependent, but GPCR-Independent Mechanism. Cell Adhesion & Migration. 2007;1(3):115-23.
212. Blair P, Flaumenhaft R. Platelet alpha-granules: basic biology and clinical correlates. Blood Rev. 2009;23(4):177-89.
213. Golebiewska EM, Poole AW. Platelet secretion: From haemostasis to wound healing and beyond. Blood Rev. 2015;29(3):153-62.
214. Majlessi L, Prados-Rosales R, Casadevall A, Brosch R. Release of mycobacterial antigens. Immunol Rev. 2015;264(1):25-45.
215. Stamm CE, Pasko BL, Chaisavaneeyakorn S, Franco LH, Nair VR, Weigele BA, et al. Screening Mycobacterium tuberculosis Secreted Proteins Identifies Mpt64 as a Eukaryotic Membrane-Binding Bacterial Effector. mSphere. 2019;4(3).
216. Ly A, Liu J. Mycobacterial Virulence Factors: Surface-Exposed Lipids and Secreted Proteins. Int J Mol Sci. 2020;21(11).

217. Simeone R, Bottai D, Frigui W, Majlessi L, Brosch R. ESX/type VII secretion systems of mycobacteria: Insights into evolution, pathogenicity and protection. Tuberculosis (Edinb). 2015;95 Suppl 1:S150-4.
218. Singh S, Saraiva L, Elkington PT, Friedland JS. Regulation of matrix metalloproteinase-1, -3, and -9 in Mycobacterium tuberculosis-dependent respiratory networks by the rapamycin-sensitive PI3K/p70(S6K) cascade. FASEB J. 2014;28(1):85-93.
219. Green J, Elkington P, Pennington C, Roncaroli F, Dholakia S, Moores R, et al. Mycobacterium tuberculosis Upregulates Microglial Matrix Metalloproteinase-1 and -3 Expression and Secretion via NF-kappaB– and Activator Protein-1–Dependent Monocyte Networks. J Immunol. 2010;184(11):6492-503.
220. CIA World Factbook. The World Factbook: Peru. 2022 [Available from: https://www.cia.gov/the-world-factbook/countries/peru/.
221. The World Bank in Peru. 2021 [Available from: https://www.worldbank.org/en/country/peru/overview#1.
222. The World Bank. GDP per capita - Peru. World Bank Open Data. 2022 [Available from: https://data.worldbank.org/
223. Johns Hopkins Coronavirus Resource Center. Mortality Analyses. 2022 [Available from: https://coronavirus.jhu.edu/data/mortality. .
224. Chacaltana J. Rapid response to COVID-19 under high informality? The case of Peru. International Labour Organization; 2020.
225. Salo WL, Aufderheide AC, Buikstra J, Holcomb TA. Identification of Mycobacterium tuberculosis DNA in a pre-Columbian Peruvian mummy. Proc Natl Acad Sci U S A. 1994;91(6):2091-4.
226. Smith-Nonini S. When "the program is good, but the disease is better": lessons from Peru on drug-resistant tuberculosis. Med Anthropol. 2005;24(3):265-96.
227. Ministerio de Salud (MINSA). Construyendo Alianzas para Detener la Tuberculosis: la Experiencia Peruana. Lima: MINSA. 2006.
228. Suárez PG, Watt CJ, Alarcón E, Portocarrero J, Zavala D, Canales R, et al. The Dynamics of Tuberculosis in Response to 10 Years of Intensive Control Effort in Peru. The Journal of Infectious Diseases. 2001;184(4):473-8.
229. Personal communication, Lic. Rosa Mayhua, CENEX, Hospital Cayetano Heredia. 2021.
230. Coronel J, Roper M, Caviedes L, Moore D. MODS: A user guide. Microscopic observation drug susceptibility assay. Lima, Peru: Universidad Peruana Cayetano Heredia; 2008.
231. Caviedes L, Lee T-S, Gilman RH, Sheen P, Spellman E, Lee EH, et al. Rapid, Efficient Detection and Drug Susceptibility Testing of Mycobacterium tuberculosis in Sputum by Microscopic Observation of Broth Cultures. J Clin Microbiol. 2000;38(3):1203-8.
232. U.K. Foreign Office Foreign Travel Advice: Peru. 2021.
233. Neelemaat F, Kruizenga H, de Vet H, Seidell J, Butterman M, Bokhorst-de v, et al. Screening malnutrition in hospital outpatients. Can the SNAQ malnutrition screening tool also be applied to this population? Clin Nutr. 2008;27(3):439-46.
234. Chang SW, Pan WS, Lozano Beltran D, Oleyda Baldelomar L, Solano MA, Tuero I, et al. Gut hormones, appetite suppression and cachexia in patients with pulmonary TB. PloS one. 2013;8(1):e54564-e.
235. Paris L, Magni R, Zaidi F, Araujo R, Saini N, Harpole M, et al. Urine lipoarabinomannan glycan in HIV-negative patients with pulmonary tuberculosis correlates with disease severity. Sci Transl Med. 2017;9(420).

236. Wilson M, Thomas D, Rubenstein L, Chibnall J, Anderson S, Baxi A, et al. Appetite assessment: simple appetite questionnaire predicts weight loss in community-dwelling adults and nursing home residents. The American Journal of Clinical Nutrition. 2005;82:1074-81.
237. Ruiz P, Vega J, Loret de Mola C, Arevalo M, Chavez K. Validez y Consistencia Interna de la Versión de 5 ítems de la Escala para Depresión del Centro de Estudios Epidemiológicos (CESD) y la Escala Auto-administrada de Depresión de Zung (EDZ). Jornadas Cientificas Universidad Peruana Cayetano Heredia 2009.
238. Ugarte-Gil C, Ruiz P, Zamudio C, Canaza L, Otero L, Kruger H, et al. Association of major depressive episode with negative outcomes of tuberculosis treatment. PLoS One. 2013;8(7):e69514.
239. He R, Chen D. Chapter 142 - Confirmatory Testing for Diagnosis of Platelet Disorders. In: Shaz BH, Hillyer CD, Reyes Gil M, editors. Transfusion Medicine and Hemostasis (Third Edition): Elsevier; 2019. p. 841-8.
240. Zeng S, Zhou X, Ge L, Ji WJ, Shi R, Lu RY, et al. Monocyte subsets and monocyte-platelet aggregates in patients with unstable angina. J Thromb Thrombolysis. 2014;38(4):439-46.
241. Baldini M, Manfredi AA, Maugeri N. Targeting platelet-neutrophil interactions in giant-cell arteritis. Curr Pharm Des. 2014;20(4):567-74.
242. Tsai JJ, Jen YH, Chang JS, Hsiao HM, Noisakran S, Perng GC. Frequency alterations in key innate immune cell components in the peripheral blood of dengue patients detected by FACS analysis. J Innate Immun. 2011;3(5):530-40.
243. Le Joncour A, Biard L, Vautier M, Bugaut H, Mekinian A, Maalouf G, et al. Neutrophil-Platelet and Monocyte-Platelet Aggregates in COVID-19 Patients. Thromb Haemost. 2020;120(12):1733-5.
244. Hottz ED, Medeiros-de-Moraes IM, Vieira-de-Abreu A, de Assis EF, Vals-de-Souza R, Castro-Faria-Neto HC, et al. Platelet activation and apoptosis modulate monocyte inflammatory responses in dengue. J Immunol. 2014;193(4):1864-72.
245. Laddha AP, Kulkarni YA. VEGF and FGF-2: Promising targets for the treatment of respiratory disorders. Respir Med. 2019;156:33-46.
246. Apte RS, Chen DS, Ferrara N. VEGF in Signaling and Disease: Beyond Discovery and Development. Cell. 2019;176(6):1248-64.
247. Polena H, Boudou F, Tilleul S, Dubois-Colas N, Lecointe C, Rakotosamimanana N, et al. Mycobacterium tuberculosis exploits the formation of new blood vessels for its dissemination. Sci Rep. 2016;6:33162.
248. Golubinskaya EP, Filonenko TG, Kramar TV, Yermola YA, Kubyshkin AV, Gerashenko AV, et al. Dysregulation of VEGF-dependent angiogenesis in cavernous lung tuberculosis. Pathophysiology. 2019;26(3-4):381-7.
249. Bien MY, Wu MP, Chen WL, Chung CL. VEGF correlates with inflammation and fibrosis in tuberculous pleural effusion. ScientificWorldJournal. 2015;2015:417124.
250. Datta M, Via LE, Kamoun WS, Liu C, Chen W, Seano G, et al. Anti-vascular endothelial growth factor treatment normalizes tuberculosis granuloma vasculature and improves small molecule delivery. Proc Natl Acad Sci U S A. 2015;112(6):1827-32.
251. Saghazadeh A, Rezaei N. Vascular endothelial growth factor levels in tuberculosis: A systematic review and meta-analysis. PLoS One. 2022;17(5):e0268543.
252. Qama D, Choi WI, Kwon KY. Immune responses in the lungs of patients with tuberculous pleural effusion without pulmonary tuberculosis. BMC Immunol. 2012;13:45.
253. Ong CW, Elkington PT, Brilha S, Ugarte-Gil C, Tome-Esteban MT, Tezera LB, et al. Neutrophil-Derived MMP-8 Drives AMPK-Dependent Matrix Destruction in Human Pulmonary Tuberculosis. PLoS Pathog. 2015;11(5):e1004917.

254. Philip-Joët F, Alessi MC, Philip-Joët C, Aillaud M, Barriere JR, Arnaud A, et al. Fibrinolytic and inflammatory processes in pleural effusions. Eur Respir J. 1995;8(8):1352-6.
255. Bark CM, Manceur AM, Malone LL, Nsereko M, Okware B, Mayanja HK, et al. Identification of Host Proteins Predictive of Early Stage Mycobacterium tuberculosis Infection. EBioMedicine. 2017;21:150-7.
256. LENTING PJ, CASARI C, CHRISTOPHE OD, DENIS CV. von Willebrand factor: the old, the new and the unknown. Journal of Thrombosis and Haemostasis. 2012;10(12):2428-37.
257. Bhaskaran K, Bacon S, Evans SJW, Bates CJ, Rentsch CT, MacKenna B, et al. Factors associated with deaths due to COVID-19 versus other causes: population-based cohort analysis of UK primary care data and linked national death registrations within the OpenSAFELY platform. The Lancet Regional Health – Europe. 2021;6.
258. Staines HM, Kirwan DE, Clark DJ, Adams ER, Augustin Y, Byrne RL, et al. IgG Seroconversion and Pathophysiology in Severe Acute Respiratory Syndrome Coronavirus 2 Infection. Emerg Infect Dis. 2021;27(1):85-91.
259. Haimovich AD, Ravindra NG, Stoytchev S, Young HP, Wilson FP, van Dijk D, et al. Development and Validation of the Quick COVID-19 Severity Index: A Prognostic Tool for Early Clinical Decompensation. Annals of Emergency Medicine. 2020;76(4):442-53.
260. Sahu AK, Amrithanand VT, Mathew R, Aggarwal P, Nayer J, Bhoi S. COVID-19 in health care workers – A systematic review and meta-analysis. The American Journal of Emergency Medicine. 2020;38(9):1727-31.
261. Gallo Marin B, Aghagoli G, Lavine K, Yang L, Siff EJ, Chiang SS, et al. Predictors of COVID-19 severity: A literature review. Reviews in Medical Virology. 2021;31(1):e2146.
262. Shang Y, Liu T, Wei Y, Li J, Shao L, Liu M, et al. Scoring systems for predicting mortality for severe patients with COVID-19. EClinicalMedicine. 2020;24:100426.
263. Zhang C, Qin L, Li K, Wang Q, Zhao Y, Xu B, et al. A Novel Scoring System for Prediction of Disease Severity in COVID-19. Frontiers in cellular and infection microbiology. 2020;10:318-.
264. Liang W, Liang H, Ou L, Chen B, Chen A, Li C, et al. Development and Validation of a Clinical Risk Score to Predict the Occurrence of Critical Illness in Hospitalized Patients With COVID-19. JAMA Internal Medicine. 2020;180(8):1081-9.
265. Yao H, Zhang N, Zhang R, Duan M, Xie T, Pan J, et al. Severity Detection for the Coronavirus Disease 2019 (COVID-19) Patients Using a Machine Learning Model Based on the Blood and Urine Tests. Frontiers in Cell and Developmental Biology. 2020;8.
266. Fan G, Tu C, Zhou F, Liu Z, Wang Y, Song B, et al. Comparison of severity scores for COVID-19 patients with pneumonia: a retrospective study. European Respiratory Journal. 2020:2002113.
267. Knight SR, Ho A, Pius R, Buchan I, Carson G, Drake TM, et al. Risk stratification of patients admitted to hospital with covid-19 using the ISARIC WHO Clinical Characterisation Protocol: development and validation of the 4C Mortality Score. BMJ. 2020;370:m3339.
268. Seow J, Graham C, Merrick B, Acors S, Pickering S, Steel KJA, et al. Longitudinal observation and decline of neutralizing antibody responses in the three months following SARS-CoV-2 infection in humans. Nat Microbiol. 2020;5(12):1598-607.
269. Ethnic Category Code 2001. NHS Data Model and Dictionary [Available from: https://datadictionary.nhs.uk/attributes/ethnic_category_code_2001.html.
270. McFadden D. Regression-based specification tests for the multinomial logit model. Journal of Econometrics. 1987;34(1):63-82.
271. Hughes G, Choudhury RA, McRoberts N. Summary Measures of Predictive Power Associated with Logistic Regression Models of Disease Risk. Phytopathology®. 2019;109(5):712-5.

272. Richardson S, Hirsch JS, Narasimhan M, Crawford JM, McGinn T, Davidson KW, et al. Presenting Characteristics, Comorbidities, and Outcomes Among 5700 Patients Hospitalized With COVID-19 in the New York City Area. JAMA. 2020.
273. Tian W, Jiang W, Yao J, Nicholson CJ, Li RH, Sigurslid HH, et al. Predictors of mortality in hospitalized COVID-19 patients: A systematic review and meta-analysis. J Med Virol. 2020;92(10):1875-83.
274. Abers MS, Delmonte OM, Ricotta EE, Fintzi J, Fink DL, de Jesus AAA, et al. An immune-based biomarker signature is associated with mortality in COVID-19 patients. JCI Insight. 2021;6(1).
275. Wang Z, Wang Z. Identification of risk factors for in-hospital death of COVID - 19 pneumonia -- lessions from the early outbreak. BMC Infect Dis. 2021;21(1):113.
276. Li J, He X, Yuan Y, Zhang W, Li X, Zhang Y, et al. Meta-analysis investigating the relationship between clinical features, outcomes, and severity of severe acute respiratory syndrome coronavirus 2 (SARS-CoV-2) pneumonia. Am J Infect Control. 2021;49(1):82-9.
277. Tai DBG, Shah A, Doubeni CA, Sia IG, Wieland ML. The Disproportionate Impact of COVID-19 on Racial and Ethnic Minorities in the United States. Clin Infect Dis. 2021;72(4):703-6.
278. Gao YD, Ding M, Dong X, Zhang JJ, Kursat Azkur A, Azkur D, et al. Risk factors for severe and critically ill COVID-19 patients: A review. Allergy. 2021;76(2):428-55.
279. Remdesivir and three other drugs for hospitalised patients with COVID-19: final results of the WHO Solidarity randomised trial and updated meta-analyses. Lancet. 2022;399(10339):1941-53.
280. Horby P, Lim WS, Emberson JR, Mafham M, Bell JL, Linsell L, et al. Dexamethasone in Hospitalized Patients with Covid-19. N Engl J Med. 2021;384(8):693-704.
281. Montgomery J, Stokes-Lampard H, Griffiths M, Gardiner D, Harvey D, Suntharalingam G. Assessing whether COVID-19 patients will benefit from critical care, and an objective approach to capacity challenges during a pandemic: An Intensive Care Society clinical guideline. Journal of the Intensive Care Society. 2021;22(3):204-10.
282. British Medical Association. COVID-19 – ethical issues. A guidance note. London: British Medical Association; 2020.
283. Tsai PH, Lai WY, Lin YY, Luo YH, Lin YT, Chen HK, et al. Clinical manifestation and disease progression in COVID-19 infection. J Chin Med Assoc. 2021;84(1):3-8.
284. Kozlov M. Omicron's feeble attack on the lungs could make it less dangerous. Nature. 2022;601(7892):177.
285. Iftimie S, López-Azcona AF, Vallverdú I, Hernández-Flix S, de Febrer G, Parra S, et al. First and second waves of coronavirus disease-19: A comparative study in hospitalized patients in Reus, Spain. PLoS One. 2021;16(3):e0248029.
286. Karagiannidis C, Windisch W, McAuley DF, Welte T, Busse R. Major differences in ICU admissions during the first and second COVID-19 wave in Germany. The Lancet Respiratory medicine. 2021;9(5):e47-e8.
287. . UK Health Security Agency. SARS-CoV-2 variants of concern and variants under investigation in England. Technical briefing: Update on hospitalisation and vaccine effectiveness for Omicron VOC-21NOV-01 (B.1.1.529) 31st December 2021.
288. Del Valle DM, Kim-Schulze S, Huang HH, Beckmann ND, Nirenberg S, Wang B, et al. An inflammatory cytokine signature predicts COVID-19 severity and survival. Nat Med. 2020;26(10):1636-43.
289. Yang Y, Shen C, Li J, Yuan J, Wei J, Huang F, et al. Plasma IP-10 and MCP-3 levels are highly associated with disease severity and predict the progression of COVID-19. J Allergy Clin Immunol. 2020;146(1):119-27.e4.

290. Laing AG, Lorenc A, Del Molino Del Barrio I, Das A, Fish M, Monin L, et al. A dynamic COVID-19 immune signature includes associations with poor prognosis. Nat Med. 2020;26(10):1623-35.
291. Arunachalam PS, Wimmers F, Mok CKP, Perera R, Scott M, Hagan T, et al. Systems biological assessment of immunity to mild versus severe COVID-19 infection in humans. Science. 2020;369(6508):1210-20.
292. Elshazli RM, Toraih EA, Elgaml A, El-Mowafy M, El-Mesery M, Amin MN, et al. Diagnostic and prognostic value of hematological and immunological markers in COVID-19 infection: A meta-analysis of 6320 patients. PLoS One. 2020;15(8):e0238160.
293. Vultaggio A, Vivarelli E, Virgili G, Lucenteforte E, Bartoloni A, Nozzoli C, et al. Prompt Predicting of Early Clinical Deterioration of Moderate-to-Severe COVID-19 Patients: Usefulness of a Combined Score Using IL-6 in a Preliminary Study. J Allergy Clin Immunol Pract. 2020;8(8):2575-81.e2.
294. Herold T, Jurinovic V, Arnreich C, Lipworth BJ, Hellmuth JC, von Bergwelt-Baildon M, et al. Elevated levels of IL-6 and CRP predict the need for mechanical ventilation in COVID-19. J Allergy Clin Immunol. 2020;146(1):128-36.e4.
295. Grifoni E, Valoriani A, Cei F, Lamanna R, Gelli AMG, Ciambotti B, et al. Interleukin-6 as prognosticator in patients with COVID-19. J Infect. 2020;81(3):452-82.
296. Zhou F, Yu T, Du R, Fan G, Liu Y, Liu Z, et al. Clinical course and risk factors for mortality of adult inpatients with COVID-19 in Wuhan, China: a retrospective cohort study. Lancet. 2020;395(10229):1054-62.
297. Shankar-Hari M, Vale CL, Godolphin PJ, Fisher D, Higgins JPT, Spiga F, et al. Association Between Administration of IL-6 Antagonists and Mortality Among Patients Hospitalized for COVID-19: A Meta-analysis. Jama. 2021;326(6):499-518.
298. Yang L, Xie X, Tu Z, Fu J, Xu D, Zhou Y. The signal pathways and treatment of cytokine storm in COVID-19. Signal Transduction and Targeted Therapy. 2021;6(1):255.
299. Huang C, Wang Y, Li X, Ren L, Zhao J, Hu Y, et al. Clinical features of patients infected with 2019 novel coronavirus in Wuhan, China. Lancet. 2020;395(10223):497-506.
300. Schulte-Schrepping J, Reusch N, Paclik D, Baßler K, Schlickeiser S, Zhang B, et al. Severe COVID-19 Is Marked by a Dysregulated Myeloid Cell Compartment. Cell. 2020;182(6):1419-40.e23.
301. Borges L, Pithon-Curi TC, Curi R, Hatanaka E. COVID-19 and Neutrophils: The Relationship between Hyperinflammation and Neutrophil Extracellular Traps. Mediators Inflamm. 2020;2020:8829674.
302. National Institute for Health and Care Excellence (NICE), Scottish Intercollegiate Guidelines Network (SIGN), and Royal College of General Practitioners (RCGP). COVID-19 rapid guideline: managing the long-term effects of COVID-19. Version 1.9, 14 January 2022. . 2022.
303. Myall KJ, Mukherjee B, Castanheira AM, Lam JL, Benedetti G, Mak SM, et al. Persistent Post-COVID-19 Interstitial Lung Disease. An Observational Study of Corticosteroid Treatment. Ann Am Thorac Soc. 2021;18(5):799-806.
304. Huang C, Huang L, Wang Y, Li X, Ren L, Gu X, et al. 6-month consequences of COVID-19 in patients discharged from hospital: a cohort study. Lancet. 2021;397(10270):220-32.
305. Qin C, Zhou L, Hu Z, Zhang S, Yang S, Tao Y, et al. Dysregulation of immune response in patients with COVID-19 in Wuhan, China. Clin Infect Dis. 2020.
306. George PM, Wells AU, Jenkins RG. Pulmonary fibrosis and COVID-19: the potential role for antifibrotic therapy. Lancet Respir Med. 2020;8(8):807-15.

307. Zhang T, Sun LX, Feng RE. [Comparison of clinical and pathological features between severe acute respiratory syndrome and coronavirus disease 2019]. Zhonghua Jie He He Hu Xi Za Zhi. 2020;43(6):496-502.
308. Shi H, Han X, Jiang N, Cao Y, Alwalid O, Gu J, et al. Radiological findings from 81 patients with COVID-19 pneumonia in Wuhan, China: a descriptive study. Lancet Infect Dis. 2020;20(4):425-34.
309. Elkington PT, Friedland JS. Matrix metalloproteinases in destructive pulmonary pathology. Thorax. 2005;61(3):259-66.
310. Lerum TV, Maltzahn NN, Aukrust P, Trøseid M, Henriksen KN, Kåsine T, et al. Persistent pulmonary pathology after COVID-19 is associated with high viral load, weak antibody response, and high levels of matrix metalloproteinase-9. Sci Rep. 2021;11(1):23205.
311. Ueland T, Holter JC, Holten AR, Müller KE, Lind A, Bekken GK, et al. Distinct and early increase in circulating MMP-9 in COVID-19 patients with respiratory failure. The Journal of infection. 2020;81(3):e41-e3.
312. Desforges M, Miletti TC, Gagnon M, Talbot PJ. Activation of human monocytes after infection by human coronavirus 229E. Virus Res. 2007;130(1-2):228-40.
313. Lartey NL, Valle-Reyes S, Vargas-Robles H, Jiménez-Camacho KE, Guerrero-Fonseca IM, Castellanos-Martínez R, et al. ADAM17/MMP inhibition prevents neutrophilia and lung injury in a mouse model of COVID-19. J Leukoc Biol. 2021.
314. Wild JM, Porter JC, Molyneaux PL, George PM, Stewart I, Allen RJ, et al. Understanding the burden of interstitial lung disease post-COVID-19: the UK Interstitial Lung Disease-Long COVID Study (UKILD-Long COVID). BMJ Open Respir Res. 2021;8(1).
315. Sigfrid L, Cevik M, Jesudason E, Lim WS, Rello J, Amuasi J, et al. What is the recovery rate and risk of long-term consequences following a diagnosis of COVID-19? A harmonised, global longitudinal observational study protocol. BMJ Open. 2021;11(3):e043887.
316. Adeloye D, Elneima O, Daines L, Poinasamy K, Quint JK, Walker S, et al. The long-term sequelae of COVID-19: an international consensus on research priorities for patients with pre-existing and new-onset airways disease. Lancet Respir Med. 2021;9(12):1467-78.
317. Kim S, Kunapuli SP. P2Y12 receptor in platelet activation. Platelets. 2011;22(1):56-60.
318. Dorsam RT, Kunapuli SP. Central role of the P2Y12 receptor in platelet activation. J Clin Invest. 2004;113(3):340-5.
319. Savi P, Herbert JM. Clopidogrel and ticlopidine: P2Y12 adenosine diphosphate-receptor antagonists for the prevention of atherothrombosis. Semin Thromb Hemost. 2005;31(2):174-83.
320. Cattaneo M, Zighetti ML, Lombardi R, Martinez C, Lecchi A, Conley PB, et al. Molecular bases of defective signal transduction in the platelet P2Y12 receptor of a patient with congenital bleeding. Proc Natl Acad Sci U S A. 2003;100(4):1978-83.
321. Hagiwara S, Iwasaka H, Hasegawa A, Oyama M, Imatomi R, Uchida T, et al. Adenosine diphosphate receptor antagonist clopidogrel sulfate attenuates LPS-induced systemic inflammation in a rat model. Shock. 2011;35(3):289-92.
322. da Costa Martins PA, van Gils JM, Mol A, Hordijk PL, Zwaginga JJ. Platelet binding to monocytes increases the adhesive properties of monocytes by up-regulating the expression and functionality of beta1 and beta2 integrins. J Leukoc Biol. 2006;79(3):499-507.
323. Hayward SE, Deal A, Rustage K, Nellums LB, Sweetland AC, Boccia D, et al. The relationship between mental health and risk of active tuberculosis: a systematic review. BMJ Open. 2022;12(1):e048945.
324. Nolan A, Condos R, Huie ML, Dawson R, Dheda K, Bateman E, et al. Elevated IP-10 and IL-6 from bronchoalveolar lavage cells are biomarkers of non-cavitary tuberculosis. Int J Tuberc Lung Dis. 2013;17(7):922-7.

325. Kibiki GS, Myers LC, Kalambo CF, Hoang SB, Stoler MH, Stroup SE, et al. Bronchoalveolar neutrophils, interferon gamma-inducible protein 10 and interleukin-7 in AIDS-associated tuberculosis. Clin Exp Immunol. 2007;148(2):254-9.
326. Bogen E. The Pathogenesis of Tuberculous Hemoptysis: A Clinical-Pathological Investigation. American Journal of Clinical Pathology. 1932;2(4):299-308.
327. Kumar Gupta D, Jenaw RK. A CROSS-SECTIONAL STUDY TO EVALUATE THE ETIOLOGICAL PROFILE OF HEMOPTYSIS AND IT S CORRELATION WITH SEVERITY. Paripex Indian Journal Of Research. 2021:45-7.
328. Ozgül MA, Turna A, Yildiz P, Ertan E, Kahraman S, Yilmaz V. Risk factors and recurrence patterns in 203 patients with hemoptysis. Tuberk Toraks. 2006;54(3):243-8.
329. Tan S, Sun D, Zhang T, Li Y, Cao Y, Njire MM, et al. Risk Factors for Hemoptysis in Pulmonary Tuberculosis Patients from Southern China: A Retrospective Study. Journal of Tuberculosis Research. 2014;02:173-80.
330. Halezeroğlu S, Okur E. Thoracic surgery for haemoptysis in the context of tuberculosis: what is the best management approach? J Thorac Dis. 2014;6(3):182-5.
331. Goncalves IM, Alves DC, Carvalho A, do Ceu Brito M, Calvario F, Duarte R. Tuberculosis and Venous Thromboembolism: a case series. Cases Journal. 2009;2:9333-.
332. Subahi EA, Alawad MJ, Abdelmahmuod EA, Sibira D, Kamal I. Pulmonary Tuberculosis With Saddle Pulmonary Embolism and Deep Vein Thrombosis: A Rare Case Report. Cureus. 2021;13(6):e15958.
333. Kechaou I, Cherif E, Ben Hassine L, Khalfallah N. Deep vein thrombosis and tuberculosis: a causative link? BMJ Case Rep. 2014;2014.
334. Dentan C, Epaulard O, Seynaeve D, Genty C, Bosson JL. Active tuberculosis and venous thromboembolism: association according to international classification of diseases, ninth revision hospital discharge diagnosis codes. Clin Infect Dis. 2014;58(4):495-501.
335. Danwang C, Bigna JJ, Awana AP, Nzalie RN, Robert A. Global epidemiology of venous thromboembolism in people with active tuberculosis: a systematic review and meta-analysis. J Thromb Thrombolysis. 2021;51(2):502-12.
336. Ambrosetti M, Ferrarese M, Codecasa LR, Besozzi G, Sarassi A, Viggiani P, et al. Incidence of venous thromboembolism in tuberculosis patients. Respiration. 2006;73(3):396.
337. Roka-Moiia Y, Palomares DE, Italiano JE, Sheriff J, Bluestein D, Slepian M. Abstract 13132: The "Thrombosis-Bleeding Paradox" of Mechanical Circulatory Support: Shear Stress Promotes Platelet Prothrombosis and Microparticle Generation While Inducing Integrin αIIbβ3 Shedding and Decreased Aggregability. Circulation. 2019;140(Suppl_1):A13132-A.
338. Bye AP, Unsworth AJ, Gibbins JM. Platelet signaling: a complex interplay between inhibitory and activatory networks. Journal of thrombosis and haemostasis : JTH. 2016;14(5):918-30.
339. Le Blanc J, Lordkipanidzé M. Platelet Function in Aging. Front Cardiovasc Med. 2019;6:109-.
340. Qiu X, Xiong T, Su X, Qu Y, Ge L, Yue Y, et al. Accumulate evidence for IP-10 in diagnosing pulmonary tuberculosis. BMC Infect Dis. 2019;19(1):924.
341. Chen YC, Chin CH, Liu SF, Wu CC, Tsen CC, Wang YH, et al. Prognostic values of serum IP-10 and IL-17 in patients with pulmonary tuberculosis. Dis Markers. 2011;31(2):101-10.
342. Blauenfeldt T, Petrone L, Del Nonno F, Baiocchini A, Falasca L, Chiacchio T, et al. Interplay of DDP4 and IP-10 as a Potential Mechanism for Cell Recruitment to Tuberculosis Lesions. Front Immunol. 2018;9:1456-.
343. Marchandot B, Sattler L, Jesel L, Matsushita K, Schini-Kerth V, Grunebaum L, et al. COVID-19 Related Coagulopathy: A Distinct Entity? J Clin Med. 2020;9(6).

344. Boccia M, Aronne L, Celia B, Mazzeo G, Ceparano M, D'Agnano V, et al. COVID-19 and coagulative axis: review of emerging aspects in a novel disease. Monaldi Arch Chest Dis. 2020;90(2).
345. Al-Samkari H, Karp Leaf RS, Dzik WH, Carlson JCT, Fogerty AE, Waheed A, et al. COVID-19 and coagulation: bleeding and thrombotic manifestations of SARS-CoV-2 infection. Blood. 2020;136(4):489-500.
346. Kowalewski M, Fina D, Słomka A, Raffa GM, Martucci G, Lo Coco V, et al. COVID-19 and ECMO: the interplay between coagulation and inflammation-a narrative review. Crit Care. 2020;24(1):205.
347. Kollias A, Kyriakoulis KG, Dimakakos E, Poulakou G, Stergiou GS, Syrigos K. Thromboembolic risk and anticoagulant therapy in COVID-19 patients: emerging evidence and call for action. Br J Haematol. 2020;189(5):846-7.
348. Neri T, Nieri D, Celi A. P-selectin blockade in COVID-19-related ARDS. Am J Physiol Lung Cell Mol Physiol. 2020;318(6):L1237-l8.
349. Panigada M, Bottino N, Tagliabue P, Grasselli G, Novembrino C, Chantarangkul V, et al. Hypercoagulability of COVID-19 patients in intensive care unit: A report of thromboelastography findings and other parameters of hemostasis. J Thromb Haemost. 2020;18(7):1738-42.
350. Philippe A, Chocron R, Gendron N, Bory O, Beauvais A, Peron N, et al. Circulating Von Willebrand factor and high molecular weight multimers as markers of endothelial injury predict COVID-19 in-hospital mortality. Angiogenesis. 2021;24(3):505-17.
351. Chen J, Ling M, Fu X, López JA, Chung DW. Simultaneous exposure of sites in von Willebrand factor for glycoprotein Ib binding and ADAMTS13 cleavage: studies with ristocetin. Arterioscler Thromb Vasc Biol. 2012;32(11):2625-30.
352. Ozaki Y, Suzuki-Inoue K, Inoue O. Platelet receptors activated via mulitmerization: glycoprotein VI, GPIb-IX-V, and CLEC-2. J Thromb Haemost. 2013;11 Suppl 1:330-9.
353. Gibbins JM. Platelet adhesion signalling and the regulation of thrombus formation. J Cell Sci. 2004;117(Pt 16):3415-25.
354. Mancini I, Baronciani L, Artoni A, Colpani P, Biganzoli M, Cozzi G, et al. The ADAMTS13-von Willebrand factor axis in COVID-19 patients. J Thromb Haemost. 2021;19(2):513-21.
355. González-López A, Astudillo A, García-Prieto E, Fernández-García MS, López-Vázquez A, Batalla-Solís E, et al. Inflammation and matrix remodeling during repair of ventilator-induced lung injury. Am J Physiol Lung Cell Mol Physiol. 2011;301(4):L500-9.
356. Amado-Rodríguez L, González-López A, López-Alonso I, Aguirre A, Astudillo A, Batalla-Solís E, et al. Anti-inflammatory effects of clarithromycin in ventilator-induced lung injury. Respir Res. 2013;14(1):52.
357. Cabrera-Benitez NE, Laffey JG, Parotto M, Spieth PM, Villar J, Zhang H, et al. Mechanical ventilation-associated lung fibrosis in acute respiratory distress syndrome: a significant contributor to poor outcome. Anesthesiology. 2014;121(1):189-98.
358. Berumen Sánchez G, Bunn KE, Pua HH, Rafat M. Extracellular vesicles: mediators of intercellular communication in tissue injury and disease. Cell Commun Signal. 2021;19(1):104.
359. Cognasse F, Hamzeh-Cognasse H, Laradi S, Chou ML, Seghatchian J, Burnouf T, et al. The role of microparticles in inflammation and transfusion: A concise review. Transfus Apher Sci. 2015;53(2):159-67.
360. Ostermeier B, Soriano-Sarabia N, Maggirwar SB. Platelet-Released Factors: Their Role in Viral Disease and Applications for Extracellular Vesicle (EV) Therapy. Int J Mol Sci. 2022;23(4).
361. Tőkés-Füzesi M, Ruzsics I, Rideg O, Kustán P, Kovács GL, Molnár T. Role of microparticles derived from monocytes, endothelial cells and platelets in the exacerbation of COPD. Int J Chron Obstruct Pulmon Dis. 2018;13:3749-57.

362. Zahran AM, El-Badawy O, Ali WA, Mahran ZG, Mahran E, Rayan A. Circulating microparticles and activated platelets as novel prognostic biomarkers in COVID-19; relation to cancer. PLoS One. 2021;16(2):e0246806.
363. Hamali HA, Saboor M, Dobie G, Madkhali AM, Akhter MS, Hakamy A, et al. Procoagulant Microvesicles in COVID-19 Patients: Possible Modulators of Inflammation and Prothrombotic Tendency. Infect Drug Resist. 2022;15:2359-68.
364. Brambilla M, Talmon M, Canzano P, Fresu LG, Brunelleschi S, Tremoli E, et al. Different Contribution of Monocyte- and Platelet-Derived Microvesicles to Endothelial Behavior. Int J Mol Sci. 2022;23(9).
365. Shet AS. Characterizing blood microparticles: technical aspects and challenges. Vasc Health Risk Manag. 2008;4(4):769-74.
366. Tomer A, Harker LA, Burstein SA. Flow cytometric analysis of normal human megakaryocytes. Blood. 1988;71(5):1244-52.
367. Schubert S, Weyrich AS, Rowley JW. A tour through the transcriptional landscape of platelets. Blood. 2014;124(4):493-502.
368. Davizon-Castillo P, Rowley JW, Rondina MT. Megakaryocyte and Platelet Transcriptomics for Discoveries in Human Health and Disease. Arteriosclerosis, thrombosis, and vascular biology. 2020;40(6):1432-40.
369. Bao J, Zhao X, Lu J, Hu Z, Hu M, Hu X, et al. Platelet transcriptome profiles provide potential therapeutic targets for elderly acute myelocytic leukemia patients. J Transl Med. 2021;19(1):388.
370. Eicher JD, Wakabayashi Y, Vitseva O, Esa N, Yang Y, Zhu J, et al. Characterization of the platelet transcriptome by RNA sequencing in patients with acute myocardial infarction. Platelets. 2016;27(3):230-9.
371. Shroff KE, Sainis KB, Sengupta SR, Kamat RS. Role of antigen-presenting cells in variation in immunogenicity of mycobacteria. Clin Exp Immunol. 1990;79(2):285-90.
372. Rangel Moreno J, Estrada García I, De La Luz García Hernández M, Aguilar Leon D, Marquez R, Hernández Pando R. The role of prostaglandin E2 in the immunopathogenesis of experimental pulmonary tuberculosis. Immunology. 2002;106(2):257-66.
373. Hernández-Pando R, Orozco-Esteves H, Maldonado HA, Aguilar-León D, Vilchis-Landeros MM, Mata-Espinosa DA, et al. A combination of a transforming growth factor-beta antagonist and an inhibitor of cyclooxygenase is an effective treatment for murine pulmonary tuberculosis. Clin Exp Immunol. 2006;144(2):264-72.
374. Byrne ST, Denkin SM, Zhang Y. Aspirin antagonism in isoniazid treatment of tuberculosis in mice. Antimicrob Agents Chemother. 2007;51(2):794-5.
375. Peres-Buzalaf C, de Paula L, Frantz FG, Soares EM, Medeiros AI, Peters-Golden M, et al. Control of experimental pulmonary tuberculosis depends more on immunostimulatory leukotrienes than on the absence of immunosuppressive prostaglandins. Prostaglandins, Leukotrienes and Essential Fatty Acids. 2011;85(2):75-81.
376. Mortensen R, Clemmensen HS, Woodworth JS, Therkelsen ML, Mustafa T, Tonby K, et al. Cyclooxygenase inhibitors impair CD4 T cell immunity and exacerbate Mycobacterium tuberculosis infection in aerosol-challenged mice. Communications biology. 2019;2:288-.
377. Schoeman JF, Janse van Rensburg A, Laubscher JA, Springer P. The role of aspirin in childhood tuberculous meningitis. J Child Neurol. 2011;26(8):956-62.